



Field-Trip Guide to Mafic Volcanism of the Cascade Range in Central Oregon—A Volcanic, Tectonic, Hydrologic, and Geomorphic Journey



Scientific Investigations Report 2017–5022–H

COVER

View north along the Cascade Range crest from the north flank of Yapoah Crater, in Three Sisters Wilderness, Oregon. Prominent peaks forming the skyline are, from left to right, the rounded shield of Belknap Crater; the jagged peaks of Mount Washington and Three Fingered Jack, both eroded stratovolcano remnants; and the better preserved edifice of Mount Jefferson. Also faintly visible in the distance, to the right of Mount Jefferson, is the snow-capped peak of still-active Mount Hood. In the foreground are mafic lava flows from Yapoah Crater. Photograph by Jim O'Connor, 2014.

Field-Trip Guide to Mafic Volcanism of the Cascade Range in Central Oregon— A Volcanic, Tectonic, Hydrologic, and Geomorphic Journey

By Natalia I. Deligne, Daniele Mckay, Richard M. Conrey, Gordon E. Grant, Emily R. Johnson, Jim O'Connor, and Kristin Sweeney

Scientific Investigations Report 2017–5022–H

**U.S. Department of the Interior
U.S. Geological Survey**

U.S. Department of the Interior

RYAN K. ZINKE, Secretary

U.S. Geological Survey

William H. Werkheiser, Acting Director

U.S. Geological Survey, Reston, Virginia: 2017

For more information on the USGS—the Federal source for science about the Earth, its natural and living resources, natural hazards, and the environment—visit <https://www.usgs.gov> or call 1–888–ASK–USGS.

For an overview of USGS information products, including maps, imagery, and publications, visit <https://store.usgs.gov>.

Any use of trade, firm, or product names is for descriptive purposes only and does not imply endorsement by the U.S. Government.

Although this information product largely is in the public domain, it may also contain copyrighted materials as noted in the text. Permission to reproduce copyrighted items must be secured from the copyright owner.

Suggested citation:

Deligne, N.I., Mckay, D., Conrey, R.M., Grant, G.E., Johnson, E.R., O'Connor, J., and Sweeney, K., 2017, Field-trip guide to mafic volcanism of the Cascade Range in central Oregon—A volcanic, tectonic, hydrologic, and geomorphic journey: U.S. Geological Survey Scientific Investigations Report 2017–5022–H, 94 p., <https://doi.org/sir20175022H>.

ISSN 2328-0328 (online)

Preface

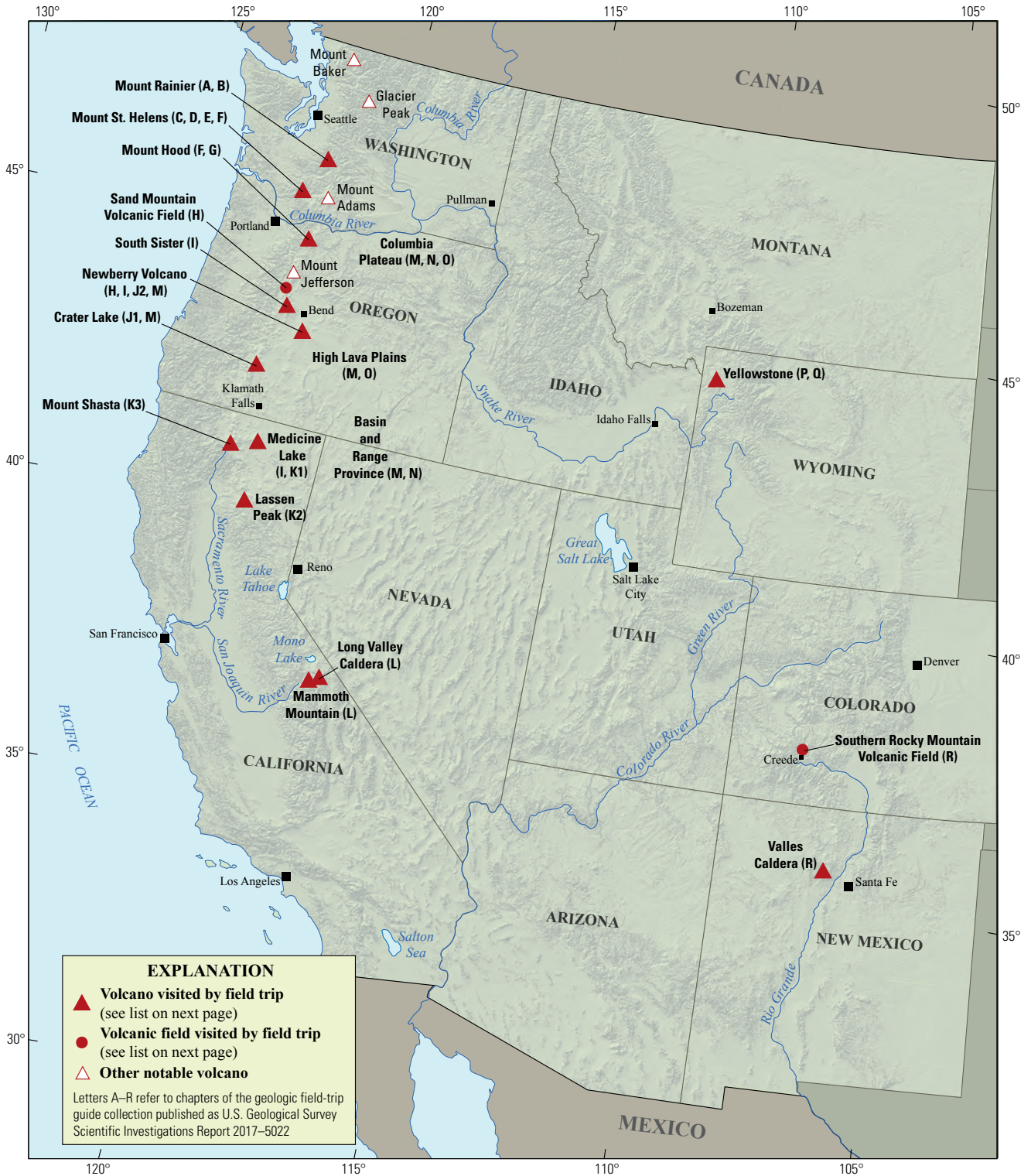
The North American Cordillera is home to a greater diversity of volcanic provinces than any comparably sized region in the world. The interplay between changing plate-margin interactions, tectonic complexity, intra-crustal magma differentiation, and mantle melting have resulted in a wealth of volcanic landscapes. Field trips in this series visit many of these landscapes, including (1) active subduction-related arc volcanoes in the Cascade Range; (2) flood basalts of the Columbia Plateau; (3) bimodal volcanism of the Snake River Plain-Yellowstone volcanic system; (4) some of the world's largest known ignimbrites from southern Utah, central Colorado, and northern Nevada; (5) extension-related volcanism in the Rio Grande Rift and Basin and Range Province; and (6) the spectacular eastern Sierra Nevada featuring Long Valley Caldera and the iconic Bishop Tuff. Some of the field trips focus on volcanic eruptive and emplacement processes, calling attention to the fact that the western United States provides opportunities to examine a wide range of volcanological phenomena at many scales.

The 2017 Scientific Assembly of the International Association of Volcanology and Chemistry of the Earth's Interior (IAVCEI) in Portland, Oregon, marks the first time that the U.S. volcanological community has hosted this quadrennial meeting since 1989, when it was held in Santa Fe, New Mexico. The 1989 field-trip guides are still widely used by students and professionals alike. This new set of field guides is similarly a legacy collection that summarizes decades of advances in our understanding of magmatic and tectonic processes of volcanic western North America.

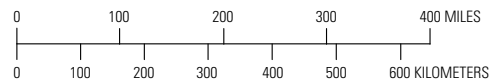
The field of volcanology has flourished since the 1989 IAVCEI meeting, and it has profited from detailed field investigations coupled with emerging new analytical methods. Mapping has been enhanced by plentiful major- and trace-element whole-rock and mineral data, technical advances in radiometric dating and collection of isotopic data, GPS (Global Positioning System) advances, and the availability of lidar (light detection and ranging) imagery. Spectacularly effective microbeam instruments, geodetic and geophysical data collection and processing, paleomagnetic determinations, and modeling capabilities have combined with mapping to provide new information and insights over the past 30 years. The collective works of the international community have made it possible to prepare wholly new guides to areas across the western United States. These comprehensive field guides are available, in large part, because of enormous contributions from many experienced geologists who have devoted entire careers to their field areas. Early career scientists are carrying forward and refining their foundational work with impressive results.

Our hope is that future generations of scientists as well as the general public will use these field guides as introductions to these fascinating areas and will be enticed toward further exploration and field-based research.

Michael Dungan, University of Oregon
Judy Fierstein, U.S. Geological Survey
Cynthia Gardner, U.S. Geological Survey
Dennis Geist, National Science Foundation
Anita Grunder, Oregon State University
John Wolff, Washington State University
Field-trip committee, IAVCEI 2017



Map of the western United States showing volcanoes and volcanic fields visited by geologic field trips scheduled in conjunction with the 2017 meeting of the International Association of Volcanology and Chemistry of the Earth's Interior (IAVCEI) in Portland, Oregon, and available as chapters in U.S. Geological Survey Scientific Investigations Report 2017–5022. Shaded-relief base from U.S. Geological Survey National Elevation Dataset 30-meter digital elevation model data.



Chapter letter	Title
A	Field-Trip Guide to Volcanism and Its Interaction with Snow and Ice at Mount Rainier, Washington
B	Field-Trip Guide to Subaqueous Volcaniclastic Facies in the Ancestral Cascades Arc in Southern Washington State—The Ohanapecosh Formation and Wildcat Creek Beds
C	Field-Trip Guide for Exploring Pyroclastic Density Current Deposits from the May 18, 1980, Eruption of Mount St. Helens, Washington
D	Field-Trip Guide to Mount St. Helens, Washington—An overview of the Eruptive History and Petrology, Tephra Deposits, 1980 Pyroclastic Density Current Deposits, and the Crater
E	Field-Trip Guide to Mount St. Helens, Washington—Recent and Ancient Volcaniclastic Processes and Deposits
F	Geologic Field-Trip Guide of Volcaniclastic Sediments from Snow- and Ice-Capped Volcanoes—Mount St. Helens, Washington, and Mount Hood, Oregon
G	Field-Trip Guide to Mount Hood, Oregon, Highlighting Eruptive History and Hazards
H	Field-Trip Guide to Mafic Volcanism of the Cascade Range in Central Oregon—A Volcanic, Tectonic, Hydrologic, and Geomorphic Journey
I	Field-Trip Guide to Holocene Silicic Lava Flows and Domes at Newberry Volcano, Oregon, South Sister Volcano, Oregon, and Medicine Lake Volcano, California
J	Overview for Geologic Field-Trip Guides to Mount Mazama, Crater Lake Caldera, and Newberry Volcano, Oregon
J1	Geologic Field-Trip Guide to Mount Mazama and Crater Lake Caldera, Oregon
J2	Field-Trip Guide to the Geologic Highlights of Newberry Volcano, Oregon
K	Overview for Geologic Field-Trip Guides to Volcanoes of the Cascades Arc in northern California
K1	Geologic Field-Trip Guide to Medicine Lake Volcano, northern California, including Lava Beds National Monument
K2	Geologic Field-Trip Guide to the Lassen Segment of the Cascades Arc, northern California
K3	Geologic Field-Trip Guide to Mount Shasta Volcano, northern California
L	Geologic Field-Trip Guide to Long Valley Caldera, California
M	Field-Trip Guide to a Volcanic Transect of the Pacific Northwest
N	Field-Trip Guide to the Vents, Dikes, Stratigraphy, and Structure of the Columbia River Basalt Group, Eastern Oregon and Southeastern Washington
O	Field-Trip Guide to Flood Basalts, Associated Rhyolites, and Diverse Post-Plume Volcanism in Eastern Oregon
P	Field-Trip Guide to the Volcanic and Hydrothermal Landscape of Yellowstone Plateau, Montana and Wyoming
Q	Field-Trip Guide to the Petrology of Quaternary Volcanism on the Yellowstone Plateau, Idaho and Wyoming
R	Field-Trip Guide to Continental Arc to Rift Volcanism of the Southern Rocky Mountains—Southern Rocky Mountain, Taos Plateau, and Jemez Volcanic Fields of Southern Colorado and Northern New Mexico

Contributing Authors

Boise State University

Brittany D. Brand
Nicholas Pollock

Colgate University

Karen Harpp
Alison Koleszar

Durham University

Richard J. Brown

Eastern Oregon University

Mark L. Ferns

ETH Zurich

Olivier Bachmann

Georgia Institute of

Technology

Josef Dufek

GNS Science, New

Zealand

Natalia I. Deligne

Hamilton College

Richard M. Conrey

Massachusetts Institute of

Technology

Timothy Grove

National Science Foundation

Dennis Geist (also with
Colgate University and
University of Idaho)

New Mexico Bureau of

Geology and Mineral

Resources

Paul W. Bauer
William C. McIntosh
Matthew J. Zimmerer

New Mexico State

University

Emily R. Johnson

Northeastern University

Martin E. Ross

Oregon Department of Geology and Mineral Industries

William J. Burns
Lina Ma
Ian P. Madin
Jason D. McClaughry

Oregon State University

Adam J.R. Kent

Portland State University

Jonathan H. Fink (also with
University of British Columbia)
Martin J. Streck
Ashley R. Streig

San Diego State University

Victor E. Camp

Smithsonian Institution

Lee Siebert

Universidad Nacional

Autónoma de San Luis Potosi

Damiano Sarocchi

University of California, Davis

Kari M. Cooper

University of Liverpool

Peter B. Kokelaar

University of Northern

Colorado

Steven W. Anderson

University of Oregon

Ilya N. Binderman
Michael A. Dungan
Daniele Mckay (also with
Oregon State University and
Oregon State University,
Cascades)

University of Portland

Kristin Sweeney

University of Tasmania

Martin Jutzeler
Jocelyn McPhie

University of Utah

Jamie Farrell

U.S. Army Corps of

Engineers

Keith I. Kelson

U.S. Forest Service

Gordon E. Grant (also with
Oregon State University)

U.S. Geological Survey

Charles R. Bacon
Andrew T. Calvert
Christine F. Chan
Robert L. Christiansen
Michael A. Clynne
Michael A. Cosca
Julie M. Donnelly-Nolan
Benjamin J. Drenth

William C. Evans
Judy Fierstein
Cynthia A. Gardner
V.J.S. Grauch
Christopher J. Harpel
Wes Hildreth
Richard P. Hoblitt
Robert A. Jensen
Peter W. Lipman
Jacob B. Lowenstern
Jon J. Major
Seth C. Moran
Lisa A. Morgan
Leah E. Morgan
L.J. Patrick Muffler
Jim O'Connor
John S. Pallister
Thomas C. Pierson
Joel E. Robinson
Juliet Ryan-Davis
Kevin M. Scott
William E. Scott
Wayne (Pat) Shanks
David R. Sherrod
Thomas W. Sisson
Mark Evan Stelten
Weston Thelen
Ren A. Thompson
Kenzie J. Turner
James W. Vallance
Alexa R. Van Eaton
Jorge A. Vazquez
Richard B. Waitt
Heather M. Wright

U.S. Nuclear Regulatory Commission

Stephen Self (also with University of
California, Berkeley)

Washington State University

Joseph R. Boro
Owen K. Neill
Stephen P. Reidel
John A. Wolff

Acknowledgments

Juliet Ryan-Davis and Kate Sullivan created the overview map, and Vivian Nguyen created the cover design for this collection of field-trip guide books. The field trip committee is grateful for their contributions.

Contents

Preface.....	iii
Contributing Authors.....	vi
Abstract.....	1
Introduction and Trip Overview.....	1
A Brief Overview of the Geologic and Physiographic Setting of the Cascade Range.....	2
Day 1: Portland to H.J. Andrews Experimental Forest (Near the Town of Blue River).....	6
In Transit—The Interstate 5 Corridor and the Willamette Valley.....	7
Stop 1: Santiam Rest Stop—A Willamette Valley Overview.....	7
Directions to Stop 1.....	7
Discussion of Stop 1.....	7
Stop 2: Leaburg Dam—Introduction to the “West Side Story”.....	9
Directions to Stop 2.....	9
Discussion of Stop 2.....	9
Stop 3: McKenzie Ranger Station.....	10
Directions to Stop 3.....	10
Discussion of Stop 3.....	10
Stop 4: Limberlost Campground—A High Cascades Stream.....	11
Directions to Stop 4.....	11
Discussion of Stop 4.....	11
Stop 5: “Lost Spring”—A Groundwater System.....	11
Directions to Stop 5.....	11
Discussion of Stop 5.....	11
Stop 6: Proxy Falls—Traversing the Collier Cone Lava Flow.....	12
Directions to Stop 6 and Description of Hike.....	12
Discussion of Stop 6.....	14
Stop 7 (Optional): White Branch—Incision into the Collier Cone Lava Flow.....	14
Directions to Stop 7 and Description of Hike.....	14
Discussion of Stop 7.....	15
End of Day 1: The H.J. Andrews Experimental Forest.....	16
Directions to H.J. Andrews Experimental Forest.....	16
Discussion of H.J. Andrews Experimental Forest.....	16
Day 2: H.J. Andrews Experimental Forest to Bend, by Way of the Sand Mountain Volcanic Field.....	16
Stop 8: Lookout Creek—A Typical Western Cascades Stream.....	18
Directions to Stop 8.....	18
Discussion of Stop 8.....	18
In Transit—The Western Cascades—High Cascades Boundary.....	19
Stop 9: Olallie Creek—Geomorphology of Western and High Cascades Streams.....	20
Directions to Stop 9.....	20
Discussion of Stop 9.....	20
Stop 10: Fish Lake—View of Sand Mountain.....	21
Directions to Stop 10.....	21
Discussion of Stop 10.....	21
Stop 11: Coldwater Cove Recreation Site—Lava, Lake, and Forest.....	21

Directions to Stop 11	21
Discussion of Stop 11	21
Stop 12: Sahalie Falls to Koosah Falls—Water Flow Over and Through Young Lava	27
Directions to Stop 12 and Description of Hike	27
Discussion of Stop 12	27
Stop 13 (Optional): Carmen Reservoir—Where the McKenzie River Goes Underground	28
Directions to Stop 13 and Description of Hike	28
Discussion of Stop 13	28
Stop 14 (Optional): “Tamolitch Pool”—Where the McKenzie River Reappears	29
Directions to Stop 14 and Description of Hike	29
Discussion of Stop 14	29
Stop 15: Clear Lake—Source of the McKenzie River	30
Directions to Stop 15	30
Discussion of Stop 15	30
Stop 16: Little Nash Crater	33
Directions to Stop 16	33
Discussion of Stop 16	33
Stop 17: Lost Lake—Tephra, Hydrology, and a Tale of Resource Management	36
Directions to Stop 17	36
Discussion of Stop 17	36
Stop 18: Mount Washington Overlook and Blue Lake Crater	42
Directions to Stop 18	42
Discussion of Stop 18	42
Stop 19 (Optional): Blue Lake Crater—A Central Cascades Maar	42
Directions to Stop 19 and Description of Hike	42
Discussion of Stop 19	42
Stop 20 (Optional): Headwaters of the Metolius River	44
Directions to Stop 20 and Description of Hike	44
Discussion of Stop 20	44
End of Day 2: Bend	46
Directions to Bend	46
Discussion of Bend	46
Day 3: Total Solar Eclipse and Various Stops in the Bend Area	46
The Total Solar Eclipse—A Celestial Interlude	46
Stop 21: Three Sisters Viewpoint and the Bend Highland	47
Directions to Stop 21	47
Discussion of Stop 21	47
Stop 22: Bull Flat and Tumalo Dam	49
Directions to Stop 22	49
Discussion of Stop 22	49
Stop 23: The Bend Pumice and the Tumalo Tuff—An Explosive Quaternary Eruption	54
Directions to Stop 23	54
Discussion of Stop 23	54
End of Day 3: Bend	54
Directions to Bend	54

Day 4: The McKenzie Pass Area	54
Stop 24: Dee Wright Observatory—McKenzie Pass and the High Cascades	56
Directions to Stop 24.....	56
Discussion of Stop 24	56
Stops 25, 26, and 27 (All Optional): Matthieu Lakes (Stop 25); Yapoah Crater and a Reflection on Holocene Mafic Volcanism Near North Sister (Stop 26); and Collier Glacier View (Stop 27).....	57
Directions to the Trailheads for Stops 25, 26, and 27 and Description of Hikes	57
Discussion of Stop 25	57
Discussion of Stop 26	57
Discussion of Stop 27	60
Stop 28 (Optional): Little Belknap Crater	63
Directions to the Trailhead for Stop 28 and Description of Hike	63
Discussion of Stop 28	63
End of Day 4: Bend.....	63
Directions to Bend.....	63
Day 5. The Bend Area	64
Stop 29. Top of Lava Butte	65
Directions to Stop 29.....	65
Discussion of Stop 29	65
Stop 30. Dillon Falls—Incursion of the Lava Butte Flow into the Deschutes River	68
Directions to Stop 30.....	68
Discussion of Stop 30	69
Stop 31. Mount Bachelor	70
Directions to Stop 31.....	70
Discussion of Stop 31	70
Stop 32. Sparks Lake.....	72
Directions to Stop 32.....	72
Discussion of Stop 32	73
Stop 33. Lava Lakes Fen	73
Directions to Stop 33.....	73
Discussion of Stop 33	73
Stop 34. Pilot Butte.....	74
Directions to Stop 34.....	74
Discussion of Stop 34	74
End of Day 5: Bend.....	74
Day 6. Bend to Portland.....	76
Stop 35. Surface-Water Diversions in Bend.....	76
Directions to Stop 35.....	76
Discussion of Stop 35	76
Stop 36. Bridge at Peter Skene Ogden State Park—Canyon-Filling Lava Flows.....	78
Directions to Stop 36.....	78
Discussion of Stop 36	78
Stop 37. Lake Billy Chinook Overlook.....	79
Directions to Stop 37.....	79

Discussion of Stop 37	79
Stop 38. Timberline Lodge at Mount Hood	81
Directions to Stop 38.....	81
In Transit—The Geology En Route from the Deschutes River near Warm Springs to Mount Hood	82
Discussion of Stop 38	82
End of Day 6: Return to Portland	83
Directions to Portland.....	83
Acknowledgments.....	83
References Cited.....	84

Figures

1. Index map of part of northwestern Oregon, showing locations of field-trip stops.....	1
2. Tectonic setting of Cascade volcanic arc	3
3. Distribution of faults and Quaternary-age volcanic vents in central Oregon Cascade Range.....	5
4. Shaded-relief map showing locations of field-trip stops on Day 1.....	6
5. Map of Willamette River Basin, showing major westward-flowing tributaries of Willamette River	7
6. Hydrographs of daily streamflow, normalized by drainage area, for McKenzie River at Belknap Hot Spring and for Little North Santiam River from part of 1960, all of 1961, and part of 1962	8
7. Mean August streamflow and percentage of High Cascades contributing area for selected tributary basins of Willamette River	8
8. Graphs of discharge versus drainage area for McKenzie River and east-west-trending subbasins of Willamette River.....	9
9. Schematic representation of discharge into McKenzie River from various sources during typical August and March flow regimes	10
10. “Lost Spring”	11
11. Shaded-relief maps showing tree-canopy heights and other selected features in White Branch valley area	12
12. Compositional plots for Collier Cone lava flow units.....	14
13. Proxy Falls, “Upper Proxy Falls” and pool into which it disappears, and lower part of “Upper Proxy Falls”.....	15
14. Shaded-relief map showing locations of field-trip stops on Day 2.....	17
15. Areal changes in wood accumulation and gravel bars in lower section of Lookout Creek, for five dates between 1977 and 2002	19
16. Conceptual cross section showing groundwater-flow paths from Cascade crest to Western Cascades.....	20
17. Shaded-relief map of upper McKenzie River catchment, showing Holocene lava flows and associated cinder cones of Sand Mountain volcanic field and other Holocene volcanic units.....	22
18. Stratigraphic relations within and among units in Nash, Sand, and Lost Lake groups of Sand Mountain volcanic field.....	23

19.	Shaded-relief map of McKenzie River from Clear Lake to Carmen Reservoir, showing detailed view of Holocene lava flows	24
20.	Shaded-relief map and photographs of Clear Lake area, showing tree canopy heights on lava flows.....	26
21.	Sahalie Falls and Koosah Falls.....	27
22.	Shaded-relief map showing infrastructure of Carmen–Smith Hydroelectric Project on upper McKenzie River	29
23.	“Tamolitch Pool”	30
24.	Shaded-relief map of Clear Lake area, showing bathymetry of Clear Lake, locations of drowned Douglas-fir trees in lake, and approximate locations of two dated Douglas-fir samples	31
25.	Drowned Douglas-fir tree in Clear Lake	32
26.	Modeled estimates of annual hydrograph and sensitivity to climate warming for McKenzie River at Clear Lake and Lookout Creek.....	33
27.	Compositional variations in units in Sand Mountain volcanic field compared with those in selected mafic volcanoes in central Oregon High Cascades.....	35
28.	Large sinkhole at Lost Lake.....	36
29.	Shaded-relief map and isopachs showing thickness of tephra deposits from Sand Mountain volcanic field.....	37
30.	Plot showing thickness versus dispersal area for Cascade-arc tephra deposits compared to those of other selected cinder-cone eruptions	38
31.	Isopach maps comparing thicknesses of tephra deposits from Sand Mountain and Volcán Parícutin, Mexico	39
32.	Plot showing sorting versus median grain size for tephra deposits from eruptions of Sand Mountain, Collier Cone, and other Cascade-arc cinder cones, as well as of Taal, Philippines	40
33.	Scanning electron microscope images of tephra clasts from Eyjafjallajökull, Iceland; Collier Cone; and Sand Mountain.....	41
34.	Pit excavated in deposit from eruption of Blue Lake crater.....	43
35.	Shaded-relief map and isopachs showing thickness of tephra deposits from Blue Lake crater.....	43
36.	Generalized geology of Black Butte–Green Ridge area	44
37.	Mean monthly discharge of Metolius River near Grandview, about 28 km west of Madras, from 1922 to 2015.....	45
38.	Shaded-relief map showing locations of field-trip stops on Day 3.....	46
39.	Shaded-relief map showing compass directions and distances to features that are visible from Three Sisters viewpoint	48
40.	Shaded-relief maps showing distribution of three Brunhes-age ash-flow tuffs erupted from Bend highland.....	50
41.	Generalized geology of Bull Flat–Tumalo Dam area.....	52
42.	Map showing generalized lines of equal hydraulic head, groundwater-flow directions, and well locations in upper Deschutes Basin	53
43.	Shaded-relief map showing locations of field-trip stops on Day 4, as well as lava flows and vents in McKenzie Pass area.....	55
44.	Shaded-relief map showing lava flows and fissures of “Matthieu Lakes vent alignment”	58
45.	Shaded-relief map and isopachs showing thickness of tephra deposits from Four in One Cone and Collier Cone	59

46.	Shaded-relief map showing locations of regional lakes that have preserved tephra deposits from central Cascade-arc cinder cones.....	60
47.	Photographs of Collier Glacier, taken from same position at Collier Glacier View, 100 years apart.....	61
48.	Oblique aerial photograph toward remnant lake, breached moraine, and downstream deposits left after 1942 debris flow from lake at Collier Glacier.....	62
49.	Graph showing indirect estimates of peak discharge for 1942 debris flow into White Branch creek.....	63
50.	Shaded-relief map showing locations of field-trip stops on Day 5.....	64
51.	Compass-wheel diagram showing distances and approximate azimuthal directions to peaks and other features that are visible from top of Lava Butte.....	66
52.	Map showing vents, fissures, and lava flows of “northwest rift zone” of Newberry Volcano.....	67
53.	Diagrammatic cross section of elevation profile of Deschutes River, showing effect of geology and topography on groundwater flow and discharge.....	68
54.	Map showing maximum and stabilized extents of “Lake Benham”.....	69
55.	Graphs showing Zr versus FeO*/MgO for chain of lava flows in Mount Bachelor region.....	71
56.	Graph showing Zr versus SiO ₂ contents of lava flows from Three Sisters volcanoes.....	71
57.	InSAR interferogram from 1996 to 2000, showing area of uplift west of South Sister.....	72
58.	Compass-wheel diagram showing distances and approximate azimuthal directions to peaks and other features that are visible from top of Pilot Butte.....	75
59.	Index map of part of northwestern Oregon, showing locations of field-trip stops on Day 6...	76
60.	Map showing diversions of Deschutes River for North Unit and Pilot Butte Canals north of Bend.....	76
61.	Hydrograph showing estimated canal leakage north of Bend and August mean flow of Crooked River.....	77
62.	Hydrographs showing relation between groundwater fluctuations and canal operation.....	78
63.	Graph of streamflow of lower Crooked River, as measured between river miles 28 and 7 during July 1994.....	79
64.	Correlation of ages of selected samples in Deschutes Basin with paleomagnetic timescale.....	80
65.	Photographs into canyons of Crooked and Deschutes Rivers taken in August 1925.....	80

Tables

1.	Petrographic descriptions of select lava flow units in the upper McKenzie River watershed.....	25
2.	Estimates of minimum and maximum volume for tephra deposits in the central Oregon Cascades and from other cinder-cone eruptions where trace deposits are known.....	38
3.	Central Oregon volcanic features visible from Dee Wright Observatory, at McKenzie Pass.....	56

2 Field-Trip Guide to Mafic Volcanism of the Cascade Range in Central Oregon

The Cascade Range is the result of subduction of the Juan de Fuca plate underneath the North American plate. This north-south-trending volcanic mountain range is immediately downwind of the Pacific Ocean, a huge source of moisture. As moisture is blown eastward from the Pacific on prevailing winds, it encounters the Cascade Range in Oregon, and the resulting orographic lift and corresponding rain shadow is one of the strongest precipitation gradients in the conterminous United States. We will see how the products of the volcanoes in the central Oregon Cascades have had a profound influence on groundwater flow and, thus, on the distribution of Pacific moisture. We will also see the influence that mafic volcanism has had on landscape evolution, vegetation development, and general hydrology.

On Day 1, we will travel from Portland southward through the Willamette Valley, then, just north of Eugene, we will turn eastward and travel up the valley of the McKenzie River, a major tributary of the Willamette River. We will discover that the river has been profoundly affected by mafic volcanism of the central Oregon Cascades. We will begin to understand the interplay among Quaternary and Holocene mafic volcanism, groundwater, and river hydrology, and we will see the first Holocene lava flow of the trip, the Collier Cone lava flow.

On Day 2, we will focus on the Sand Mountain volcanic field of the central Oregon Cascades—its volcanic history, its geochemistry, its effect on the hydrology of the McKenzie River, and its forest development. This 76-km² field, which was erupted about 3 ka, tapped at least two magma sources, its relatively small spatial and temporal extent notwithstanding.

The highlight of Day 3 will be a total solar eclipse, which we will experience at near maximum totality in the Oregon high desert. Afterwards we will resume our exploration of the central Oregon Cascades, using Bend as our base.

The aim of Day 4 will be to explore the Holocene mafic volcanic rocks and deposits in the McKenzie Pass area, between the Three Sisters volcanic cluster to the south and Belknap Crater to the north. We will be offering a choice of hikes that range from moderately difficult to strenuous (but with stunning views). Alternatively, this day could also be a rest day in the Bend area.

On Day 5, we will focus on the Quaternary and Holocene, mafic and other types of volcanic rocks and deposits south of and within the Bend area. As we explore the variety of volcanism in the region, we will consider the volcanic hazards and the hydrological implications of future volcanic activity on the city of Bend.

We will return to Portland on Day 6, aiming to be back in the early afternoon. We will make several stops along the way, including a visit to Timberline Lodge on Mount Hood.

This field trip is an updated and expanded version of a 2009 field trip developed by Kathy Cashman, Natalia Deligne, Marshall Gannett, Gordon Grant, and Anne Jefferson for the 2009 Geological Society of America Annual Conference. The Cashman and others (2009) guide, in turn, used several stops from a 2002 field trip by Dave Sherrod, Marshall Gannett, and Ken Lite (Sherrod and others, 2002). We've also drawn on field guides by Rick Conrey, Ed Taylor, Julie Donnelly-Nolan, and Dave Sherrod (Conrey and others, 2002a); Bob Jensen, Julie Donnelly-Nolan,

and Daniele McKay (Jensen and others, 2009); and Willie Scott and Cynthia Gardner (Scott and Gardner, 1990). In addition, we've drawn on papers by Brittain Hill and Ed Taylor (Hill and Taylor, 1990); Judy Fierstein, Wes Hildreth, and Andy Calvert (Fierstein and others, 2011); and Allison Aldous, Marshall Gannett, Mackenzie Keith, and Jim O'Connor (Aldous and others, 2015). Rather than omitting or attempting to rewrite the descriptions of these stops, we've included parts of them as originally written, with some minor modifications as needed. We've clearly indicated the figures and descriptions of stops that are derived from these earlier field guides and papers. We thank the authors for putting together such valuable resources.

A Brief Overview of the Geologic and Physiographic Setting of the Cascade Range

[Modified from Cashman and others (2009)]

The Cascade Range extends from northern California into southern Canada. In central Oregon, the Cascade Range, which is 50 to 120 km wide, is bounded on west by the Willamette Valley and on the east by the Deschutes Basin. The Cascade volcanic arc has been active for about 40 million years, owing to the convergence of the North American and Juan de Fuca plates, although volcanism has not been continuous in either space or time throughout this period (Sherrod and Smith, 2000). The Oregon Cascades are commonly divided into the Western Cascades and the High Cascades physiographic subprovinces, which differ markedly in their degree of dissection, owing mainly to the near absence of Pliocene and Quaternary volcanoes in the Western Cascades. This apparent eastward shift in volcanism is the result of clockwise rotation of the North American plate; the same rotation has resulted in the apparent westward migration in the Northern Cascades (fig. 2; see also, Wells and others, 1998; McCaffrey and others, 2007; Wells and McCaffrey, 2013). From the Three Sisters volcanic cluster north to Mount Hood, the young (Pliocene to Quaternary) High Cascades occupy a structural graben formed by a northward-propagating rift (Conrey and others, 2002a, 2004), which has affected both the composition of the erupted magma and the patterns of groundwater flow.

The volcanic rocks and deposits of the Western Cascades consist of a thick, mixed assemblage of mafic lava flows (mostly of andesitic composition) and ash-flow and ash-fall tuffs, with minor silicic intrusive bodies and stocks that range in age from middle Eocene to early Pliocene (40–5 Ma). Rocks along the western margin of the Western Cascades tend to be older, and they decrease in age toward the boundary with the High Cascades; in some places in the Western Cascades, intracanyon lava flows from the High Cascades fill the upper valleys. Rocks have been locally altered by hydrothermal processes, particularly in contact aureoles that surround granitic stocks. The landscape, which has been covered repeatedly by montane glaciers and dissected by rivers, is prone to frequent mass wasting by landslides, debris flows, and

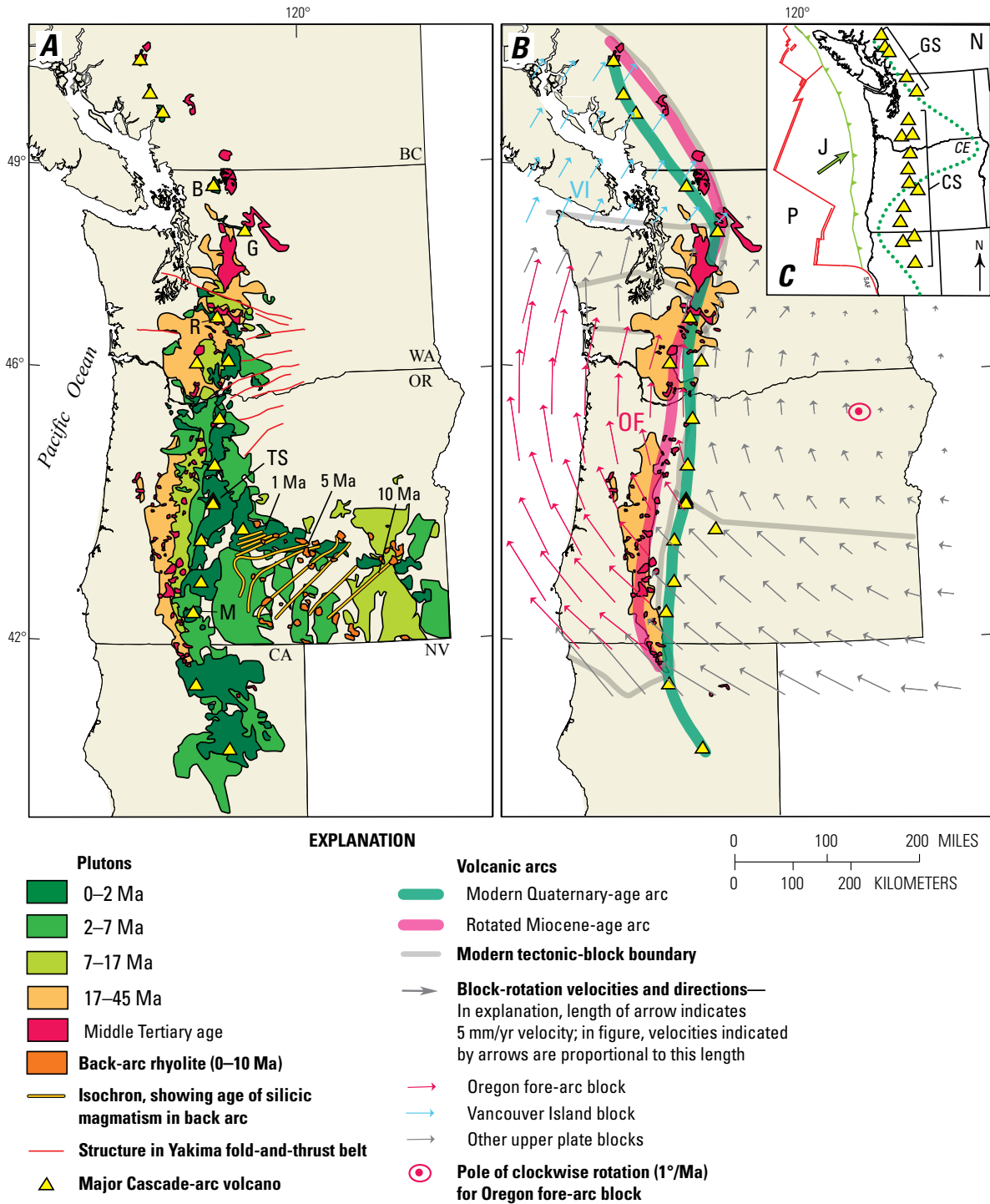


Figure 2. Tectonic setting of Cascade volcanic arc. Modified from Wells and McCaffrey (2013). Triangles show major Cascade-arc volcanoes. A, Ages of Cascade-arc and back-arc rocks (Smith, 1993; Sherrod and Smith, 2000; Massey and others, 2005; Hildreth, 2007). Major Cascade arc volcanoes: B, Mount Baker; G, Glacier Peak; M, Mount McLoughlin; R, Mount Rainier; TS, Three Sisters volcanic cluster. B, Block-rotation velocities and directions from Global Positioning System (GPS) model of McCaffrey and others (2007); velocities are regularized velocities of minimum-misfit-block model derived from GPS data. GPS model simultaneously solves for locking on block-boundary faults (including megathrust fault) and block rotation; one needs to remove effect of locking to get long-term plate-tectonic motions shown in figure. Velocities match sense of offset of ancestral, mostly Miocene Cascade-arc plutons from active arc axis. Tectonic blocks: OF, Oregon fore-arc block; VI, Vancouver Island block (note that pole of rotation of Vancouver Island block is outside of figure). C, Plate-tectonic setting of Cascade arc. Tectonic plates: J, Juan de Fuca; N, North American; P, Pacific. Single red lines show faults (SAF, San Andreas Fault). Double red lines show spreading centers. Green barbed line shows Cascadia subduction zone (barbs on upper plate); green arrow shows direction of convergence of Juan de Fuca plate). Arc segments (from Hildreth, 2007): CS, Cascade; GS, Garibaldi. Dotted green line shows position of Mesozoic orocline and Columbia embayment (CE).

4 Field-Trip Guide to Mafic Volcanism of the Cascade Range in Central Oregon

earthflows. Consequently, the topography is extremely rugged: the elevations range from 200 to 1,800 m, the ridges are sharp and dissected, and the slopes are steep, dipping 30 degrees or more. Stream channels range from high-gradient bedrock channels to alluvial gravel to boulder-bed rivers.

In the Western Cascades, outcrops are commonly obscured by the dense native coniferous forests of Douglas-fir (*Pseudotsuga menziesii*), western hemlock (*Tsuga heterophylla*), and western red cedar (*Thuja plicata*). Trees in this region, which can grow to reach great heights (>80 m) and ages (>500 years old), are subject to episodic wildfires and, more recently, intensive logging on both public and private lands. At one time in the 1980s, timber harvest from the Willamette National Forest, which includes much of the Western Cascades, produced more than 20 percent of the nation's softwood timber. The legacy of this harvest remains as a distinct pattern of regenerating clearcuts of various sizes and shapes. Precipitation of as much as 2,500 mm/yr typically falls between November and April as both rain and snow (at elevations lower than 400 m and higher than 1,200 m, respectively), with the intervening elevations, which make up much of the landscape, constituting a "transitional snow zone."

Extending along the eastern margin of the Western Cascades is the modern volcanic arc of the High Cascades, a north-south-trending belt 30 to 50 km wide of late Miocene to Holocene volcanic rocks. In central Oregon, the High Cascades form a broad ridge composed of a 2- to 3-km-thick sequence of lava flows that fill a graben formed in the older rocks (Smith and Taylor, 1983; Smith and others, 1987; Taylor, 1990b; Sherrod and Smith, 1990; Sherrod and others, 2004). High Quaternary stratovolcanoes are constructed on top of the flows; the stratovolcanoes have rhyolitic to basaltic compositions and are composed of interlayered thin lava flows and pyroclastic deposits overlying cinder cones (Taylor, 1981). The location of the High Cascades at the western margin of the Basin and Range Province places it in a zone of crustal extension, which influences both its structural features and its volcanic history. Most striking is the density of Quaternary volcanoes in the Oregon Cascade Range, which contains 1,054 vents within 9,500 km² (fig. 3; see also, Hildreth, 2007). At least 466 Quaternary volcanoes are in the Three Sisters reach, which we will traverse; many of these have a pronounced north-south alignment of vents, and most are mafic (basalt or basaltic andesite; Hildreth, 2007). Sherrod and Smith (1990) estimated an average mafic magma production rate in the central Oregon Cascades of about 3 to 6 km³ per linear kilometer of arc per million years during the Quaternary. Mafic activity has continued into postglacial times, with 290 km³ of magma erupted from the Cascade Range over the past 15 ka. Hildreth (2007) estimated that 21 percent of the erupted material forms mafic eruptive products from cones and shields and that most of these edifices are within the Oregon Cascade Range.

The crest of the Oregon Cascade Range has an average elevation of 1,500 to 2,000 m, with several of the highest volcanoes exceeding 3,000 m. The conical morphology of mafic shield volcanoes and stratovolcanoes is best preserved

on the younger edifices—Middle Sister, South Sister, and Mount Bachelor—as the older cones have been deeply eroded by Pleistocene glaciation. The High Cascades have also been extensively and repeatedly glaciated by thick montane ice sheets but are relatively undissected by streams (drainage density is about 1–2 km/km²; Grant, 1997), and many primary volcanic features are generally preserved. Most winter precipitation falls as snow in this zone, with occasional summer thunderstorms contributing to the water budget. Forests east of the crest are a mix of alpine and subalpine hemlocks and firs (*Tsuga* and *Abies* spp.) that transition abruptly into a more open forest of ponderosa pine (*Pinus ponderosa*) and lodgepole pine (*Pinus contorta*) in response to the abrupt decline in rainfall just east of the crest. Much of the land is in public ownership and is managed by the U.S. Forest Service and the Bureau of Land Management for timber harvesting, livestock grazing, and recreation. Of the High Cascades subprovince in central Oregon, 25 percent is in wilderness areas managed by the U.S. Forest Service. The Pleistocene glacial record is better preserved (and mapped) on the east side than on the west side of the crest, owing to the lower rainfall amounts (~300 mm/year), the more subdued topography, and the limited opportunity for fluvial erosion (Scott, 1977; Scott and Gardner, 1992; Sherrod and others, 2004).

To the east, the Oregon Cascade Range is bounded by the upper Deschutes Basin, a volcanic landscape dominated by a thick (>700 m) sequence of lava flows, pyroclastic rocks, and volcanoclastic deposits of Cascade Range origin, as well as fluvial gravels deposited between about 7 and 4 Ma in a broad depositional basin (Smith, 1986b). These deposits extend eastward into upland areas consisting of early Tertiary volcanic rocks of the John Day and Clarno Formations. Interspersed throughout are local eruptive centers in a wide variety of sizes, compositions, and eruptive styles. The most prominent eruptive center off the axis of the Cascade Range is Newberry Volcano, which forms the southeast boundary of the Deschutes Basin. Lava flows from Newberry Volcano blanket a large part of the central Deschutes Basin, and they partly fill canyons of the ancestral Deschutes and Crooked Rivers. The volcanic eruptions that formed the rocks of the Deschutes Formation culminated with the downfaulting of a depression along the axis of the Cascade Range in central Oregon (Allen, 1966; Smith and others, 1987). The Pleistocene deposits in this part of the Cascade Range are largely restricted to this axial graben.

The primary feature that controls regional groundwater flow on the east side of the Cascade Range is the pronounced permeability contrast between the early Tertiary rocks and the late Miocene and younger deposits (Lite and Gannett, 2002). Deposits of the Miocene and Pliocene Deschutes Formation are highly permeable and, along with the younger volcanic deposits, host a continuous regional groundwater system that extends from the Cascade Range to the depositional contact with the early Tertiary deposits in the eastern part of the basin. The High Cascades subprovince is the principal source of recharge to this regional aquifer system.

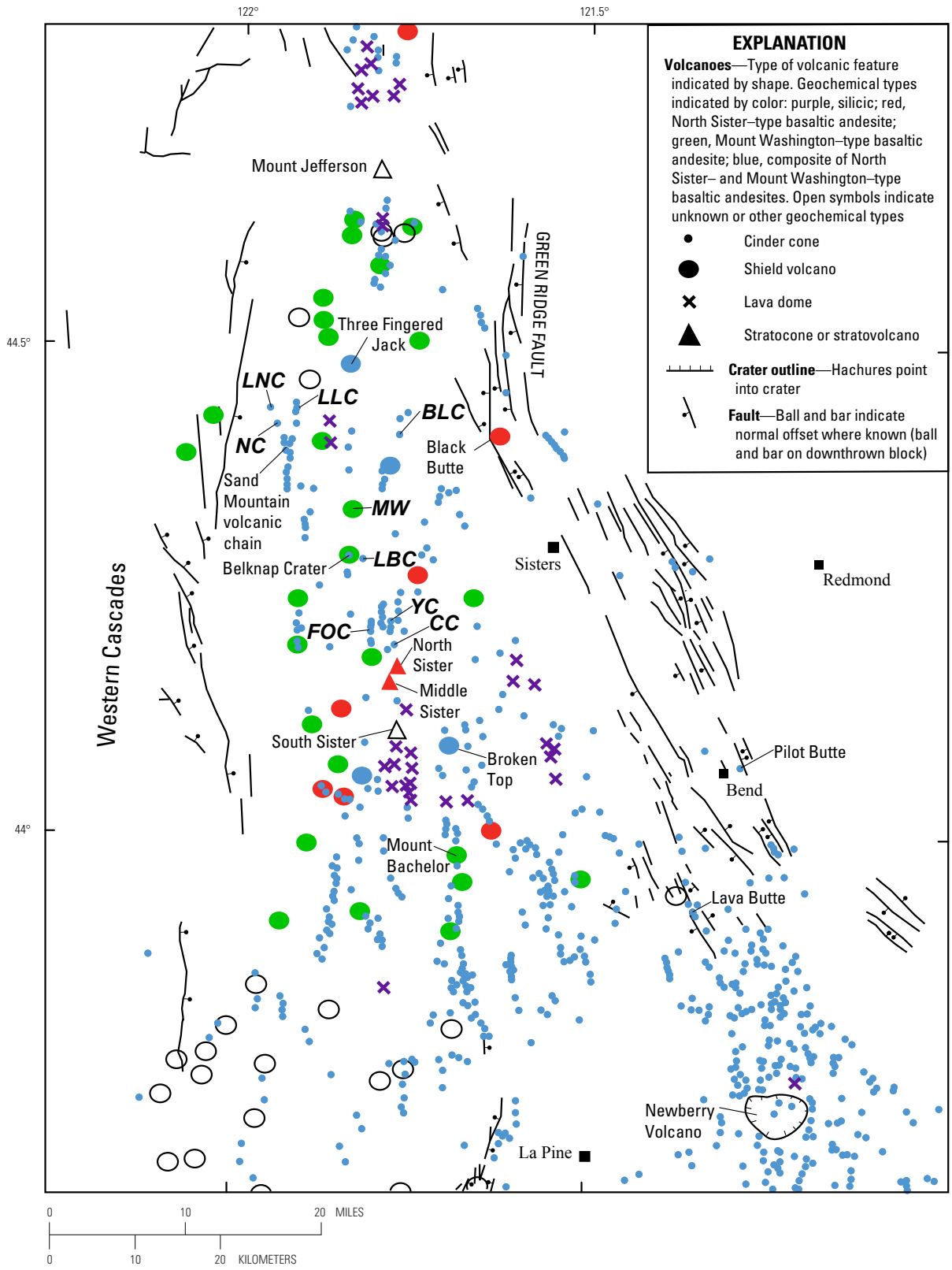


Figure 3. Distribution of faults and Quaternary-age volcanic vents in central Oregon Cascade Range (modified from Sherrod and others, 2004; Conrey and others, 2004; Schmidt and Grunder, 2009); monogenetic mafic vents tend to be found along lineaments that mimic exposed faults, both in length and in orientation (Hughes and Taylor, 1986). Also shown is distribution of two main types of basaltic andesite, North Sister and Mount Washington types (from Conrey and others, 2004). Abbreviations: BLC, Blue Lake crater; CC, Collier Cone; FOC, Four in One Cone; LBC, Little Belknap crater; LLC, Lost Lake chain; LNC, Little Nash Crater; MW, Mount Washington; NC, Nash Crater; YC, Yapoah Crater.

Day 1: Portland to H.J. Andrews Experimental Forest (Near the Town of Blue River)

[Note that State Highway 242, required to access Stops 4 through 7, is closed in winter and spring; check with the Oregon Department of Transportation (<http://www.tripcheck.com/Pages/RCmap.asp?curRegion=0&mainNav=RoadConditions>) or the Willamette National Forest (<http://www.fs.usda.gov/alerts/willamette/alerts-notice>) before you travel to see whether the highway is open or closed]

On Day 1 of the field trip, we will travel from Portland to the Oregon Cascades (see fig. 4). The goal of the day is to understand the hydrogeological controls (tectonic and volcanic) of the central Oregon Cascades. At the end of the day, we will take a short hike across a young Holocene lava flow to see a disappearing waterfall. The locations of, and relations between, these features reflect the tectonics, glaciations, and volcanism in the region.

We will travel south through the Willamette Valley, with a short break (Santiam rest area, Stop 1) to observe and discuss the geology of the Willamette Valley and the geologic controls on

the hydrologic regimes of the westward-flowing tributaries of the Willamette River.

Just north of Eugene, we will turn east and follow the McKenzie River valley into the Oregon Cascades. At Leaburg Dam (Stop 2), we will discuss the hydrogeology of the McKenzie River. Our next stop is the McKenzie Ranger Station (Stop 3), which has a large, three-dimensional map of the central Oregon Cascades. From there we will enter the glaciated White Branch valley, and we will have lunch at Limberlost Campground (Stop 4), along a High Cascades stream. At “Lost Spring” (Stop 5), we will discuss the relation between groundwater and Quaternary lava flows in the High Cascades.

We will continue up White Branch valley to the westernmost extent of the Collier Cone lava flow. On a short hike we will traverse the Collier Cone lava flow to Proxy Falls (Stop 6) to see a waterfall that disappears beneath the lava flow.

Another option would be a hike farther up White Branch valley along the Linton Lake trail to see the incision of White Branch creek into the Collier Cone lava flow (optional Stop 7).

At the end of the day, we will retrace our steps down White Branch valley to the McKenzie River valley to spend the night near Blue River (a tributary of the McKenzie River) at the H.J. Andrews Experimental Forest.

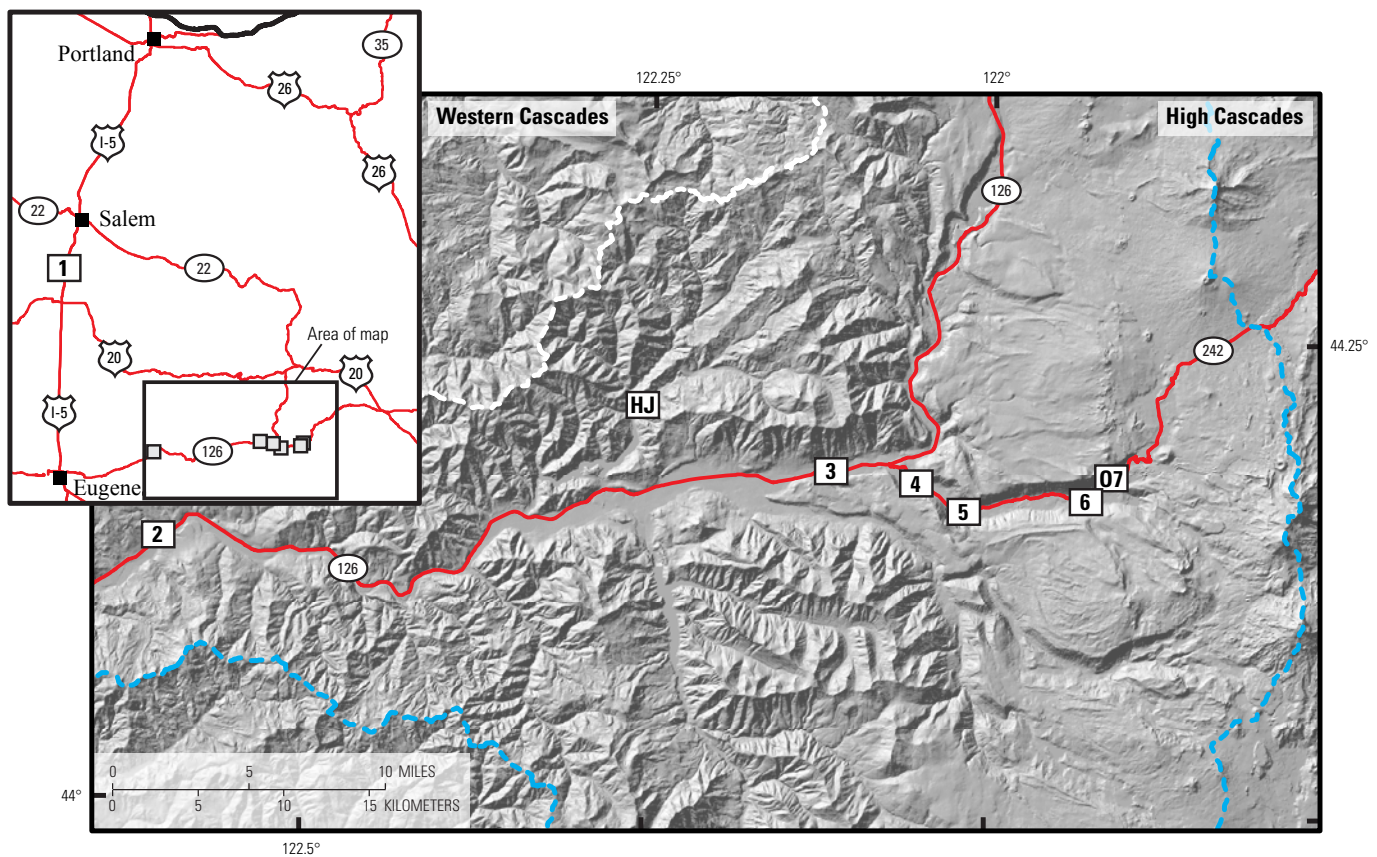


Figure 4. Shaded-relief map showing locations of field-trip stops on Day 1. Field-trip stops shown by white rectangles; stop numbers are inside rectangles (0, optional stop; HJ, H.J. Andrews Experimental Forest [end of Day 1]; note that location of Stop 1 is shown on regional inset map). Dashed blue line shows boundary of McKenzie River watershed (from Oregon Watershed Enhancement Board, 2014–2016). Shaded relief derived from 10-m digital elevation models (from Oregon Geospatial Enterprise Office, 2008). Roads from Oregon Department of Transportation (2015). Oregon state outline from Bureau of Land Management (2001).

In Transit—The Interstate 5 Corridor and the Willamette Valley

[Modified from Cashman and others (2009)]

Heading south from Portland, we will traverse the Willamette Valley, part of a broad structural low extending from the Puget Lowland to just south of Eugene that has existed for at least 15 million years (O'Connor and others, 2001b). The valley, a broad alluvial plain, 30 to 50 km wide, is flanked by the sedimentary rocks of the Coast Range to the west and the volcanic rocks of the Cascade Range to the east. The valley slopes gently north, with elevations ranging from 120 m at Eugene to 20 m at Portland. The hills that the road traverses south of Portland and near Salem represent incursions of lava flows from the east, some of which are also faulted upward; the Salem Hills in particular are underlain by Miocene Columbia River Basalt flows that were erupted in eastern Washington and followed the path of the paleo-Columbia River toward the ocean prior to the construction and uplift of the High Cascades.

The Quaternary history of the Willamette Valley, which has been the subject of geological investigations for over 100 years, reflects the dramatic interplay between erosion and deposition from the Willamette River and its tributaries, as well as backwater flooding and lacustrine deposition from catastrophic flooding of the Columbia River. The valley is floored by and filled with Quaternary gravels brought down by tributaries that drain the Cascade Range and, to a lesser extent, the Coast Range (O'Connor and others, 2001a). This thick (>100 m) alluvium is capped by a thinner (>10 m) but more extensive sequence of sand and silt of late Pleistocene age that was deposited owing to backwater effects during the immense Missoula floods in the Columbia River drainage system. Multiple episodes of outbreak flooding occurred as Glacial Lake Missoula repeatedly filled and then drained as its glacial dams failed catastrophically, resulting in rhythmically bedded, fine-grained deposits draped over older alluvium, into which the modern Willamette River is now incised. The flat valley floor is, thus, a constructional terrace approximately 15,000 years old. The Missoula flood deposits, which thin to the south, can be traced as far south as just north of Eugene. The total volume of these deposits is approximately 50 km³, and the volume of water that deposited this material is estimated at 250 km³, which is equivalent to 10 years of the annual flow of the Willamette River at Salem.

Stop 1: Santiam Rest Stop—A Willamette Valley Overview

Directions to Stop 1

Take Interstate 5 south to Salem. After passing through the Salem Hills, enter the wide southern part of the Willamette Valley. The Santiam rest area is near Mile Post (MP) 241. Stop here for a bathroom break and to hear an introduction to the Willamette Valley.

Discussion of Stop 1

[Modified from Cashman and others (2009)]

The Santiam River is one of the major westward-flowing tributaries of the Willamette River (fig. 5). Drainage area at the U.S. Geological Survey (USGS) gaging station (Santiam River at Jefferson) 5.7 km upstream is 4,580 km²; the confluence of the Santiam and Willamette Rivers is about 8 km downstream from our location.

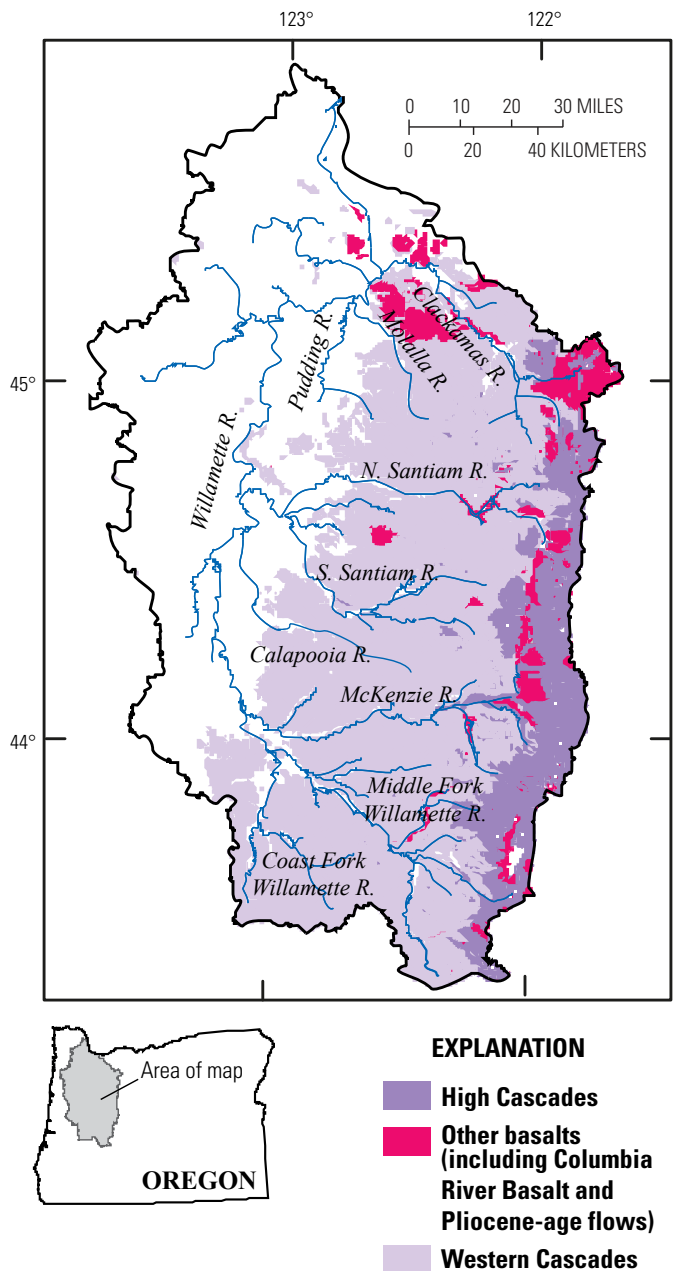


Figure 5. Map of Willamette River Basin, showing major westward-flowing tributaries of Willamette River. Also shown is approximate distribution of basalts from High Cascades and Western Cascades subprovinces, as well as other basalts in basin (including Columbia River Basalt and Pliocene-age flows). From Tague and Grant (2004); geology from Walker and MacLeod (1991).

The pattern of streamflow in the Santiam River and the other rivers that drain the western margin of the Cascade Range is one of the themes of this field trip, namely the geologic control of hydrologic regimes in volcanic landscapes. This characteristic of Cascade Range streams, which was generally described by Russell (1905), Meinzer (1927), and Stearns (1929, 1931), more recently has been the subject of extensive work (Ingebritsen and others, 1992, 1994; Grant, 1997; Gannett and others, 2001, 2003; Tague and Grant, 2004; Jefferson and others, 2006, 2007, 2008).

Understanding the role of geology in hydrologic regimes first requires an appreciation of how annual variation in precipitation controls runoff. The first rains of the hydrologic year typically begin in mid- to late October, following a prolonged summer drought of three to four months. Early fall storms, therefore, must satisfy a pronounced soil-moisture deficit before any significant runoff can occur. Once this deficit has been satisfied and soils are near saturated—a condition that normally occurs by early to mid-November—streamflow becomes more synchronized with precipitation, rising and falling in response to passage of frontal storms from the Pacific. At higher elevations (above about 1,200 m), however, precipitation typically falls as snow, building the winter snowpack, so that the upper elevations of westward-draining rivers do not normally contribute much to streamflow until the spring melt.

A pattern of repeated rising and falling streamflow during the winter is clearly visible in the hydrograph for the Little North Santiam River, one of the tributaries of the Santiam River that drains the Western Cascades landscape exclusively (fig. 6). Some of these rises may be augmented by melting snow during periods of rain; these “rain-on-snow” events are generally responsible for the largest floods in the Willamette Valley, such as the ones that occurred in December 1861, December 1964, and February 1996. As precipitation diminishes in the spring, a minor snowmelt rise occurs in late April or May, followed by a distinct recession into

very low flows, which typically persist until the first fall rains begin the cycle anew.

The steep, deeply dissected landscape and the permeable but shallow soils of the Western Cascades respond quickly to precipitation recharge but have little storage (Tague and Grant, 2004). For this reason, the overarching pattern of flashy winter responses and very low summer flows is the characteristic signature of rivers that drain Western Cascades landscapes.

Contrast this pattern with that of the upper McKenzie River, which is located about 50 km to the southeast and drains the High Cascades landscape (see hydrograph in fig. 6). The McKenzie River Basin receives precipitation amounts that are similar to those of the Little North Santiam River, although more winter moisture falls as snow in the McKenzie River Basin owing to its higher elevation. This snow-dominated regime delivers water to the permeable volcanic rocks and relatively modest relief of the High Cascades subprovince, resulting in subsurface recharge and groundwater flow that buffers the hydrograph response of streams. Major increases in streamflow are effectively limited to only the largest winter storms. A significant snowmelt peak occurs in the spring, and the summer flow recession is much less pronounced; the high base flows are sustained throughout the summer, supported by discharge from volcanic aquifers (Jefferson and others, 2006).

Larger rivers, such as the Santiam and Willamette Rivers, are hybrids of these two distinct flow regimes, and they demonstrate streamflow characteristics that are typical of both High Cascades and Western Cascades streams; the relative amounts of each type of streamflow are directly proportional to the areal percentages of their basins that drain either the High Cascades or Western Cascades subprovinces (Tague and Grant, 2004). These trends are best illustrated by low-flow regimes, including absolute flow volume (fig. 7) and trajectories of longitudinal change in discharge with distance downstream (fig. 8), both of which are directly correlated

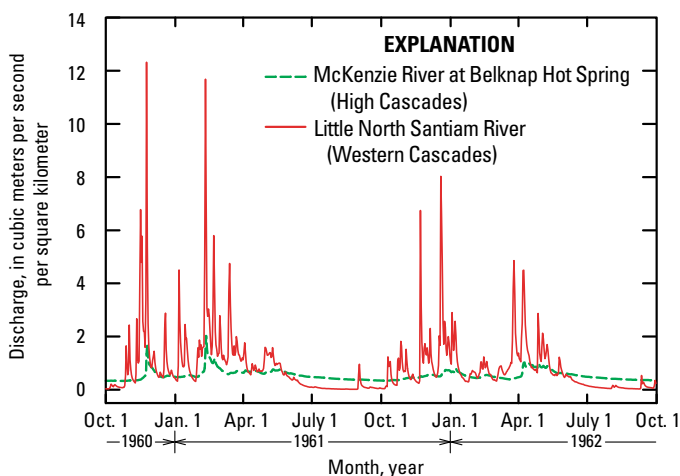


Figure 6. Hydrographs of daily streamflow, normalized by drainage area, for McKenzie River at Belknap Hot Spring (predominantly High Cascades subprovince) and for Little North Santiam River (Western Cascades subprovince) from part of 1960, all of 1961, and part of 1962. From Tague and Grant (2004); discharge data from U.S. Geological Survey streamflow-data archive.

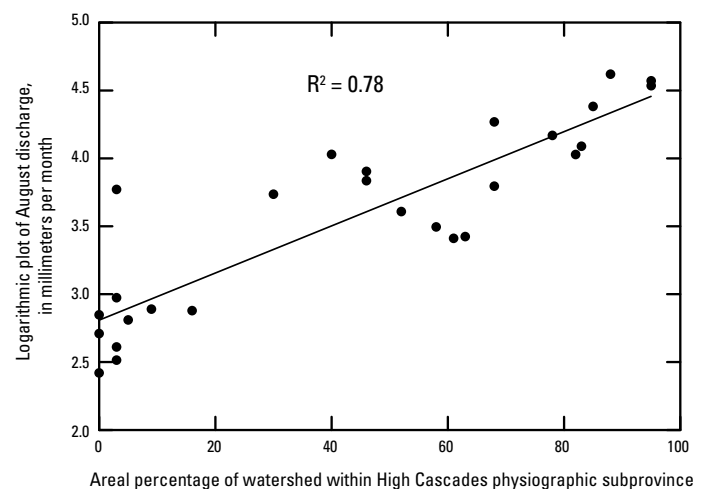


Figure 7. Mean August streamflow and percentage of High Cascades contributing area for selected tributary basins of Willamette River. Best-fit line and coefficient of determination (R^2) shown. From Cashman and others (2009); data from Tague and Grant (2004).

with the percentage of High Cascades rocks in the basin area. Summer low flows essentially come from young volcanic rocks in the High Cascades, and winter peak flows are due to runoff over older, less porous volcanic rocks in the Western Cascades.

The drainage of the Santiam River at Jefferson, just upstream of Stop 1, is 15 percent High Cascades by area, with the North Santiam River (drainage area, 1,990 km²) at 28 percent, and the slightly larger South Santiam River (drainage area, 2,590 km²) at 5 percent (fig. 8B). Therefore, the Santiam River is primarily a Western Cascades stream that has some High Cascades influence, in contrast it to the McKenzie River (discussed at the next several stops).

Stop 2: Leaburg Dam—Introduction to the “West Side Story”

Directions to Stop 2

Leave the Santiam rest area (cross the Santiam River) and head south on Interstate 5. Follow I-5 south for 48 miles (78 km) through the Willamette Valley. Just after MP 198, on the outskirts of Eugene, cross the McKenzie River, roughly 3 miles (5 km) upstream from its confluence with the Willamette River. Take Exit 194A east onto Interstate 105/State Highway 126 toward Springfield. Follow I-105 for 6.4 miles (10.3 km) to a stoplight at Main Street. Turn left (east) onto Highway 126 and follow for 17.7 miles (28.5 km) to Leaburg Dam. Cross the McKenzie River again at Hendricks Bridge Wayside, just after MP 11. Shortly after MP 19, cross a power canal where water diverted from the McKenzie River is transported almost 10 miles (16 km) downstream to a hydroelectric-power-generation facility. Leaburg Dam is immediately before MP 24; turn right across a bridge into the parking area.

Discussion of Stop 2

[Modified from Cashman and others (2009)]

The McKenzie River valley crosses the Western Cascades, extending to the High Cascades in its upper reaches (fig. 4). At Leaburg Dam, the McKenzie River has a drainage area of 2,637 km², of which 61 percent is classified as being of High Cascades origin (Tague and Grant, 2004). Contrast this with McKenzie River at the Belknap Springs Resort (40 km upstream) where the drainage area is only 374 km², of which 95 percent is of High Cascades origin. The McKenzie River at Leaburg Dam is a hybrid of flow-regime types but is dominated overall by the High Cascades, particularly in summer. Comparison of the sources of water during low and high flow shows the relative contribution of water from the High and Western Cascades and highlights the importance of groundwater discharge during the summer (fig. 9). As a result of the contrasting drainage mechanisms in the High and Western Cascades, the McKenzie River has a nonlinear drainage-discharge relation, particularly during the summer dry season when nearly two-thirds of the water in the McKenzie River is derived from High Cascades aquifers (fig. 8A). Over the next few days, we will investigate the ways in which the geology of the High Cascades, which is dominated by Quaternary mafic lava flows, controls the hydrology of this region.

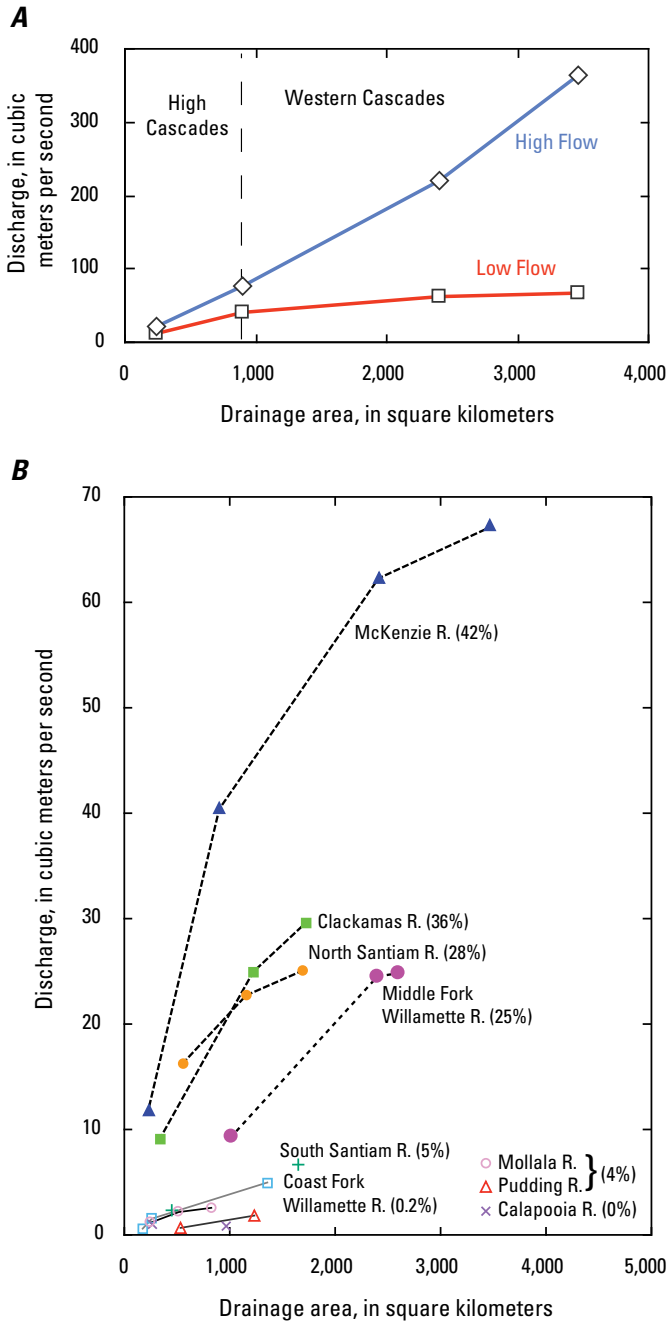


Figure 8. Graphs of discharge versus drainage area for (A) McKenzie River (for high and low flow) and (B) east-west-trending subbasins of Willamette River (for low flow), showing effect of contributions from High Cascades basins. Areal percentages of High Cascades basin contributions shown in parentheses. Measurements for high flow taken on March 1, 1950; for low flow, on September 1, 1950. From Cashman and others (2009), modified from Tague and Grant (2004).

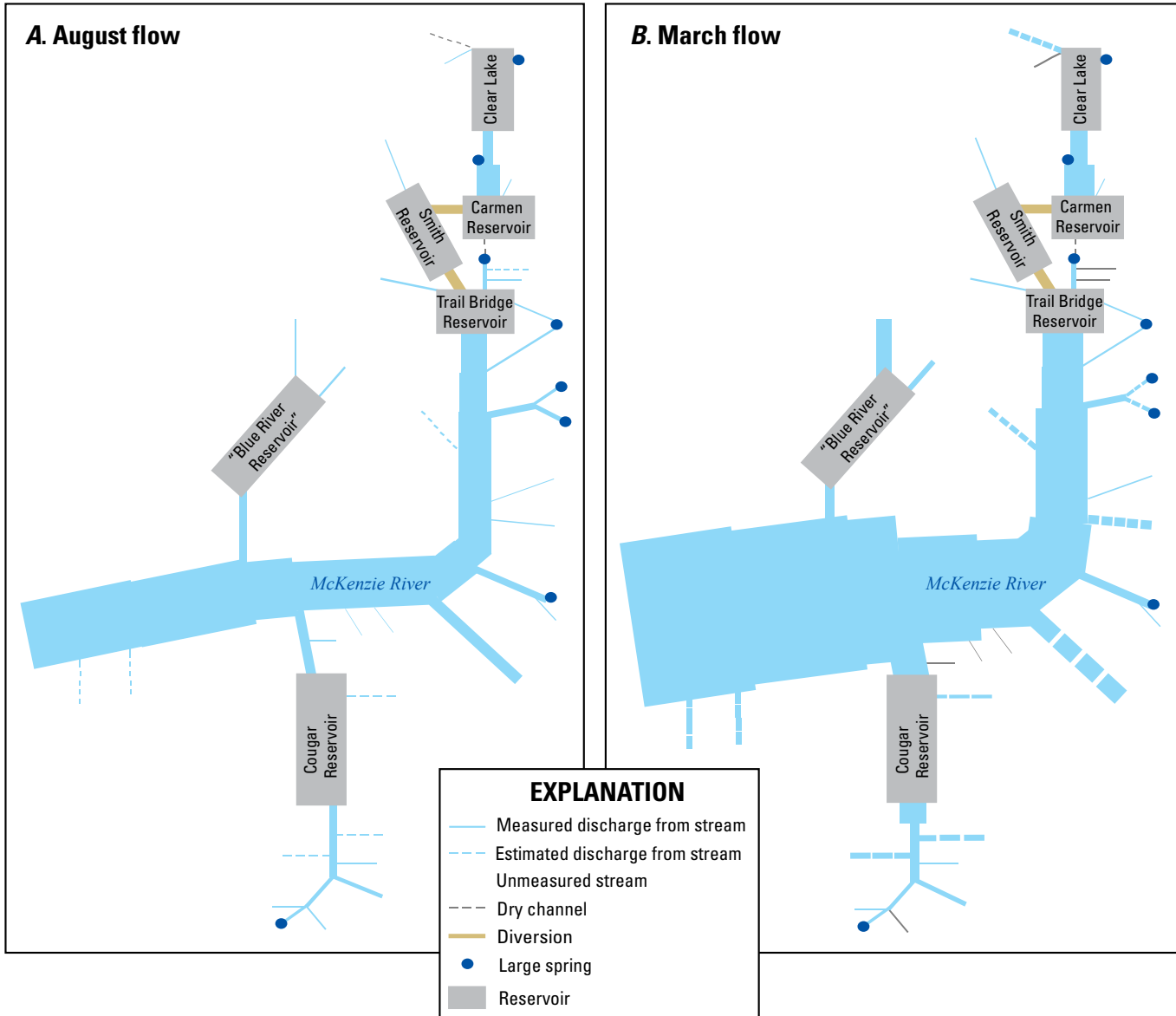


Figure 9. Schematic representation of discharge into McKenzie River from various sources during typical (A) August (low) and (B) March (high) flow regimes. Line thicknesses indicate relative contributions to discharge; lengths, distances, and angles not to scale. Modified from Jefferson and others (2007).

Stop 3: McKenzie Ranger Station

Directions to Stop 3

From Leaburg Dam, follow Highway 126 east for 28.6 miles (46.0 km) to the McKenzie Ranger Station on the right, after MP 52. Turn into the parking area; stop briefly here to hear an overview of the geography of the upper McKenzie River. Bathrooms are available inside the ranger station. Note that the last place to get gasoline is just after MP 47, at the Shell station on the right (south) side of the highway.

Discussion of Stop 3

The McKenzie Ranger Station is at the site of the 1934 Civilian Conservation Corps Belknap Camp. Workers from this camp, among other projects, built the Dee Wright Observatory, which we will see on Day 4 (Stop 24). The main hall has a three-dimensional map of the central Oregon Cascades. Note that this is a good place to purchase maps and, for those who are following this field-trip guide after the IAVCEI Conference–sponsored field trip (August 19–24, 2017) has ended, a Northwest Forest Pass, which is required at a number of field-trip stops.

Stop 4: Limberlost Campground—A High Cascades Stream

Directions to Stop 4

Continue east on Highway 126 for another 2.2 miles (3.5 km) to the intersection with State Highway 242; turn right (east) onto Highway 242 and climb toward McKenzie Pass through White Branch valley. Here, outcrops of till mark the most recent termination of the glacial tongue that carved out White Branch valley (fig. 4). Follow Highway 242 for 1 mile (1.6 km); turn left at the sign for Limberlost Campground (Forest Service Road 220); if you pass MP 58, you have gone too far. Display a Northwest Forest Pass in your vehicle when parked; we will have lunch here. Primitive bathrooms are available at the campground.

Discussion of Stop 4

[Modified from Cashman and others (2009)]

This scenic U.S. Forest Service campground is bordered by Lost Creek, a channel fed by large springs and also by glaciers located on the west flank of the Three Sisters volcanic cluster. The geomorphic form of the channel is typical of a spring-dominated stream: a rectangular channel cross section, an absence of bedforms and exposed gravel bars, a lack of a well-developed floodplain, mature vegetation down to the water level, and stable woody-debris accumulations (Manga and Kirchner, 2000). These

attributes reflect the extremely stable flow regimes and lack of floods that characterize High Cascades streams.

Stop 5: “Lost Spring”—A Groundwater System

Directions to Stop 5

Follow Highway 242 east for about 1 mile (1.6 km) past MP 58; a small meadow will be on the left at the end of a right bend. Turn left onto a dirt track; park under the big tree; if you pass MP 60, you have gone too far. Display a Northwest Forest Pass in your vehicle when parked.

Discussion of Stop 5

[Modified from Cashman and others (2009), including changes to second paragraph]

“Lost Spring” (once called “Lost Creek Spring”) (fig. 10) lies at the distal end of White Branch valley, which was carved by glacial ice that accumulated in and flowed from the vicinity of North Sister and Middle Sister volcanoes. As noted by Lund (1977), a stream that enters the upper part of a valley usually has the same name as the stream that flows out the lower end; however, this is not the case here, where the stream name changes from White Branch in the upper part of the valley to Lost Creek in the lower part. This name change reflects the complex hydrology of the area and the fact that the flow of water is largely through, rather than over, the young mafic lava flows that fill the valley. This



Figure 10. “Lost Spring.”
Photograph by Natalia Deligne, 2008.

valley, with its transient surface-water flow, provides an elegant example of the hydrology of the High Cascades, where young and highly permeable volcanic rocks form aquifers for subsurface transport of water from the high peaks to the valleys below.

Two young mafic lava flows fill White Branch valley. The late Pleistocene Sims Butte lava flow traveled nearly all the way down White Branch valley (fig. 11A; see also, Sherrod and others, 2004). The younger Collier Cone lava flow (1,600±100 ¹⁴C yr B.P.; Scott, 1990) originated on the northwest flank of North Sister and advanced westward into White Branch valley, partly covering the Sims Butte lava flow.

“Lost Spring” is actually a complex of small outlet springs that emerge from the terminus of the Sims Butte lava flow (see, for example, Stearns, 1929) and flow into a series of interconnected channels and ponds. At a mean discharge of 6 m³/s (212 ft³/s), the spring complex has the largest discharge of any of the springs that flow into the McKenzie River, and it also exhibits more seasonal discharge fluctuations than other McKenzie River springs. Similar to other springs that feed the upper McKenzie River, its estimated recharge area (114 km²) is substantially different from its topographic watershed area (197 km²), indicating that modern topography is not the main constraint on groundwater catchments (Jefferson and others, 2006). It also has (1) the highest temperature (6.3 °C) of any of the cold springs in the area, (2) the largest component of mantle-derived volatile constituents (as estimated from ³He/⁴He ratios), and (3) the longest estimated transit time (54.5 yr; Jefferson and others, 2006). These data suggest that the water emerging from “Lost Spring” is a mixture of deep-derived (warm) water, which rises along a fault zone 5 km upstream (Ingebritsen and others, 1994), and shallow-derived (cold) groundwater.

South of “Lost Spring,” a channel of White Branch creek may also contain water. White Branch creek originates at the toe of Collier Glacier (fig. 11B), on the northwest flank of Middle Sister and just south of Collier Cone. As Collier Glacier retreated in the 20th century, a lake formed behind the terminal moraine, which was breached catastrophically in July 1942 and again in 1954–56 (see optional Stop 27). Peak discharge from the 1942 breach is estimated at 140 m³/s (4,944 ft³/s), and the resulting flood formed a debris flow that traveled 7.5 km downstream to where the preexisting channel of White Branch creek disappears into the Collier Cone lava flow (O’Connor and others, 2001a). Under current conditions, White Branch creek is ephemeral from Collier Glacier downstream to its junction with

discharge from “Lost Spring.” Surface flow is discontinuous in the stream, and, in some places, no channel is identifiable (for example, 1 km upstream from “Lost Spring”). In places, the channel is well defined on the Collier Cone lava flow (for example, north of Linton Lake, as shown on fig. 11C), and we interpret the channel as having resulted from vigorous glacial-meltwater discharge during the advancing of glaciers of the Little Ice Age (about 1400–1900 C.E.).

About 750 m upvalley from “Lost Spring,” White Branch emerges from the Sims Butte lava flow in a seasonally fluctuating spring. Discharge in this spring ranges from 0 to 2 m³/s (0–70 ft³/s), peaking in March and late June and drying up from late summer to midwinter. When the White Branch spring is discharging water, the water has the same temperature and oxygen-isotopic composition as the water in “Lost Spring.” We infer that the two springs discharge from the same aquifer but that seasonal fluctuations in the water table result in a perennial flow to “Lost Spring” and an intermittent flow to White Branch spring (Jefferson and others, 2006). Just downstream and to the south of the springs, White Branch plunges over a small, 3-m-high waterfall into a short slot canyon, before joining Lost Creek and flowing into the McKenzie River below Belknap Hot Spring.

Stop 6: Proxy Falls—Traversing the Collier Cone Lava Flow

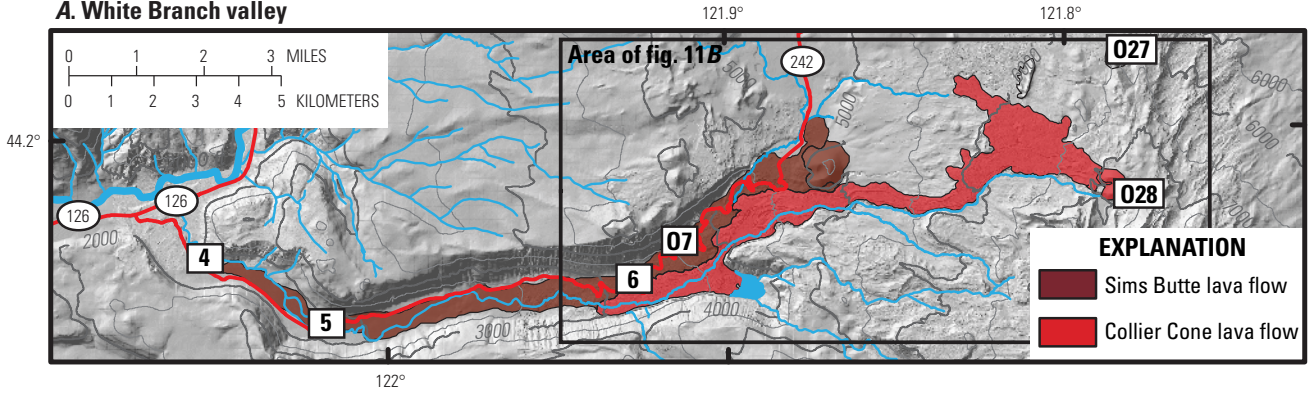
Directions to Stop 6 and Description of Hike

Follow Highway 242 east to the well-marked Proxy Falls trailhead, just past MP 64. Park in the parking area or on the side of the road. Display a Northwest Forest Pass in your vehicle when parked.

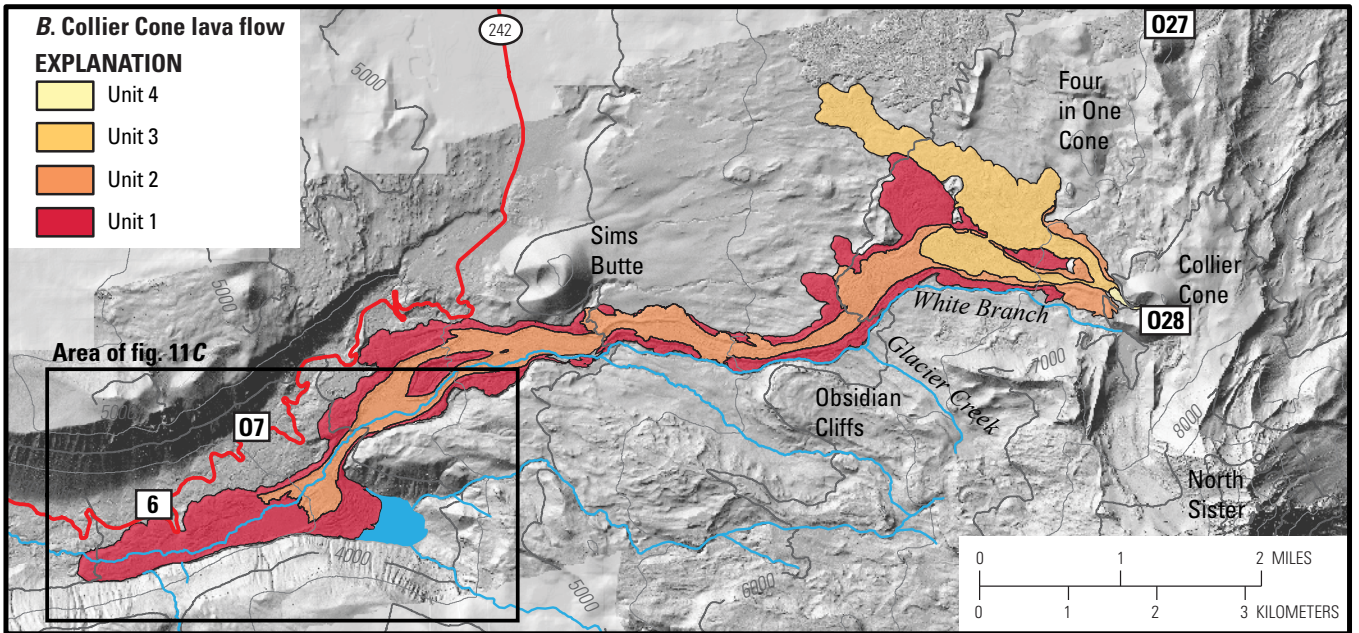
The Proxy Falls loop hike (distance, 1.5 miles [2.3 km]) starts from the Proxy Falls parking area. The loop can be hiked in either direction, but the U.S. Forest Service signage assumes a counterclockwise direction; in the counterclockwise direction, Proxy Falls (informally known as “Lower Proxy Falls”) is reached first. The hike is clearly marked and relatively flat and easy, but it is not wheelchair accessible. Dogs on a leash are permitted. No potable water is available at the trailhead. The hike is within the Three Sisters Wilderness; self-issue permits, which are available at the trailhead, are

Figure 11. Shaded-relief maps showing tree-canopy heights and other selected features in White Branch valley area. Field-trip stops shown by white rectangles; stop numbers are inside rectangles (0, optional stop). Shaded relief and tree-canopy heights derived from lidar imagery (from Oregon Department of Geology and Mineral Industries, 2007–2010; National Center for Airborne Laser Mapping, 2008; Oregon Department of Geology and Mineral Industries, 2011b) where available and from 10-m digital elevation models (from Oregon Geospatial Enterprise Office, 2008) elsewhere. Contours derived from digital elevation models. Drainage from Pacific Northwest Hydrography Framework Group (2005b) and also traced from lidar imagery. Roads from Oregon Department of Transportation (2015); trails from U.S. Forest Service (2017). *A*, Overview of White Branch valley area, showing lava flows from Sims Butte (Priest and others, 1988) and Collier Cone (Deardorff and Cashman, 2012). Note that “Lost Spring” (see fig. 10) is located at Stop 5. Contour interval, 500 ft. *B*, Units of Collier Cone lava flow (modified from Deardorff and Cashman, 2012). Contour interval, 500 ft. *C*, Map of tree-canopy heights (from Deligne and others, 2013) in area surrounding westernmost extent of Collier Cone lava flow. White outlines show upper and lower alluvial flats on Collier Cone lava flow (from Deligne and others, 2013). Contour interval, 250 ft.

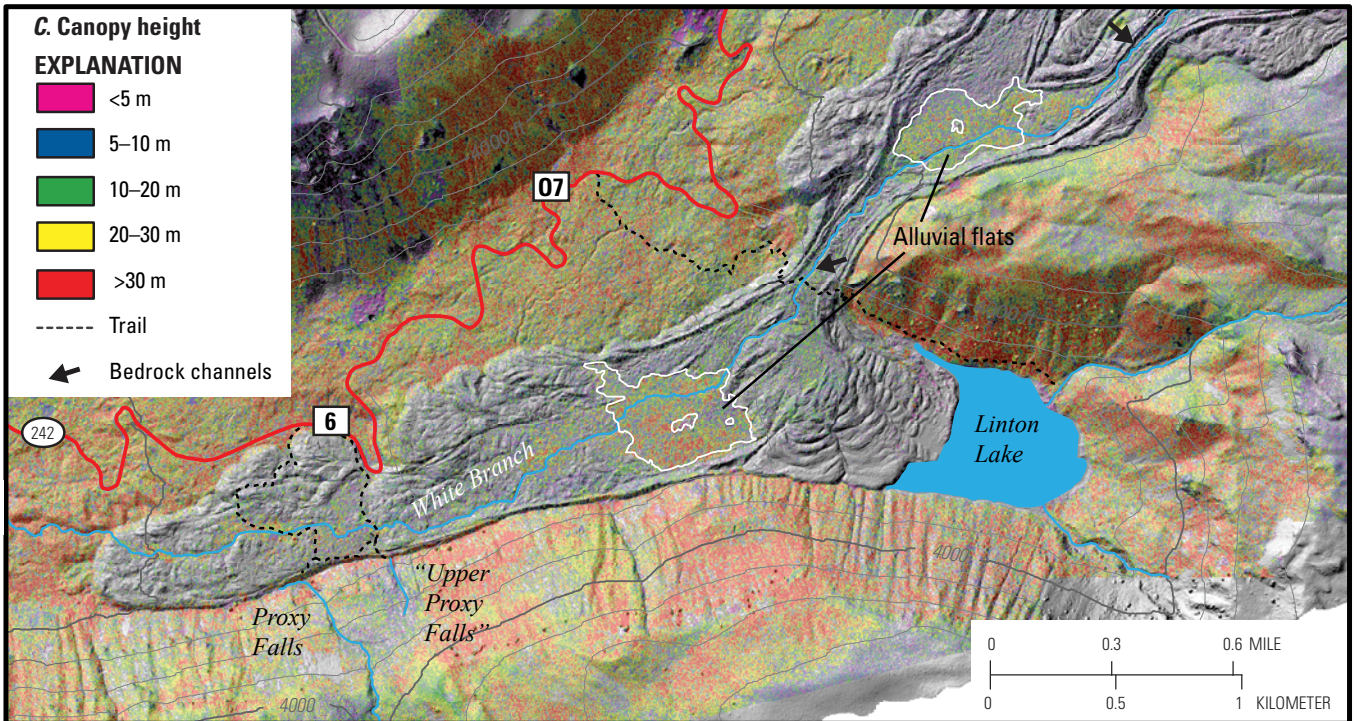
A. White Branch valley



B. Collier Cone lava flow



C. Canopy height



required to enter. Sampling or collecting is not allowed without a permit. Leave no trace.

Discussion of Stop 6

The Proxy Falls loop trail traverses the distal end of the about-1,600-yr-B.P. Collier Cone lava flow and the (typically dry) White Branch creek that has been incised into the lava (note that optional Stop 7 will provide a better view of the incised channel). Note also that we will see Collier Cone on Day 4, but today we will hike across its andesitic lava flows (unit 1 on figs. 11, 12).

Collier Cone is considered to be a monogenetic cone. Its lava flows, which cover about 0.17 km², range in composition from basaltic andesite to dacite (fig. 12; see also, Deardorff and Cashman, 2012). (Note that these flows are discussed in more detail on Day 4, at optional Stop 26.) Andesitic lava flows (unit 1 on fig. 11B) traveled 13.6 km westward from the vent,

making them some of the longest Holocene lava flows in the central Oregon Cascades (fig. 11). Whereas most lava flows in the central Oregon Cascades are considerably shorter (<5 km), the observation that flows can, in some cases, travel relatively long distances is a concern for transportation networks if further volcanism should occur in the area. Few transportation corridors link eastern and western Oregon, and a lava flow that disrupts one or more corridors could cause severe transportation problems in the region.

The Collier Cone lava flow developed a complex surface morphology because it is made up of multiple flow units, which created multiple levees, and also because it interacted with the surrounding topography (fig. 11; see also, Deardorff and Cashman, 2012). The effects of topography are pronounced in White Branch valley: to the south, flows of unit 1 (fig. 11B) are confined by the steep walls of the U-shaped valley; on its north edge, however, the flows have lobate structures associated with lateral spreading. Lava flows of units 1 and 2 (fig. 11B) likely were confined to the southern part of White Branch valley, owing to preexisting Sims Butte lava flows.

[Remainder of Stop 6 description is modified from Cashman and others (2009)]

The hydrology of the Proxy Falls area was described in detail by Lund (1977), who noted that the Proxy Falls area consists of several waterfalls that have different sources (fig. 13). “Upper Proxy Falls” (fig. 13B) originates in springs that emerge from an older lava flow about 200 m above the valley floor; these springs feed streams that flow down two ravines before joining at “Upper Proxy Falls.” “Upper Proxy Falls” is remarkable because the water disappears into the Collier Cone lava flow: at the bottom of “Upper Proxy Falls” lies a pool that has no outlet (fig. 13C). Proxy Falls (fig. 13A; informally known as “Lower Proxy Falls”) is fed by Proxy Creek, which traverses a glacially carved hanging valley. Below the falls, Proxy Creek continues along the south edge of the Collier Cone lava flow until it ends, where it flows on top of the Sims Butte lava flow; there, it loses much of its water to the underlying lava flow. All of the waters from this system, as well as Linton Lake and White Branch, ultimately emerge at “Lost Spring” to form Lost Creek (Stop 5).

Stop 7 (Optional): White Branch—Incision into the Collier Cone Lava Flow

Directions to Stop 7 and Description of Hike

Continue eastward on Highway 242 for 1.8 miles (2.9 km) to Alder Springs Campground; if you pass MP 66, you’ve gone too far. Park in the parking area or on the side of the road. Display a Northwest Forest Pass in your vehicle when parked. A primitive bathroom is available at the campground, but no potable water.

The hike to White Branch creek (round-trip distance, 1.5 miles [2.4 km]) starts from the Linton Lake trailhead, on the other side of the road opposite (immediately south of)

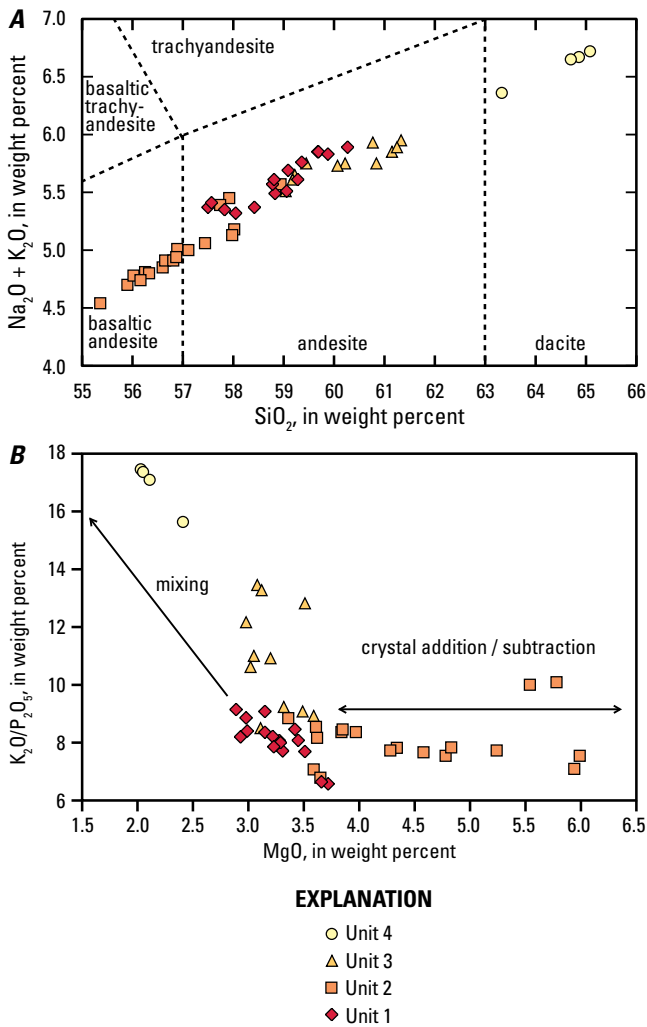


Figure 12. Compositional plots for Collier Cone lava flow units. Data from Deardorff and Cashman (2012). A, Na₂O + K₂O versus SiO₂ contents, in wt. percent. Total alkali-silica fields from Le Bas and others (1986). B, K₂O/P₂O₅ versus MgO contents, in wt. percent. Mixing and crystal addition and subtraction trends from Allègre and others (1977).

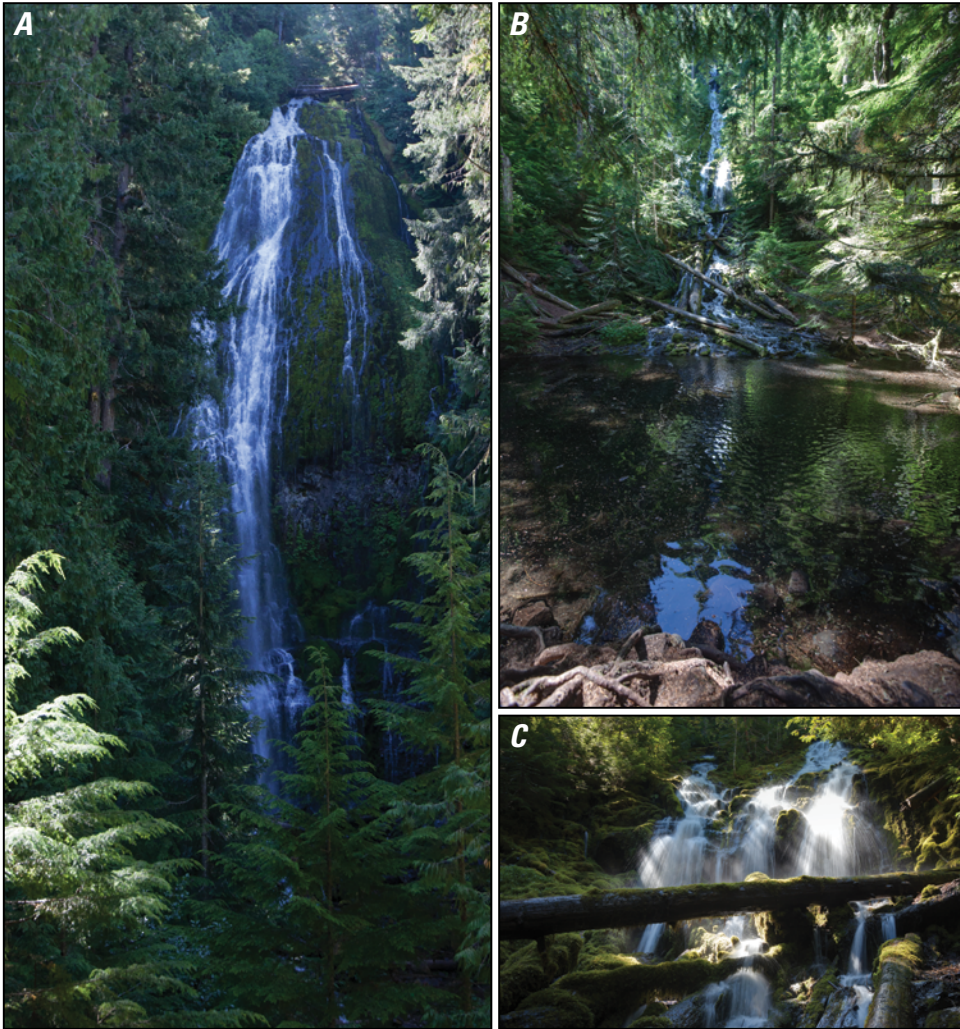


Figure 13. A, Proxy Falls. B, “Upper Proxy Falls” and pool into which it disappears. C, Lower part of “Upper Proxy Falls.” Photographs by Marli Miller, 2016.

Alder Springs Campground. The trail is easy to follow but is not wheelchair accessible. Dogs on a leash are permitted. The hike is within the Three Sisters Wilderness; self-issue permits, which are available at the trailhead, are required to enter. Sampling or collecting is not allowed without a permit. Leave no trace.

Note that you can continue on the trail to Linton Lake for an out-and-back hike (round-trip distance, 3 miles [4.9 km]).

Discussion of Stop 7

After hiking 0.75 miles (1.2 km) on the Linton Lake trail, you will encounter the Collier Cone lava flow; its outer levees are associated with unit 1 (fig. 11B). Shortly thereafter, you will cross a second set of levees, which marks the outer boundary of unit 2 (fig. 11B). After hiking about 30 m (near $44^{\circ}10'25''$ N., $121^{\circ}54'9''$ W.), you will cross a dry stream channel. This is White Branch creek, an ephemeral channel that has a unique history.

The incision of White Branch creek into Collier Cone lava flow as seen here appears at first glance to be a regional anomaly. As has been apparent at the last few stops, surface water and

incised fluvial channels are quite rare in the High Cascades, owing to the high permeability of young, blocky lava flows. Typically, this hydrological regime persists until lava-flow permeability is reduced by in situ weathering, a process that takes between about ten thousand to one million years (Jefferson and others, 2010). Despite the inhospitable conditions for fluvial processes, White Branch creek has incised as much as 8 m into Collier Cone lava flow and deposited more than 0.2 km^3 of alluvium onto the flow (fig. 11C; see also, Deline and others, 2013).

The constructional nature of volcanic processes presents a unique opportunity for quantifying geomorphic processes by providing easily dateable initial conditions. Topographic patterns and drainage-network organization are highly dependent on initial conditions, which are nearly impossible to constrain in most erosional landscapes (Perron and Fagherazzi, 2012). At this stop, however, we can see the earliest stages of fluvial incision and, using the temporal and spatial constraints of the Collier Cone lava flow, can infer the incision history of White Branch creek.

Field observations of the channel and its alluvial stratigraphy suggest that White Branch creek conveys both outburst floods from Collier Glacier (located about 10 km

upstream) and smaller, interannual flows related to snowmelt (O'Connor and others, 2001b; Sweeney and Roering, 2017). Evidence for large flood events that originated from Collier Glacier includes the presence of obsidian clasts in channel sediment, the source of which must be Obsidian Cliffs (fig. 11B), and discrete, normally graded flood deposits in the alluvial plains. Despite the clear influence of glaciation, Sweeney and Roering (2017) showed using numerical modeling that, even with low-magnitude snowmelt flows, these interannual events can result in appreciable incision. Nevertheless, glacial-outburst floods likely play a crucial role in the initiation of channel formation, either by rapidly plucking loose lava blocks or by filling in macroporosity cavities with sediment.

[Next paragraph is modified from Cashman and others (2009)]

The Collier Cone lava flow created two lakes as it flowed down the valley and blocked streams: Spring Lake, northeast of Sims Butte, and Linton Lake, which is fed by both Obsidian and Linton Creeks. Obsidian Creek seasonally carries snowmelt runoff but is dry in the summer; Linton Creek is perennial, fed from springs west of Middle Sister. Linton Lake has no surface outlet. In July and August 2004, Linton Creek had an average discharge of 1.46 m³/s (51 ft³/s), and, during that same period, lake levels dropped about 3 m. This drop is unlikely to be solely the result of evaporation, on the basis of a comparison with the evaporation rate of Crater Lake (1,883 m elevation), which is 1.2 m/yr (Redmond, 1990). The elevation of Linton Lake is 1,067 m, and so its evaporation rate is probably higher than that of Crater Lake but not likely to exceed 3 m/yr. Thus, all of the water discharge lost from Linton Creek in the summer, plus some water stored in the lake, is recharging groundwater. Several small sinkholes that are visibly and audibly draining lake water are present along the margin of Collier Cone lava flow. The water that flows out of Linton Lake probably mingles with both upstream water from White Branch creek and downstream water introduced at Proxy Falls, emerging from the distal end of Sims Butte lava flow at “Lost Spring.”

As you retrace your steps back to Alder Springs Campground, note the vegetation on the Collier Cone lava flow. In places, large Douglas-fir and western hemlock trees have grown on the lava flow, which is remarkable given the young age of the lava flow, the lack of soil, and the scarcity of surface moisture. At two places on the Collier Cone lava flow, large amounts of sediment have been deposited on the flow (“alluvial flats” noted on fig. 11C); these two areas host mature forests that are indistinguishable from those that are adjacent to the lava flow. Trees are present elsewhere on the lava flow but are less concentrated, and they generally are shorter than the ones off the flow. Although trees are able to grow on young lava flows, they will preferentially grow and thrive on young lava flows in places where a soil-like substrate has been deposited on the flow (Deligne and others, 2013), either by water (as is the case here) or as tephra (which we will see tomorrow at the Sand Mountain volcanic field).

End of Day 1: The H.J. Andrews Experimental Forest

Directions to H.J. Andrews Experimental Forest

Retrace the route west, following Highway 242 to its intersection with Highway 126. Turn left (west) onto Highway 126 and follow it 15.3 miles (24.6 km), passing through the town of McKenzie Bridge. Turn right (north) at the “Blue River Reservoir” sign onto U.S. Forest Service Road 15 (just after MP 44). Drive up the hill and away from the McKenzie River, following the edge of Blue River Lake. After 3.8 miles (6.1 km), you will cross the Lookout Creek bridge. Just past the bridge, turn right onto Forest Service Road 130 at the sign for H.J. Andrews Experimental Forest Headquarters. Park in the parking area.

Discussion of H.J. Andrews Experimental Forest

Since 1948, the H.J. Andrews Experimental Forest has been the nexus of groundbreaking work on forest and stream ecosystems. As part of the National Science Foundation’s Long Term Ecological Research (NSF-LTER) program, researchers from throughout the world have worked cooperatively with the U.S. Forest Service Pacific Northwest Research Station, with Oregon State University, and with the Willamette National Forest to develop concepts and tools needed to predict effects of natural disturbance, land use, and climate change on ecosystem structure, function, and species composition. Long-term field experiments and measurement programs have focused on climate dynamics, streamflow, water quality, and vegetation succession (<http://andrewsforest.oregonstate.edu>).

The H.J. Andrews Experimental Forest is also home to the U.S. Geological Survey’s debris-flow flume, a field-scale experimental facility that enables researchers to test mathematical models of flow dynamics. Past studies have used ultrasonic imaging, force plates, and “smart rocks” that have embedded accelerometers to measure experimental flows and inform hazard mitigation (Iverson and others, 1992).

Day 2: H.J. Andrews Experimental Forest to Bend, by Way of the Sand Mountain Volcanic Field

[Note that Forest Service Road 770, required to access Stop 11, is closed from mid-November to mid-May, and other Forest Service roads that access stops on Day 2 also may be closed because of snow accumulation or for the season; please inquire at the McKenzie Ranger Station before you travel to see whether the roads are open or closed]

On Day 2 of the field trip, we will focus primarily on the physical volcanology and geochemistry of Sand Mountain volcanic field and its influence on, and interaction with, the

local and regional hydrology (see fig. 14). The Sand Mountain volcanic field, which was erupted about 3 ka, includes more than 20 cones and 13 eruptive units, as well as associated lava flows that collectively cover more than 70 km² and a tephra blanket that covers more than 150 km². The total dense-rock-equivalent⁹ eruptive volume of the Sand Mountain volcanic field is between 1.5 and 3 km³.

We will start the day by looking at the contrast in morphology of a typical Western Cascades stream (Lookout Creek; Stop 8) with that of rivers that are dominated by High Cascades streamflow regimes (Olallie Creek; Stop 9).

We will then travel up the McKenzie River catchment to Fish Lake (Stop 10) for a sighting of Sand Mountain and an overview of the Sand Mountain volcanic field. We will

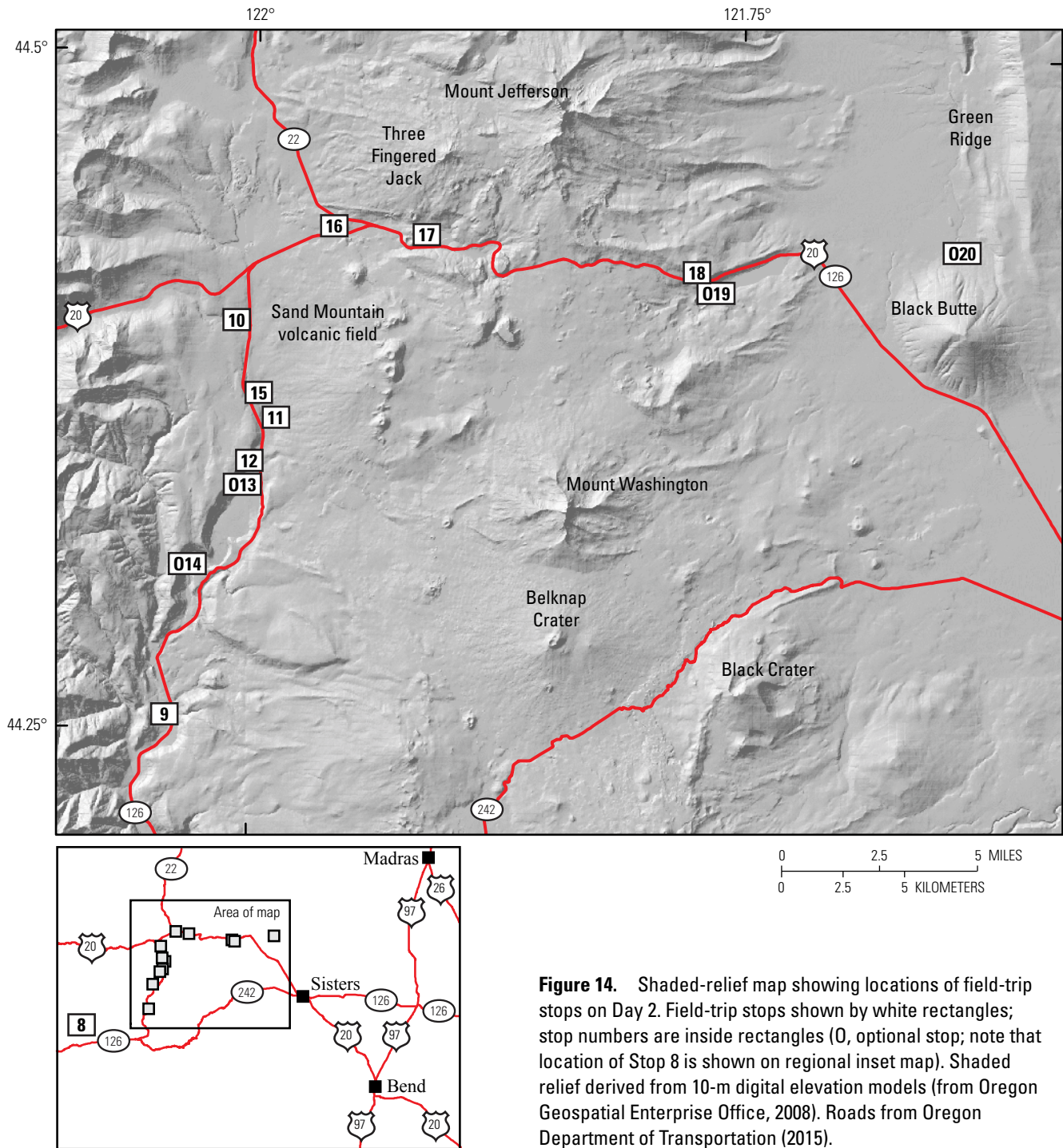


Figure 14. Shaded-relief map showing locations of field-trip stops on Day 2. Field-trip stops shown by white rectangles; stop numbers are inside rectangles (0, optional stop; note that location of Stop 8 is shown on regional inset map). Shaded relief derived from 10-m digital elevation models (from Oregon Geospatial Enterprise Office, 2008). Roads from Oregon Department of Transportation (2015).

⁹ Dense-rock-equivalent (DRE) volume is the equivalent volume of unerupted magma.

then retrace our steps to follow the McKenzie River's journey across the Sand Mountain volcanic field. We will visit the south end of Clear Lake (Coldwater Cove Recreation Site; Stop 11) to see the spring-fed headwaters of the McKenzie River, which have been dammed by lava flows of the Sand Mountain volcanic field, and we will look at several Sand Mountain volcanic field lavas flows and the outlet to Clear Lake. Next we will hike from Sahalie Falls to Koosah Falls (Stop 12), two stunning waterfalls that owe their existence to the Sand Mountain volcanic field.

Two optional stops would continue to follow the McKenzie River. At Carmen Reservoir (optional Stop 13), the McKenzie River seasonally occupies a channel but primarily flows underground through an about-7-ka lava flow of unknown origin. The river then reappears at the exquisite "Tamolitch Pool" (optional Stop 14), which can be accessed with a hike either from Carmen Reservoir or Trail Bridge Reservoir.

We will return to the headwaters of the McKenzie River for lunch at Clear Lake (Stop 15), then we will travel by rowboat to Great Spring, which provides about 10 percent of Clear Lake's water. After lunch, we will visit a cinder cone in Sand Mountain volcanic field (Little Nash Crater; Stop 16) where we will discuss the geochemical story of the Sand Mountain volcanic field. Our final Sand Mountain volcanic field stop will be at Lost Lake (Stop 17) where we will discuss the Sand Mountain volcanic field's tephra story, as well as a resource-management decision at Lost Lake that failed owing to the poor understanding of hydrology within a young volcanic landscape.

Once our tour of the Sand Mountain volcanic field is complete, we will cross Santiam Pass on our way to Bend, which will serve as our base for the rest of the field trip. En route we will stop at the Mount Washington overlook (Stop 18) for good views of the glacially sculpted cone of Mount Washington and a view of Blue Lake crater, the result of another recent eruption.

Two more optional stops are possible here. Blue Lake crater (optional Stop 19) is a young maar that is accessible by way of a short hike. Further east, on the north flank of Black Butte, is Metolius Spring, the headwaters of the Metolius River (optional Stop 20), which is a major spring-fed tributary of the Deschutes River. Also prominent in the landscape at this location is Green Ridge, the escarpment of the eastern bounding fault of the graben in which this part of the High Cascades resides.

From the valley that contains Blue and Suttle Lakes, the road descends the flank of the High Cascades, crossing glacial-outwash deposits and Quaternary lava flows, to the central Oregon high desert; the precipitation gradient between the west and east sides of Santiam Pass is one of the steepest

in North America, and its effects are clearly visible in the vegetation.

Stop 8: Lookout Creek—A Typical Western Cascades Stream

Directions to Stop 8

Note that Stop 8 is located within the H.J. Andrews Experimental Forest, where the previous day's field trip ended, and so no directions to Stop 8 are needed.

Discussion of Stop 8

[Modified from Cashman and others (2009)]

Lookout Creek, located near the main H.J. Andrews Experimental Forest Headquarters, is a classic Western Cascades stream, and it has a drainage area of 64 km². Characteristic features of this Western Cascades stream include (1) a planform morphology dominated by coarse-grained lateral and marginal bars of flood origin, now colonized by broadleaf alders, cottonwoods, and willows; (2) a well-defined floodplain of mixed fluvial and debris-flow origin, now colonized by an old-growth Douglas-fir forest; (3) a well-defined channel morphology of step-pool sequences; and (4) marginal but occasionally channel-spanning accumulations of large woody debris (Grant and others, 1990).

Channel and valley-floor morphology, processes, and changes in this reach, which have been extensively studied and described (for example, Grant and others, 1990; Nakamura and Swanson, 1993; Grant and Swanson, 1995; Faustini, 2001; Swanson and Jones, 2002; Dreher, 2004), reveal interactions among fluvial processes, debris flows from upstream tributaries, growth and disturbance of riparian vegetation, and dynamics of large woody debris. In particular, this reach has been affected by repeated debris flows generated during major storms in 1964 and 1996. These debris flows, which entered the Lookout Creek channel approximately 2 km upstream, transitioned into bedload-laden floods that dramatically mobilized accumulations of large woody debris, stripped mature and old-growth riparian forests, and deposited large coarse-cobble bars that now support a young forest of alders and conifers. The stratigraphy of older deposits on which the current old-growth forest now grows reveals a similar origin. These reaches undergo a decades-long sequence of morphologic changes after large floods that are driven both by fluvial reworking of flood deposits and morphologic adjustments around large pieces of wood that have fallen from the adjacent forest stand (fig. 15).

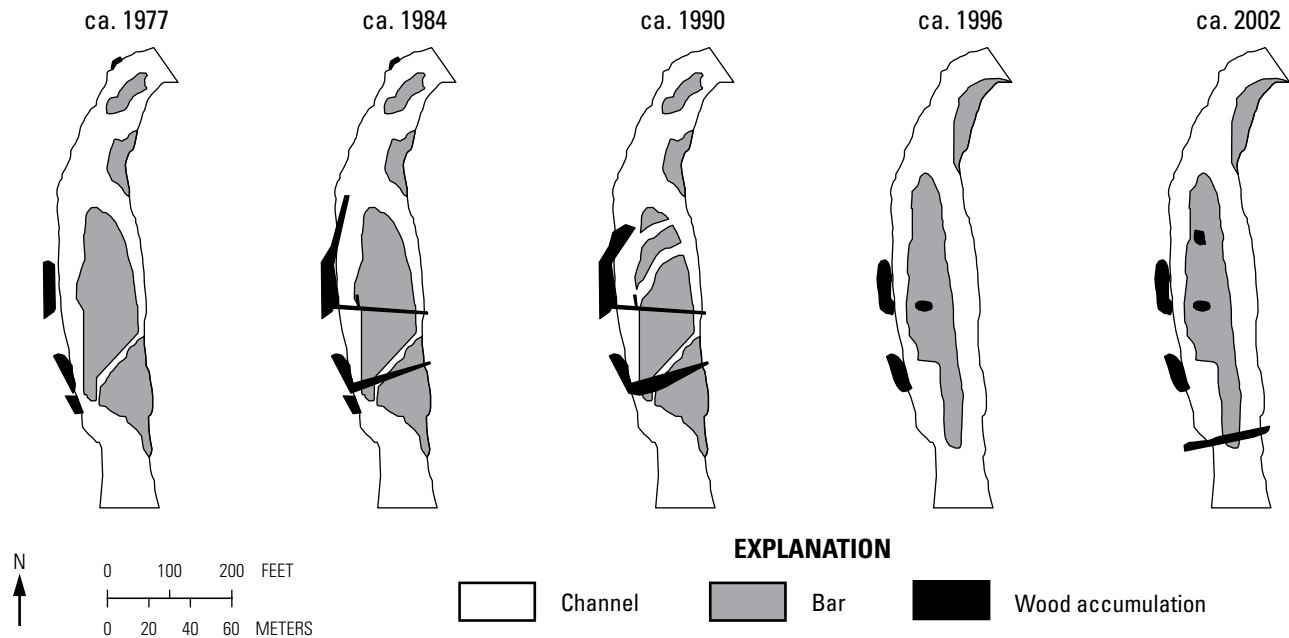


Figure 15. Areal changes in wood accumulation (black areas) and gravel bars (gray areas) in lower section of Lookout Creek, for five dates between 1977 and 2002. Modified from Dreher (2004).

In Transit—The Western Cascades–High Cascades Boundary

[Slightly modified from Cashman and others (2009)]

Just beyond the turnoff for Highway 242, the McKenzie River (and Highway 126) makes an abrupt turn to the north. From here to its headwaters, the McKenzie River flows along the western boundary of the Central Cascades graben that lies between the High Cascades and the Western Cascades. Within the graben, nearly 3 km of subsidence has occurred over the last 5 million years (Conrey and others, 2002a).

The Western Cascades–High Cascades boundary is traversed by several ridge-capping lava flows, resulting in a topographic inversion that illustrates the persistent effects of erosion-resistant lava flows on landscape form. These lava flows can also be used to estimate incision rates across this boundary. Lookout Ridge, which separates Lookout Creek from the McKenzie River, is capped by 8- to 6-Ma lavas from the ancestral High Cascades (Conrey and others, 2002a). These ridge-capping lavas probably originated as intracanyon lava flows and, therefore, mark the course of the ancestral McKenzie River. The elevation difference between the summit of Lookout Ridge (1,341 m) and the modern McKenzie River at the town of McKenzie Bridge (396 m) yields an average incision rate of 0.12 to 0.16 mm/yr. Similar calculations for Foley Ridge (634 m), a 0.8- to 0.6-Ma intracanyon flow on the south side

of the McKenzie River near the ranger station (454 m), indicate an incision rate of 0.23 to 0.3 mm/yr. These rates bracket estimates for the Middle Santiam River of 0.14 mm/yr over the past 5 Ma (Conrey and others, 2002a), as well as rates for the Western Cascades of 0.28 to 0.33 mm/yr from 3.3 to 2 Ma and 0.14 to 0.17 mm/yr since 2 Ma (Sherrod, 1986).

Along the graben-bounding fault zone, several hot springs discharge into the McKenzie River or its tributaries, including the privately owned Belknap Hot Spring and also another one on Deer Creek (known as “Bigelow Hot Spring”) that is submerged during high flows of the McKenzie River. The thermal waters are inferred to recharge near the Cascade Range crest, move in flow paths several kilometers deep, and emerge along faults, which interrupt the downgradient flow of water (Ingebritsen and others, 1994). The waters discharge at temperatures of 46 to 79 °C, are enriched in sodium, calcium, and chlorine, and contain a magmatic signature in their helium isotopes. Discharge at individual hot springs ranges from 5 to 24 L/s. Total discharge of geothermal water in the central Oregon Cascades is less than 0.2 percent of annual groundwater recharge but represents 148 MW of heat discharge (Ingebritsen and others, 1994). To date (2017), no geothermal-energy production has been developed, but numerous exploratory wells have been drilled.

The deep-flowing thermal water captures most of the geothermal heat and magmatic gasses migrating upward through the west slope of the High Cascades (fig. 16). As a result, water

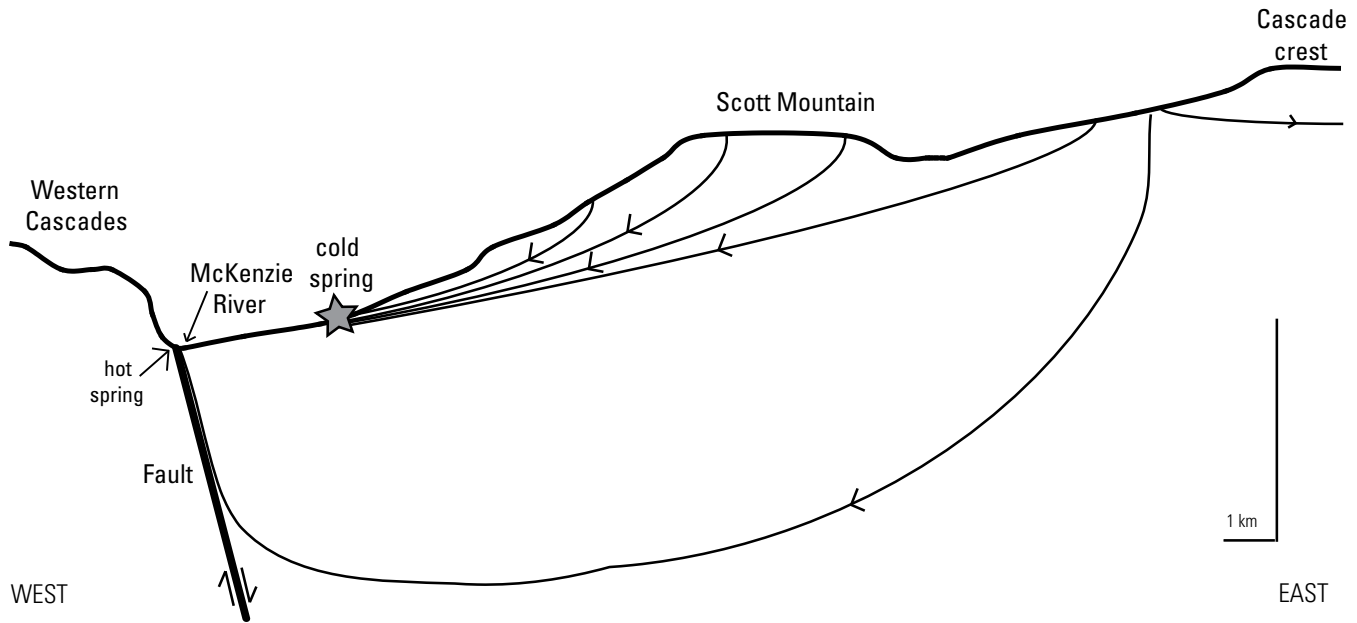


Figure 16. Conceptual cross section showing groundwater-flow paths (arrows) from Cascade crest to Western Cascades (from Jefferson and others, 2006). Hot springs are found where deep groundwater-flow paths are interrupted by faults (Ingebritsen and others, 1994), whereas cold springs result from more shallow groundwater-flow paths.

flowing from the large nonthermal springs (1) is close to the temperature at the mean recharge elevation inferred from stable isotopes, (2) has low total dissolved solids, and (3) has a helium-isotope ratio close to that of the atmosphere.

As we will see over the course of the next few days, the central Cascades graben has a profound effect on the extent of young lava flows and the local, regional, and statewide hydrology.

Stop 9: Olallie Creek—Geomorphology of Western and High Cascades Streams

Directions to Stop 9

Exit the H.J. Andrews Forest Headquarters and turn left onto Forest Service Road 15. Follow the Blue River Lake 3.8 miles (6.1 km) to Highway 126. Turn left and follow the highway for about 18 miles (29.0 km) to Olallie Creek Campground, shortly after MP 13. Park at the north end of the campground. A primitive bathroom is available at the campground from late spring to early fall.

Discussion of Stop 9

[Modified from Cashman and others (2009)]

This stop offers an excellent opportunity to observe the contrast in morphology between Western Cascades and High Cascades streams. Unvegetated, channel-flanking gravel bars, large boulders, well-developed step-pool sequences, and

woody-debris pieces and accumulations that indicate fluvial transport are all characteristic of Western Cascades streams (Stop 8). Contrast this with the Olallie Creek channel here, a spring-fed High Cascades stream characterized by (1) a planform morphology that shows few emerged gravel bars and is dominated by stable wood accumulations, as indicated by moss growth and nurse logs; (2) mature conifers at the channel margin and the absence of well-defined floodplain and flood-reset broadleaf species; (3) a chaotic and poorly defined channel-unit structure; and (4) stable, channel-spanning wood accumulations that show little evidence of fluvial transport. High Cascades channels reflect near-constant flow regimes, absence of flooding, and limited sediment and wood transport.

Lidar imagery suggests that the path of Olallie Creek is controlled by the position of lava flow margins, and the creek is fed by two springs less than 800 m apart at the heads of two tributary channels. The northern spring discharges $1.7 \text{ m}^3/\text{s}$ ($60 \text{ ft}^3/\text{s}$) of $4.5 \text{ }^\circ\text{C}$ water that cascades down a steep slope of lava from Scott Mountain, whereas the southern spring emerges from under a talus pile, discharging $2.3 \text{ m}^3/\text{s}$ ($81 \text{ ft}^3/\text{s}$) at a constant $5.1 \text{ }^\circ\text{C}$ (Jefferson and others, 2006). Both springs discharge more water than what falls as precipitation in their watersheds, showing that groundwater flowpaths cross modern topographic divides (Jefferson and others, 2006). Flowpaths are inferred to follow lava geometries that were influenced by now-observed paleotopography. Using water temperature and hydrogen and oxygen stable isotopes, Jefferson and others (2006) showed that the two springs that feed Olallie Creek receive groundwater from different source areas, with the southern spring recharging at elevations lower than those of the northern spring. Olallie Creek and its springs illustrate the

dominant influence of constructional volcanic topography on pathways of both groundwater and surface water.

Stop 10: Fish Lake—View of Sand Mountain

Directions to Stop 10

Exit the campground and turn left (north) onto Highway 126. Follow the highway for 11 miles (17.7 km) to Fish Lake, at MP 2. Turn left (west) to access the Fish Lake Interpretative Day Use site. A Northwest Forest Pass is not required when parked here.

Discussion of Stop 10

Fish Lake is a seasonal lake: it is full for a few weeks a year, in late spring and early summer during snow melt, and it is a meadow the rest of the year. We will stop here to hear an introduction to the Sand Mountain volcanic field, which is today's focus.

The Sand Mountain volcanic field (fig. 17) includes the Sand Mountain chain of cones, Nash Crater, Little Nash Crater, and the Lost Lake chain of cones; it consists of 23 vents and lava flows (collectively covering 76 km²) and a tephra blanket that extends to the east. The tephra will be discussed at Stop 17; for now we will focus on the vents and lava flows.

The first scientific investigation of the Sand Mountain volcanic field was undertaken by Stearns (1929), who was scouting for potential dam sites; he reported on lava flows near Clear Lake (Stop 11) and on waterfalls further down the McKenzie River valley (Stops 12, 14). Williams (1957) undertook early reconnaissance mapping to tie together the lava flows that surround Clear Lake with the Sand Mountain chain of vents. Taylor (1965) completed the first full map of the Sand Mountain volcanic field; Taylor's mapping provided the foundation for the most recent U.S. Geological Survey geologic map of the area (Sherrod and others, 2004). However, the geologic map and volcanic history of the Sand Mountain volcanic field has recently been revised and expanded by Deligne and others (2016), which we will present here.

Deligne and others (2016) mapped the lava flows and vents of the Sand Mountain volcanic field, and they identified 15 separate eruptive units on the basis of geochemistry (see Stop 16). Three of these units are "orphan" units, meaning that they do not have an associated vent, likely owing to either vent burial or vent reoccupation. The separate eruptive units have been informally grouped by geochemistry into the Lost Lake group (4 units), the Sand group (5 units), and the Nash group (4 units) (fig. 17). An additional two units are part of the Sand Mountain volcanic field but do not fit into a group.

Studies from the 1960s to early 2000s suggested that the Sand Mountain volcanic field was erupted intermittently over 1,500 years during the last 4,000 years (Benson, 1965; Taylor, 1965; Chatters, 1968; Champion, 1980; Taylor, 1990a; Sherrod and others, 2004). However, paleomagnetic studies indicate that the Lost Lake, Sand, and Nash groups were erupted within

a few decades of each other, and more recent cosmogenic and radiocarbon dating indicated that this occurred about 3 ka (Deligne and others, 2016). In general, the Lost Lake group is the oldest in the sequence of eruptive activity, and the Nash group is the youngest (fig. 18).

Fish Lake is both bordered on the east and dammed by Fish Lake lava flows (unit FL in the Lost Lake group; fig. 17). The barren lava flows slightly to the north, and on the other side, of Highway 126 are Nash-group lava flows (unit N in the Nash group; fig. 17). You can see Sand Mountain to the east-southeast from Fish Lake, across lava flows of the Nash group.

Stop 11: Coldwater Cove Recreation Site—Lava, Lake, and Forest

Directions to Stop 11

Exit the Fish Lake parking area and turn right (south) onto Highway 126. Go past the turnoff for Clear Lake, and, after MP 4, cross a bridge, then immediately turn left onto Forest Service Road 770 and follow the signs for Coldwater Cove Recreation Site. If you reach the turnoff for Sahalie Falls, you have gone too far.

We will make two brief stops along Forest Service Road 770 on the way to the Coldwater Cove Recreation Site boat launch: the first will be as soon as is feasible after turning onto Forest Road 770, and the second will be about 0.5 miles after the turnoff from Highway 126, immediately after a bridge (park alongside the road). After these brief stops, continue to the end of the road (stay to the right at intersections) to the Coldwater Cove Recreation Site boat launch. Display a Northwest Forest Pass in your vehicle when parked. Primitive bathrooms are available near the boat launch.

Discussion of Stop 11

Forest Road 770 initially traverses part of the Clear Lake South lava flow (unit CLS in the Sand group; fig. 17). This lava flow dammed Clear Lake, which is the highest permanent source of the McKenzie River. As it filled, Clear Lake drowned a forest of Douglas-fir (see Stop 15). At our first brief stop is an opportunity to see the Clear Lake South lava flow.

Our second brief stop will be within the Coldwater Cove lava flow (unit CWC in the Lost Lake group; fig. 17), which is remarkable for its pronounced levees (fig. 19). The Coldwater Cove lava flow is an "orphan" lava flow (that is, not associated with a vent), thought to be one of the oldest in the Sand Mountain volcanic field (Deligne and others, 2016). Note that we will be seeing the Coldwater Cove lava flow again at Stop 15.

At the end of Forest Road 770 is the Coldwater Cove Recreation Site boat launch. Coldwater Cove Recreation Site is at the southeast end of Clear Lake, which is bounded by lava flows of the Sand Mountain volcanic field on its northern, eastern, and southern margins and by the Horse Creek Fault Zone along its western margin (figs. 14, 19). Note that we will be further discussing Clear Lake at Stop 15; for now we will focus on lava flows and vegetation.

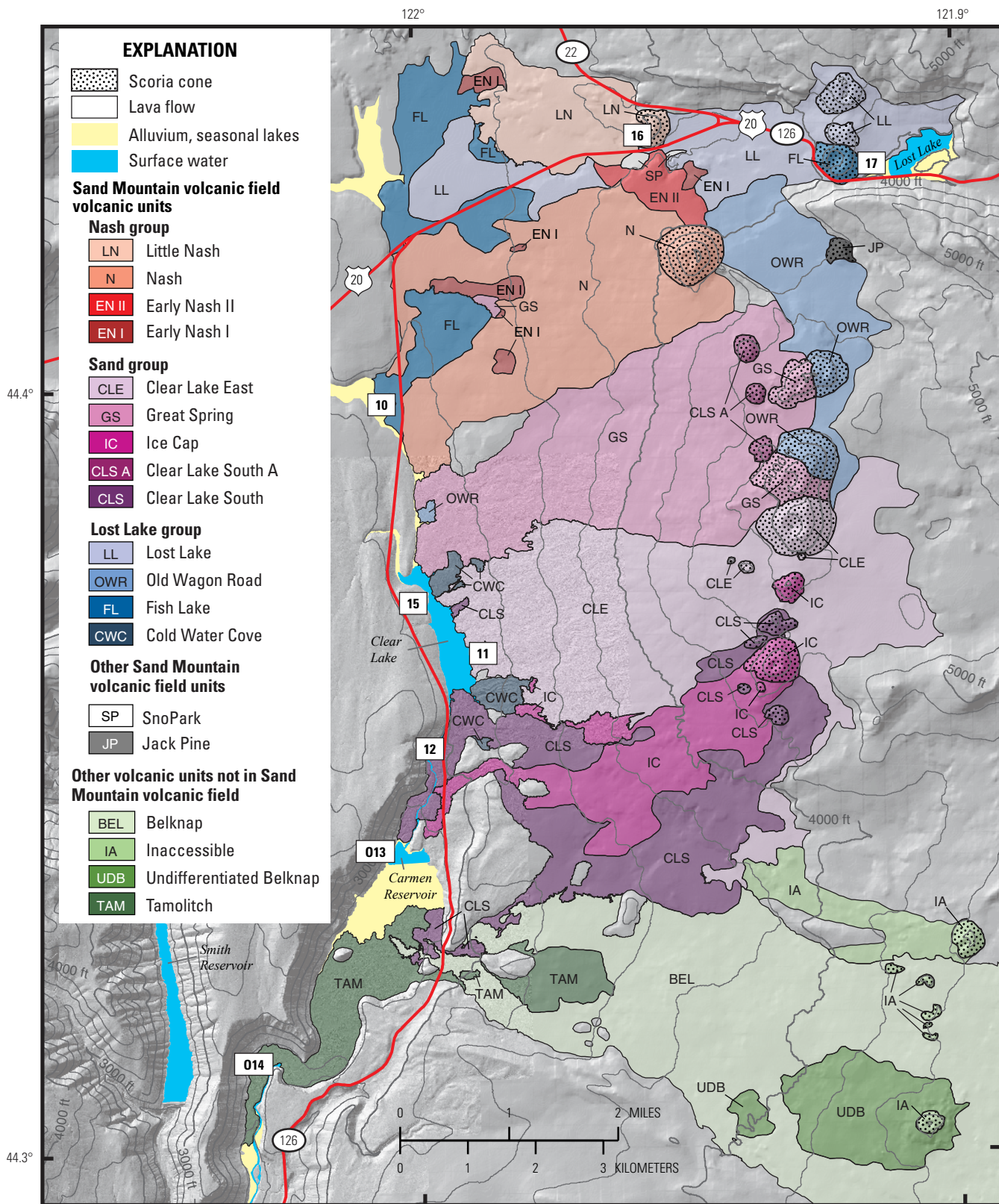


Figure 17. Shaded-relief map of upper McKenzie River catchment, showing Holocene lava flows and associated cinder cones of Sand Mountain volcanic field and other Holocene volcanic units (modified from Deligne and others, 2016). Bare areas (that is, areas that lack color) consist of older, glaciated, Pleistocene-age volcanic rocks. Field-trip stops shown by white rectangles; stop numbers are inside rectangles (0, optional stop). Note that “Tamolitch Pool” (see fig. 23) is at Stop 14. Shaded relief derived from lidar imagery (from Oregon Department of Geology and Mineral Industries, 2007–2010) where available and from 10-m digital elevation models (from Oregon Geospatial Enterprise Office, 2008) elsewhere. Contours derived from digital elevation model; contour interval, 250 ft. Drainage and roads traced from lidar imagery.

A. NASH GROUP STRATIGRAPHY

Little Nash -?- Nash
 Early Nash II
 Early Nash I

Possibly contemporaneous units

Clear Lake East
 Ice Cap

Remainder of Sand Mountain volcanic field units

B. SAND GROUP STRATIGRAPHY

Belknap

Clear Lake East
 Great Spring -?- Ice Cap

Possibly contemporaneous units

Nash group } Clear Lake East and Ice Cap only
 Lost Lake } (younger than Great Spring)

Clear Lake South A -?- Clear Lake South
Cold Water Cove

Fish Lake, Old Wagon Road
 Other Sand Mountain volcanic field units

Tamolitch

C. LOST LAKE GROUP STRATIGRAPHY

Nash group
 Lost Lake
 Great Spring

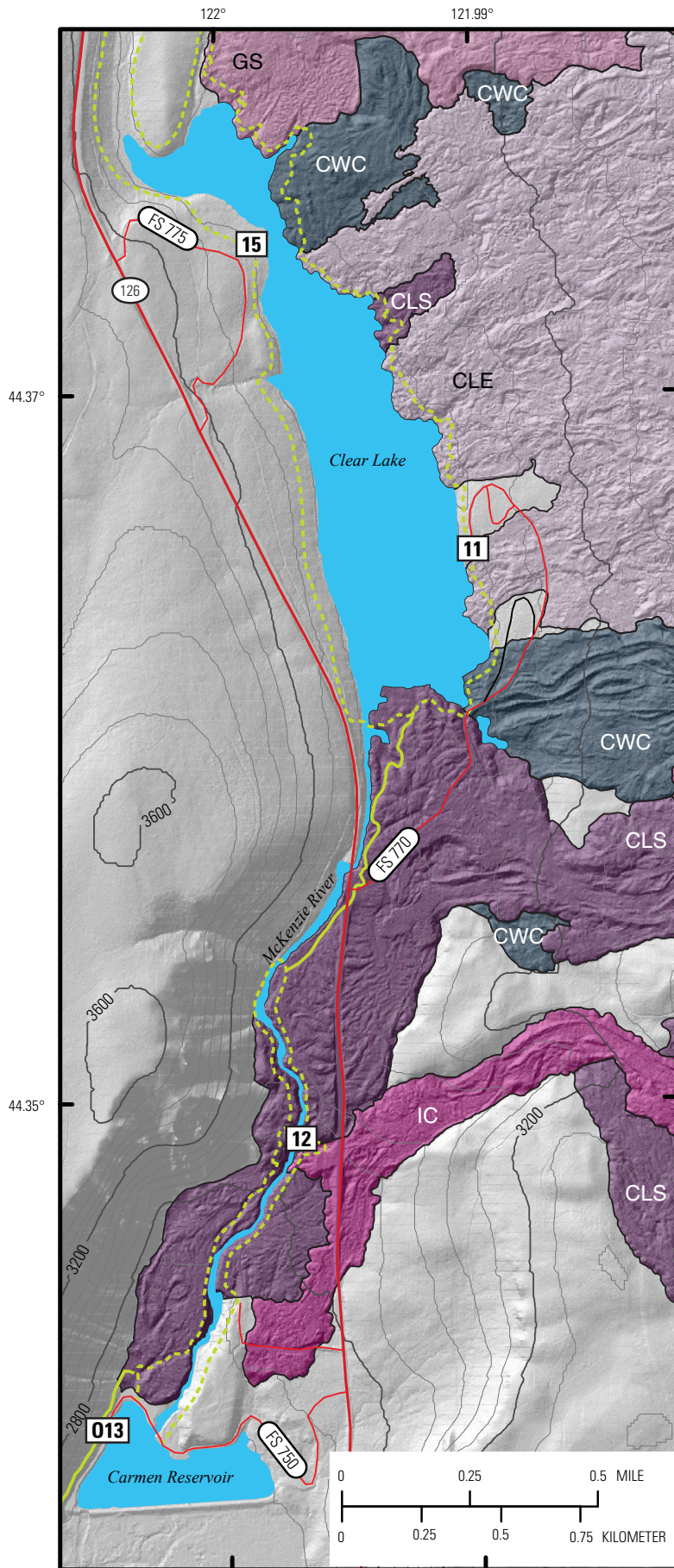
Possibly contemporaneous units

Clear Lake East
 Ice Cap

Fish Lake -?- Old Wagon Road
 Cold Water Cove

Snobark } Remainder of Sand group
 Jack Pine }

Figure 18. Stratigraphic relations within and among units in (A) Nash, (B) Sand, and (C) Lost Lake groups of Sand Mountain volcanic field (from Deligne and others, 2016); see figure 17 for areal distribution of units. Within each stratigraphic group, units not part of that group are shown in italic type; younger units shown above older units; units that have similar stratigraphic relations above and below but that lack stratigraphic control as to which is older are placed side by side, separated by question mark (-?-). Possibly contemporaneous units from other groups are shown to right of groups; brackets show temporal range of possible overlap.



EXPLANATION
Sand Mountain volcanic field volcanic units

Sand group

- CLE Clear Lake East
- GS Great Spring
- IC Ice Cap
- CLS Clear Lake South

Lost Lake group

- CWC Cold Water Cove

Figure 19. Shaded-relief map of McKenzie River from Clear Lake to Carmen Reservoir, showing detailed view of Holocene lava flows in figure 17 (modified from Deligne and others, 2016). Bare areas (that is, areas that lack color) consist of older, glaciated, Pleistocene-age volcanic rocks. Field-trip stops shown by white rectangles; stop numbers are inside rectangles (0, optional stop). Dashed green lines show Clear Lake loop and Waterfall loop hiking trails; solid green line shows McKenzie River National Recreation Trail where it connects these two loop trails. Shaded relief derived from lidar imagery (from Oregon Department of Geology and Mineral Industries, 2007–2010). Contours derived from digital elevation models (from Oregon Geospatial Enterprise Office, 2008); contour interval, 100 ft. Drainage, roads, and trails traced from lidar imagery; traces of some trails supplemented by Global Positioning System tracks from Deligne (2012).

The campground and boat launch are on Pleistocene lavas that predate the Sand Mountain volcanic field; these glacially smoothed Pleistocene lavas are clearly visible in lidar imagery (fig. 19). North of the campground is the relatively barren Clear Lake East lava flow (unit CLE of the Sand group; fig. 17), one of the youngest units (and youngest lava flows) of the Sand Mountain volcanic field (fig. 18). Follow the trail that departs north from the Coldwater Cove Recreation Site boat launch a few tens of meters to see the Clear Lake East lava flow. The Clear Lake East lava flow is distinctive within the Sand Mountain volcanic field owing to its high plagioclase content (10–15 percent), having laths as much as 2 mm long; it also contains about 2 percent olivine (table 1).

Note that this trail is part of both the 4.6-mile-long (7.4-km-long) Clear Lake loop trail (fig. 19), which goes around the lake, and the 26-mile-long (42-km-long) McKenzie River National

Recreation Trail, which starts close to Fish Lake and finishes near the McKenzie Ranger Station (see Stop 3).

The amount of soil and vegetation cover can vary greatly in this area (fig. 20), which Stearns (1929) noted in his preliminary investigations of the area. The Pleistocene lava flows at Coldwater Cove Recreation Site have continuous soil and forest cover; however, the Clear Lake South (CLS) and Coldwater Cove (CWC) lava flows have discontinuous soil cover (lava blocks are readily visible) yet host a relatively continuous forest. The Clear Lake East lava flow (CLE), on the other hand, which erupted within a few decades of the Clear Lake South and Coldwater Cove lava flows, has no soil cover and sparse vegetation. This huge discrepancy in soil and forest cover between lava flows of very similar age was studied by Deligne and others (2013), who found that the “soil” that covers the Clear Lake South and Coldwater

Table 1. Petrographic descriptions of select lava flow units in the upper McKenzie River watershed.

[See figure 17 for more information on map-unit groups and eruptive units. Slightly modified from Deligne and others (2016)]

Eruptive unit	Phenocrysts	Groundmass
Sand group		
Clear Lake East	10–15 percent plagioclase 2 percent olivine Plagioclase: mostly laths, as much as 2 mm long Olivine: generally 1 mm in diameter, some glomerocrysts	Microcrystalline plagioclase and olivine
Great Spring	5 percent olivine <1.5 percent plagioclase Olivine: generally ≤1 mm, can be as much as 3 mm in diameter Plagioclase: mostly laths, small	Highly microcrystalline plagioclase and olivine
Ice Cap	3 percent olivine <1 percent plagioclase Olivine: generally ≤2 mm, can be as much as 3 mm in diameter Plagioclase: generally equant (few laths) Large glomerocrysts of olivine and plagioclase	Microcrystalline plagioclase and olivine
Clear Lake South	7 percent olivine <0.1 percent plagioclase Olivine: bimodal size distribution of submillimeter- and 1–4-mm-diameter-sized grains; larger grains, typically >2 mm	Microcrystalline plagioclase (abundant) and olivine
Lost Lake group		
Coldwater Cove	5 percent olivine Trace plagioclase Olivine: bimodal size distribution of submillimeter- and 1–2-mm-diameter-sized grains	Highly microcrystalline plagioclase and olivine
Other		
Belknap	1 percent olivine Trace plagioclase Olivine: generally ≤1 mm, can be as much as 4 mm diameter (rare) Overall, few phenocrysts Very glassy and vesicular	Very glassy
Tamolitch	10 percent plagioclase 5 percent olivine Plagioclase: as much as 2 mm diameter Olivine: ≤1 mm diameter Glomerocrysts of olivine and plagioclase common	Very crystalline, although glass visible

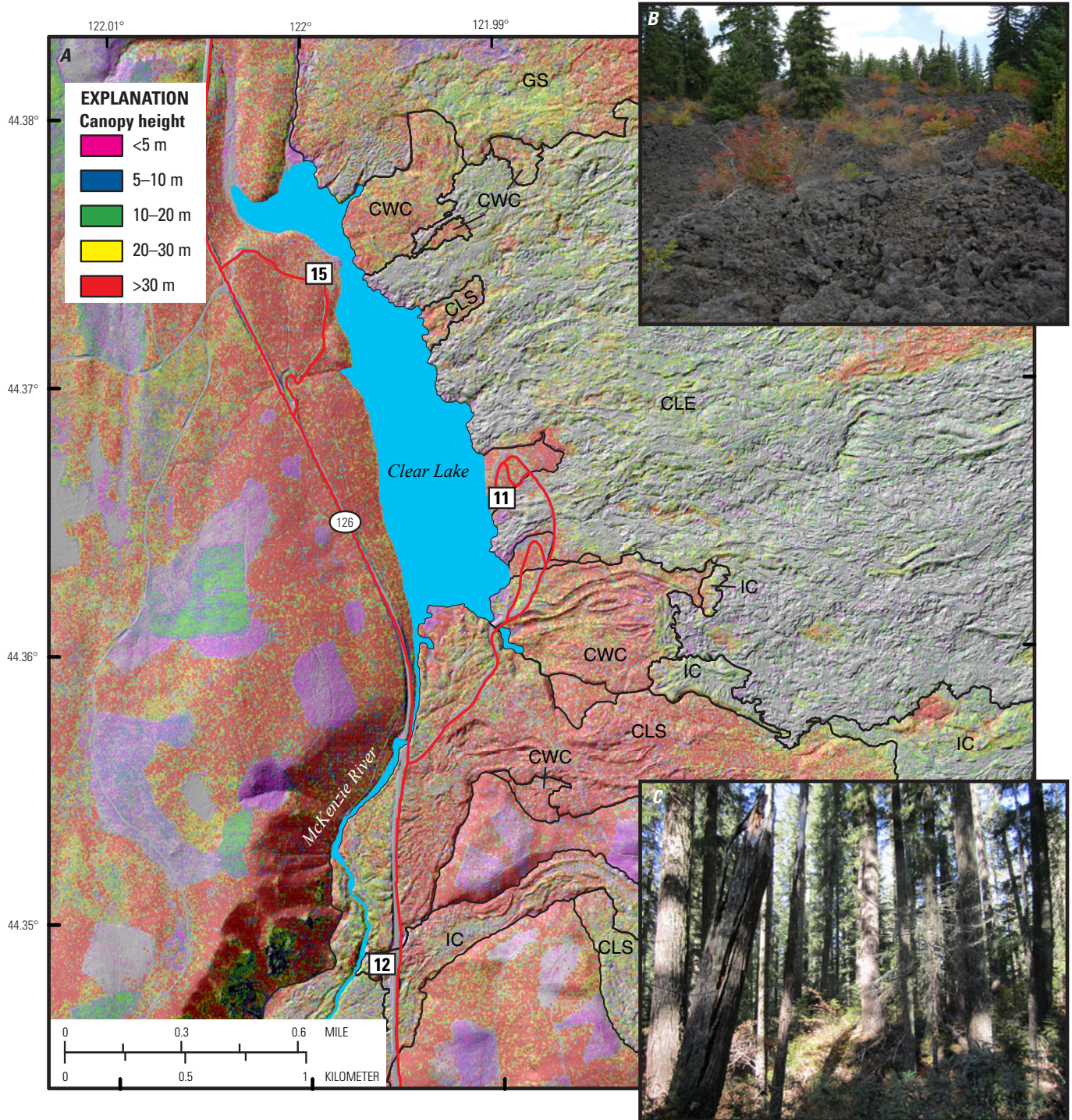


Figure 20. Shaded-relief map and photographs of Clear Lake area. *A*, Shaded-relief map of Clear Lake area (similar to area depicted in fig. 19), showing tree-canopy heights (from Deligne and others, 2013) on lava flows. Clear-cut patches west of Clear Lake are clearly visible. Lava-flow units (from Deligne and others, 2016; see figs. 17 and 18 for stratigraphic relations): CLE, Clear Lake East; CLS, Clear Lake South; CWC, Cold Water Cove; GS, Great Spring; IC, Ice Cap. Field-trip stops shown by white rectangles; stop numbers are inside rectangles. Shaded relief and tree-canopy heights derived from lidar imagery (from Oregon Department of Geology and Mineral Industries, 2007–2010). Drainage and roads traced from lidar imagery. *B*, Photograph of sparse vegetation on Clear Lake East lava flow. Photograph by Natalia Deligne, 2007. *C*, Photograph of forested area on Clear Lake South lava flow. Photograph by Natalia Deligne, 2011.

Cove lava flows is actually tephra of the Sand Mountain volcanic field, and this fine material provides a soil-like substrate for trees to grow on. Forests can quickly establish themselves on lava flows that have a soil-like substrate: for the Collier Cone lava flow (see Stop 7), this soil-like substrate is debris-flow sediment; for the lava flows in the Sand Mountain volcanic field, it is tephra of the Sand Mountain volcanic field. Thus, within the Sand Mountain volcanic field, lava flows that predate the end of the explosive phase host relatively mature forests, whereas flows that postdate the explosive phase are relatively barren (Deligne and others, 2013).

Worth relating here is a story about how one of the first ages was determined on Clear Lake lava flows. The age was determined on a sample collected by Taylor (1965) of a drowned Douglas-fir near Coldwater Cove Recreation Site. Taylor attempted to collect this sample by tying a cable to the drowned tree near the boat launch, then tying the cable to his truck and winching the tree out. Unfortunately, the cable snapped, nearly taking Taylor's head off in the process; fortunately, the tree was ultimately uprooted, sampled, and then dated.

Stop 12: Sahalie Falls to Koosah Falls—Water Flow Over and Through Young Lava

Directions to Stop 12 and Description of Hike

Return to Highway 126 and turn left (south). After 0.5 mile (0.8 km), turn right into the Sahalie Falls parking area. A Northwest Forest Pass is not required when parked here. Primitive bathrooms are available in the parking area.

The hike from Sahalie Falls to Koosah Falls (distance, 0.3 miles [0.5 km]) follows the trail downstream. The trail, which is clearly marked, is mostly downhill and easy, but it is not wheelchair accessible. At Koosah Falls, exit to the parking area.

For those who want to see both Sahalie Falls and Koosah Falls on foot, they both can be reached on a 3-mile (4.8-km) round-trip hike (the Waterfall loop trail). For those who want to see both waterfalls but do not want to hike the entire Waterfall loop trail, we recommend arranging for a shuttle pickup at Koosah Falls before hiking from Sahalie Falls to Koosah Falls.

The Waterfall loop trail (distance, 3 miles [4.8 km]), which we will not do today, continues from Koosah Falls to just north of Carmen Reservoir, then it loops around the west side of the McKenzie River past Sahalie Falls, crosses a bridge, and goes back down to Sahalie Falls. The Waterfall loop can also be done in the opposite direction, with access points at Carmen Reservoir, Sahalie Falls, and Koosah Falls. The Waterfall loop trail is not wheelchair accessible, although the trail to Sahalie Falls is. Dogs on a leash are permitted.

To drive from Sahalie Falls to Koosah Falls, exit the Sahalie Falls parking area and turn right (south) onto Highway 126. After 0.3 miles (0.5 km), turn right (west) into Koosah Falls and Ice Cap Creek Campground. Follow the road to the day use area in the campground.

Discussion of Stop 12

Sahalie and Koosah (“Heaven” and “Sky” in the Chinook language, respectively) Falls (fig. 21) are waterfalls that tumble over lobes of the Clear Lake South lava flow (unit CLS of the Sand group; fig. 17), which is responsible for the damming of Clear Lake (see, for example, Taylor, 1981; Sherrod and others, 2004; Deligne, 2012; Deligne and others, 2016). The waterfalls were first described by Stearns (1929). Today we will hike between these two waterfalls.

The McKenzie River flows south from Clear Lake. Initially its channel lies between Holocene Clear Lake South lava flows (CLS) to the east and older, glaciated, Pleistocene-age volcanic rocks to the west (fig. 19). One kilometer downstream of the outlet, the river flows onto the Clear Lake South lava flow (near the intersection of Highway 126 and Forest Road 770) and follows what appears to be a lava channel; lava-flow levees can be observed on both sides of the river (Deligne, 2012). Unlike at Collier Cone and White



Figure 21. A, Sahalie Falls. B, Koosah Falls. Photographs by Marli Miller, 2016.

Branch creek (optional Stop 7), not much channel incision appears to have occurred along this stretch of the McKenzie River.

At Sahalie Falls, the river plunges 23 m over a lobe of the Clear Lake South lava flow (CLS). Numerous springs also emerge from the lava flow where it is exposed at the base of Sahalie Falls. Interestingly, the base of Sahalie Falls is at the same elevation as the bottom of Clear Lake, suggesting that the valley profile was flat prior to the eruption of the Clear Lake South lava flow (Deligne, 2012). Note that the Sahalie Falls parking area is on a different unit, the Ice Cap lava flow (unit IC of the Sand group; figs. 17, 19).

South of Sahalie Falls, the McKenzie River channel traverses another lobe of the Clear Lake South lava flow (CLS), then it plunges 24 m off the lava flow at Koosah Falls. A number of springs are also visible at the base of Koosah Falls. South of Koosah Falls, the McKenzie River flows between the Clear Lake South lava flow and a Pleistocene unit to the east until it reaches Carmen Reservoir.

A curious feature of the upper McKenzie River channel is the pronounced amphitheatrelike shapes of Sahalie and Koosah Falls, which suggest headwall erosion. Preliminary measurements suggest that Sahalie and Koosah Falls have retreated 30 and 50 m, respectively. Given a flow age of about 3 ka, this suggests minimum retreat rates of 1 and 1.6 cm/yr, respectively. However, very little sediment is transported along this stretch of the McKenzie River, which suggests a limited capacity for erosion. Interestingly, small shallow potholes are present on top of Sahalie Falls, suggesting that rare high-discharge events may transport bedloads that have large clasts capable of quickly eroding the bed.

[Remainder of Stop 12 description is modified from Cashman and others (2009)]

Koosah Falls and nearby “Ice Cap” spring illustrate the multiple surface and subsurface flow paths of water through young volcanic terrains. Although water flows over a young lava flow at this location, evidence also exists for additional flow of water through the lava flows in this part of the McKenzie River. Between Clear Lake and Carmen Reservoir, a distance of only about 1.6 miles (2.5 km), about 6 m³/s (212 ft³/s) of flow is added to the river. Much of this water is discharged directly into the channel, as is illustrated just below Koosah Falls where springs discharge along flow boundaries within the valley walls. “Ice Cap” spring, on the other side of the Koosah Falls parking area, demonstrates that flow paths and discharge areas can be strongly controlled by local lava-flow topography. “Ice Cap” spring, appropriately named for its 4.7 °C temperature, feeds an 0.35 m³/s (12 ft³/s) creek that parallels the McKenzie River for 400 m before entering Carmen Reservoir (Cashman and others, 2009).

Stop 13 (Optional): Carmen Reservoir—Where the McKenzie River Goes Underground

Directions to Stop 13 and Description of Hike

Return to Highway 126 and turn right (south), then immediately turn right again (west) onto Forest Service Road 750. Follow the road around the north end of Carmen Reservoir, and park at the end of the road. Display a Northwest Forest Pass in your vehicle when parked.

The round-trip hike (distance, 1.6 miles [2.6 km]) joins the McKenzie River National Recreational Trail, either from the end of Forest Service Road 750 (a little scrambling up to the trail is required) or from the sign on the northwest end of Carmen Reservoir. Follow the trail southward for 0.8 miles (1.3 km) to a bridge that crosses the (generally dry) river channel. The hike is mostly flat and easy. Dogs on a leash are permitted.

Discussion of Stop 13

[Modified from Cashman and others (2009)]

Carmen Reservoir is part of a water-diversion-and-power-generation complex operated by the Eugene Water and Electric Board (EWEB). In 1958, the EWEB was issued a license by the Federal Energy Regulatory Commission to establish and operate the hydroelectric system, which became operational in 1963. At present (2017), the EWEB is in the final stages of renewing the license.

The McKenzie River flows for 2.5 km from Clear Lake to Carmen Reservoir. There, water is diverted to Smith Reservoir by way of an underground, 3,469-m-long, 3.9-m-diameter tunnel to join water from the Smith River. The combined water is then run through a second tunnel (2,217 m long by 4.1 m diameter) to Trail Bridge Reservoir. In this second tunnel, power that is generated has a maximum power output of 118 MW. At Trail Bridge Reservoir, water is returned to the McKenzie River, and the flow rates are closely controlled to mimic natural conditions (figs. 9, 22).

Directly south of Carmen Reservoir, no surface water flows from the McKenzie River, although this is not solely a function of the Carmen–Smith Reservoir diversion. Stearns (1929) noted that, at this location in September 1926, the McKenzie River “generally flows only in the spring, for during the rest of the year the water sinks into the permeable lava in the valley floor” (Stearns, 1929, p. 176). Stearns noted that the McKenzie River flows underground between the present-day Carmen Reservoir and “Tamolitch Pool” (“Lower Falls” in Stearns, 1929), where it reemerges after flowing either beneath or through an about-7-ka lava flow (Deligne

and others, 2016). The diversion has decreased the amount of water traveling through this stretch by about one-half: the discharge rate at “Tamolitch Pool” in October 2003 was 4.1 m³/s (Jefferson and others, 2006), which is roughly one-half of the discharge rate of 9.9 m³/s estimated by Stearns (1929).

From the southwestern margin of Carmen Reservoir, the McKenzie River National Recreational Trail eventually reaches a footbridge over the dry McKenzie River channel. Note that, despite the lack of surface flow and the young age of the lava, the channel is well defined and composed of large angular boulders. Farther downstream, boulders within the

channel are imbricated. Both channel creation and boulder imbrication require substantially larger surface flows than have been observed historically in this stretch of the McKenzie River. The valley itself was glacially carved, and several of the unusual morphologic features in this area, including the steep cliffs and the amphitheater immediately north of “Tamolitch Pool,” reflect this origin.

Stop 14 (Optional): “Tamolitch Pool”—Where the McKenzie River Reappears

Directions to Stop 14 and Description of Hike

Retrace your route around the north end of Carmen Reservoir, then follow Forest Service Road 750 to Highway 126; turn right (south) onto Highway 126. In 1.1 miles (1.8 km), Highway 126 will traverse the fresh-looking lava flows of the about-1,500-yr-B.P. Belknap lava flows (unit BEL; fig. 17), which are bracketed in age by the Clear Lake South lava flows (CLS) to the north and the about-7-ka Tamolitch lava flow (unit TAM; fig. 17) to the south. Shortly after MP 10, turn right (west) onto Forest Service Road 730 and cross the bridge to Trail Bridge Reservoir. Immediately after the bridge, turn right (north) at the intersection with Forest Service Road 655. Follow Forest Road 655 for about 0.4 miles (0.6 km) until it makes a sharp left turn; this is the Tamolitch Falls trailhead. Display a Northwest Forest Pass in your vehicle when parked.

From the Tamolitch Falls trailhead, hike north on the McKenzie River National Recreational Trail. The trail is clearly marked and is relatively easy, with a slight uphill gradient. “Tamolitch Pool” is about 2 miles (3.2 km) from the trailhead. The round-trip hike is 4 miles (6.4 km) long. As “Tamolitch Pool” is on the McKenzie River National Recreational Trail, another option is to continue along the trail from (optional) Stop 13 to “Tamolitch Pool,” a 6-mile-long (9.6-km-long) round-trip hike from Carmen Reservoir or a 5-mile-long (8-km-long) hike between Carmen Reservoir and the (optional) Stop 14 trailhead.

Discussion of Stop 14

“Tamolitch Pool,” also known as “Blue Pool,” is one of the most stunning sites in the central Oregon Cascades (fig. 23). From the Trail Bridge Reservoir trailhead, it is a 4-mile-long (6.4-km-long) round-trip hike on the McKenzie River National Recreational Trail.

The trail follows the McKenzie River upstream in a glacially carved valley. In about a mile (1.6 km), the trail crosses onto the basaltic Tamolitch lava flow (TAM; fig. 17); “Tamolitch Pool” is less than 1 mile (1.6 km) upstream from here. The Tamolitch

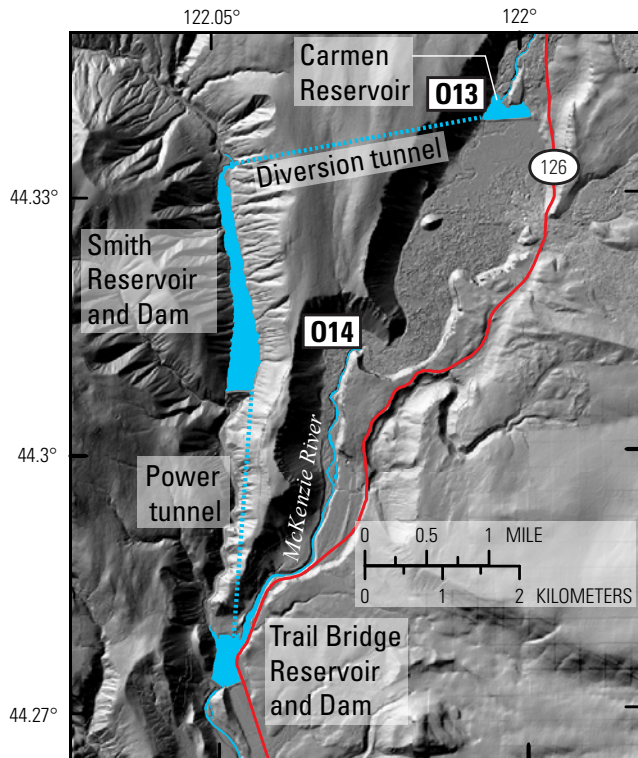


Figure 22. Shaded-relief map showing infrastructure of Carmen–Smith Hydroelectric Project on upper McKenzie River. Modified from Cashman and others (2009). River water is collected at Carmen Reservoir and diverted to Smith River drainage, then it is transferred back to McKenzie River drainage at Trail Bridge Reservoir for purpose of power generation. Field-trip stops shown by white rectangles; stop numbers are inside rectangles (0, optional stop). Shaded relief derived from lidar imagery (from Oregon Department of Geology and Mineral Industries, 2007–2010) where available and from 10-m digital elevation models (from Oregon Geospatial Enterprise Office, 2008) elsewhere. Surface water and roads traced from lidar imagery.



Figure 23. View to south of “Tamolitch Pool.” Outlet to McKenzie River is at far end of pool. Photograph by Marli Miller, 2016.

lava flow, which is of unknown origin (but is not part of the Sand Mountain volcanic field), likely erupted about 7 ka (Deligne and others, 2016), making it the oldest postglacial lava flow to enter the upper McKenzie River valley (fig. 17). It was erroneously mapped by Taylor (1965) and Sherrod and others (2004) as being an about-1,500-yr-B.P., late-stage Belknap flow. The lava flow has tumuli, pāhoehoe ropes, and, in several places, tree molds, some of which are along the trail slightly south of “Tamolitch Pool.” These tree molds, first noted by Stearns (1929), are vertical features that have a diameter similar to that of the largest trees along the trail.

As discussed in (optional) Stop 13, the McKenzie River disappears south of Carmen Reservoir, flowing through the Tamolitch lava flow (TAM) before reappearing at “Tamolitch Pool.” As noted earlier (and as observed by Stearns, 1929), this disappearance is not caused by the Carmen–Smith Reservoir diversion scheme.

“Tamolitch Pool” is remarkably clear and blue, and it has with a temperature of 5.4 °C (Jefferson and others, 2006). Water appears blue because the longer wavelengths of light (red and green) are absorbed when they interact with water molecules, leaving the shorter wavelengths (blue and violet) visible. Suspended particles in water scatter this light and may reflect other colors back to the surface, limiting the depth of view. In extremely pure water (that is, having a low concentration of suspended particles), light is able to pass through many meters of blue-colored water, and the refracted and scattered light we see remains blue. The deeper the clear water is, as in “Tamolitch Pool” and in many mountain lakes, the more blue the color.

Stop 15: Clear Lake—Source of the McKenzie River

[Note that, if you are following this field-trip guide after the IAVCEI Conference–sponsored field trip (August 19–24, 2017) has ended, we recommend that you hike to Great Spring by taking the Clear Lake loop trail]

Directions to Stop 15

From either Sahalie Falls, Koosah Falls (Ice Cap Creek Campground), Carmen Reservoir, or Trail Bridge Reservoir, return to Highway 126 and turn left (north). Soon after MP 4, turn right onto Forest Service Road 775 (at the sign for the Clear Lake Resort). Follow the road downhill to the parking area by the lake. Clear Lake Resort operates a restaurant, rental cabins, and a boat dock that has rowboat rentals. Bathrooms are available in the restaurant. A Northwest Forest Pass is not required when parked here.

We will have lunch here, and, after lunch, we will rent rowboats and then row to Great Spring. Note that no boat dock or ramp is located near Great Spring; we will be coming ashore on the north side of the inlet toward Great Spring and securing the boats as best we can. Great Spring can also be reached on foot by hiking along the 5-mile-long (8-km-long) Clear Lake Loop trail, either in the clockwise direction from the Clear Lake Resort or in the counterclockwise direction from the Coldwater Cove Recreation Site boat ramp (the shortest round trip hiking option, at 2.4 miles [3.9 km]).

Discussion of Stop 15

Clear Lake, which was briefly discussed at Stop 11, is bounded on three sides by lava flows of the Sand Mountain volcanic field (fig. 19). At this stop, we will focus on Clear Lake and Great Spring, which is close to the contact between two lava flows of the Sand Mountain volcanic field.

Clear Lake’s name stems from its remarkable clarity, which results from the inability of most organisms to grow in the 4.0 °C spring water that feeds the lake (Jefferson and others, 2006); roughly 10 percent of the water in Clear Lake comes from Great Spring (Stearns, 1929), which is situated on its northeastern shore. Great Spring emerges from beneath the Great Spring lava flow (unit GS of the Sand group; fig. 17), a few meters from its contact with the Coldwater Cove lava flows (unit CWC of the Lost Lake group; fig. 17). Stearns (1929) suggested that the Great Spring lava flow buried a preexisting creek, leading to the formation of the spring. The remainder of the water in Clear Lake comes from small springs along the edges and bottom of the lake. In addition, seasonal (late spring and early summer) runoff enters Clear Lake from the north in Ikenick and Fish Lake Creeks and, from the west, in a small, unnamed creek.

The lake is divided into three zones (fig. 24A; see also, Johnson and others, 1985; Deligne, 2012): a northern zone (maximum depth, 18 m); a southern zone, which covers most of the lake (maximum depth, 54 m); and a “pinched” zone that separates the northern and southern zones (maximum depth, 7 m). The southern zone is characterized by a deep, flat bottom and a shallow platform at the southernmost part of the lake, south of the Coldwater Cove Recreation Site boat ramp. The Clear Lake Resort boat dock is situated on the western margin of the “pinched” zone.

Submerged Douglas-fir trees are visible (fig. 25) from the Clear Lake Resort boat dock. These trees were drowned after the Clear Lake South lava flow (unit CLS of the Sand group; fig. 17) dammed the ancestral McKenzie River; the trees have been preserved in the cold water. Deligne (2012) mapped the location of 57 submerged trees (fig. 24A): in the northern and “pinched” zones, all trees are visible from the surface; in contrast, most trees

in the southern zone were not visible at the surface. In addition, divers from the Eugene Dive Club have observed many more submerged trees in the deepest parts of the lake that cannot be detected at the surface (Deligne, 2012).

An interesting part of Clear Lake’s story is that of the alternating bands of oxidized and fresh lavas (figs. 24B–24D) found along the margin of the Clear Lake East lava flow (unit CLE, the youngest unit of the Sand group; fig. 17), north of the Coldwater Cove Recreation Site boat ramp (Deligne, 2012). Thin sections (fig. 24C) show that these parts of the flow are quite glassy, suggesting that the flows were quenched by water. These alternating bands of oxidized and fresh lavas are not found south of the Coldwater Cove boat ramp where the Clear Lake East lava flowed onto a shallow (<10 m deep) platform. From this we infer that, at the time of the Clear Lake East lava flow, the lake level was more than 10 m lower than

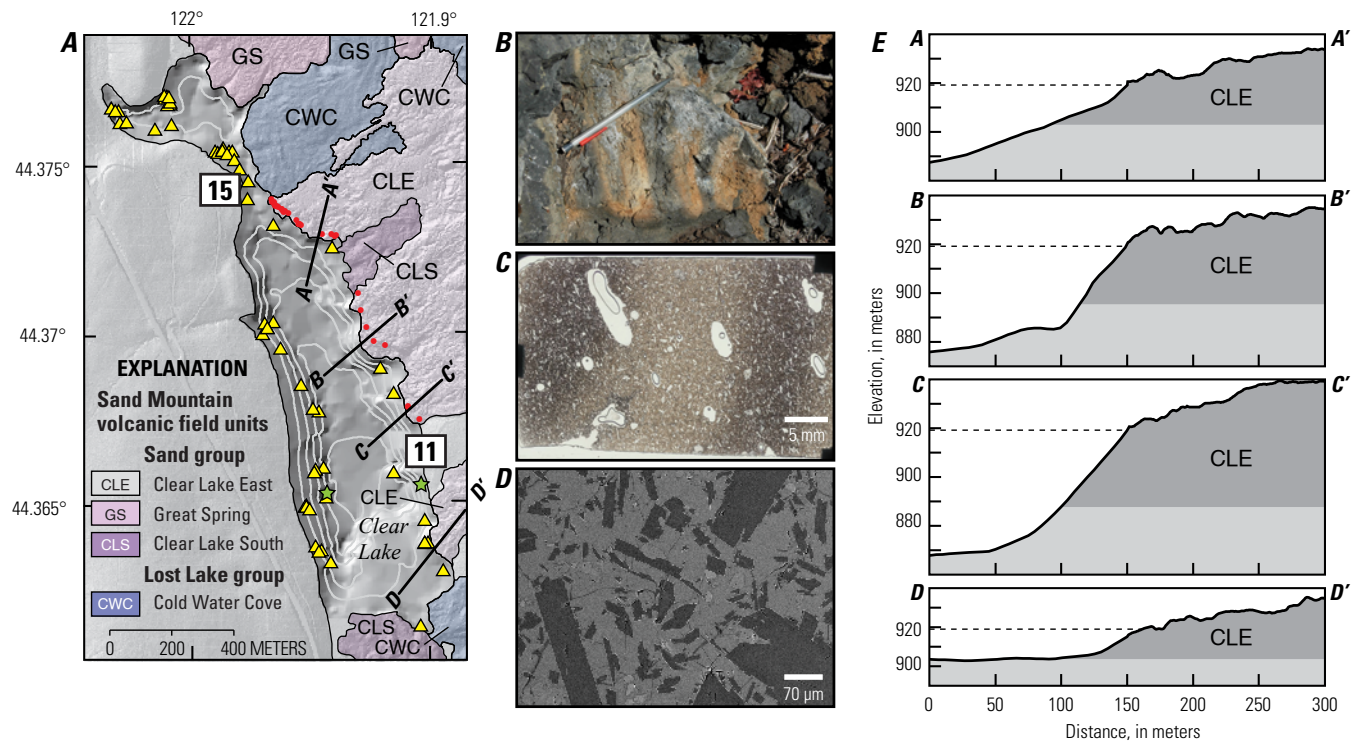


Figure 24. A, Shaded-relief map of Clear Lake area, showing bathymetry of Clear Lake, locations of drowned Douglas-fir trees (yellow triangles) in lake, and approximate locations of two dated (¹⁴C) Douglas-fir samples (green stars; Deligne and others, 2013). Modified from Deligne (2012). Also shown are lava flows of Sand Mountain volcanic field (from Deligne and others, 2016) and locations of topographic profiles shown in figure 24E; red dots indicate locations of Clear Lake East lava flows that contain oxidation bands shown in figure 24B. Field-trip stops shown by white rectangles; stop numbers are inside rectangles. Onshore shaded relief derived from lidar imagery (from Oregon Department of Geology and Mineral Industries, 2007–2010). Clear Lake boundary from traced from lidar imagery. Shaded-relief bathymetry and bathymetric contours from Deligne (2012); contour interval, 10 m. B, Photograph of Clear Lake East lava flow that contains oxidation bands. Photograph by Natalia Deligne, 2009. C, Photograph of thin section of Clear Lake East lava that contains oxidation bands (shown in figure 24B). Photograph by Lucy Walsh, 2011. D, Scanning electron microscope image of thin section in figure 24C, showing high glass content (light-gray areas). Image by Lucy Walsh, 2011. E, Topographic profiles that extend onshore from Clear Lake, showing schematic thicknesses of Clear Lake East lava flows (CLE; dark-gray layer) overlying presumably Pleistocene-age rocks (light-gray layer). Dashed line shows elevation of modern lake surface (919 m). Modified from Deligne (2012).

Figure 25. Drowned Douglas-fir tree in Clear Lake. Photograph by Natalia Deligne, 2009.



its current level. An alternative explanation is that banding only occurs when lava flows enter water more than 10 m deep. As lava flows entered the lake, lake level may have risen owing to water displacement.

Another intriguing observation is the oversteepened flow front of the Clear Lake East lava flow (CLE) where it enters the lake. These flow fronts were mapped using a fish-finding device (Deligne, 2012), and a pronounced difference in flow-front thickness was observed on either side of the Coldwater Cove boat ramp: north of the boat ramp, flow fronts are as much as 25 m thick, whereas south of the boat ramp, flow fronts are about 10 m thick, a more typical thickness for this lava flow. This may reflect the presence (north of the boat ramp) and absence (south of the boat ramp) of ponded water at the time that the Clear Lake East lava flow was erupted. Although no classic water-interaction features such as pillow basalt or hyaloclastite are present, quenching of the flow at the former lake boundary may have oversteepened the flow front. The observation that the flow extends into the current lake only to a depth of 20 to 30 m before stopping abruptly on a very steep slope ($\sim 20\text{--}30^\circ$) rather than flowing about 60 m farther west onto the flat platform at the bottom of the lake (fig. 24E) also suggests that the Clear Lake East lava flow was stopped, possibly by water, prior to reaching its natural destination.

Roughly 140 years separate the dates of death of a tree rooted at 40 m depth ($3,000 \pm 73$ calibrated yr B.P.; Deligne and others, 2013) and a tree rooted at a shallower (4 m) depth ($2,856 \pm 92$ calibrated yr B.P.; Licciardi and others, 1999); these two dates are statistically different at the 95 percent confidence level (error bars, 2σ). The 40-m-deep tree most likely drowned shortly after the emplacement of the Clear Lake South lava flow (CLS), whereas the 4-m-deep tree most likely drowned after the emplacement of the Clear Lake East lava flow (CLE). Given that the current water depth at the Clear Lake outlet is

about 5 m, the date of death of the 4-m-deep tree likely coincided with the establishment of the modern McKenzie River.

The modern volume of the lake is about $1.27 \times 10^7 \text{ m}^3$. If the fill rate is equal to the discharge rate at the Clear Lake outlet, Clear Lake would fill in 17 days; at a fill rate equal to the discharge rate into Carmen Reservoir (that is, the combined water flow out of the lake and through the lava dam), Clear Lake would fill in 10 days (Deligne, 2012). These estimates are orders of magnitude faster than the approximately 140 years that it apparently took for the lake to fill, suggesting that the Clear Lake South lava flow (CLS) was an extremely leaky dam for a long period of time. As was discussed at Stop 12, it remains a leaky dam.

[Remainder of Stop 15 description is modified from Cashman and others (2009)]

Clear Lake also provides a good opportunity to consider how the hydrology of this volcanic landscape is likely to change under conditions of a warming climate (fig. 26). Work by Tague and Grant (2009) suggested that streams in the Western Cascades are likely to respond quite differently from those in the High Cascades. Both downscaled climate models and empirical observations indicate that snowpacks in the Cascade Range are melting on the order of 1 to 3 weeks earlier than they did a few decades ago, and the snowpacks will continue to diminish in the future as the climate warms (Mote, 2003; Mote and others, 2005; Nolin and Daly, 2006; Jefferson and others, 2008; Tague and others, 2008). The consequences of reduced snowpacks and earlier melting on streamflow are likely to play out differently in the Western Cascades than in the High Cascades. Simulations of effects of future climate warming on streamflow using RHESSys (Regional Hydro-Ecologic Simulation System), a distributed-parameter, spatially explicit hydrologic model, reveal that streams in the Western Cascades will recede earlier in the year to minimum streamflow

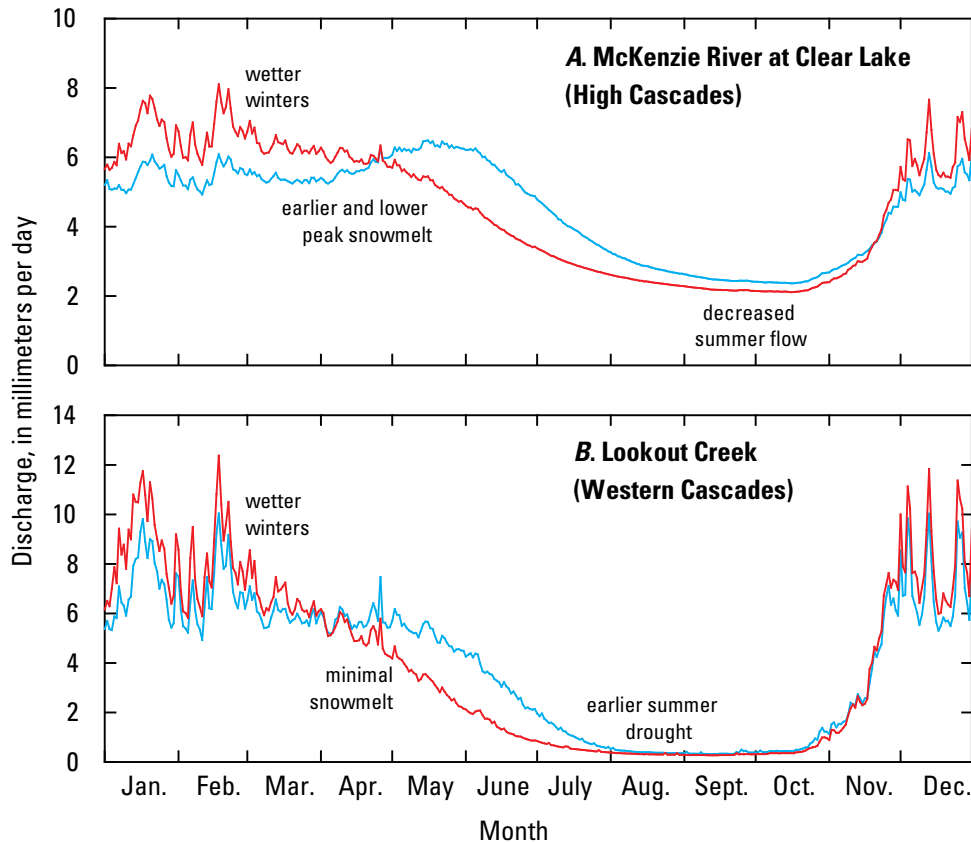


Figure 26. Modeled estimates of annual hydrograph and sensitivity to climate warming for (A) McKenzie River at Clear Lake and (B) Lookout Creek. Blue lines show estimated streamflow using base-line meteorologic data; red lines show estimated streamflow from 1.5 °C of warming. Mean unit discharge computed by averaging RHESSys (Regional Hydro-Ecologic Simulation System) estimates of daily streamflow (normalized by drainage area) for each day of year for 30-year climate record. From Cashman and others (2009), modified from Tague and Grant (2009).

levels that are similar to those currently observed in summer months (fig. 26B; modified from Tague and Grant, 2009). These low flows are remarkably stable year-to-year under all climatic conditions because they are constrained by an absence of significant groundwater storage. Streams in the High Cascades, on the other hand, will lose discharge peaks that are due to snowmelt and also recede earlier but, because of large groundwater storage flux, will continue to recede throughout the summer (fig. 26A). These results suggest that streams in the High Cascades will have winter flow levels that are higher than in the past, but they will also lose a larger proportion of their summer discharge than that of streams in the Western Cascades under conditions of climate warming.

Stop 16: Little Nash Crater

Directions to Stop 16

From Clear Lake Resort, return to Highway 126 and turn right (north). Continue north for about 3.3 miles (5.3 km) to where Highway 126 merges with Highway 20. Turn right (east) onto Highway 20 and continue for about 2.5 miles (4 km) to Forest Service Road 820 (located just past the road sign marked Little Nash Sno-Park, on the right side of Highway 20); turn left (north). Follow Forest Road 820 about 0.3 miles (0.5 km) to the top of Little Nash Crater.

Important note: be aware of quarry operations—if heavy machinery is being operated or other quarry activity is happening, we recommend that you skip this stop.

Discussion of Stop 16

Little Nash Crater, one of the northernmost vents of the Sand Mountain volcanic field, is disappearing, owing to quarry operations by the Oregon State Department of Transportation. The view from the top includes parts of the Sand Mountain volcanic field and several Brunhes-age (younger than about 0.8 Ma) mafic shield volcanoes, as well as older volcanic rocks that cap the scarp that bounds the High Cascades graben on the west. The dissected and glacially eroded western skyline is dominated by these older, chiefly 7.2- to 5.8-Ma rocks (Black and others, 1987; Priest and others, 1987). This stop is primarily for the view but can also be an opportunity to hunt for rare inclusions of quartz, perhaps vein quartz, that have been found in the scoria.

[Next two paragraphs are modified from Conrey and others (2002a)]

As is evident from this vantage point, the rather modest slope of the west scarp of the graben is much less steep than that of the east escarpment of the High Cascades graben along Green Ridge. The slope is modest because it essentially is a dip slope underlain by eastward-tilted fault blocks. The steepest parts of the scarp, which are just east of the higher summits, generally coincide with

major faults. The modest slopes east of the steeper scarps are underlain by eastward-tilted fault blocks in a zone that is generally about 5 km wide. Faulting also affects the sections that are exposed on the higher summits, which are generally tilted a few degrees eastward, as can be seen from here in Scar Mountain (note the prominent dark lava layer over the light-colored sedimentary layer) and Bachelor Mountain (northeast of Scar Mountain).

A sense of the young, north-striking faulting along the upper McKenzie River can be gained from the distant view to the south of the north-trending ridge between Carmen and Smith Reservoirs. The ridge is capped chiefly by reversely polarized, Matuyama-age (2.6–0.8 Ma) lava that has age-equivalent downfaulted blocks east of the McKenzie River (Avramenko, 1981; also, R. Conrey, unpub. data, 1997).

Maxwell Butte (relatively undissected) and Three Fingered Jack (heavily eroded), two prominent High Cascades mafic shield volcanoes, are visible to the northeast. Neither has been dated, but Maxwell Butte displays only minor erosion from glaciation and so is likely to be no older than 20 ka, whereas Three Fingered Jack probably experienced at least two major glaciations and, therefore, is likely older than 150 ka. To the southeast, the most prominent summit is the central plug of the eroded Mount Washington, another glaciated mafic shield volcano. The degree of dissection suggests an age that is somewhat younger than that of Three Fingered Jack. Also visible to the southeast (to the left of Mount Washington) is the late Pleistocene basaltic andesite cinder cone of Hoodoo Butte (and its ski area), which was largely shielded from glacial erosion because the steep-sided andesitic tuya of Hayrick Butte just upslope blocked glacial ice from overriding the easily erodible cinder cone (Sherrod and others, 2004). The view of Hayrick Butte is partly obscured from here. Hayrick Butte represents a rare eruption of intermediate-composition magma similar to that of Hogg Rock, located along the mafic-dominated arc between the Three Sisters volcanic cluster to the south and Mount Jefferson to the north.

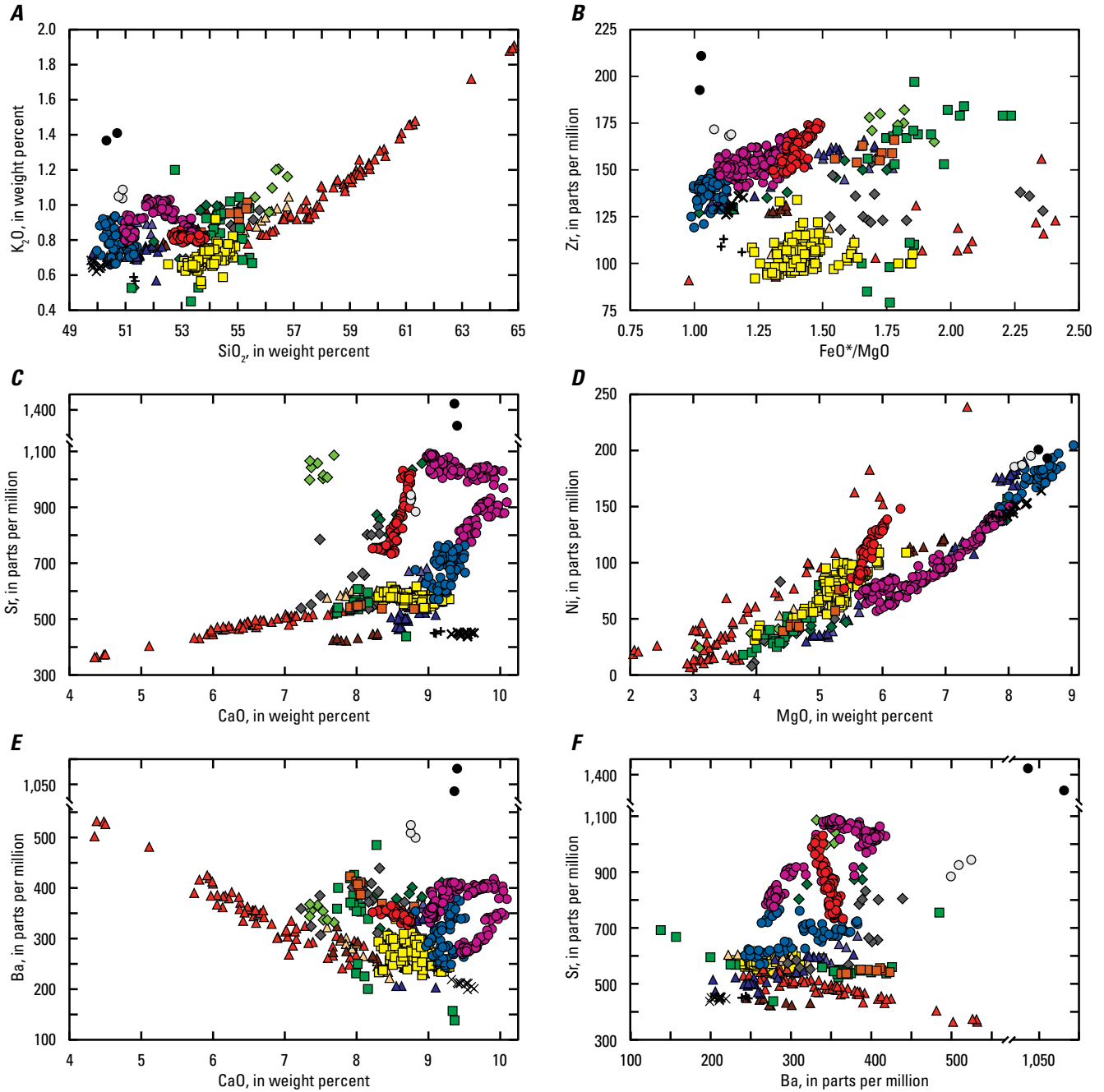
The large cinder cone to the right (northwest) of Mount Washington is Nash Crater, the vent for at least two lava flows that flowed westward nearly to the McKenzie River (Sherrod and others, 2004; Deligne and others, 2016). The lava compositions from Nash Crater and Little Nash Crater are very similar, and both overlie the newly recognized “orphan” “Early Nash” lavas (units “EN I” and “EN II” of Deligne and others, 2016). Unit “EN II” was erupted from a vent (or vents) now buried by Nash Crater. To the left (southeast) of Nash Crater lies the northernmost vent of the chain of cinder cones of the Sand Mountain volcanic field. The vents of the Sand Mountain volcanic field fed extensive lavas that flowed primarily westward (to Clear Lake, as is seen at Stops 11 and 15) but also to the northwest, south, and east. Almost due east from our vantage point is the Lost Lake cinder cone chain (see Stop 17); lavas from those vents flowed westward to the McKenzie River drainage and dammed it, forming both Lava Lake and Fish Lake. Lavas from the Nash Crater and Little Nash Crater eruptions, as well as from the “Early Nash” eruptions, overlie the Lost Lake lavas.

Compositional variation in the Sand Mountain volcanic field is complex (fig. 27) and worthy of additional study. We

sampled extensively during our mapping, owing to the complex geology, the difficulty in distinguishing sparsely phyrific hand specimens, and the need to correlate lavas with scoria from vents. The composition of individual lavas is relatively homogeneous, therefore allowing us to positively distinguish different eruptive events (Deligne and others, 2016). The homogeneity of individual flows is especially notable compared with those of other Holocene eruptions in central Oregon such as, for example, Collier Cone and Yapoah Crater (Deardorff and Cashman, 2012; see also, figs. 12, 27 of this report).

The Sand Mountain volcanic field consists of basalt and basaltic andesite exclusively, with a range from 50 to 54 wt. percent SiO_2 (fig. 27A). The basaltic lavas at Sand Mountain are all similar to the common High Cascades calc-alkaline basalt as defined by Schmidt and others (2008) and Rowe and others (2009). The basaltic andesite compositions at Sand Mountain are mostly unlike those of the two types of basaltic andesite most commonly found in central Oregon (Hughes and Taylor, 1986). The most common is the Mount Washington type, which has higher incompatible-element (for example, K, Zr, Ba) concentrations when compared with the more atypical incompatible-element-poor North Sister type (Hughes and Taylor, 1986; Schmidt and Grunder, 2009). Data from the type volcanoes are shown in figure 27. Several High Cascades mafic shield volcanoes (for example, Three Fingered Jack and Black Crater) have erupted both Mount Washington and North Sister types of lava during their lifetimes, with the North Sister type commonly following the Mount Washington type. The compositional variations in both of these magma types are consistent with a strong crystal fractionation control. For example, the increase of K_2O with SiO_2 , the increase of Zr with FeO^*/MgO ratio, the decline of Sr and increase of Ba with declining CaO, and the decline of Ni with MgO (fig. 27) are all consistent with crystal fractionation of the common minerals (olivine, Cr-spinel, clinopyroxene, and plagioclase) that are found as phenocrysts in High Cascades mafic lava. The Sr concentrations of these common lava types normally do not exceed 600 ppm, whereas most of the Sand Mountain lavas contain more than 700 ppm (and as much as 1,100 ppm) Sr (fig. 27C). The lavas at Sand Mountain are more similar to those erupted from the less common type of central Oregon mafic shield volcano that is enriched in Sr (but not in K), such as Maxwell Butte and Turpentine Peak (older than, and north of, Maxwell Butte).

Any fractionation that has affected the compositional variations at Sand Mountain, consistent with the decline of Ni with MgO and the coupled increase in Zr and FeO^*/MgO (fig. 27B), was likely a very deep crustal process where plagioclase either was not present or was unstable, as is suggested by the incompatible behavior of Ba, Sr, and CaO (figs. 27C, 27E). Several variations suggest that mixing of magmas from different sources was important, to account for the increase in K_2O but little or no change in SiO_2 in the Lost Lake and Sand Mountain group lavas, as well as the continuous variations in Sr but little or no change in CaO or Ba (figs. 27C, 27F). The earliest eruptions of the volcanic field, the Jack Pine and SnoPark lava flows (fig. 17), are compositionally much



EXPLANATION

Sand Mountain volcanic field

- Nash group
- Sand group
- Lost Lake group
- SnoPark
- Jack Pine

Other units not in Sand Mountain volcanic field

- + Inaccessible
- × Tamolitch

Three Sisters region

- ▲ Belknap Crater and Little Belknap
- ▲ Collier Cone
- ▲ Yapoah Crater
- ▲ Sims Butte
- ▲ Scott Mountain
- ◆ Black Crater
- ◆ Maxwell Butte
- ◆ Turpentine Peak

Major stratovolcanoes

- North Sister
- Mount Washington
- Three Fingered Jack

Figure 27. Compositional variations in units in Sand Mountain volcanic field compared with those in selected mafic volcanoes in central Oregon High Cascades. Stratigraphic relations of Sand Mountain volcanic field shown in figures 17 and 18. Data sources: R. Conrey, unpub. data (2003); Schmidt (2005); Deardorff and Cashman (2012); Deligne and others (2016). *A*, K_2O versus SiO_2 ; *B*, Zr versus FeO^*/MgO (measure of fractionation; FeO^* is total Fe calculated as FeO); *C*, Sr versus CaO; *D*, Ni versus MgO; *E*, Ba versus CaO; *F*, Sr versus Ba.

different from the other Sand Mountain lavas, as well as from the Sr-rich basaltic andesite type noted above; they resemble the rare Sr- and K-rich shoshonite lavas found throughout the High Cascades (see, for example, Bacon, 1990).

The chemical data indicate that at least two, and more likely three or more, sources were involved in Sand Mountain magma genesis. One of the sources could be the calc-alkaline basaltic magma that gives rise to the common Mount Washington-type basaltic andesite. If that basaltic magma had fractionated deep in the crust, both Sr and CaO would have behaved as incompatible elements. The second source could be the K-poor, Sr-rich type of basaltic andesite found in the central Cascades. That type may be related to similar K-poor, but Sr-rich, andesite that is hypothesized to have been derived from deep-crustal partial melting of mafic granulite, which is found at several High Cascades stratovolcanoes (for example, at Mount Jefferson [Conrey and others, 2001] and Crater Lake [Ankney and others, 2013]). Mixing of common Cascade Range calc-alkaline basalt with such andesite would yield Sr-rich basaltic andesite, which would account for the steep and continuous changes in composition found at Sand Mountain. An additional shoshonitic source is required for the Jack Pine lava flow eruption, and perhaps for the SnoPark lava flow eruption as well. A further source, or perhaps process, is required to account for the high Ni content, versus MgO, found in the Nash group lavas (fig. 27D). Many of the more evolved (that is, <5.5 wt. percent MgO) High Cascades basaltic andesites have higher Ni than Cr contents, a feature not restricted to any magma type (and also common in many highly evolved mafic rocks). But the high Ni content seen in the Nash group, as well as in some of the more primitive Belknap Crater lavas (fig. 27D), is puzzling and indicates either mixing with a unique Belknap Crater-type source or an assimilation(?) process that enriches mafic magma in Ni relative to Cr (not shown but closely correlated with MgO, unlike Ni). Schmidt and Grunder (2011) demonstrated that mafic magma recharge in an open system chamber can account for an increase in the Ni/Mg ratio seen at the polygenetic North Sister volcano, but we are uncertain that a recharge model is applicable to a monogenetic eruption. However, recent determinations of both

magmatic CO₂ and hydrothermal Cl⁻ flux rates in the Cascade Range indicate that volatile fluxes and, hence, mafic magma intrusion rates may be relatively constant, unlike the punctuated record of eruptions (James and others, 1999; Evans and others, 2004; Ingebritsen and others, 2014). If that is correct, even monogenetic eruptions could be sampling magma bodies that have undergone multiple recharge events.

Stop 17: Lost Lake—Tephra, Hydrology, and a Tale of Resource Management

Directions to Stop 17

From Little Nash Crater, return to Highway 20 and turn left (east). Continue east for about 0.9 miles (1.5 km) to where Highway 22 merges with Highway 20. Continue east on Highway 20 for about 1.6 miles (2.6 km), then turn left (north) onto Forest Service Road 835. Follow the road for 0.6 miles (0.9 km) to a small day use parking area near the northwestern shore of Lost Lake. Display a Northwest Forest Pass in your vehicle when parked.

From the day use parking area, several unmarked trails head southeastward toward Lost Lake. Follow the most prominent trail for about 600 ft (about 180 m) to several shallow sinkholes. Note that the trails and sinkholes may or may not be accessible, depending on the water level in the lake.

Discussion of Stop 17

We stop at Lost Lake because it is a pleasant area that has picnic tables and pit toilets, and it is the site of several interesting stories. We will take this opportunity to discuss the tephra component of the Sand Mountain volcanic field, and we will touch on the hydrology of Lost Lake and how it may have been altered by recent resource-management practices.

Lost Lake is a shallow, closed-basin lake that has several sinkholes in the lakebed (fig. 28). Lake levels fluctuate annually

Figure 28. View to southwest of large sinkhole at Lost Lake. Photograph by Daniele McKay, 2016.



by more than 1 m, the highest water levels occurring during spring snowmelt and the lowest at the end of the summer. Water that drains from Lost Lake by way of subsurface is inferred to reemerge in Clear Lake (Jefferson and Grant, 2003), an inference that is based on the fact that quite a bit of relief is present that would preclude drainage to the north and east of Lost Lake and also that all of the youngest lava flows flowed south into the Clear Lake topographic watershed.

An interesting (but poorly documented) account tells some of the recent management history of the lake. Lost Lake, which is popular for sport fishing, hosts a naturalized population of brook trout, and it is annually stocked with rainbow trout by the Oregon Department of Fish and Wildlife (A. Farrand, oral commun., 2016). According to a draft management plan by Oregon Department of Fish and Wildlife, the water level in Lost Lake had been stabilized in 1957 by blocking two surface outlets located along the northwestern shore of the lake (Oregon Department of Fish and Wildlife, 1982). In 1987 several holes were excavated to provide additional refuge areas for fish (A. Farrand, oral commun., 2016); presumably, these are the sinkholes that can be seen in the lakebed during low-water periods. However, excavations to make

the lake deeper likely achieved the opposite result by increasing the permeability of the substrate and, thus, reducing the overall water level of the lake. The Oregon Department of Fish and Wildlife sealed and refilled at least one of the holes (A. Farrand, oral commun., 2016); in addition, the U.S. Forest Service has found evidence that people have tried to seal some of the sinkholes with boulders, wood, and other debris (T. Baker, oral commun., 2016). A 2015 news video that shows water draining into one of the sinkholes was widely circulated on the internet (<https://www.youtube.com/watch?v=wqlhmXJeb5s>).

The location of Lost Lake near the Sand Mountain volcanic field would make it an ideal basin to preserve tephra from the Sand Mountain cinder cones. However, sediment cores from the lake show poor stratigraphy; therefore, if tephra from the Sand Mountain volcanic field is present, it cannot be discerned from tephra from other sources. Tephra from the Sand Mountain volcanic field is preserved in other lakes, in wetlands, and on dry land near Lost Lake (fig. 29). The mapped extent of the tephra deposit covers an area of about 154 km², and the deposit is more than 2 m deep as far as 9 km from the vent and more than 1 m deep about 12 km from the vent. The volume of the mapped

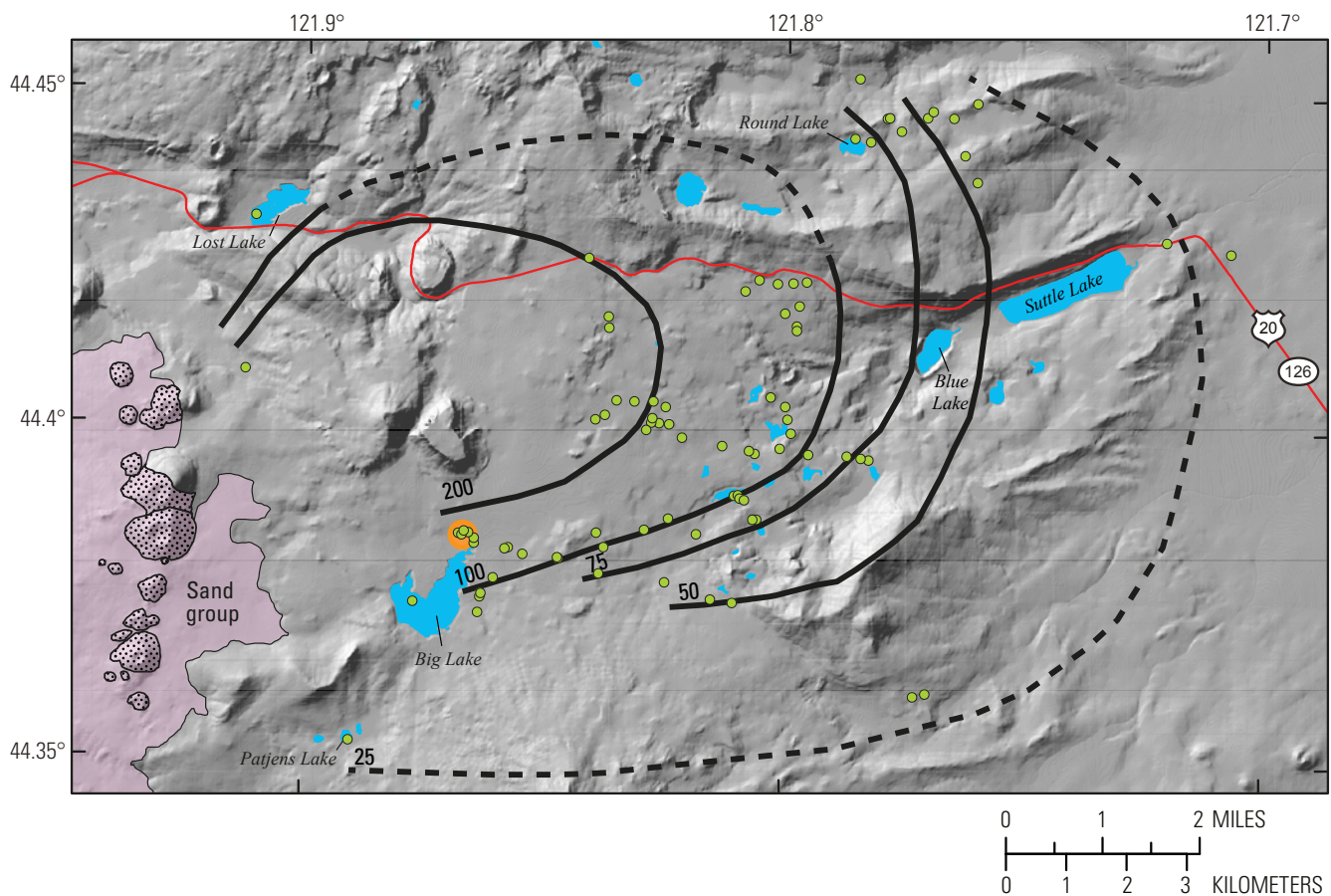


Figure 29. Shaded-relief map and isopachs showing thickness (in centimeters) of tephra deposits from Sand Mountain volcanic field. Modified from McKay (2012). Isopachs dashed where inferred or poorly constrained. Green dots show locations where tephra-deposit thicknesses were measured; large orange dot shows location where complete tephra stratigraphy was described and sampled. Pink shading shows extent of lava flows from Sand group; stippled areas are vents (from Deligne and others, 2016). Shaded relief derived from 10-m digital elevation models (from Oregon Geospatial Enterprise Office, 2008). Lakes from Pacific Northwest Hydrography Framework Group (2005a). Roads from Oregon Department of Transportation (2015).

deposit, as estimated from isopachs, is about 0.387 km³ (table 2). In general, the deposit is well exposed east of the vents, but, to the west, it is obscured by the extensive Sand Mountain volcanic field and by the steep slopes and dense vegetation of the Western Cascades, making it very difficult to trace the extent of the tephra deposit in that direction. Therefore, the deposit has not been mapped to the west, and, thus, the total area and volume of the tephra deposit likely are significantly underestimated.

Reconstructing accurate isopachs for tephra deposits can be difficult because the deposits are easily eroded, can be reworked by biotic activity, or are covered by subsequent lava flows from the same vent or other vents within the volcanic field. It can be especially difficult to reconstruct areas covered by trace deposits

(in this case, less than 25 cm thick) because thin deposits often are eroded or reworked quickly. For these reasons, tephra production from cinder cones is often either underestimated or not accounted for at all; however, original volumes can be estimated using thinning trends for tephra deposits from well-documented, historic cinder-cone eruptions where trace deposits were measured shortly after the eruption (fig. 30). This method gives a maximum-volume estimate of 1.13 km³ for the Sand Mountain tephra that is based on the thinning trend for the 1943–52 eruption of Volcán Paricutin, Mexico (table 2), which is a good analog for the Sand Mountain eruption because the isopachs for both deposits cover similar areal extents (fig. 31). Although this approach is an improvement on the minimum-volume estimate in table 2, the maximum-volume

Table 2. Estimates of minimum and maximum volume for tephra deposits in the central Oregon Cascades and from other cinder-cone eruptions where trace deposits are known.

Vent name	Volume (km ³)		Reference
	Minimum	Maximum	
Four in One Cone	0.002	0.003	Mckay (2012)
Collier Cone	0.037	0.069	Mckay (2012)
Sand Mountain	0.387	1.13	Mckay (2012)
Volcán Cerro Negro, Nicaragua	0.002	0.003	Hill and others (1998)
Volcán Paricutin, Mexico	0.325	1.3	Fries (1953); Luhr and Simkin (1993)
Cinder Cone, Lassen Volcanic National Park, Calif., U.S.A.	0.024	0.035	Clynne and Muffler (2010)
Sunset Crater, Ariz., U.S.A.	0.486	0.972	Ort and others (2008)

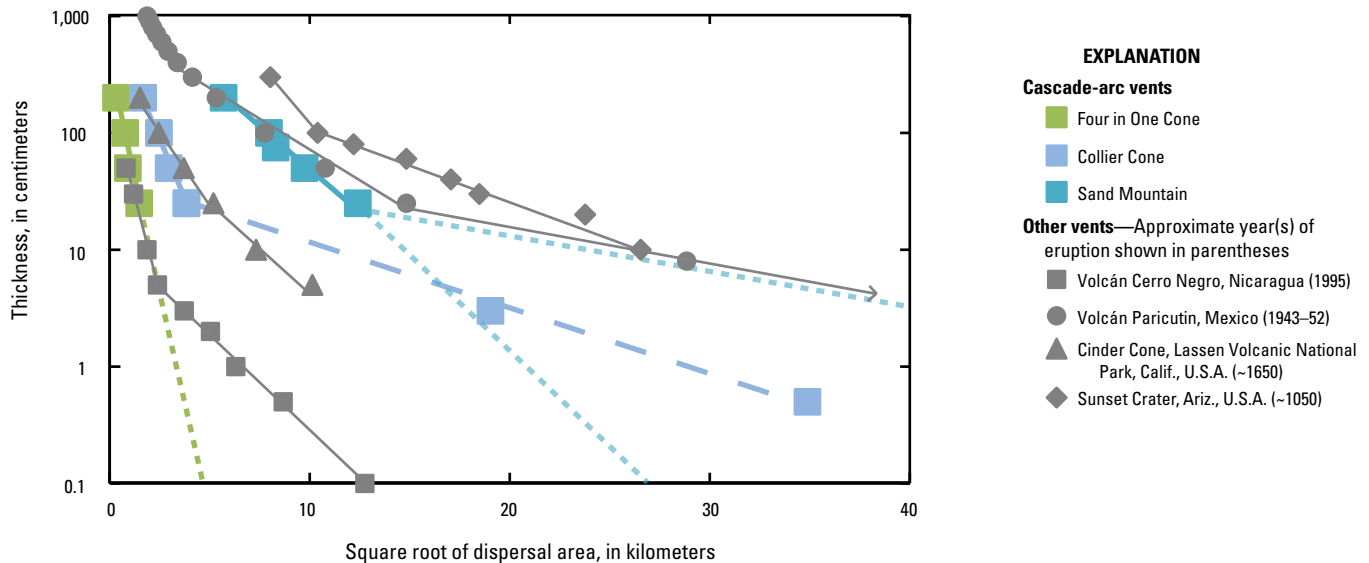


Figure 30. Plot showing thickness versus dispersal area for Cascade-arc tephra deposits (colored data points and lines) compared to those of other selected cinder-cone eruptions (gray data points and lines). Modified from McKay (2012). For Cascade-arc vents, solid lines connect points derived from isopachs at least 25 cm thick; dashed line for Four in One Cone represents estimated thinning trend; dashed line for Collier Cone connects data points, which are derived from trace deposits preserved in lake sediments; upper and lower dashed lines for Sand Mountain represent minimum and maximum estimates, respectively, for thinning trends. Arrow on thinning trend for Volcán Paricutin indicates that thinning trend extends outside of graph to 0.1 cm thickness, which corresponds to dispersal area of 242.24 km². Data source for Four in One Cone, Collier Cone, and Sand Mountain is McKay (2012). Data sources for other cinder-cone eruptions: Cinder Cone, Clynne and Muffler (2010); Sunset Crater, Ort and others (2008); Volcán Cerro Negro, Hill and others (1998); Volcán Paricutin, Fries (1953).

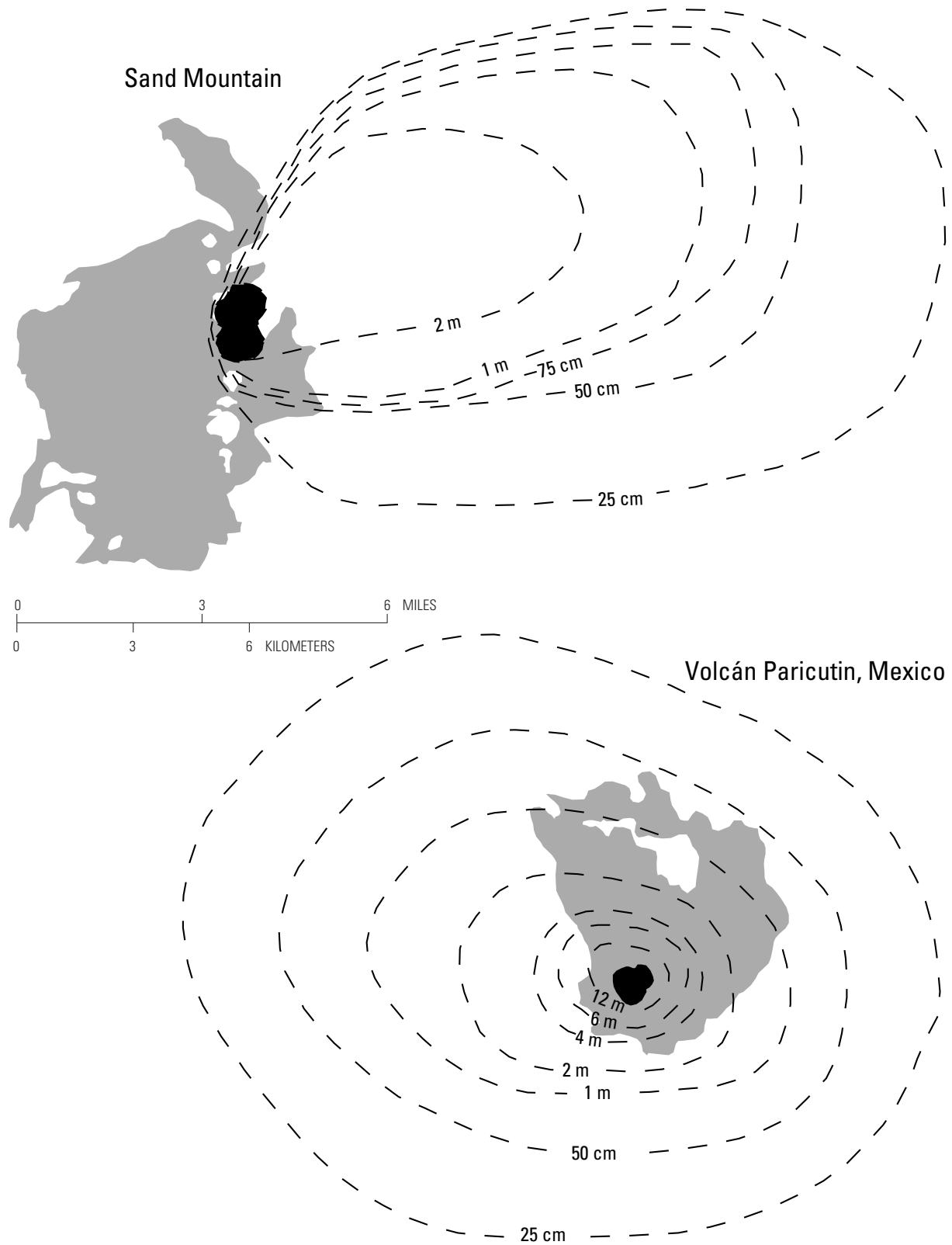


Figure 31. Isopach maps comparing thicknesses of tephra deposits (dashed lines) from Sand Mountain (Mckay, 2012) and Volcán Paricutin, Mexico (Segerstrom, 1956). Black areas, cinder-cone vents; gray areas, extent of lava flows (extent of Sand Mountain lava flows from Deligne and others, 2016; extent of Volcán Paricutin lava flows modified from Segerstrom, 1956).

estimate of 1.13 km³ is still likely to be an underestimate because it does not account for tephra deposited west of the vents where steep topography, vegetation, and (or) lava flows may obscure the deposits.

The Sand Mountain tephra deposit is striking in that it is consistently fine grained at every location where it has been recorded, making it easily recognizable in the field. The deposit lies stratigraphically above a gray, clay-rich paleosol that contains rounded pebbles and cobbles and, in many locations, abundant lenses of charcoal. The stratigraphy of the deposit is characterized by hundreds of interbedded layers of fine-, medium-, and coarse-grained ash. The entire deposit is very well sorted and is dominated by clasts that range from about 0.5 mm to 100 μ m (fig. 32); lapilli-sized clasts are completely absent throughout the entire deposit. Grain-size distributions and sorting have been used to make interpretations about eruption styles at mafic vents. Eruptive activity at other Cascade Range cinder cones can be categorized as Hawaiian, Strombolian, or violent Strombolian on the basis of grain size and sorting of the tephra deposits, but most of the Sand Mountain deposit does not fall into any of these categories (fig. 32).

Grain-size and sorting data from Taal, Philippines, also are shown in figure 32 (see also, Waters and Fisher, 1971). The Taal eruption was characterized by phreatomagmatic activity that produced wet pyroclastic-surge deposits. Although the Sand Mountain deposit resembles that of the Taal eruption in terms of grain-size distributions, Sand Mountain tephra layers are much better sorted. Individual layers within the deposit are very thin

(several millimeters to several centimeters thick) and laminar, and they show no cross-stratification. These bedding features, along with the extremely well sorted nature of the deposit, indicate that the Sand Mountain tephra sequence is dominated by fall deposits rather than pyroclastic-surge deposits, which are characterized by crossbedding and poorly sorted layers (fig. 32).

Microtextural features of the Sand Mountain tephra indicate that magma interacted with water during the eruption. Figure 33 compares magmatic and phreatomagmatic features of tephra clasts from the 2010 eruption of Eyjafjallajökull, Iceland, with those of tephra clasts from Sand Mountain and Collier Cone (on the north flank of North Sister). Magmatic tephra clasts have fluidal shapes and abundant microvesicles (figs. 33A, 33B); in contrast, phreatomagmatic clasts are denser and have blocky, equant shapes and stepped fractures (figs. 33C, 33D), both of which are characteristic of brittle fragmentation caused by interaction with water (see, for example, Heiken, 1972; Wohletz, 1983; Büttner and others, 1999; Dellino and Kyriakopoulos, 2003). Sand Mountain clasts are very similar to those produced during phreatomagmatic phases of the Eyjafjallajökull eruption. Additionally, clast surfaces show evidence of very fine microscale cracking that indicates rapid quenching by water (fig. 33E; see also, for example, Büttner and others, 1999; Dellino and Kyriakopoulos, 2003). These microtextural features are present throughout the entire stratigraphy of the Sand Mountain tephra deposit.

Grain-size distributions, sorting, and microtextures of the Sand Mountain tephra indicate that the eruption was characterized by phreatomagmatic activity but that ash particles were transported by an eruption column rather than by wet base surges that are typically associated with phreatomagmatic eruptions. The eruption may have been similar to phreatomagmatic phases of the 2010 Eyjafjallajökull eruption. Fall deposits from Eyjafjallajökull are well sorted, fine grained, and dominated by ash-sized clasts and rare lapilli clasts (Dellino and others, 2012). Grain-size distributions from Eyjafjallajökull reported in Dellino and others (2012) are very similar to those of Sand Mountain; however, the volume of tephra produced by the Sand Mountain eruption is considerably larger than the about 0.14 km³ produced by Eyjafjallajökull (Gudmundsson and others, 2010), indicating that either the Sand Mountain eruption was much more explosive or the activity was prolonged over a longer period of time.

The relatively large tephra deposit from Sand Mountain indicates that tephra from central Oregon mafic vents can travel considerable distances. Future eruptions could have consequences for transportation, agriculture, and infrastructure throughout central Oregon. Widespread disruption of transportation during the 2010 Eyjafjallajökull eruption in Iceland is well documented (see, for example, Barratt and Fuller, 2010; Gudmundsson and others, 2012; Alexander, 2013). Effects of tephra on agriculture and infrastructure are also well documented and can be severe, especially in arid regions similar to central Oregon (see, for example, Craig and others, 2016). Tephra deposits that are less than 10 mm thick can be enough to cause tooth abrasion in livestock (see, for example, Wilson and others, 2011; Craig and others, 2016) and disrupt photosynthesis in crops (see, for example, Cook and others, 1981; Craig and others, 2016).

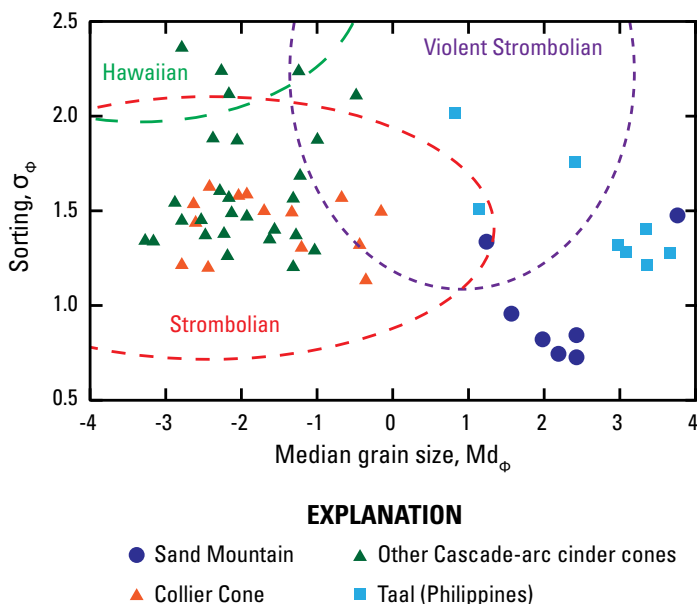


Figure 32. Plot showing sorting (σ_{ϕ}) versus median grain size (Md_{ϕ}) for tephra deposits from eruptions of Sand Mountain, Collier Cone, and other Cascade-arc cinder cones, as well as of Taal, Philippines. Fields defining eruption styles from Walker and Croasdale (1972), Parfitt (1998), Houghton and Gonnermann (2008), and Pioli and others (2008). Data from Taal represent phreatomagmatic activity that produced wet surge deposits (Waters and Fisher, 1971).

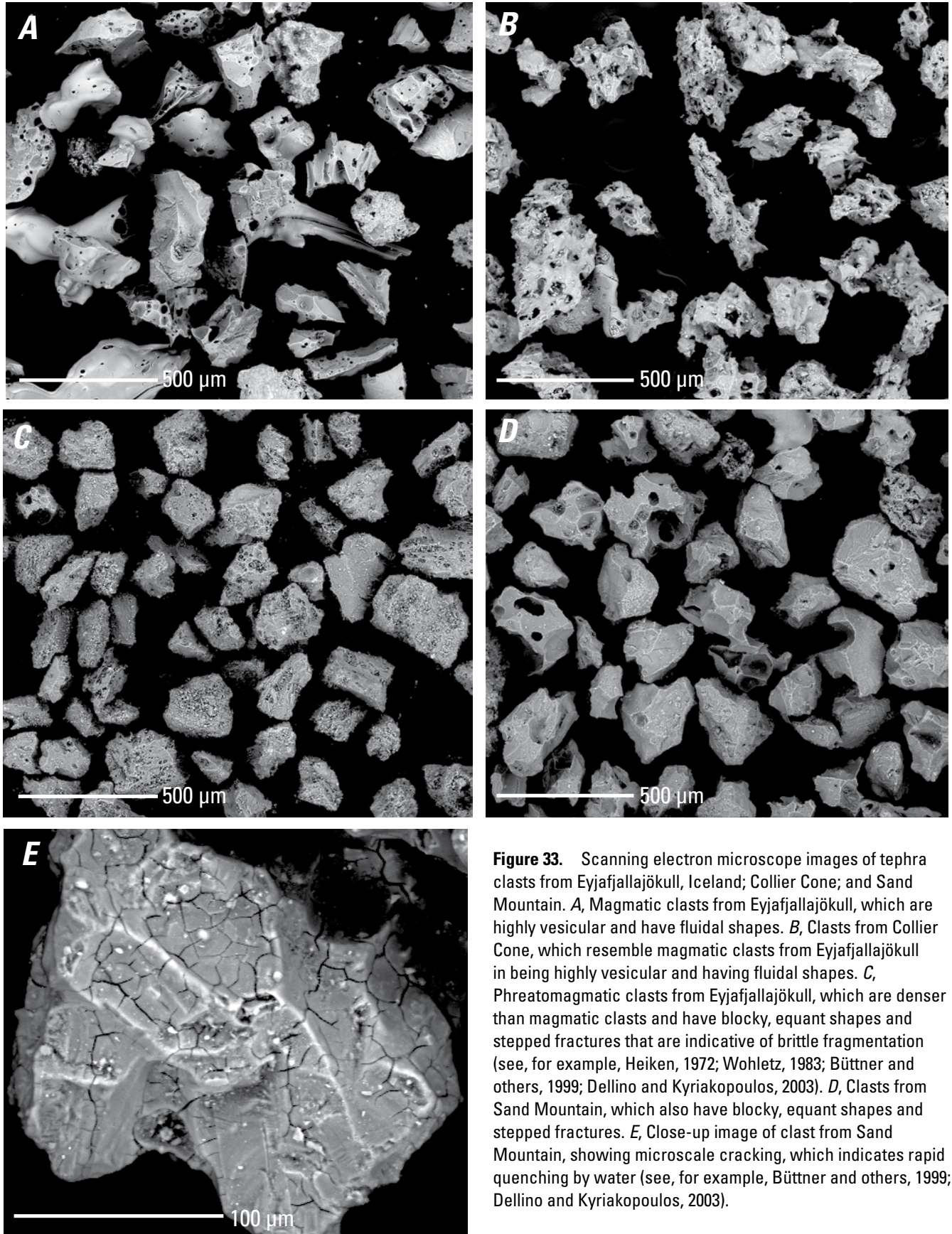


Figure 33. Scanning electron microscope images of tephra clasts from Eyjafjallajökull, Iceland; Collier Cone; and Sand Mountain. *A*, Magmatic clasts from Eyjafjallajökull, which are highly vesicular and have fluidal shapes. *B*, Clasts from Collier Cone, which resemble magmatic clasts from Eyjafjallajökull in being highly vesicular and having fluidal shapes. *C*, Phreatomagmatic clasts from Eyjafjallajökull, which are denser than magmatic clasts and have blocky, equant shapes and stepped fractures that are indicative of brittle fragmentation (see, for example, Heiken, 1972; Wohletz, 1983; Büttner and others, 1999; Dellino and Kyriakopoulos, 2003). *D*, Clasts from Sand Mountain, which also have blocky, equant shapes and stepped fractures. *E*, Close-up image of clast from Sand Mountain, showing microscale cracking, which indicates rapid quenching by water (see, for example, Büttner and others, 1999; Dellino and Kyriakopoulos, 2003).

Stop 18: Mount Washington Overlook and Blue Lake Crater

Directions to Stop 18

From Lost Lake, return to Highway 20 and turn left (east) onto the highway. Continue east around the western margin of Hogg Rock (about 3 miles [4.8 km] from Lost Lake). Cross Santiam Pass in about 1.5 miles (2.4 km) and continue another about 3.9 miles (6.3 km) to the Mount Washington and Blue Lake crater overlook, on the right.

Discussion of Stop 18

[Modified from Cashman and others (2009)]

From Lost Lake, Highway 20 passes Hogg Rock, one of two andesitic tuyas that resulted from Pleistocene volcanism in this area (the other tuya is Hayrick Butte, to the south). Hogg Rock has an age of 0.08 Ma (Hill and Priest, 1992), which is correlative with the onset of Wisconsin-age glaciation. The spectacular exposure of glassy, fine-scale columnar jointing in the Hogg Rock roadcut provides an example of ice-contact morphology, in which the columnar jointing formed by rapid cooling of the lava at the ice (water) interface (see, for example, Lescinsky and Fink, 2000).

This stop consists of two parts: first, a photography stop that has a spectacular view of Mount Washington and, second, an overlook of Blue Lake maar crater, another form of lava-water interaction. Blue Lake crater is discussed in (optional) Stop 19.

Mount Washington is a mafic shield volcano composed of basaltic lava flows, accumulations of palagonitic tuff (evidence of subglacial eruption), and a central micronorite plug (Hughes and Taylor, 1986; Taylor, 1990a; Conrey and others, 2002a). No isotopic ages for Mount Washington have yet been published, but all samples have normal-polarity magnetization, which, when considered with the geomorphology, indicates that Mount Washington is younger than 0.78 Ma (that is, the time of the Brunhes-Matuyama reversal).

Stop 19 (Optional): Blue Lake Crater—A Central Cascades Maar

Directions to Stop 19 and Description of Hike

From the Mount Washington and Blue Lake crater overlook, turn left (west) onto Highway 20 and backtrack about 0.8 miles (1.3 km) to the road sign for Corbett Memorial State Park. Turn left (south) into the parking area for the trail to Corbett Memorial State Park. From here, the roads are rough and may be seasonally closed or, at best, are unmaintained, so be prepared to hike the rest of the route if necessary (round-trip distance, 1–4 miles [1.5–6.5 km], depending on road conditions).

From the west end of the parking area, take Forest Service Road 2076 for about 0.7 miles (1.1 km), then turn left (south) onto Forest Service Road 200. The road is steep and in poor condition. Follow Forest Road 200 as it winds downhill for about 1 mile (1.6 km) and then makes a right-angle turn; however, do not turn but, instead, go straight onto Forest Service Road 250 and follow it for about 0.5 miles (0.8 km) to where it ends. The cinder slope that rises above the road's end is the west rim of Blue Lake crater. The southwest side of the crater, located within Corbett Memorial State Park, can be explored; a short hike up to the rim will afford excellent views of the lake (note that the northeast side of the crater is located on private land and should be avoided). Take note of the vesicular tephra and the large blocks and bombs that have been deposited around the west crater rim.

Discussion of Stop 19

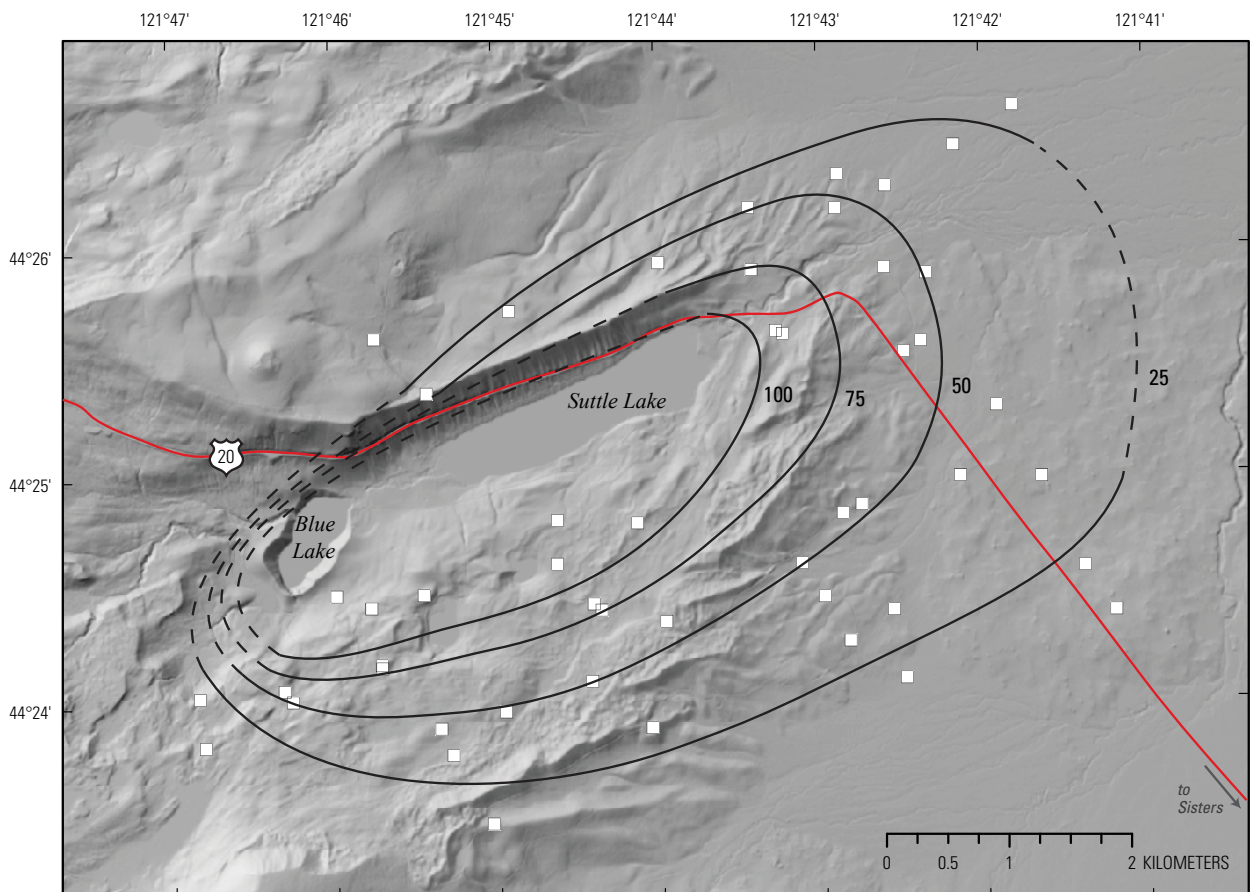
Blue Lake crater sits east of the Cascade Range crest. The lake that occupies the crater is about 0.8 km long and 0.5 km wide, and it is very deep (>95 m) for its size. Blue Lake, as well as the elongate Suttle Lake to the east, occupy an east-northeast-trending valley carved by glaciers during the Last Glacial Maximum. Blue Lake is cold (2.5 °C at depths of >10 m below the surface) and is fed by springs; its low temperature and low biological productivity contrast sharply with that of Suttle Lake, which is shallow, warm, eutrophic, and glacial in origin (Johnson and others, 1985).

Blue Lake crater is commonly referred to as a maar because the eruption produced a deep, now-lake-filled depression below the previous ground level that cut into the underlying country rock (see, for example, Fisher and Schmincke, 1984). Blue Lake is rimmed by crater walls of agglutinate, tephra, and bombs; the crater walls are thickest (less than about 60 m) on the west side of the lake but are absent near the outlet where the lake drains into Suttle Lake to the east. Although classified as a maar, deposits at Blue Lake crater indicate a more complex eruptive sequence; the eruption transitioned from an early, minor phreatomagmatic phase to a dominantly magmatic (volatile-driven) phase. Thin (<30 cm) surge deposits are present locally at or near the base of the deposits, indicative of magma-water interaction during eruption initiation (fig. 34). Overlying the surge deposits are fall deposits dominated by vesicular scoria that appear to be the products of a magmatic (Strombolian to violent Strombolian) eruption, although dense layers of lithic fragments of country rock are also present throughout the deposits. Tephra deposits, which reach a maximum depth near the vent of more than 5 m, can be found about 8 km to the east-northeast (fig. 35). The entire deposit volume (estimated from the isopachs) is about 4×10^7 m³. Additionally, large (less than about 2 m in diameter) bombs and lithic blocks that were ejected during the eruption are found in abundance around the west rim of the crater. No lava flows are associated with the Blue Lake crater eruption.

Figure 34. Pit excavated in deposit from eruption of Blue Lake crater. Base of deposit (white line) is thin layer of tephra fall, overlain by phreatomagmatic surge deposits (light-colored layer). Rest of deposit is dominantly magmatic, vesicular tephra fall. Scale shown is approximate, varying with pit depth.



Figure 35. Shaded-relief map and isopachs showing thickness (in centimeters) of tephra deposits from Blue Lake crater, which are dominantly found east-northeast of crater. Isopachs dashed where inferred or poorly constrained. White squares show locations where tephra-deposit thicknesses were measured. Shaded relief derived from 10-m digital elevation models (from Oregon Geospatial Enterprise Office, 2008). Road from Oregon Department of Transportation (2015).



The magma erupted from Blue Lake crater is basaltic andesite in composition (52–54.5 wt. percent SiO_2 ; Ruscitto and others, 2010) and contains abundant, large (<2 mm) olivine phenocrysts. Analyses of the preruptive volatile contents revealed that the magmas were relatively volatile rich (~3–3.6 wt. percent H_2O), which corresponds to crystallization pressures of about 150 to 200 MPa (Ruscitto and others, 2010). These data suggest that the magma was stored at depth prior to eruption and that the relatively gas-rich magma likely drove the magmatic phase of the eruption.

[Remainder of Stop 19 description is modified from Cashman and others (2009)]

Age constraints for Blue Lake crater, which are summarized in Sherrod and others (2004), include a maximum age of $3,440 \pm 250$ ^{14}C yr B.P., reported by Taylor (1965) for a tree limb located at the interface between tephra from Blue Lake crater and the underlying Sand Mountain tephra, as well as a minimum age of $1,330 \pm 140$ ^{14}C yr B.P., for charred forest litter beneath cinders from a chain of spatter cones 6 km south-southwest of, and on the same trend as, Blue Lake crater. Sherrod and others (2004) preferred the minimum age for Blue Lake crater because of both the petrographic similarities in the erupted magma and the alignment of the vents. However, a sediment core obtained from Round Lake, 3.6 km north-northwest of Blue Lake, contains a thin (~1 cm) layer at a depth of 94.5 cm of mafic ash that is geochemically similar to the Blue Lake crater tephra. If this correlation is correct, we can constrain the minimum age of Blue Lake crater to $1,860 \pm 25$ ^{14}C yr B.P. on the basis of age constraints from organic material that overlies ash from Blue Lake crater present in that same core (C. Long, written commun., 2011).

Stop 20 (Optional): Headwaters of the Metolius River

Directions to Stop 20 and Description of Hike

From the Mount Washington and Blue Lake crater overlook, turn right (east) onto Highway 20. Follow Highway 20 for about 6.3 miles (10.1 km) to Forest Service Road 14 (also known as Southwest Camp Sherman Road) and turn left (north); the turn is marked with a road sign for Metolius River and Camp Sherman. After about 2.7 miles (4.3 km), take a slight right (to the east) at the Y-shaped intersection and continue about 1.6 miles (2.6 km), still on Forest Road 14 (note that this part of the road is also known as Southwest Metolius River Road). Turn left (west) at the signs for the Head of the Metolius and follow the short road to the parking area.

The hike is short (less than 0.25 miles [0.4 km]) on a paved path to Metolius Spring (actually, several springs are located in this area). The path is wheelchair accessible. Dogs on a leash are permitted.

Discussion of Stop 20

[Modified from Cashman and others (2009)]

The Metolius River emerges from headwaters springs at the base of Black Butte and flows northward along the base of Green Ridge for roughly 30 km until it turns east and flows another 30 km to join the Deschutes River (fig. 36). The catchment of the Metolius River includes approximately 50 km of the axis of the Cascade Range. Mean annual discharge of the Metolius River ($42 \text{ m}^3/\text{s}$ [$1,483 \text{ ft}^3/\text{s}$]) accounts for roughly one-third of the mean annual discharge of the upper Deschutes Basin ($124 \text{ m}^3/\text{s}$ [$4,379 \text{ ft}^3/\text{s}$]), as measured at the gaging station near Madras.

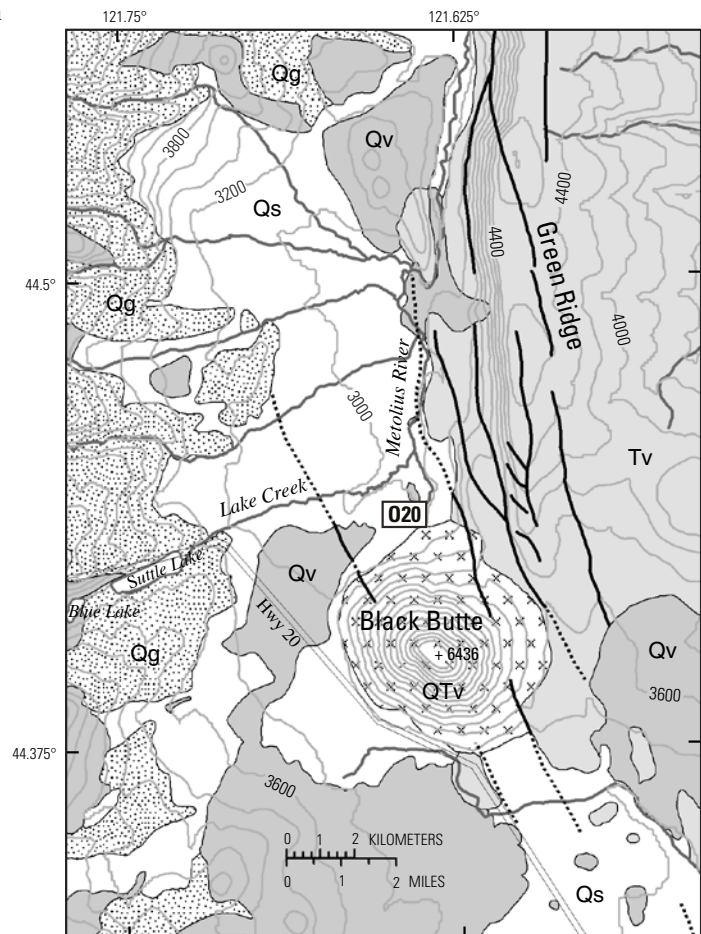


Figure 36. Generalized geology of Black Butte–Green Ridge area (modified from Cashman and others, 2009; geology from Lite and Gannett, 2002). Map units, listed oldest to youngest: Tv, Tertiary volcanic rocks; QTV, Quaternary and Tertiary volcanic vents and deposits; Qv, Quaternary volcanic deposits; Qg, Quaternary glacial drift; Qs, Quaternary alluvium and glacial outwash deposits, undivided. Thick black lines show faults: solid where location is certain; dotted where location is inferred or concealed. Field-trip stop shown by white rectangle; stop number is inside rectangle (O, optional stop). Base map from U.S. Geological Survey, scale 1:100,000 (Madras, 1975; Bend, 1980); contour interval, 200 ft.

The Metolius River is largely spring fed, as evidenced by its remarkably constant discharge (fig. 37). Most of the groundwater discharging to the stream emerges from springs along the main stem or lower parts of Cascade Range tributaries, mostly within 20 km of the headwaters springs along the west side of Green Ridge. Measurements of flow at the headwaters springs range from 2.8 to 3.6 m³/s (98–126 ft³/s). Surprisingly, only about four discharge measurements from this site have been published.

James and others (2000) included the Metolius River headwaters springs in their analysis of groundwater flow in the Deschutes Basin, which included measurements of temperature, stable isotopes, and noble gases. The temperature of the headwaters springs is about 8.2 °C. The near-surface groundwater temperature at the mean recharge elevation inferred from oxygen-isotope data (2,200 m) is closer to 3 °C, indicating that the headwaters springs contain considerable geothermal heat. If one uses an average flow rate (3.1 m³/s [109 ft³/s]) and a conservative 4 °C rise in temperature along its flow path, the groundwater that discharges at the Metolius River headwaters springs represents a geothermal-heat output of about 50 MW. Blackwell and others (1982) and Ingebritsen and others (1994) described a geothermal heat flux of over 100 mW/m² in the High Cascades. To pick up 50 MW, the groundwater that discharges at the Metolius River headwaters springs would need to intercept all of the geothermal heat over an area of 400 to 500 km²; the entire upper Metolius Basin encompasses about 1,160 km². A 400- to 500-m² contributing area for the headwaters springs is consistent with topography and surface-drainage patterns in the Metolius Basin and adjacent basins. A mass balance by Gannett and Lite (2004) indicated that a flux of approximately 23 m³/s (800 ft³/s) flows to

the Metolius River drainage from adjacent basins. The near-zero surface heat flux observed in the High Cascades (Ingebritsen and others, 1994) indicates that regional groundwater is indeed intercepting most of the geothermal heat flux.

Groundwater discharging at the Metolius River headwaters springs not only picks up geothermal heat along its flow path but magmatic volatiles as well. Analysis of carbon- and helium-isotope data by James and others (1999, 2000) indicated that the Metolius River headwaters springs contain a component of magmatic CO₂ and helium.

The age of water can be roughly calculated from mass-balance considerations (Gannett and others, 2003). Assuming a 400-km² contributing area, a mean aquifer thickness of 300 m (consistent with estimates by Gannett and Lite, 2004), a porosity of 10 percent, and an average discharge of 3.1 m³/s, mean residence time would be about 120 years. James and others (2000) reported a tritium content of 4.0 TU,¹⁰ however, indicating that the Metolius River headwaters springs contain at least some component of modern water.

Black Butte, from which the Metolius River emerges, is described by Sherrod and others (2004) as “a mildly eroded, steep sided lava cone whose pyroclastic center remains unexposed.” Lavas of Black Butte are basaltic andesite that contains 5 to 10 percent plagioclase (1–2 mm phenocrysts) and 3 to 5 percent olivine (1–2 mm phenocrysts). The potassium-argon (whole rock) age of the lava 1 km northeast of the summit is 1.43±0.33 Ma (Hill and Priest, 1992). Lavas of Black Butte exhibit reversed-polarity magnetization. The relatively pristine morphology of Black Butte stands in stark contrast to the glacially ravaged appearance of younger volcanic centers to the west. Black Butte was not glaciated, owing to the rain-shadow effect of the High Cascades.

Black Butte sits at the south end of Green Ridge, the east escarpment of the north-trending, 30-km-wide by 50-km-long High Cascades graben (see, for example, Conrey and others, 2002a). Formation of the graben commenced at approximately 5.4 Ma, and, since then, the northern part of the upper Deschutes Basin has been effectively cut off from High Cascades volcanic centers (Smith and others, 1987; Sherrod and others, 2004). Green Ridge is capped by lava that has an age of approximately 5 Ma. Displacement continued into the early Pleistocene, as lavas of Black Butte are offset by structures related to Green Ridge. Total offset exceeds 1 km on the basis of drill-hole data at Santiam Pass (Hill and Priest, 1992; Sherrod and others, 2004).

The channel morphology of the upper part of the Metolius River should look familiar, as it is similar to the morphology of the spring-fed streams that we have seen on the west side of the Cascade Range. As on the west side, spring-fed streams on the east side are characterized by a constant flow throughout the year, so that they lack the geomorphic features that are associated with either high-flow events or substantial variations in flow such as gravel bars and cutbanks. Streams are usually close to bankfull stage because seasonal stage variations are minimal, commonly on the order of a few to several inches. Vegetation typically extends right to the edge of the water, and flows required to mobilize large woody debris are lacking, and

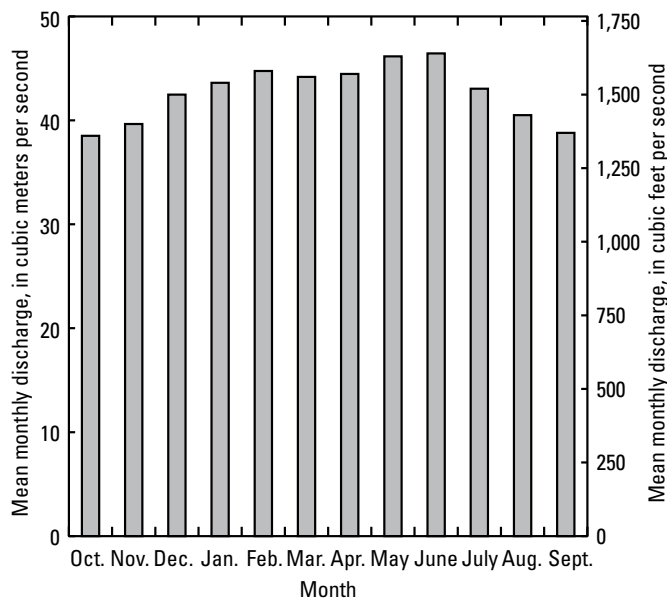


Figure 37. Mean monthly discharge of Metolius River near Grandview (gage no. 14091500), about 28 km west of Madras, from 1922 to 2015. Modified from Cashman and others (2009); discharge data from U.S. Geological Survey streamflow-data archive.

¹⁰ TU = tritium unit, the ratio of 1 tritium atom to 10¹⁵ hydrogen atoms.

so trees tend to stay in the stream and become covered with moss and grass. The hydrology and geomorphology of spring-fed channels in the Deschutes Basin was described by Whiting and Stamm (1995) and Whiting and Moog (2001).

End of Day 2: Bend

Directions to Bend

Return to Highway 20 and continue east for about 9 miles (14.5 km) to Sisters (fig. 38). The highway, which skirts Black Butte, is underlain primarily by glacial outwash and sparse outcrops of older rocks of the Deschutes Formation (~7.5–4.5 Ma). From Sisters, continue southeast on Highway 20 for about 20 miles (32 km) to Bend.

Discussion of Bend

Bend is central Oregon's largest city. Western settlement of Bend began with a commercial sawmill operation at the start of the 20th century. Since about the year 2000, the population has exploded with many who are drawn to the outdoor recreational opportunities in the area (downhill skiing, snowboarding, cross-country skiing, rock climbing, kayaking, rafting, hiking, mountain biking, and so on), along with the pleasant climate.

Bend is also home to a large number of craft breweries. One reason why breweries in this area have been so successful is the quality of the local water. Bend water is so clean that ingredients have to be added to many beers to improve the taste. The water has very low sulfate, chloride, sodium, magnesium, and calcium concentrations, and the total alkalinity is only 70 ppm, nearly the equivalent of distilled water (The Beer Detective, 2014).

Day 3: Total Solar Eclipse and Various Stops in the Bend Area

[Note that, if you are following this field-trip guide after the IAVCEI Conference–sponsored field trip (August 19–24, 2017) has ended (that is, after the solar eclipse has occurred), we recommend that you visit Stops 21, 22, and 23 on Day 2, en route from Sisters to Bend]

On Day 3 of this IAVCEI Conference–sponsored field trip, we will focus on matters of a celestial nature: our morning will be occupied by viewing the total solar eclipse that occurs today (August 21, 2017). We anticipate considerable traffic after the eclipse, and so a modest number of stops (fig. 38) are scheduled for the afternoon, including a viewpoint that showcases the Three Sisters volcanic cluster (Stop 21). Next, we will see the products of a large explosive Quaternary eruption, the Tumalo Tuff and the Bend Pumice (Stop 22). Finally, we will stop at the location of a dam and reservoir that has never held water (Stop 23); here, we will examine the Tertiary and Quaternary deposits on either side of the Tumalo Fault, a principal strand of the fault zone that bounds the central Cascades graben to the east.

The Total Solar Eclipse—A Celestial Interlude

[Note that only during totality (that is, when the moon completely blocks the sun) can the eclipse be viewed directly; at all other times, the eclipse must be viewed with protective eyewear or glasses]

Total solar eclipses are a rare and unforgettable experience, a dramatic convergence of celestial cyclicality and terrestrial opportunity. Today's (August 21, 2017) event will be the first total solar eclipse in the United States in 26 years (and the first seen in the conterminous United States in more than 37 years). The path of totality will travel over Oregon, Idaho, Wyoming, and then into the Midwestern United States, passing through the Ozark Plateau, the Appalachian Mountains, and South Carolina before heading out to sea.

As we are anticipating very congested roads before, during, and after the eclipse, we will work to position ourselves so that only minimal travel is required in the morning. Our field trip will intersect the path of the eclipse near Sisters, which will experience totality beginning at 10:19 a.m., Pacific Standard Time (although the partial eclipse will start approximately one hour earlier). At our location, we will experience a little more than 30 seconds of totality.

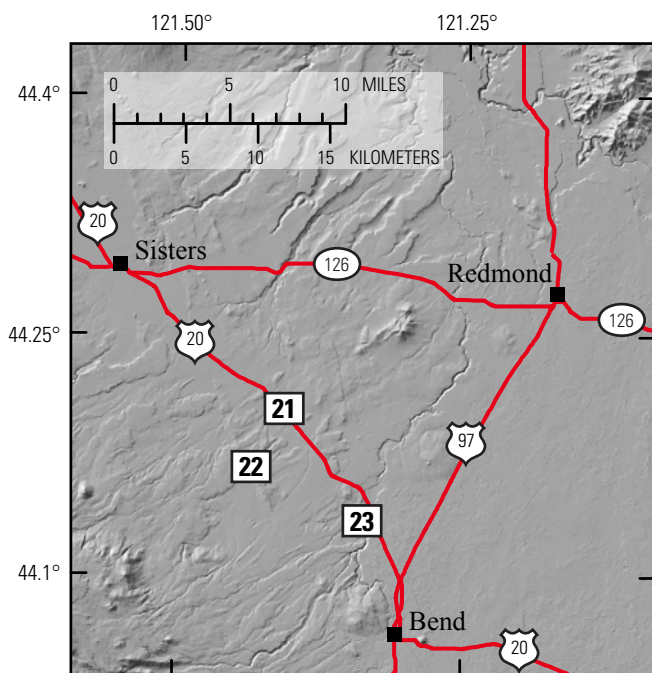


Figure 38. Shaded-relief map showing locations of field-trip stops on Day 3. Field-trip stops shown by white rectangles; stop numbers are inside rectangles. Shaded relief derived from 10-m digital elevation models (from Oregon Geospatial Enterprise Office, 2008). Roads from Oregon Department of Transportation (2015).

Stop 21: Three Sisters Viewpoint and the Bend Highland

Directions to Stop 21

From Bend, take Highway 20 northwest toward Sisters. About 5 miles (8 km) past the town of Tumalo (just before MP 9), turn right (north) into the Three Sisters viewpoint, marked with a sign. Note that there is also a viewpoint on the south side of the highway for eastbound traffic.

Discussion of Stop 21

The Three Sisters viewpoint lies on glacial outwash deposits. Most of the small buttes visible near the viewpoint, and in the middle ground that surrounds it, are underlain by lava or cinder deposits of the Deschutes Formation (McDannel, 1989; Taylor and Ferns, 1994; Taylor, 1998). Figure 39 shows a simplified compass wheel of features that are visible from this viewpoint.

From the Three Sisters viewpoint, Mount Jefferson, the prominent glaciated and glacier-covered stratovolcano, is visible on the skyline to the north-northwest. The andesitic and dacitic stratovolcano is fairly small and young, mostly less than 300 ka (Conrey, 1991); however, the volcano rests atop a broad field of intermediate-composition to silicic flows, domes, and volcanoes that extends 15 km along the Cascade arc north of Mount Jefferson. The oldest of these rocks is about 1.5 Ma; an older (4–2 Ma) field of andesitic- to rhyolitic-composition-dominated volcanism adjoins the younger (1.5 Ma) field on its northeast side (Yogodzinski, 1985), and an even older (6–4 Ma) Crag Creek unit of intermediate-composition and silicic rocks underlies it on its northwest side (Conrey, 1991). In addition, many of the 6- to 5-Ma silicic tuffs in the northern Deschutes Basin were emplaced along eastward-trending paleodrainages, suggesting that they had sources near the present-day Mount Jefferson (see summary in Conrey and others, 2004). The pattern of volcanic rocks and deposits, thus, demonstrates that the Mount Jefferson area has been a locus of intermediate-composition and silicic volcanism for some 7 million years. Both north and south of Mount Jefferson, the Cascade arc chiefly consists of mafic lava flows and shield volcanoes. The petrology of volcanic rocks in the Mount Jefferson area is dominated by the mixing of a diverse set of mafic magmas with two crustally derived magmas, one a rhyodacite and, the other, a strontium-rich andesite (Conrey and others, 2001).

Visible to the east (right) of Mount Jefferson (fig. 39) are three Pliocene basaltic andesite shield volcanoes (Armstrong and others, 1975). Two of these, Akawa Butte (farthest east) and Little Akawa Butte, overlie rocks of the Deschutes Formation (Sherrod and others, 2004) east of Green Ridge (not visible), the major scarp that bounds the east side of the High Cascade graben. The third, Bald Peter, is within the graben, close to Mount Jefferson (Yogodzinski, 1985).

In a visual arc from south (left) of Mount Jefferson to almost due west of here (fig. 39) are one mafic shield volcano or stratovolcano and several large mafic shield volcanoes:

from north to south (right to left), these are Black Butte, Three Fingered Jack, Mount Washington, Black Crater, Trout Creek Butte, and North Sister.

Black Butte is a prominent, reversely magnetized shield volcano that was erupted over the junction of the north-northwest-striking Tumalo Fault and the north-south-striking Green Ridge Fault; it is cut by strands of the Tumalo Fault (Sherrod and others, 2004). Black Butte is east of the Cascade Range crest and, thus, avoided glaciation, and so it appears to be much younger from a distance than its 1.43 Ma potassium-argon age (Hill and Priest, 1992) would suggest. It is composed of incompatible-element-poor, North Sister-type basaltic andesite (R. Conrey, unpub. data, 2003).

Three Fingered Jack is an undated, gutted shield volcano that has multiple summits. As was discussed at Stop 16, the composition of its lavas includes both the Mount Washington and the North Sister basaltic andesite types (R. Conrey, unpub. data, 1990).

Mount Washington is a prominent, eroded shield volcano that has a high central pinnacle. The pinnacle, which is the central intrusive plug of the edifice, is surrounded by more readily erodible, near-vent scoria and ash and is flanked by a resistant apron of lava (Sherrod and others, 2004).

Black Crater is a shield volcano near McKenzie Pass that is barely dissected, which suggests that it is younger than its 50 ka age. Trout Creek Butte is an older (532 ka), flat-topped, normally magnetized shield volcano (Taylor, 1987; Hildreth and others, 2012).

North Sister is a prominent, large, basaltic andesite shield volcano or stratovolcano, the northernmost (and oldest) of the Three Sisters volcanic cluster (Schmidt and Grunder, 2009; Hildreth and others, 2012). The most recent $^{40}\text{Ar}/^{39}\text{Ar}$ dates range from 120 to 45 ka (Hildreth and others, 2012); previously, $^{40}\text{Ar}/^{39}\text{Ar}$ dates on stratigraphically older units suggested an older age of about 400 ka (Schmidt and Grunder, 2009). If the Matthieu Lakes fissure is considered to be part of North Sister, then the youngest age of North Sister can be extended to about 11 ka (Schmidt and Grunder, 2009). The central plug of the volcano, along with a large number of dikes and a palagonitic complex on its east-northeast side, have been exposed by glacial erosion (Schmidt and Grunder, 2009). The presence of the palagonitic complex suggests that much of the earlier eruptive history occurred during a glacial epoch. The North Sister basaltic andesite is homogenous (53–55 wt. percent SiO_2) and is noteworthy for its very low incompatible-element concentrations (Hughes and Taylor, 1986; Schmidt and Grunder, 2011).

Visible to the south (left) of North Sister (fig. 39) are its “sister” stratovolcanoes, Middle Sister and South Sister. Middle Sister is the youngest stratovolcano of the Three Sisters volcanic cluster, having mostly been built between 25 and 18 ka; the oldest dated eruptions are about 40 ka (Hildreth and others, 2012). Middle Sister lava is quite variable, ranging in composition from 52 to 65 wt. percent SiO_2 (Hildreth and others, 2012). One notable feature of the volcano is the thick dacite lava stack in the saddle between Middle and North Sister, informally called “Step Sister.” The summit and west

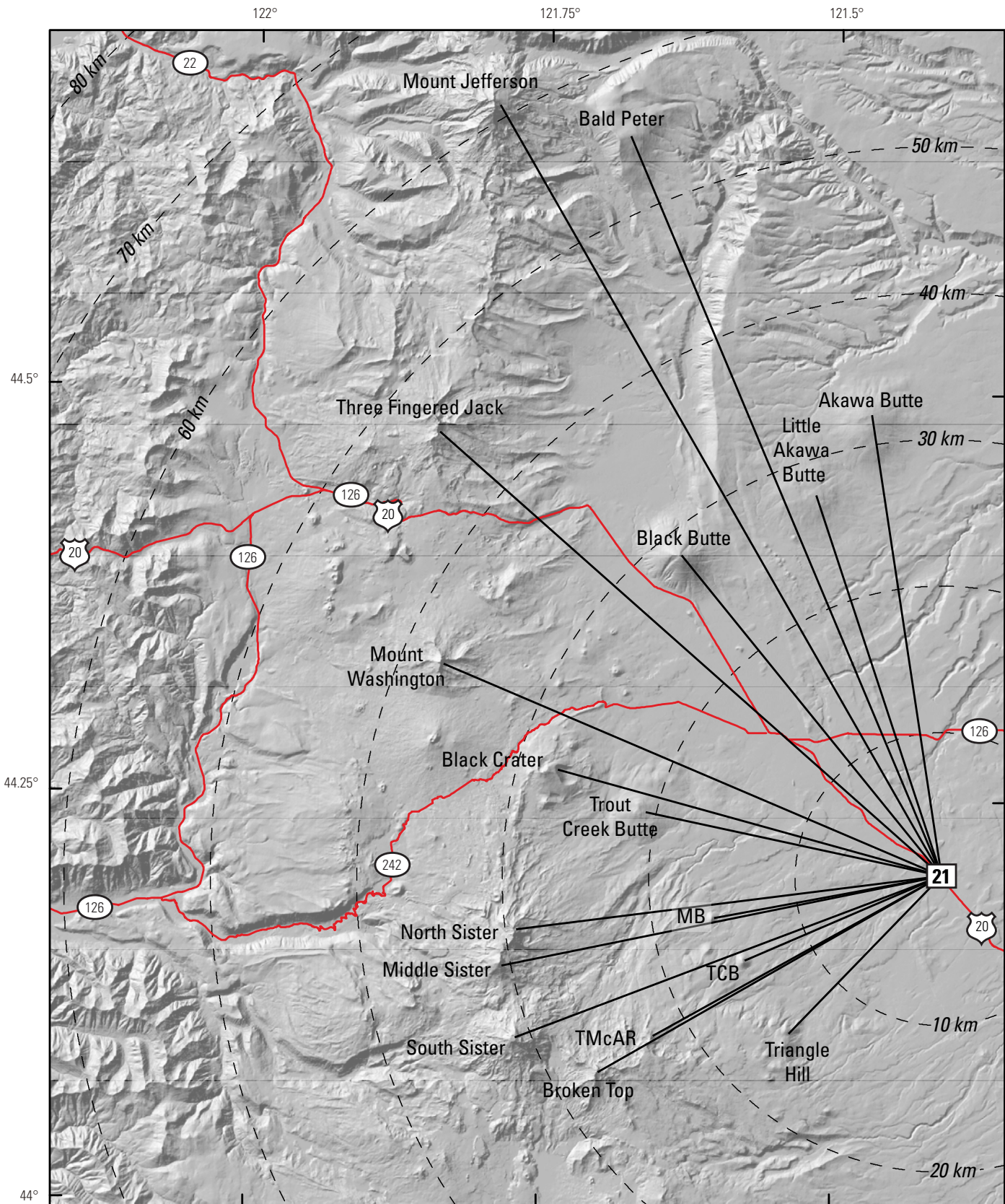


Figure 39. Shaded-relief map showing compass directions and distances (dashed lines) to features that are visible from Three Sisters viewpoint (Stop 21; location shown by stop number in white rectangle). Abbreviations: MB; Melvin Butte; TCB, Three Creek Butte; TMcAR, Tam McArthur Rim. Shaded relief derived from 10-m digital elevation models (from Oregon Geospatial Enterprise Office, 2008). Roads from Oregon Department of Transportation (2015).

slopes of Middle Sister are covered with plagioclase- and olivine-rich basaltic andesite (Hildreth and others, 2012).

South Sister was chiefly constructed contemporaneously with Middle Sister; its $^{40}\text{Ar}/^{39}\text{Ar}$ ages range from 50 to 22 ka. The early eruptive history of South Sister was dominated by rhyolite, followed by voluminous andesite and dacite flows; its summit is capped with basaltic andesite (see Hildreth and others, 2012, and references contained therein). The east flank of the volcano is cut by the 2-ka, 5-km-long linear chain of Devils Lake rhyolite domes (Scott, 1987).

Visible just below North Sister is Melvin Butte, a rhyolite dome that has a high silica composition (74 percent SiO_2), similar to that of the Bend Pumice (Hill, 1992; Taylor and Ferns, 1995). An unnamed dome that has a similar composition is visible beneath the saddle between Middle Sister and South Sister. Visible just left of South Sister is a third, similar dome, Three Creek Butte (Hill, 1992; Taylor and Ferns, 1995). These three domes were likely emplaced during eruption of the plinian Bend Pumice and the overlying Tumalo Tuff (fig. 40). On the east end of the Bend highland lies Triangle Hill, a 340 ± 20 ka andesitic cinder cone (Hill and Duncan, 1990; Hill, 1992) that overlies the probable vent for the Bend Pumice and the Tumalo Tuff (fig. 40); the andesite of Triangle Hill contains fragments of the Tumalo Tuff (Hill, 1992). Several rhyolite domes and cinder cones of mafic to intermediate composition lie in a 4-km-diameter, roughly circular area that is centered on Triangle Hill (Sherrod and others, 2004); the circular area outlines a prominent negative gravity anomaly (fig. 40).

To the southwest is the prominent cirque headwall Tam McArthur Rim, composed of diverse lava types that include basaltic andesite, dacite, and rhyodacite (Taylor, 1978). The presence of several large dikes beneath the rim suggests that most of the lava was vented locally. Hill and Duncan (1990) obtained a potassium-argon age of 213 ± 9 ka on a thick rhyodacite lava that caps the section. Overlying the lavas of Tam McArthur Rim is Broken Top, a heavily dissected, basaltic andesite shield volcano topped by a modest stratocone (Taylor, 1987; Webster, 1992). Broken Top is undated, but its age likely is about 300 to 150 ka (Hildreth and others, 2012).

The Bend highland (also known as the “Tumalo Volcanic Center” or the “Silicic Highland;” Taylor, 1987; Hill, 1988) is a prominent, broad, west-northwest-trending ridge that extends southeast of the Three Sisters volcanic cluster about 20 km, toward Bend. All surface exposures on the highland are of normal-polarity, mafic, intermediate-composition, and silicic rocks (Sherrod and others, 2004). One geothermal exploration drill hole penetrated 1,200 ft (366 m) of normal-polarity, chiefly silicic rocks. Beneath the presumed Brunhes-age (younger than about 0.8 Ma) cap, a diverse series of mafic, intermediate-composition, and silicic pyroclastic rocks were cored to a total depth of 3,430 ft (1,045 m). Potassium-argon ages determined on rocks in the drill core, which range from 1.7 to 0.6 Ma, were compromised by alteration, and they also were inconsistent with the stratigraphy. Because the Bend highland trends west-northwest, the Brunhes-age lavas likely were channeled into

northeastward-flowing drainages on its north flank. In addition, lavas of the about-5-Ma Deschutes Formation northeast of the highland (including the exposures along Highway 20), as well as ash-flow tuffs in the southern Deschutes Basin, were channeled along northeastward-flowing paleodrainages (see Sherrod and others, 2004, and references contained therein). The Brunhes-age ash-flow tuffs (fig. 40) whose sources are on or near the highland have counterparts in the petrologically similar, and even more numerous and voluminous, ash-flow tuffs of the Deschutes Formation. Several of the older tuffs can be traced from the Deschutes Basin upstream along the Deschutes River and its tributary creeks a considerable distance to the southwest where they are truncated by the Tumalo Fault (a major strand of the Sisters Fault Zone; Sherrod and others, 2004). The map distribution, therefore, suggests that the tuffs had sources in or near the Bend highland (Smith and Taylor, 1983; Smith, 1986b; Conrey and others, 2004), which further suggests that the Bend highland has long been a feature of the central Cascade Range. In addition, the highland may be the reason that magma easily penetrates the crust along the projected extension of the Brothers Fault Zone, a broad, west-northwest-striking zone of small-offset, en echelon normal faults. The Brothers Fault Zone, which extends for 240 km across eastern Oregon, separates the extensional basin-and-range faults in southern Oregon from the compressional folds in northern Oregon (Lawrence, 1976; Walker and Nolf, 1981).

Stop 22: Bull Flat and Tumalo Dam

Directions to Stop 22

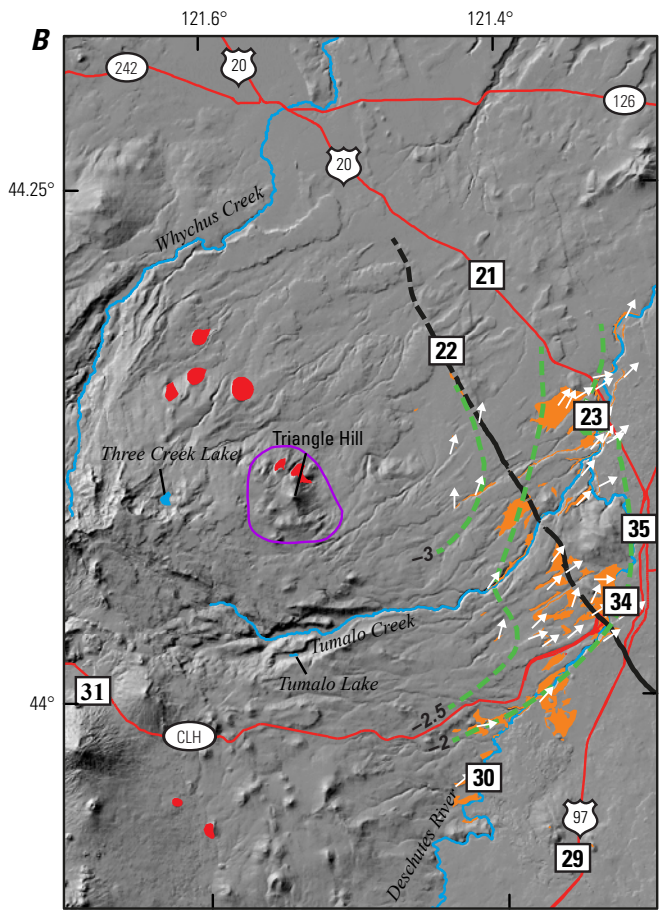
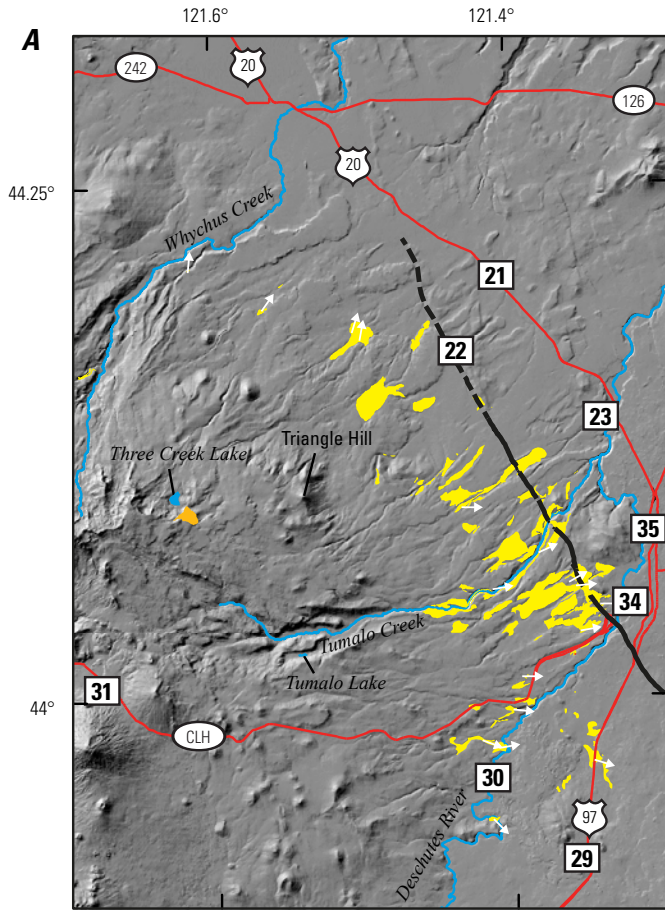
Turn left (east) onto Highway 20 and continue for about 3.2 miles (5.1 km) to the Couch Market Road exit. Turn right (west) onto Couch Market Road and continue for about 3.5 miles (5.6 km), until it ends at Sisemore Road. Turn right (north) onto Sisemore Road and continue for about 0.2 miles (0.3 km) to where the road crosses Tumalo Dam. The road is narrow at this location, but several pullouts are located about 0.1 miles (0.15 km) west of the dam.

Discussion of Stop 22

[Modified from Sherrod and others (2002)]

Traveling southeastward from Sisters, we have generally followed the Sisters Fault Zone, which consists of nearly 50 mapped faults across a 60-km-long, 5- to 15-km-wide zone; our stop here, which is about midway along it, is at the most prominent strand, the Tumalo Fault, which extends nearly continuously for 47 km. Along the Tumalo Fault, Pliocene lava flows of the Deschutes Formation have experienced at least 60 to 70 m of normal offset at Tumalo Dam. Quaternary lava flows younger than 0.78 Ma in the same area have escarpments of only 6 to 10 m.

50 Field-Trip Guide to Mafic Volcanism of the Cascade Range in Central Oregon



EXPLANATION

- Shevlin Park Tuff
- Welded agglutinate lava
- Tumalo Tuff and Bend Pumice, undivided
- Rhyolite and dacite domes that are chemically similar to the Tumalo Tuff
- Desert Spring Tuff
- Unnamed dome that is chemically similar to the Desert Spring Tuff
- Gravity low
- 2.5 --- Isopleths, in Φ units

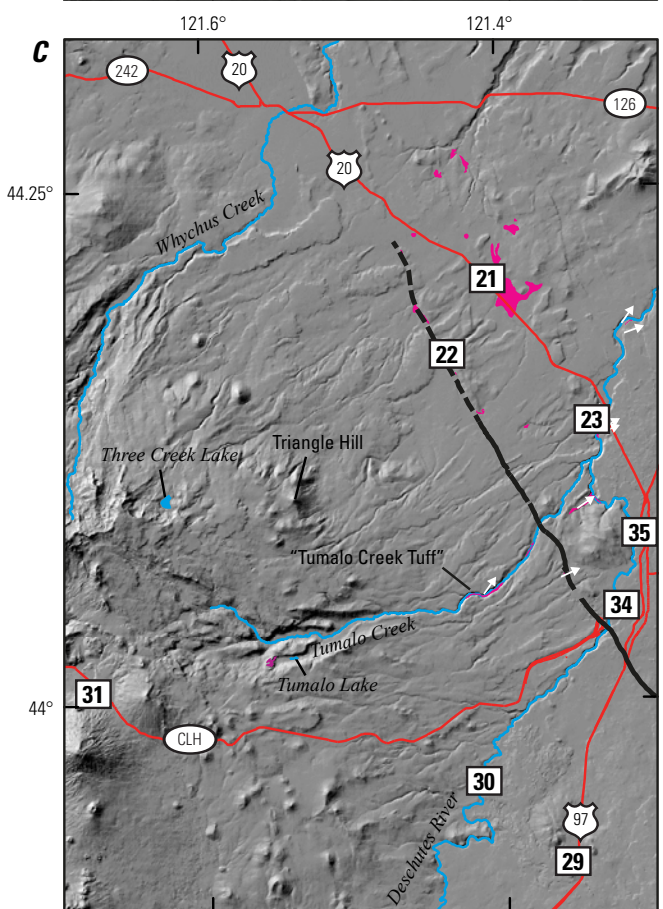
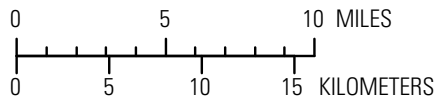


Figure 40. Shaded-relief maps showing distribution of three Brunhes-age (younger than 0.78 Ma) ash-flow tuffs erupted from Bend highland (from Scott and Gardner, 1992; MacLeod and others, 1995; Sherrod and others, 2004). Modified from Conrey and others (2004). Thick black line shows Tumalo Fault (from Sherrod and others, 2004): solid where location is known; dashed where location is approximate. White arrows show pumice-imbriation orientations (from Mimura, 1984), which are assumed to represent flow directions during emplacement. Field-trip stops shown by white rectangles; stop numbers are inside rectangles. Cascade Lakes Highway (Highway 46) is labeled as 'CLH.' Shaded relief derived from 10-m digital elevation models (from Oregon Geospatial Enterprise Office, 2008). Lakes from Pacific Northwest Hydrography Framework Group (2005a); other drainage from Pacific Northwest Hydrography Framework Group (2005b). Roads from Oregon Department of Transportation (2015) and University of Oregon Map and Aerial Photography Library (available at https://library.uoregon.edu/map/gis_data/county_trans.html). *A*, Distribution of the Shevlin Park Tuff, about 200 ka (Kuehn and Negrini, 2010; Hildreth and others, 2012). Vent is not known but may be near Three Creek Lake, where compositionally similar welded agglutinate lava is found. *B*, Distribution of the Tumalo Tuff and Bend Pumice, undivided. Ar-Ar age for the Tumalo Tuff of 440 ± 6 ka on plagioclase separate is from Lanphere and others (1999). Gravity low (from Sherrod and others, 2004) around Triangle Hill cinder cone, which includes xenoliths of the Tumalo Tuff, likely marks primary vent for Bend Pumice–Tumalo Tuff eruption, and pumice isopleths (from Hill, 1992) are consistent with that source; however, pumice-imbriation orientations suggest that flow was from southwest. Composition of rhyolite and dacite domes (chemistry from Hill, 1992) is similar to that of pumice in the Tumalo Tuff. *C*, Distribution of the Desert Spring Tuff, about 630 ka (M.A. Lanphere and D.E. Champion, written commun., 2003). Bulk compositions, mineral chemistry, and paleomagnetic orientations suggest that the Desert Spring Tuff is related to unnamed dome near Tumalo Lake (Conrey and others, 2002b; also, D.E. Champion, written commun., 2003). Note that the "Tumalo Creek Tuff" (in Tumalo Creek) was mapped as the Desert Spring Tuff by Mimura (1992); however, the "Tumalo Creek Tuff" has a different composition than that of the Desert Spring Tuff and, thus, is likely unrelated to it (Conrey and others, 2004).

Here we can see the geomorphic and stratigraphic contrasts across the Tumalo Fault (fig. 41). On the northeast (upthrown) side of the fault are Pliocene strata of the Deschutes Formation, chiefly basaltic andesite lava flows. An andesitic ignimbrite (62 percent SiO_2 ; Smith, 1986b) interlayered in the Deschutes Formation is visible in the roadcut at the eastern dam abutment. Rocks of the Deschutes Formation exposed here are probably about 5 to 4 Ma, although no isotopic ages have been reported from this area. Offset of at least 70 m is indicated by both the height of the ridge of Deschutes Formation strata northeast of the fault and the absence of Deschutes Formation strata visible at the surface southwest of the fault. Cross sections by Taylor and Ferns (1994) suggested that the Deschutes Formation is buried by 50 m of volcanoclastic deposits in the downthrown block, in which case dip separation along the fault is 120 m.

On the southwest (downthrown) side of the Tumalo Fault is alluvium that floors Bull Flat, a treeless basin upstream from (south of) the dam. Middle Pleistocene pyroclastic-flow deposits are exposed locally where banked against Deschutes Formation strata exposed in the upthrown block or where the alluvium is thin on the floor of Bull Flat. It is likely that the about-0.6-Ma Desert Spring Tuff has been displaced several meters along the fault here because no outcrops of the tuff are found on the downthrown side, but they are present on the upthrown side near the dam. Displacement of younger pyroclastic-flow deposits is difficult to quantify because the pyroclastic flows may have overtopped topographic barriers and were deposited across a wide range of elevations.

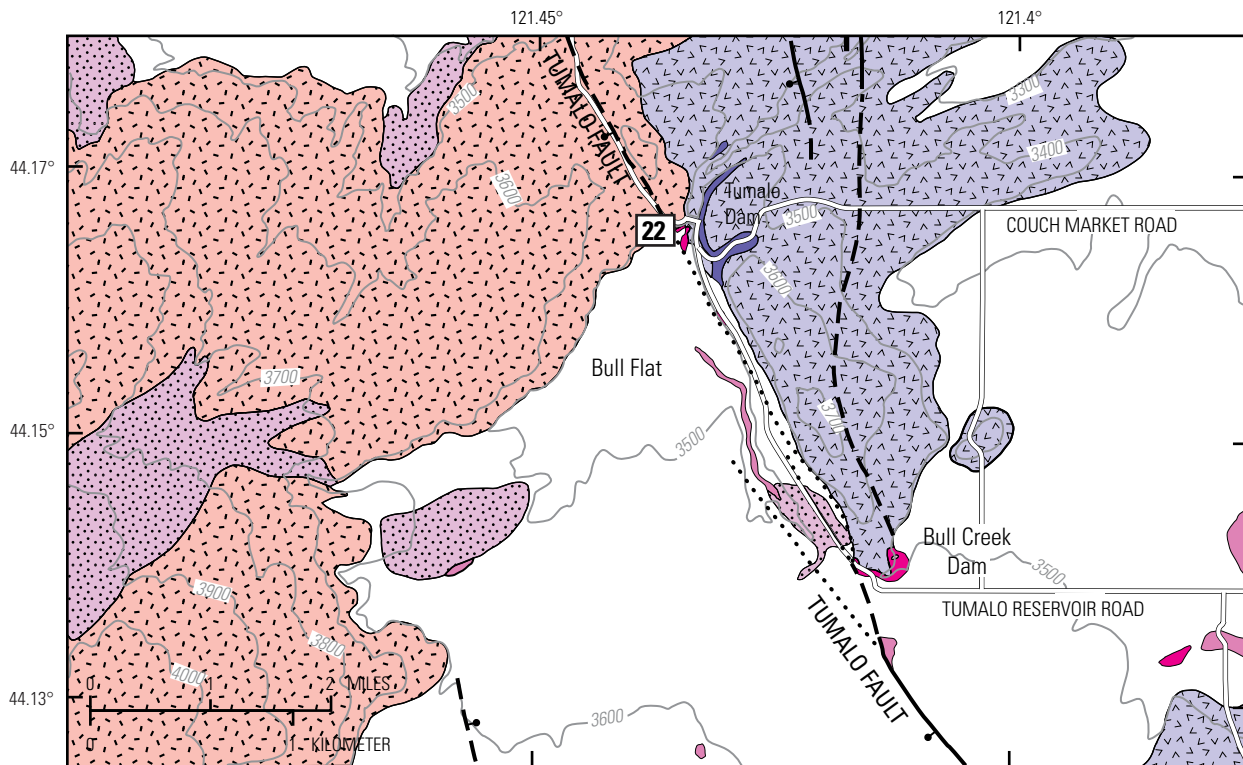
Bull Flat is an alluvial basin that likely has received sedimentary and volcanic deposits during at least the past million years. The water-table altitude is about 840 m in this area, and the depth to water in wells averages about 150 m. Neither the depth nor the lithology of the subsurface fill is known; however, we do know that the rate of stream incision across the Tumalo Fault in this area has kept pace with the rate

of uplift because the distribution of all pyroclastic flows 0.6 Ma and younger suggests that they escaped through channels cut through the upthrown block.

The western abutment of the Tumalo Dam is a basaltic andesite lava flow. Topographic escarpments only 6 to 10 m high mark the trace of the Tumalo Fault across this flow. The flow, which possesses normal-polarity thermal-remanent magnetization, is thought to be younger than 0.78 Ma. The lava flow is overlain upslope by the 0.2-Ma Shevlin Park Tuff.

The story of Tumalo Dam and its failed reservoir is one of broken promises and unfulfilled dreams, similar to many that surround the land-grab development history of the arid west. In the 1890s, homesteaders were lured to this area by promises of free land and abundant water for irrigation (Winch, 1984–85). By 1913, however, the private developers had gone bankrupt, and the promised water and delivery canals had not materialized. The State of Oregon then stepped in to fulfill promises made to homesteaders and the federal government, and Tumalo Dam was part of the attempt to provide the promised irrigation water. The dam, constructed in 1914, is a 22-m-tall earth-fill structure that has a steel-reinforced concrete core. The outlet was a 2.5×2.5 -m-wide, concrete-lined tunnel, 123 m long. Flow through the outlet was to be controlled from the small house at the end of the dam. The reservoir was to cover 447 ha ($4.47 \times 10^6 \text{ m}^3$) and impound $24.7 \times 10^6 \text{ m}^3$ of water. The dam was completed and the sluice gates closed on December 5, 1914.

Prior to construction, geologists expressed concern about permeability of the strata that bound the reservoir. These concerns were confirmed early in the winter of 1915 as the water level in the reservoir, still at only a fraction of its capacity, was falling at a rate of 0.2 m per day. When runoff increased in March and April and the water level started to rise, large sinkholes developed not far south of the dam, along the eastern margin of the reservoir (and perhaps along the Tumalo Fault). The largest sinkhole, 9×15 m across and 3 to 8 m deep, was



EXPLANATION

	Alluvium		Deschutes Formation
	Shevlin Park Tuff		Lava flows
	Tumalo Tuff and Bend Pumice, undivided		Pyroclastic-flow deposits
	Basaltic andesite		Fault—Solid where location is accurate; dashed where location is inferred, dotted where location is concealed. Ball and bar on downthrown side
	Desert Spring Tuff		

Figure 41. Generalized geology of Bull Flat–Tumalo Dam area (modified from Sherrod and others, 2002; geology from Taylor and Ferns, 1994). Field-trip stop shown by white rectangle; stop number is inside rectangle. Base map from U.S. Geological Survey, scale 1:24,000 (Tumalo Dam, 1962 [revised 1981]); contour interval, 100 ft.

swallowing water at an estimated rate of 5.7 m³/s. Attempts to seal the reservoir failed, and so Tumalo Dam was never used. An excellent history of the Tumalo Dam project is provided in Winch (1984–85).

The Sisters Fault Zone is roughly on strike with a steep, regional groundwater gradient that characterizes the Deschutes Basin, which extends northwestward from Bend for 60 km to Suttle Lake in the Cascade Range (fig. 42). However, the fault zone and groundwater gradient are displaced from each other by roughly 10 km, the groundwater gradient lying closer to the topographic slope of the Cascade Range. No evidence exists

that indicates that the Sisters Fault Zone has had a measurable effect on the distribution of groundwater. This observation is unsurprising stratigraphically because the upper Miocene and lower Pliocene strata of the Deschutes Formation on the upthrown side of faults along the fault zone are similar in permeability to the upper Pliocene and Pleistocene deposits along the downthrown side. Thus, permeability contrasts across the faults likely are few. Groundwater damming would probably occur only if these faults had created substantial gouge, or if fault offsets occurred rapidly enough or were sufficiently great to create either numerous small or one or more extensive closed basins.

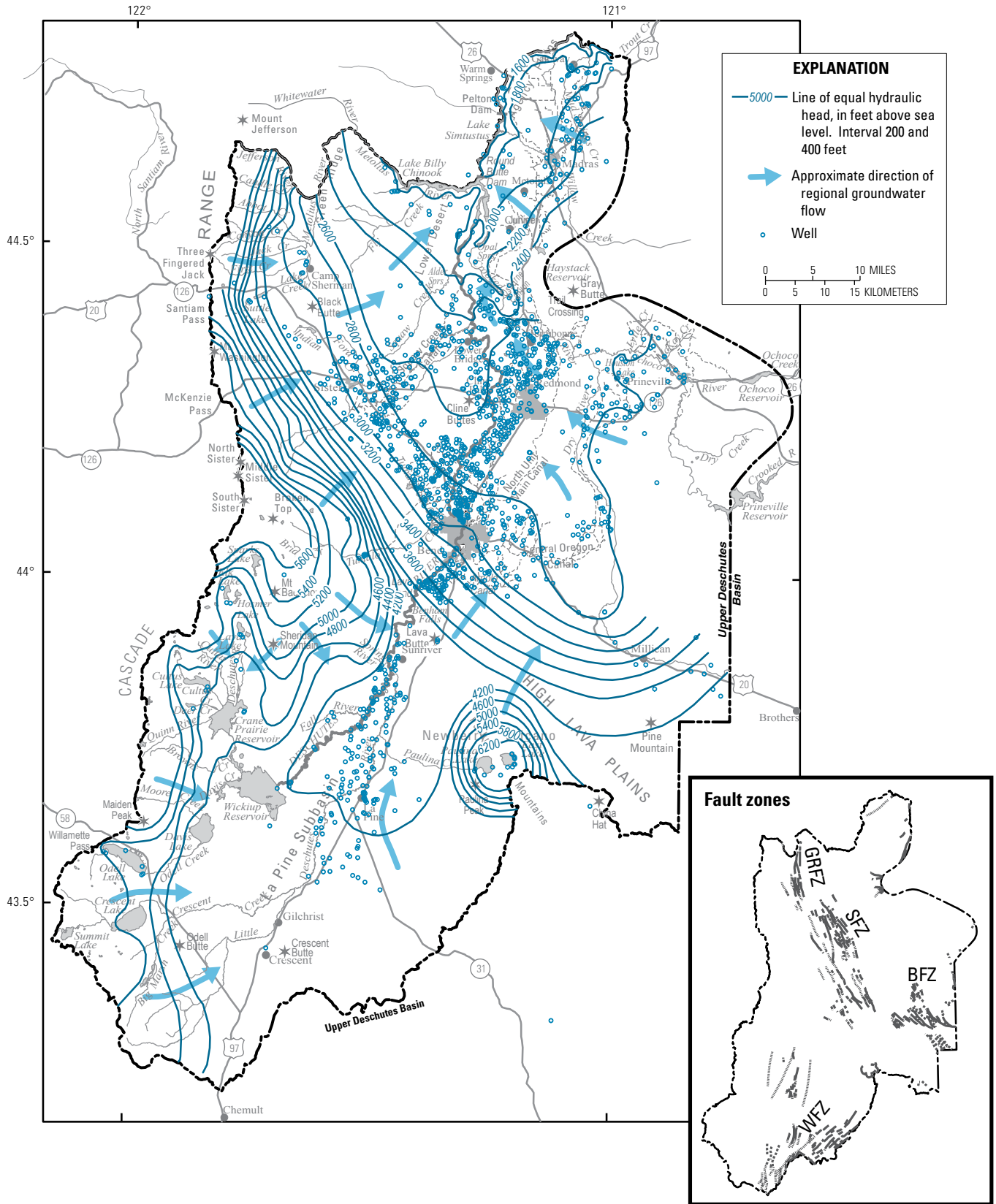


Figure 42. Map showing generalized lines of equal hydraulic head, groundwater-flow directions, and well locations in upper Deschutes Basin. Modified from Gannett and others (2001). Base map from U.S. Geological Survey, scale 1:250,000 (Bend, 1971; Crescent, 1970). Inset map shows faults in basin (solid where location is accurate; dashed where location is approximate or inferred; dotted where location is concealed): BFZ, Brothers Fault Zone; GRFZ, Green Ridge Fault Zone; SFZ, Sisters Fault Zone; WFZ, Walker Fault Zone.

Stop 23: The Bend Pumice and the Tumalo Tuff— An Explosive Quaternary Eruption

Directions to Stop 23

Return to the intersection of Couch Market and Sisemore Roads. Stay to the right (south) on Sisemore Road and continue for about 2.1 miles (3.4 km) to Tumalo Reservoir Road. Turn left (east) onto Tumalo Reservoir Road and continue for about 3.6 miles (5.8 km) to Bailey Road. Turn right (south) onto Tumalo Reservoir Road (Bailey Road continues straight ahead) and continue on Tumalo Reservoir Road for about 0.5 miles (0.8 km) to an excellent exposure of the Bend Pumice and the Tumalo Tuff. A pullout is on the right (south) side of the road.

Discussion of Stop 23

[Modified from Hill and Taylor (1990)]

The area west of Bend contains at least five ash-flow tuffs and two major pumice-fall deposits that range in age from about 0.65 to 0.2 Ma. These pyroclastic units were erupted from a large silicic-vent complex called the Bend highland (also known as the “Tumalo Volcanic Center,” Hill, 1988), located east of Broken Top volcano and west of Bend. The Bend highland, which encompasses the “silicic highland” of Taylor (1978), forms a broad, 20-km-long, west-northwest-trending belt of silicic domes and andesitic cinder cones.

Here we see excellent exposures of the about-0.4-Ma Bend Pumice of Taylor (1981), a rhyodacitic, vitric, lapilli-fall tuff that is best exposed along the roads that lead to Tumalo State Park. The 2-m-thick basal zone of the Bend Pumice, which consists of pumice lapilli, ash, and perlitic obsidian, has been locally reworked and mixed with gravel and sand. The basal zone, which is thought to represent the preliminary stage of a climactic eruption (Hill, 1985), is overlain by 3 to 13 m of air-fall lapilli and ash, the average grain sizes of which progressively increase upsection. Westward increases in average grain size, unit thickness, and size of volcanic rock fragments (Hill, 1985) all indicate that the Bend Pumice was erupted from the Bend highland (fig. 40). In addition, the major- and trace-element composition of the Bend Pumice is nearly identical to that of several silicic domes preserved in the Bend highland (Hill, 1988).

Also exposed at this location are several faults of the Sisters Fault Zone (Sherrod and others, 2004), which offset the Bend Pumice and the Tumalo Tuff. To see them, walk about 0.1 km eastward on a small dirt road that skirts the base of the exposure.

Immediately above the Bend Pumice is the Tumalo Tuff of Taylor (1981), a pink to tan, rhyodacitic, vitric ash-flow tuff. The nonerosive basal contact of the Tumalo Tuff and the absence of a normally graded top to the Bend Pumice indicate that the Tumalo Tuff was produced through collapse of the Bend Pumice eruption column. The Bend Pumice and the overlying Tumalo Tuff

represent the eruption of at least 10 km³ of nearly homogeneous, rhyodacitic magma (Hill, 1985).

Both the Bend Pumice and the Tumalo Tuff have a distinct mineral assemblage: plagioclase (An₂₀), ferrohypersthene (Wo₃En₄₀Fs₅₇), augite (Wo₄₁En₄₁Fs₁₈), fresh black hornblende, magnetite, ilmenite, apatite, and zircon. The ferrohypersthene are the most iron-rich orthopyroxenes that have been observed in the central Oregon Cascades. Banded pumice, which represents the mingling of rhyodacitic and unrelated dacitic magmas (Hill, 1985), is found in proximal (western) exposures. Although imbrication of pumice clasts in the Tumalo Tuff indicates a northeastward direction of flow (Mimura, 1984), the direct association with the Bend Pumice indicates that the Tumalo Tuff was erupted from the Bend highland and channeled by northeast-trending drainages (Hill, 1985).

End of Day 3: Bend

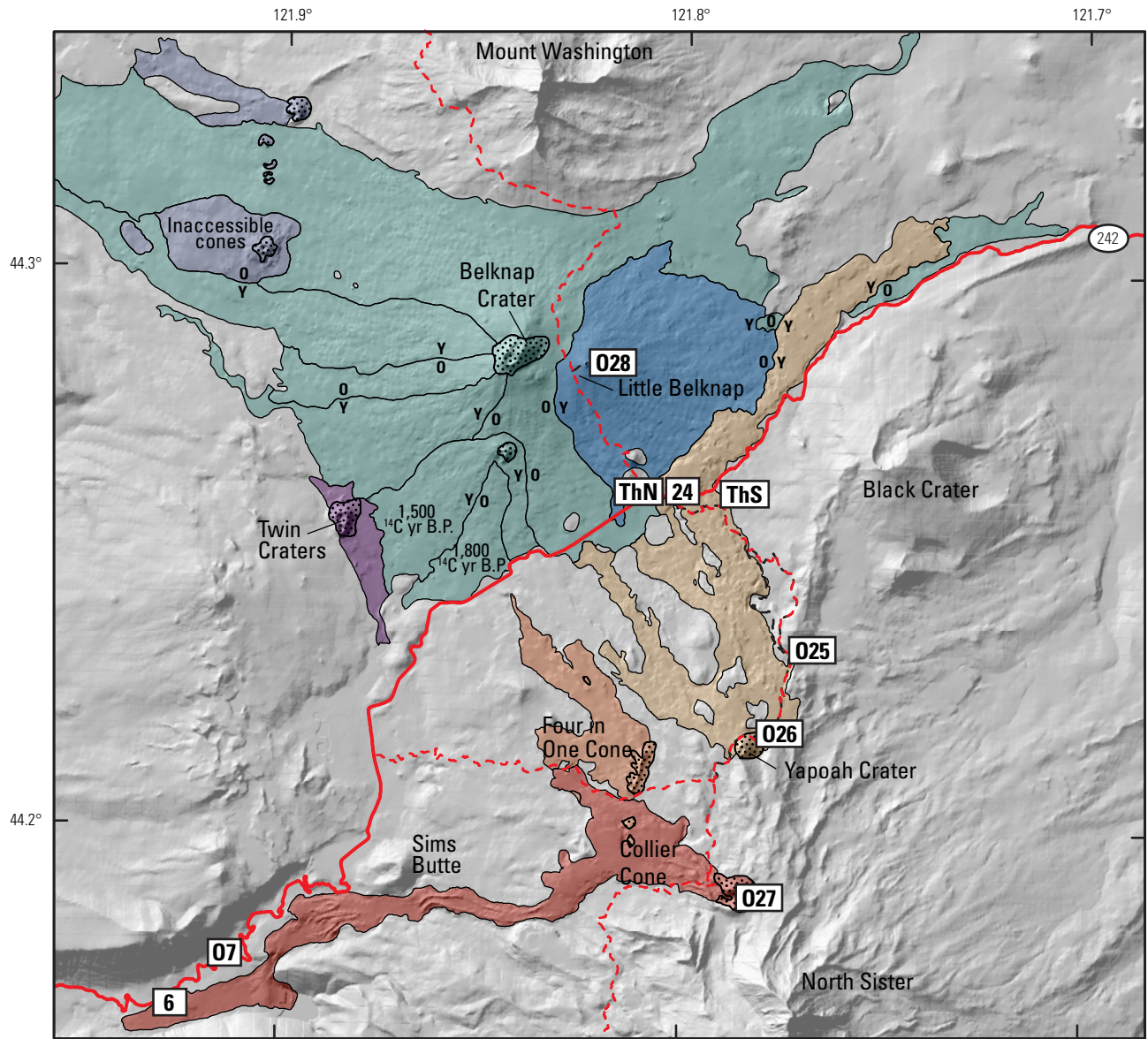
Directions to Bend

Continue on Tumalo Reservoir Road about 0.5 miles (0.8 km) to O.B. Riley Road and turn left (north). Continue on O.B. Riley Road for about 1.2 miles (1.9 km) to Highway 20 and turn right (east). Follow Highway 20 about 3 miles (4.8 km) to Bend.

Day 4: The McKenzie Pass Area

[Note that Highway 242, required to access all stops today, is closed in winter and spring; check with the Oregon Department of Transportation (<http://www.tripcheck.com/Pages/Rcmap.asp?curRegion=0&mainNav=RoadConditions>) or the Willamette National Forest (<http://www.fs.usda.gov/alerts/willamette/alerts-notices>) before you travel to see whether the highway is open or closed]

On Day 4 of the field trip, we will focus on Holocene volcanism of the McKenzie Pass area (fig. 43). McKenzie Pass is one of three passes that cross the central Oregon Cascades, the others being Santiam Pass to the north, which we crossed on Day 2, and Willamette Pass to the south. It is situated between Belknap Crater to the north and the Three Sisters volcanic cluster to the south, and it has numerous mafic Holocene lava flows nearby. We will go to Dee Wright Observatory for an impressive view of the central Oregon Cascades (Stop 24); from there, several hiking options will be available, ranging from moderate to strenuous. The most strenuous, and most stunning, is a hike to Collier Cone (optional Stop 27), the source of the Collier Cone lava flow we saw on Day 1. Shorter hikes along the same trail go Matthieu Lakes (optional Stop 25) and Yapoah Cone (optional Stop 26). Another possibility is to hike north to Little Belknap crater (optional Stop 28).



EXPLANATION

- Collier Cone
- Four in One Cone
- Yapoah Crater
- Belknap Crater
- Little Belknap crater
- Twin Craters
- Inaccessible cones

Figure 43. Shaded-relief map showing locations of field-trip stops on Day 4 (and also two from Day 1). Also shown are Holocene lava flows and vents (stippled areas) in McKenzie Pass area; relative ages (O, older; Y, younger) and radiocarbon ages of lava flows shown where known (from Sherrod and others, 2004; Koch and others, 2010). Dashed lines show trails. Field-trip stops shown by white rectangles; stop numbers are inside rectangles (O, optional stop; ThN, trailhead for optional Stop 28; ThS, trailhead for optional Stops 25–27). Shaded relief derived from 10-m digital elevation models (from Oregon Geospatial Enterprise Office, 2008). Roads from Oregon Department of Transportation (2015); trails from U.S. Forest Service (2017).

Stop 24: Dee Wright Observatory—McKenzie Pass and the High Cascades

Directions to Stop 24

From Bend, take Highway 20 northwest to Sisters. After passing through downtown Sisters, turn left (west) onto Highway 242 (McKenzie Highway). Follow Highway 242 for about 15 miles (24 km) to the parking area for Dee Wright Observatory.

Discussion of Stop 24

Dee Wright Observatory is located at an elevation of 1,581 m, at the summit of McKenzie Pass. This stone structure, which was constructed by the Civilian Conservation Corps in 1935, was named for the foreman who oversaw the project. If the day is clear, we will have a spectacular view from the top of the observatory of Pleistocene to Holocene volcanic rocks of the central Oregon

Cascades; table 3 lists the features that are visible from this location. The most prominent peaks include North Sister and Middle Sister to the south and Belknap Crater, Mount Washington, and Mount Jefferson to the north. Also evident are numerous older mafic composite volcanoes and cinder cones, as well as the young cinder cones to the south (Four in One Cone and Yapoah Crater) and Belknap Crater to the north, all three of which are the sources of the young lava flows that surround us (fig. 43).

Dee Wright Observatory is built on a basaltic andesite lava flow from Yapoah Crater (optional Stop 26), one of the young cinder cones that can be seen at the base of North Sister (the other is Collier Cone, the source of the Collier Cone lava flow, which we saw on Day 1). See (optional) Stops 26 and 27 for description of young Holocene volcanism near North Sister. To the west and northwest of Dee Wright Observatory are lava flows from Belknap Crater (fig. 43); these flows were described by Williams (1976) as being “one of the largest and most impressive sheets of recent lava anywhere in the United States.” See (optional) Stop 28 for a description of the volcanism of Belknap Crater and Little Belknap Crater.

Table 3. Central Oregon volcanic features visible from Dee Wright Observatory, at McKenzie Pass.

[Descriptions from U.S. Geological Survey Cascades Volcano Observatory, as well as from Conrey and others (2002a), Sherrod and others (2004), and Schmidt and Grunder (2009); ages (in parentheses) provided where known]

Azimuth (°)	Feature	Description
1	Mount Jefferson	andesitic-dacitic stratovolcano
7	Cache Mountain	glaciated basaltic andesite shield volcano (0.88 Ma)
11	Bald Peter	glaciated remnant of basaltic andesite shield volcano (2.2 Ma)
20	Dugout Butte	glaciated basaltic shield volcano and forested foreground
30	Green Ridge	eastern bounding fault of graben (7.5–5 Ma)
40	Black Butte	basaltic andesite shield volcano (1.42 Ma)
82	Black Crater	basaltic andesite shield volcano (about 50 ka?)
105–155	Matthieu Lakes fissure	basaltic andesite–andesite vents (75–11 ka)
167	Yapoah Crater	basaltic andesite cinder cone (about 2,000 yr B.P.)
168	North Sister	basaltic andesite shield volcano or stratovolcano
171	Collier Cone	basaltic andesite cinder cone (about 1,600 yr B.P.)
174	Middle Sister	stratovolcano of variable age and composition
178	Little Brother	basaltic shield volcano (coeval with, or older than, North Sister)
188	Four in One Cone	basaltic andesite and andesite cinder cones (about 2,000 yr B.P.)
195	Huckleberry Butte	glaciated basalt
197	The Husband	eroded core of basaltic andesite shield volcano (<0.42 Ma)
218	Condon Butte	basaltic andesite shield volcano
235	Horsepasture Mountain	part of cap rocks of Western Cascades (8–5 Ma)
256	Scott Mountain	basaltic shield volcano
282	“South Belknap” cone	basaltic andesite flank vent (1,800–1,500 yr B.P.)
309	Belknap Crater	basaltic andesite and andesite shield volcano (2,635–1,500 yr B.P.)
321	Little Belknap	basaltic andesite flank vent (2,900 yr B.P.)
340	Mount Washington	glaciated basaltic andesite shield volcano

Stops 25, 26, and 27 (All Optional): Matthieu Lakes (Stop 25); Yapoah Crater and a Reflection on Holocene Mafic Volcanism Near North Sister (Stop 26); and Collier Glacier View (Stop 27)

Directions to the Trailheads for Stops 25, 26, and 27 and Description of Hikes

[Note that the hike descriptions and maps in this field-trip guide are not a substitute for a good topographic or trail map. Maps are available at the McKenzie Ranger Station (Stop 3) and at most outdoor recreational stores in Oregon]

From the Dee Wright Observatory, travel east (toward Sisters) on Highway 242 for 1 mile (1.6 km) and then turn right (south) toward the Lava Camp Lake trailhead. Follow the gravel road to the trailhead. Display a Northwest Forest Pass in your vehicle when parked.

The hikes to Stops 25, 26, and 27 follow the Pacific Crest National Scenic Trail (PCT). The routes follow relatively flat parts of the PCT and are very scenic. The hikes are within the Three Sisters Wilderness; self-issue permits, which are available at trailheads, are required to enter. Sampling or collecting is not allowed without a special use permit. Leave no trace.

The round-trip hike from the Lava Camp Lake trailhead to Matthieu Lakes (Stop 25) is 6 miles (9.5 km). The round-trip hike from the trailhead to Yapoah Crater (Stop 26), by way of Matthieu Lakes, is 11 miles (18 km). The most strenuous, but also the most stunning, hike is to Collier Cone (Stop 27), which is the source of the Collier Cone lava flow that we saw on Day 1; the round-trip distance is 16 miles (26 km).

The hike from the Lava Camp Lake trailhead to Matthieu Lakes (Stop 25) travels south along the PCT. Roughly 1.2 miles (2 km) after entering the Three Sisters Wilderness, the trail splits: the PCT goes to the left, but the trail to North Matthieu Lake and South Matthieu Lake goes to the right. The trail will rejoin the PCT at South Matthieu Lake; from there, you may return to the Lava Camp Lake trailhead if desired.

To hike from the Lava Camp Lake trailhead to Yapoah Crater (Stop 26), follow the PCT past South Matthieu Lake for about 2 miles (3 km) to Yapoah Crater; the trail at this point is either traversing or bordering lava flows from Yapoah Crater.

To hike all the way to Collier Cone (Stop 27) from the Lava Camp Lake trailhead, follow the PCT past Matthieu Lakes and Yapoah Crater (Stops 25 and 26, respectively), then continue south on the PCT. In a meadow 0.5 miles (0.8 km) south of Yapoah Crater, the Scott Trail intersects the PCT coming from the west (the Scott Trail passes south of Four in One Cone); stay straight on the PCT. A bit before Collier Cone, you will cross Minnie Scott Spring, which is an untreated water source. You will encounter the Collier Cone lava flow as you cross a lava levee at Opie Dilldock Pass; bear left to the cone. Collier Glacier View is on the south rim of Collier Cone (44.186650° N., 121.791425° W.); from there you should have good views of North Sister, Middle Sister, and Collier Glacier, as well as the Collier Cone lava flow descending westward.

Discussion of Stop 25

North and South Matthieu Lakes border the at-least-11-km-long Pleistocene “Matthieu Lakes vent alignment” of cinder cones, lava flows, and fissure-fed agglutinate, which represent an eruptive volume of 0.4 km³ (fig. 44; see also, Schmidt and Grunder, 2009; Hildreth and others, 2012). Although the “Matthieu Lakes vent alignment” is considered to be part of the North Sister basaltic andesites, it also represents the shift in volcanism from North Sister proper to its flanks (Schmidt and Grunder, 2009). Near North Sister, lavas of the “Matthieu Lakes vent alignment” are 0.3 to 5 m thick, but, elsewhere, they can be as thick as 30 m where they ponded or were embanked against ice (Schmidt and Grunder, 2009). Eruptive materials from the “Matthieu Lakes vent alignment” range in age from 59 to 20 ka (Hildreth and others, 2012). In the Holocene, Yapoah Crater and Collier Cone both erupted on the western margin of the “Matthieu Lakes vent alignment.”

Discussion of Stop 26

Although eruptive materials from the Yapoah Crater eruption have not been dated directly, stratigraphic constraints suggest that they are about 2 ka. Tephra from Yapoah Crater immediately overlies silicic ash produced during the eruptions of Rock Mesa and the Devils Hill chain, near South Sister (about 2,300–2,000 ¹⁴C yr B.P.; Scott, 1987). In addition, tephra from Four in One Cone (1,980±160 ¹⁴C yr B.P.; Scott, 1990) overlies Yapoah Crater lavas. Yapoah Crater lavas also overlie lavas from Little Belknap crater (currently dated at 2,883±175 ¹⁴C yr B.P., although this age appears to be too old; see Chatters, 1968; Taylor, 1968, 1990a; Sherrod and others, 2004).

The moderately porphyritic basaltic andesite (Sherrod and others, 2004) lava flows from Yapoah Crater flowed northward toward McKenzie Pass, then they flowed eastward an additional 8 km toward Sisters.

Of the three young mafic (basaltic andesite) eruptions in this area—Yapoah Crater, Four in One Cone, and Collier Cone—Yapoah Crater is the oldest, and Collier Cone is the youngest. Four in One Cone is actually a chain of overlapping cinder cones erupted from a fissure system; four vents are located at the “cone,” and an additional two are about 1 km to the south. The length of the entire chain of vents is about 2 km, and the section of overlapping cones that make up Four in One Cone is about 1 km long. The highest cone in the Four in One Cone complex, located at the south end of the overlapping vents, is about 68 m tall. Each of the cones are breached to the northwest by basaltic andesite (about 56 wt. percent SiO₂) to andesite (58–59 wt. percent SiO₂) lava flows (Sherrod and others, 2004) that extend about 4 km from the vents. Large sections of cone material have been rafted to the northwest by these flows. The tephra blanket is well exposed east of the vents where it lies stratigraphically above tephra and lava from Yapoah Crater. A radiocarbon age of 1,980±160 ¹⁴C yr B.P. was obtained from charred needles and twigs in the lower 20 cm of the Four in One Cone tephra deposit, about 300 m east of the vents (Scott, 1990; Sherrod and others, 2004).

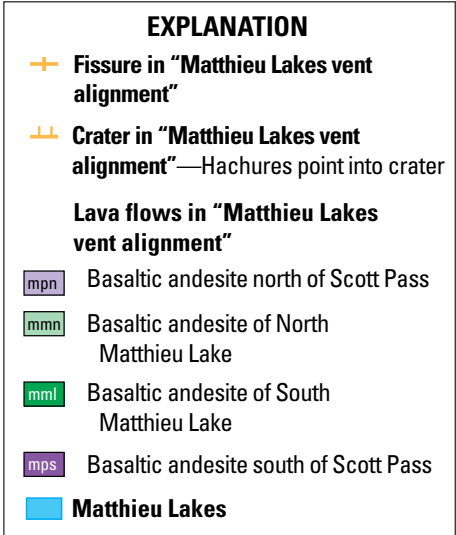
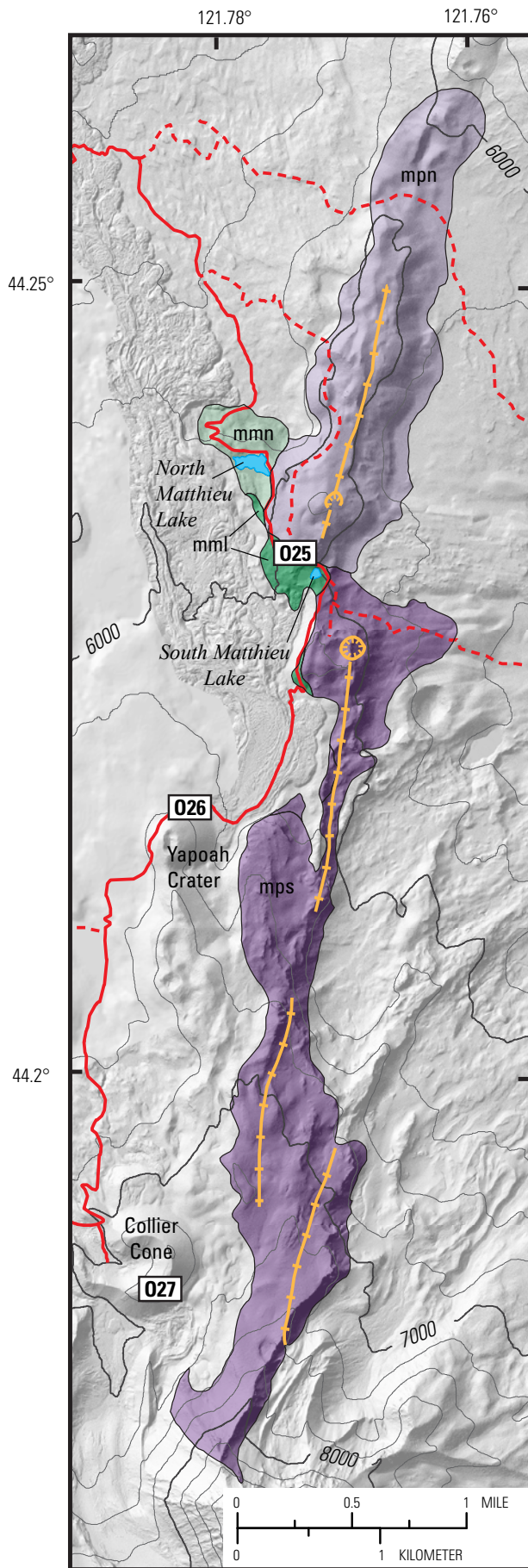


Figure 44. Shaded-relief map showing lava flows and fissures of "Matthieu Lakes vent alignment" (from Sherrod and others, 2004; Koch and others, 2010; Hildreth and others, 2012; Robinson and others, 2012; in addition, see Schmidt and Grunder, 2009, for detailed mapping that breaks units of "Matthieu Lakes vent alignment" into more subunits). Field-trip stops shown by white rectangles; stop numbers are inside rectangles (0, optional stop). Solid red line shows trail that is traversed between field-trip stops (note that much of trail follows Pacific Crest Trail); other trails shown by dashed red lines. Shaded relief derived from lidar imagery (from Oregon Department of Geology and Mineral Industries, 2011a,b) where available and from 10-m digital elevation models (from Oregon Geospatial Enterprise Office, 2008) elsewhere. Contours derived from digital elevation model; contour interval, 250 ft. Lake boundaries from Robinson and others (2012). Trails from U.S. Forest Service (2017).

Collier Cone is located on the northwest flank of North Sister, about 3 km southeast of Four in One Cone and about 3 km south of Yapoah Crater. The cone is about 150 m high and is breached to the west by multiple flows of basaltic andesite, andesite, and dacite lava (fig. 12; see also, Schick, 1994; Sherrod and others, 2004; Deardorff and Cashman, 2012) that extend about 14 km west of the vent (fig. 11B). The southwest side of Collier Cone is mantled by glacial till deposited during the late Neoglacial phase of ice advance (Sherrod and others, 2004). Tephra from Collier Cone is well exposed east of the vent where it lies stratigraphically above tephra from Yapoah Crater. Collier Cone lava flows surround and overlap the southern vents associated with Four in One Cone, as well as the southern part of the Four in One Cone tephra deposit. A radiocarbon age of $1,600 \pm 100$ ^{14}C yr B.P. was obtained from charcoal beneath Collier Cone tephra (Sherrod and others, 2004).

The Collier cone lavas contain troctolite xenoliths that are interpreted to be mafic cumulates, as well as silicic xenoliths that are similar in composition to the Obsidian Cliffs, located about 4 km southwest of the vent (Schick, 1994). As discussed in Deardorff and Cashman (2012), the composition of the second unit erupted likely has additional olivine and plagioclase crystals relative to that of the first unit erupted. Interestingly, the increase in

the K_2O/P_2O_5 ratio with declining MgO content (fig. 12B) cannot be due to crystal fractionation but, instead, is most likely due to mixing. Modeling by Mordensky (2012) of both equilibrium and fractional crystallization of the Collier Cone parent magma suggested that subtraction of crystals changes the K_2O/P_2O_5 ratio only very slightly up or down.

The mapped extents of tephra deposits from Four in One Cone and Collier Cone cover areas of about 1.4 km² and about 14.7 km², respectively (fig. 45); volume estimates that are based on isopachs are 0.002 km³ and 0.037 km³, respectively. The Four in One Cone tephra deposit has a maximum thickness of more than 2 m immediately east of the cones but thins rapidly to the east, suggesting a short-lived explosive phase. The Collier Cone eruption produced a thicker (more than 2.5 m thick, 1 km east of the vent) tephra blanket, although its full extent is unknown. Regional lakes preserve trace deposits of Collier Cone tephra (fig. 46) that can be used to estimate the thinning trend for trace deposits, which, along with estimates that are based on thinning trends for tephra deposits from well-documented cinder-cone eruptions, gives a maximum volume estimate of 0.69 km³ for the Collier Cone tephra deposit (fig. 30; table 2).

Detailed examinations of the tephra deposits from Four in One Cone and Collier Cone suggest that explosive activity at Four in One Cone ranged from Hawaiian to low-energy Strombolian, whereas the Collier Cone eruption was high-energy Strombolian to violent Strombolian (fig. 32). Violent Strombolian eruptions are characterized by moderately high (6–8 km) ash columns that produce widespread tephra deposits (see, for example, Walker, 1973; Pioli and others, 2008). The presence of the Sand Mountain tephra deposit (discussed at Stop 17) and the Collier Cone tephra deposit clearly shows that this type of high-energy mafic volcanism can occur in the central Oregon Cascades.

[Remainder of Stop 26 discussion is modified from Cashman and others (2009)]

Products of Yapoah Crater, Four in One Cone, and Collier Cone all have genetic affinities to magma produced at North Sister (see, for example, Conrey and others, 2002a; Schmidt and Grunder, 2009). Although the magmas are similar in composition, they are not identical, suggesting that each batch of magma had a slightly different source. Additionally, all three show surprising variability in composition: Collier Cone lavas, for example, show extensive

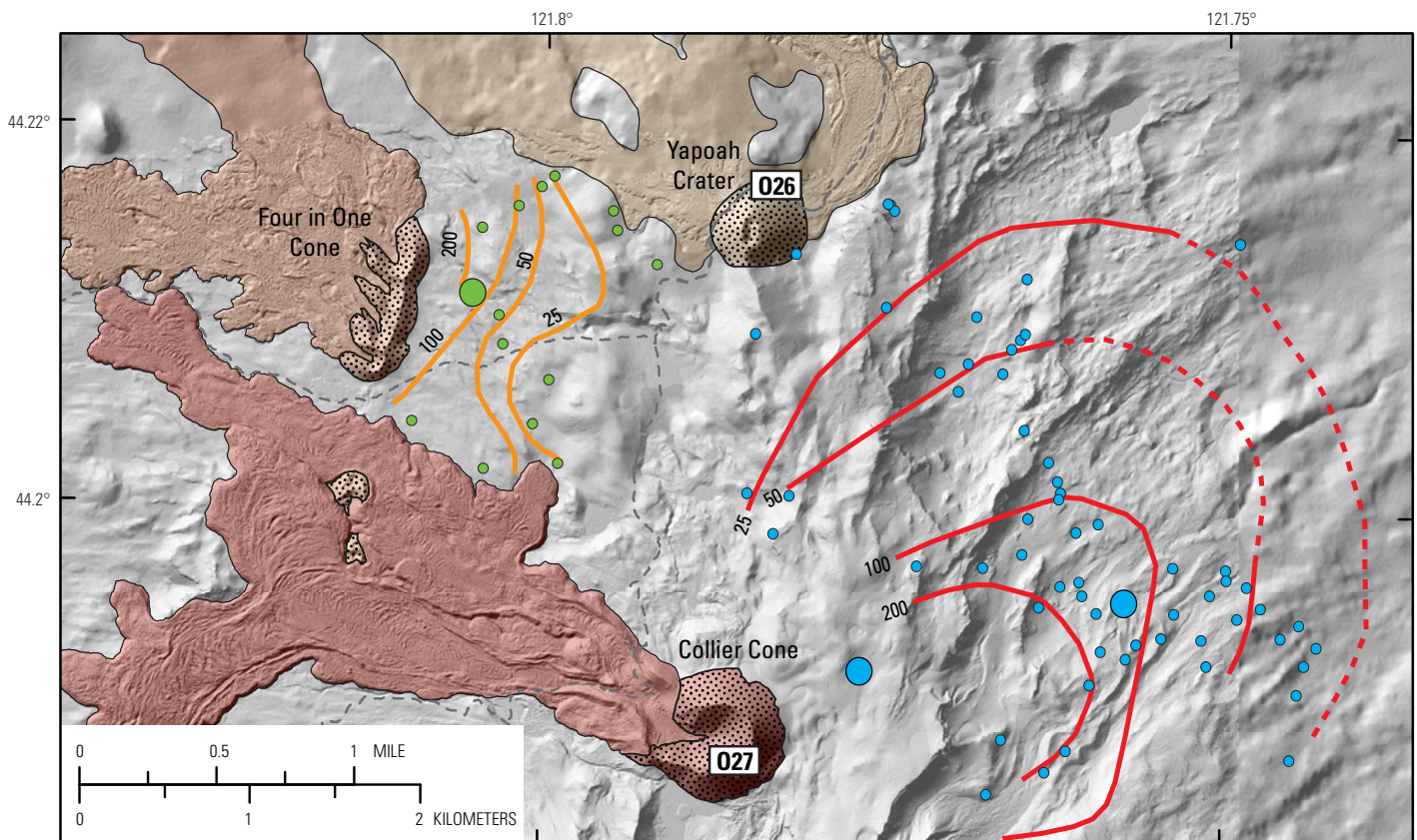


Figure 45. Shaded-relief map and isopachs showing thickness (in centimeters) of tephra deposits from Four in One Cone (orange lines) and Collier Cone (red lines). Isopachs dashed where inferred or poorly constrained. Dots show tephra localities (green, tephra from Four in One Cone; blue, tephra from Collier Cone): small dots, locations where tephra thicknesses were measured; large dots, locations where complete tephra stratigraphy was described and sampled. Also shown are Holocene lava flows and vents (stippled areas) (from Sherrod and others, 2004; Koch and others, 2010; Deardorff and Cashman, 2012). Field-trip stops shown by white rectangles; stop numbers are inside rectangles (0, optional stop). Dashed gray lines show trails. Shaded relief derived from lidar imagery (from National Center for Airborne Laser Mapping, 2008; Oregon Department of Geology and Mineral Industries, 2011b) where available and from 10-m digital elevation models (from Oregon Geospatial Enterprise Office, 2008) elsewhere. Trails from U.S. Forest Service (2017).

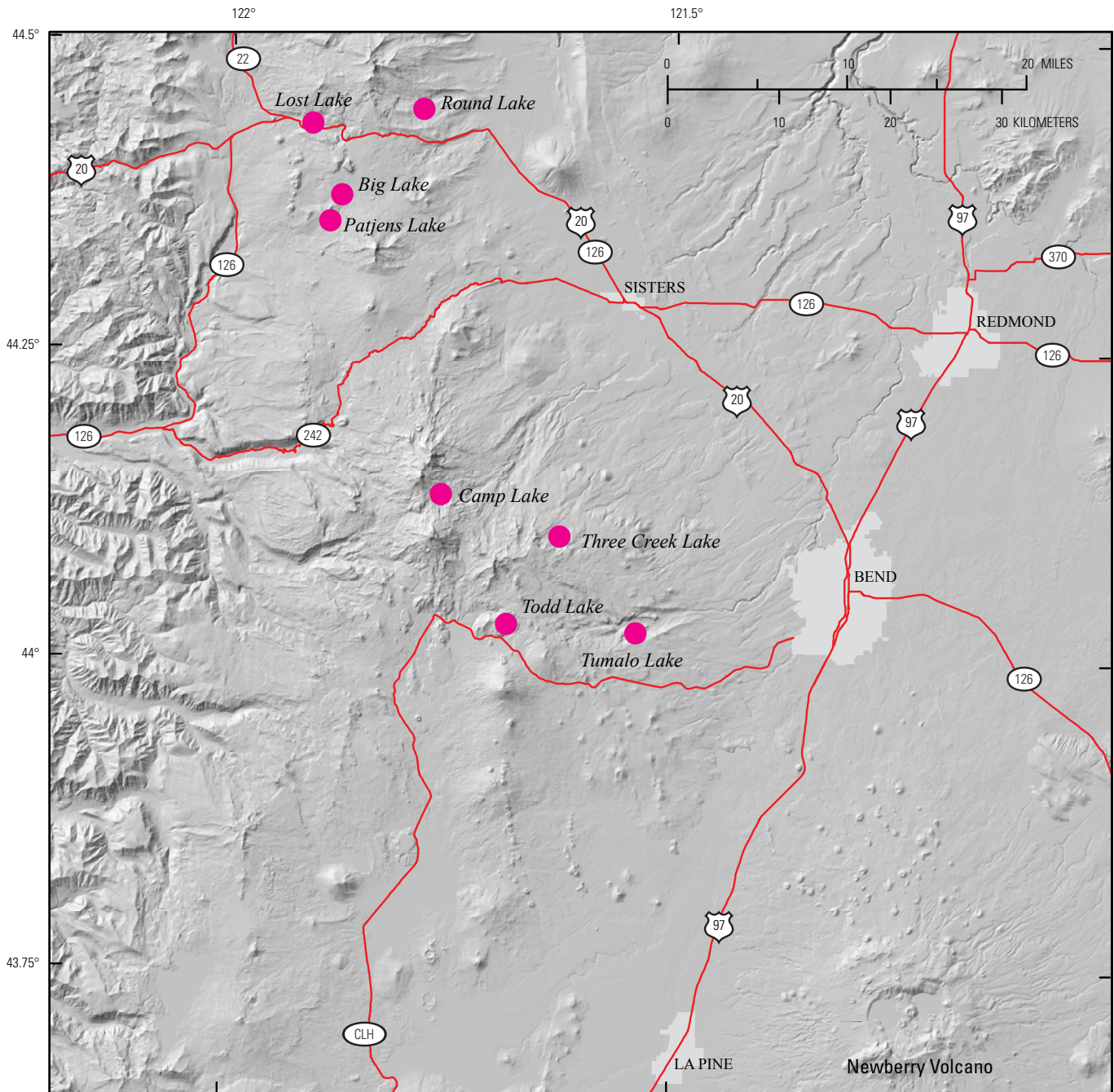


Figure 46. Shaded-relief map showing locations of regional lakes (magenta dots) that have preserved tephra deposits from central Cascade-arc cinder cones (Mckay, 2012). Cascade Lakes Highway (Highway 46) is labeled as 'CLH.' Shaded relief derived from 10-m digital elevation models (from Oregon Geospatial Enterprise Office, 2008). Roads from Oregon Department of Transportation (2015) and University of Oregon Map and Aerial Photography Library (available at https://library.uoregon.edu/map/gis_data/county_trans.html).

heterogeneities in both major-element and phenocryst contents (Schick, 1994; Deardorff and Cashman, 2012). Variations in SiO_2 content are similar to those observed during the 1943–52 eruption of Volcán Parícutin, Mexico, which have been interpreted to reflect assimilation of silicic upper crustal rocks in shallow dikes and sills (Wilcox, 1954; Erlund and others, 2010). Silicic xenoliths present in tephra and lava deposits from both Collier Cone and Four in One Cone (Taylor, 1965; Schick, 1994) may explain much of the chemical variation observed in these two eruptive sequences.

Discussion of Stop 27

Before we discuss Collier Glacier View, we will briefly discuss the lava flows at Collier Cone. On Day 1 (Stops 6, 7), we saw the westernmost extent of the Collier Cone lava flows (fig. 11C), which are among the earliest products of the eruption. From Opie Dilldock Pass immediately prior to reaching Collier Cone, all four lava units of the eruption (fig. 11B; see also, Deardorff and Cashman, 2012), which range in composition

from basaltic andesite to dacite (fig. 12), can be seen. Unit 1 not only flowed down White Branch valley but also had a second lobe that surrounded two vents from Four in One Cone. Unit 2 ponded within the cone and subsequently breached it, rafting parts of the cone; unit 2 also produced levees within unit 1 levees, leading to sets of levees in places (for example, the ones seen on the trail to Stop 7). Unit 3 produced two lobes that remained on the McKenzie Pass plateau (that is, they did not descend into White Branch valley). Dacitic unit 4, the last lava to erupt, is a small flow that is confined to the cone area. Modeling has suggested that unit 1 was emplaced in 2 to 3 months;

unit 2, in less than 6 months; and unit 3, in a bit over a month (Deardorff and Cashman, 2012). Thus, the eruption likely lasted less than a year.

Collier Glacier View is of interest because of the history of Collier Glacier and related events. At the peak of the Little Ice Age in the mid- to late 1800s, Collier Glacier View would have been under ice; even in the early 1900s, ice extended to the base of Collier Cone (fig. 47). At its maximum Little Ice Age extent, Collier Glacier was probably the largest glacier in Oregon, covering about 2.3 km² (O'Connor and others, 2001a), but, by the early 2000s, it had diminished to about 0.8 km².

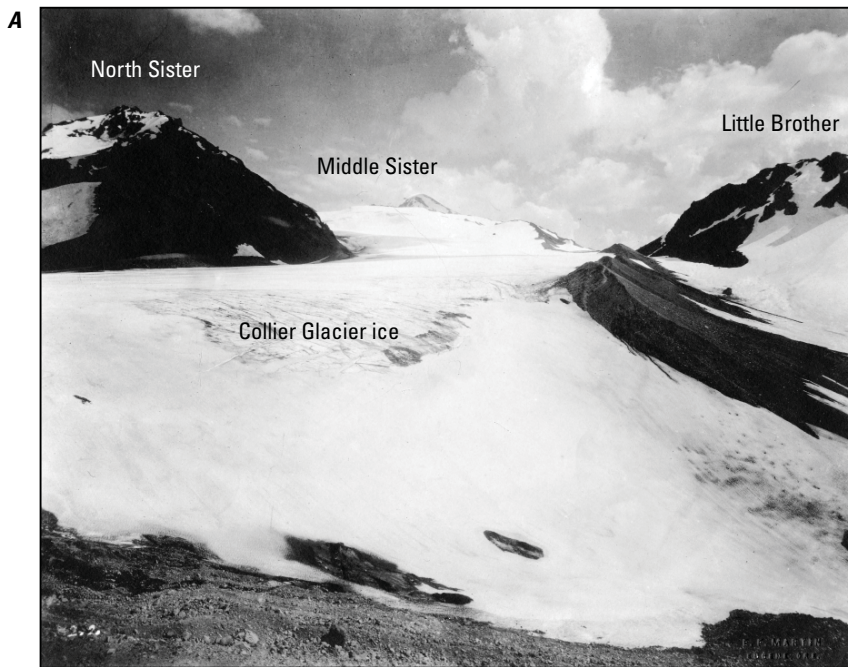
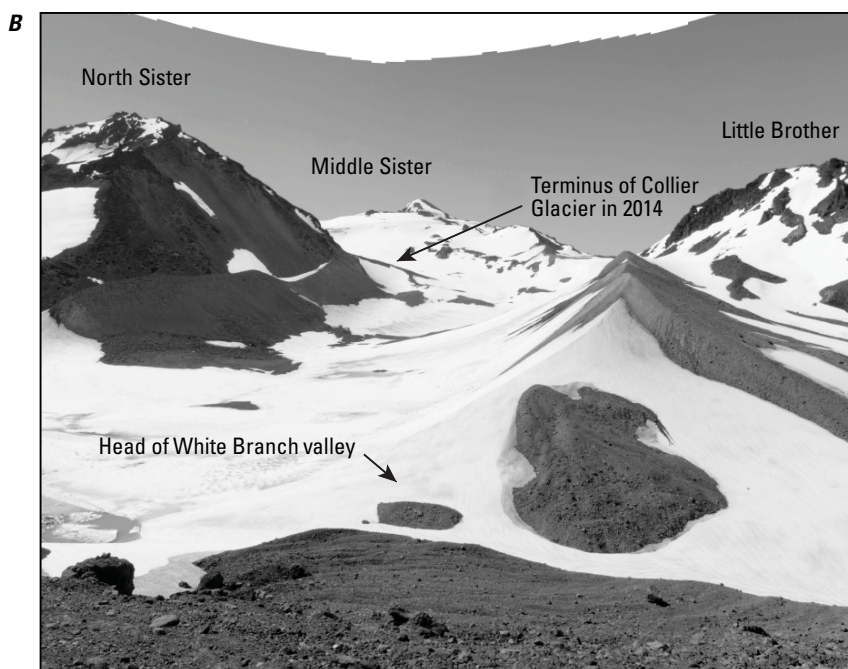


Figure 47. Photographs to south-southeast of Collier Glacier, taken from same position at Collier Glacier View, 100 years apart. *A*, Photograph taken by E.F. Martin on July 14, 1914 (scanned from postcard provided by Gerald W. Williams), showing Collier Glacier, which flows 2 km northwest from saddle between North Sister and Middle Sister, and its terminus in foreground, in head of White Branch valley. *B*, Photograph taken by Jim O'Connor on July 10, 2014, showing approximate position of terminus, which is obscured by snow. Note that photograph has been warped to account for different lens characteristics between cameras (white area at top of photograph is artifact of this process).



The former extent and thickness of the ice is easily visualized by imagining the immense space between the 100-m-high lateral moraines, built up as Collier Glacier descended the poorly consolidated stratovolcanoes. Its retreat has also been documented and analyzed by photographs, both aerial (vertical) and oblique, taken by many over the years (fig. 47; see also, Hopson, 1960; O'Connor and others, 2001a,b; O'Connor, 2013). Photogrammetric analysis of aerial photographs shows that remnant parts of Collier Glacier thinned by more than 40 m between 1957 and 2010 (Ohlschlager, 2015).

As glaciers retreated and thinned in the Cascade Range, particularly in the early 1900s, lakes formed in the moraine-rimmed voids between the diminished glacier termini and Little Ice Age moraines. Such lakes are especially common on the erodible stratovolcanoes, where Little Ice Age moraines are large. In the Mount Jefferson and Three Sisters Wilderness areas, 12 debris flows resulted from 4 complete and 8 partial breaches of moraine-dammed lakes. Most of these moraine-dam breaches occurred between 1930 and 1950 (O'Connor and others, 2001a), but one was as recent as 2012 (Sherrod and Wills, 2014). Some of the resulting debris flows traveled several kilometers downstream before transforming into sediment-laden floods.

Two of these debris flows emanated from a lake impounded by the moraine of Collier Glacier (O'Connor and others, 2001a). According to Ruth Hopson Keen, who photographed from Collier Glacier View almost annually between 1933 and 1973, the lake first formed between August 1933 and September 1934, and it grew until 1940 as Collier Glacier melted back from Collier Cone. At its maximum extent, the remnant lake covered 100,000 m² and had a volume of 670,000 m³ (fig. 48). The first breach, in July 1942, was the largest, releasing nearly 500,000 m³ of water. The second breach and debris flow occurred between 1954 and 1956 (fig. 48).

The larger 1942 flow was one of the largest of the historic moraine-dammed-lake debris flows in the Cascade Range. Like many outbursts from moraine-dammed lakes, its flow rate increased downstream as it entrained material from the moraine (fig. 49). The maximum possible outflow at the breach was about 150 m³/s, but the flow increased to about 500 m³/s at Sawyer Bar, 1 km downstream, as it entrained about 120,000 m³ of till and outwash from the eroding moraine. The debris flow continued 8 km downstream, entraining material in steep reaches and depositing it in lower gradient reaches before dying out on the lava flow from Collier Cone.

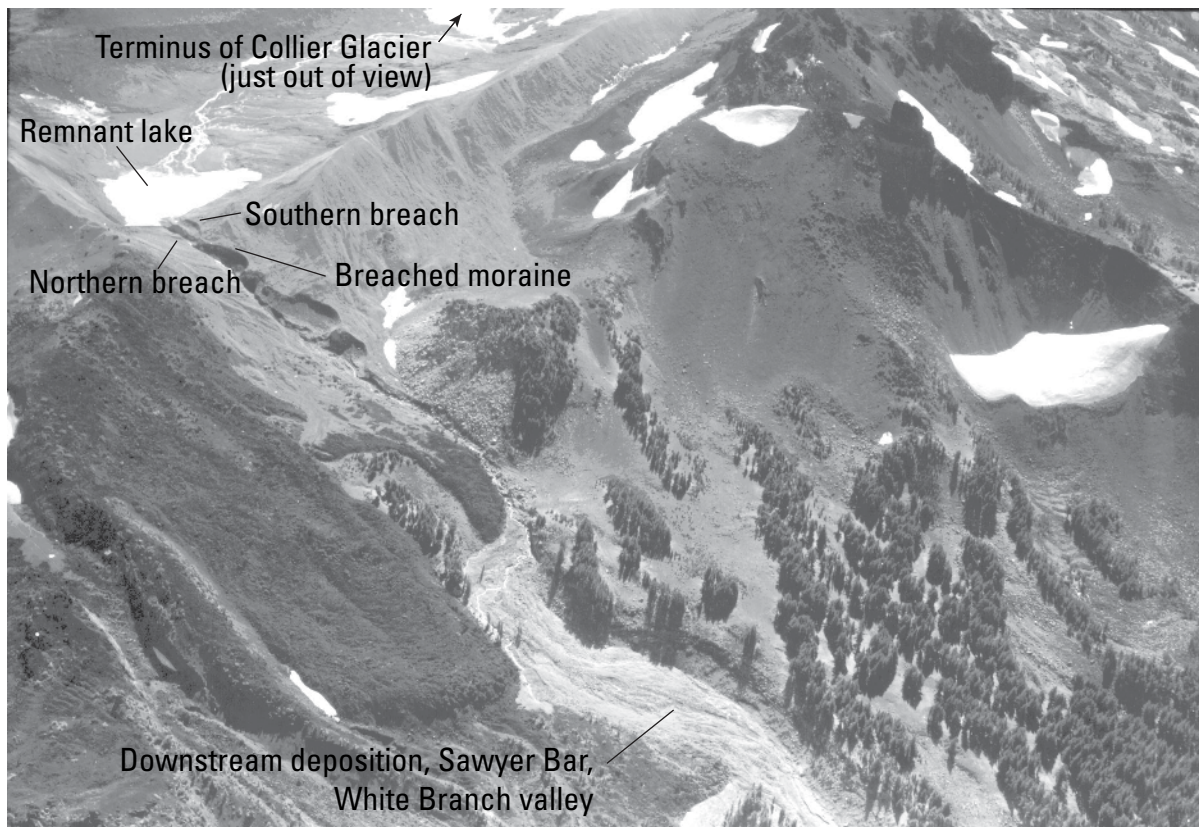


Figure 48. Oblique aerial photograph to southeast toward remnant lake, breached moraine, and downstream deposits left after 1942 debris flow from lake at Collier Glacier, which resulted from southern breach and caused most of incision visible in moraine and downstream deposition into White Branch valley at Sawyer Bar. In this view, lake drains through second, northern breach that formed between 1954 and 1956. Photograph by Ackroyd Photography, October 1956.

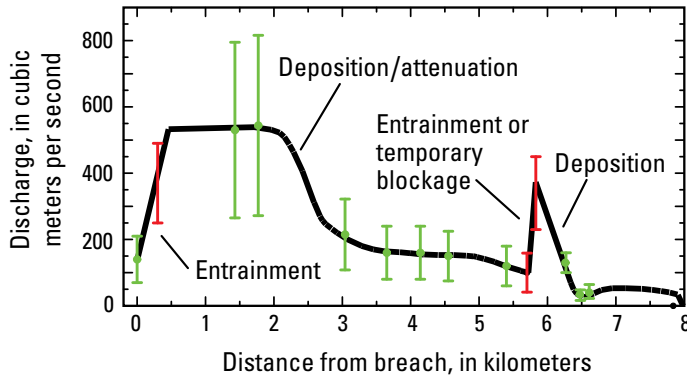


Figure 49. Graph showing indirect estimates of peak discharge for 1942 debris flow into White Branch creek. From O'Connor and others (2001a). Curve is interpretation of how peak discharge varied downstream, annotated with inferences of processes that are controlling changes in peak discharge. Green points and error bars are critical-flow estimates; red ranges are velocity-area estimates.

Although these outburst floods from moraine-dammed lakes may not be significant hazards in the wilderness areas of the Three Sisters region, they are one consequence of the many related to the climate-change effects of global warming and the resulting diminishment of alpine ice (O'Connor and Costa, 1993). For example, deglaciated areas are a source of debris flows and sediment that causes downstream channel aggradation and the burying of bridges and roads, most notably since the 1980s near Mount Hood (Pirrot, 2010) and Mount Rainier (Legg and others, 2014). Such hazards and processes are likely to continue as glaciers and perennial snow are lost from the tall, steep, and unstable stratovolcanoes of the Pacific Northwest.

Stop 28 (Optional): Little Belknap Crater

Directions to the Trailhead for Stop 28 and Description of Hike

[Note that the hike descriptions and maps in this field-trip guide are not a substitute for a good topographic or trail map. Maps are available at the McKenzie Ranger Station (Stop 3) and at most outdoor recreational stores in Oregon]

From the Dee Wright Observatory, travel west on Highway 242 for 0.5 mile (0.8 km). The trailhead is the McKenzie Pass access point to the Pacific Crest National Scenic Trail (PCT). The hike is within the Mount Washington Wilderness; self-issue permits, which are available at trailheads, are required to enter. Sampling or collecting is not allowed without a special use permit. Leave no trace. Dogs are not permitted.

The round-trip hike to Little Belknap crater (distance, 5.2 miles [8.4 km]) follows a relatively flat part of the PCT, but it is exposed and has little shade. The trail traverses blocky lava flows, and so good hiking boots are essential.

From the trailhead, hike north on the PCT for 2.4 miles (3.9 km). At a clearly marked intersection, leave the PCT and take the trail to the right (east) to Little Belknap crater. From here, the summit is less than 0.25 miles (0.4 km) away, although some scrambling will be required to make it to the top. A snow shelter at the summit will provide shade for lunch.

Discussion of Stop 28

From Little Belknap crater, we will have a good view of Belknap Crater, Mount Washington to the north, and the Three Sisters volcanic cluster to the south. Little Belknap crater is part of the Belknap shield-volcano complex, consisting of numerous vents that include Belknap Crater, “South Belknap” (an unnamed cone south of Belknap Crater), and Little Belknap crater. Little Belknap crater has a few short lava tubes near its summit (Craig, 1993). This lava-tube system is unusual in that it is spread over two levels; apparently, the lower level drained the upper level (Craig, 1993). Use extreme caution if you choose to explore these tubes.

[Remainder of Stop 28 description is modified from Cashman and others (2009)]

Unlike Collier Cone, Yapoah Crater, and Four in One Cone to the south, Belknap Crater lavas are primarily basaltic in composition and are slightly enriched in K_2O , which continues a trend noted by Schmidt and Grunder (2009) of a general decrease in SiO_2 in younger lavas from North Sister to McKenzie Pass. Belknap Crater also differs in that it is a mafic shield volcano formed by numerous eruptions from the same vent. An eruption of Belknap Crater at about 1,500 ^{14}C yr B.P. sent flows toward the McKenzie River valley (fig. 17). The oldest exposed Belknap Crater lavas, which lie to the northeast, have not been dated; however, lava flows from “South Belknap,” which form numerous interfingering small channels and flows that have blocky surfaces, have been dated at $2,635 \pm 50$ ^{14}C yr B.P. (Licciardi and others, 1999). In addition, overlying lava flows from Little Belknap crater have been dated at 2,883 ^{14}C yr B.P. (Taylor 1968, 1990a), a date that seems too old for the young morphology of Little Belknap crater and its stratigraphic relation with Belknap Crater (Sherrod and others, 2004). Together these eruptions have created a shieldlike edifice cored by a cinder cone. The lava flows have surface morphologies that range from blocky to pāhoehoe; the pāhoehoe flows from Little Belknap crater created kipukas, which are islands of older lavas surrounded by younger lavas. In Hawaii, kipukas create biological islands that can preserve rare species or promote rapid evolution of isolated insect populations.

End of Day 4: Bend

Directions to Bend

Return to Highway 242 (McKenzie Highway) and travel east for 15 miles (24 km) to Sisters, then take Highway 20 southeast for 20 miles (32 km) to Bend.

Day 5. The Bend Area

[Note that some roads we plan to take on Day 5 are subject to seasonal closures, so please check their status before you travel: (1) Lava Lands Visitor Center and the road to the top of Lava Butte (Stop 29) are typically open from May to October, but operating days and hours vary throughout the season; check with the Deschutes National Forest (<https://www.fs.usda.gov/recarea/deschutes/recarea/?recid=38394>) to see their status. (2) Parts of Highway 46 (also known as the Cascade Lakes Highway), required to access Stops 32 and 33, are closed at Mount Bachelor in winter and spring; check with the Oregon Department of

Transportation (<http://www.tripcheck.com/Pages/RCmap.asp?curRegion=0&mainNav=RoadConditions>) or the Deschutes National Forest (<http://www.fs.usda.gov/alerts/deschutes/alerts-notice>) to see whether the highway is open or closed. (3) Although trails to the summit can be accessed year-round, the road to the summit of Pilot Butte (Stop 34) in Bend is closed seasonally; check with Oregon State Parks (http://oregonstateparks.org/index.cfm?do=v.dsp_Notices) to see the status of the summit road]

On Day 5 of the field trip, we will focus on late Pleistocene and Holocene volcanism in the Bend area (fig. 50). Two general themes will guide our discussions during today's stops, (1) interactions between volcanism and regional hydrology, and

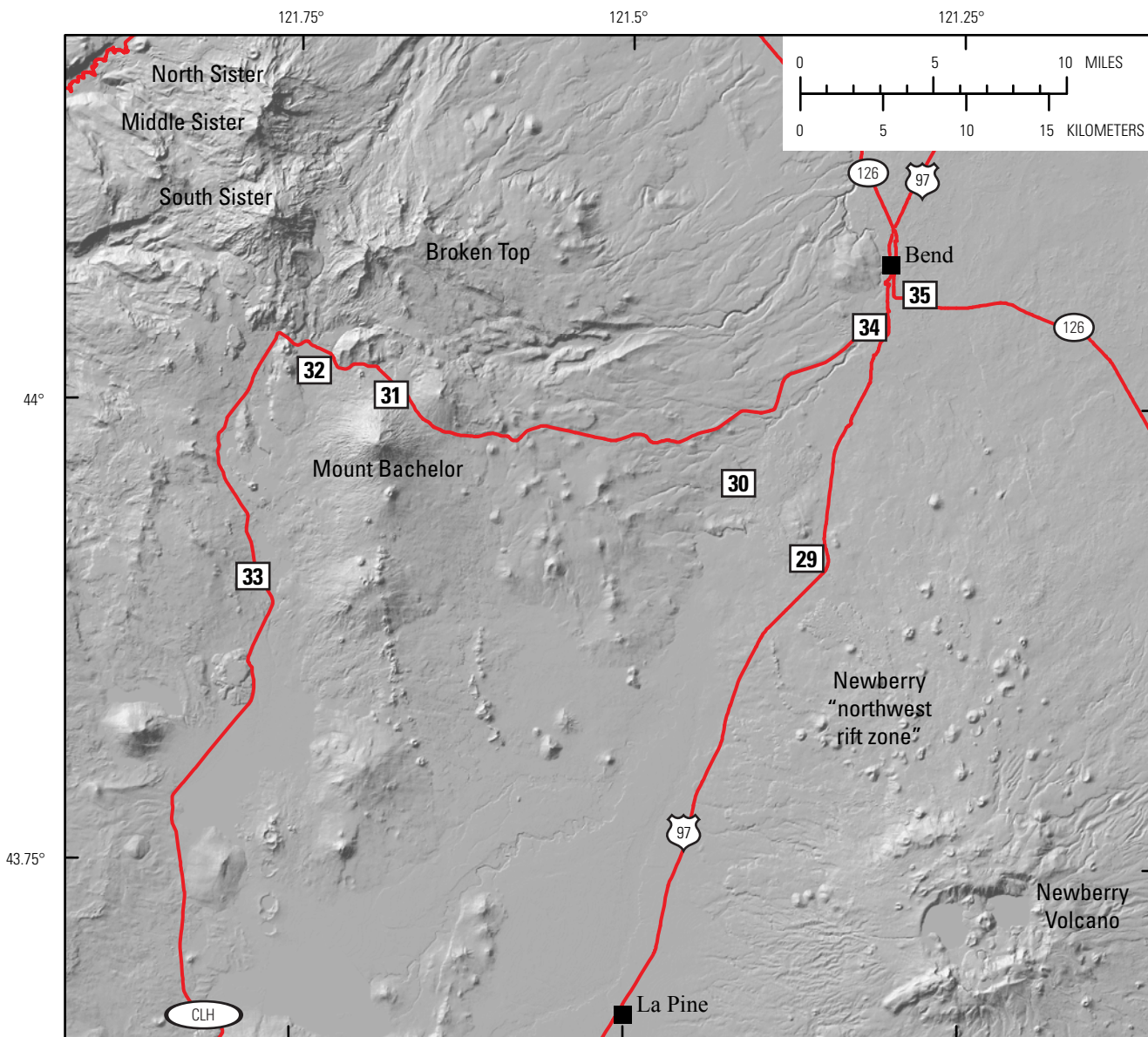


Figure 50. Shaded-relief map showing locations of field-trip stops on Day 5. Field-trip stops are shown by white rectangles; stop numbers are inside rectangles. Cascade Lakes Highway (Highway 46) is labeled as 'CLH.' Shaded relief derived from 10-m digital elevation models (from Oregon Geospatial Enterprise Office, 2008). Roads from Oregon Department of Transportation (2015) and University of Oregon Map and Aerial Photography Library (available at https://library.uoregon.edu/map/gis_data/county_trans.html).

(2) volcanic hazards associated with a rapidly developing urban area within a young volcanic landscape.

We will start the day with an overview from the top of Lava Butte, one of many cinder cones that dot the “northwest rift zone” of Newberry Volcano (Stop 29). Lava Butte sits near the north end of a sediment-filled graben (the La Pine Subbasin) that separates Newberry Volcano from the Cascade Range. Flows from Lava Butte displaced the Deschutes River westward against older deposits, resulting in a series of waterfalls that includes Dillon Falls (Stop 30).

From Lava Butte, we will return to Bend, then we will travel west on Highway 46 (also known as the Cascade Lakes Highway) to the Deschutes River and Dillon Falls (Stop 30). From there we will continue on Highway 46 to Mount Bachelor and the Three Sisters volcanic cluster area. At Mount Bachelor, we will take one of the ski lifts, which remains operational during summer months, to the midmountain lodge for lunch and for spectacular views of the Three Sisters volcanic cluster and its surrounding volcanoes (Stop 31).

After lunch, we will continue west on Highway 46 to Sparks Lake (Stop 32), which is dammed by lava flows from “Egan Cone,” on the north slope of Mount Bachelor. Our last stop on Highway 46 will be Lava Lake fen, a spring-fed wetland that has unusually high plant biodiversity (Stop 33). From there we will return to Bend; we will end our day with a visit to the top of Pilot Butte (Stop 34), where we will discuss volcanic hazards in the Bend area.

Stop 29. Top of Lava Butte

Directions to Stop 29

From Bend, take Highway 97 south toward Klamath Falls. Follow Highway 97 for about 11 miles (17.7 km) to the entrance to Lava Lands Visitor Center on the west side of the highway. If the visitor center is open, take the immediate right turn (north) through the entrance gate. If the visitor center is not open, go straight on Forest Service Road 9702 (Crawford Road) for about 0.1 mile (0.2 km) and turn right (north) into the entrance for the west end of the visitor center parking area; trails can be accessed from the west end of the parking area. Display a Northwest Forest Pass in your vehicle when parked.

Lava Lands Visitor Center and Lava Butte are part of Newberry National Volcanic Monument, which is managed by the Deschutes National Forest. During hours of visitor center operation, a \$5 fee per vehicle (current as of 2017), which includes entrance to all other locations on the monument, will be charged, unless you have a Northwest Forest Pass, in which case you will not need to pay an additional fee to access the visitor center or other locations on the monument. During peak season, a shuttle runs to the summit of Lava Butte (round-trip cost, an additional \$2 per person; during times in which the shuttle is in operation, personal vehicles may not be used to access the summit of Lava Butte.

Discussion of Stop 29

[Modified from Cashman and others (2009)]

From the splendid vista atop Lava Butte, a few hundred large and small volcanoes and nearly two-thirds of the upper Deschutes Basin can be seen. Newberry Volcano, which dominates the southern skyline, has multiple cinder cones and recent lava flows that are visible in the middle distance. To the west, hundreds of cinder cones, domes, large and small shield volcanoes, and stratovolcanoes of the Cascade Range are visible. On a clear day, the entire central section of the Cascade Range can be seen, from Mount Scott and the remnants of Mount Mazama (Crater Lake) in the south, to Mount Adams in the north. Figure 51 shows a simplified compass wheel that indicates the direction and distance to many features that are visible from this lookout.

[Modified from Jensen and others (2009)]

Newberry Volcano is a large, shield-shaped composite volcano that lies south of Bend, at the intersection of the Cascade Range and the High Lava Plains geologic province. Lava Butte is the northernmost vent along the Holocene “northwest rift zone” (informal name first used by Peterson and Groh, 1965), a nearly continuous zone of mafic vents and flows that extends 31 km from Lava Island on the Deschutes River to the north wall of Newberry caldera (fig. 52).

The “northwest rift zone” eruption postdates deposition of Mazama ash, the product of the eruption that formed Crater Lake about 7,650 years ago (Hallett and others, 1997). MacLeod and others (1995) listed 11 radiocarbon dates from eight flows along the “northwest rift zone,” as reported by five different sources. Calibrated radiocarbon ages range from 7,240 to 6,610 yr B.P., and they average 6,927 calendar yr B.P. Herein we use an even 7,000 calendar yr B.P. as an estimate of the age of Lava Butte.

The Lava Butte eruption began on a 2.4-km-long fissure and then became localized at the site of Lava Butte (fig. 52). The eruption produced a 150-m-high cinder cone, several spatter ramparts, and lava flows that cover more than 23 km². Chemical analyses of Lava Butte and its lavas yield silica contents of 55.3 to 56.2 wt. percent SiO₂ (McKay and others, 2009), whereas lava flows from individual vents of the “northwest rift zone” are variable in composition, ranging from basalt of the Sugarpine vents to basaltic andesites and andesites of Lava Butte and Mokst Butte (fig. 52; see also, MacLeod and others, 1995; Jensen, 2006), which suggests that they may not be the result of a single eruption.

Vents along the “northwest rift zone” provide examples of the types of mafic eruptions that have occurred on the flanks of Newberry Volcano. Individual vents in this zone have produced spatter ramparts, cinder cones of various sizes, both ‘a’ā and pāhoehoe lava flows, and tephra blankets. Physical characteristics of these erupted materials demonstrate that not all cinder-cone eruptions are the same. Vents for some flows produced low spatter ramparts and lava flows dominated by pāhoehoe, which are products typical of Hawaiian-style eruptions. Other vents produced small cinder cones and lava flows dominated by ‘a’ā, which are products typical of low-energy Strombolian-style

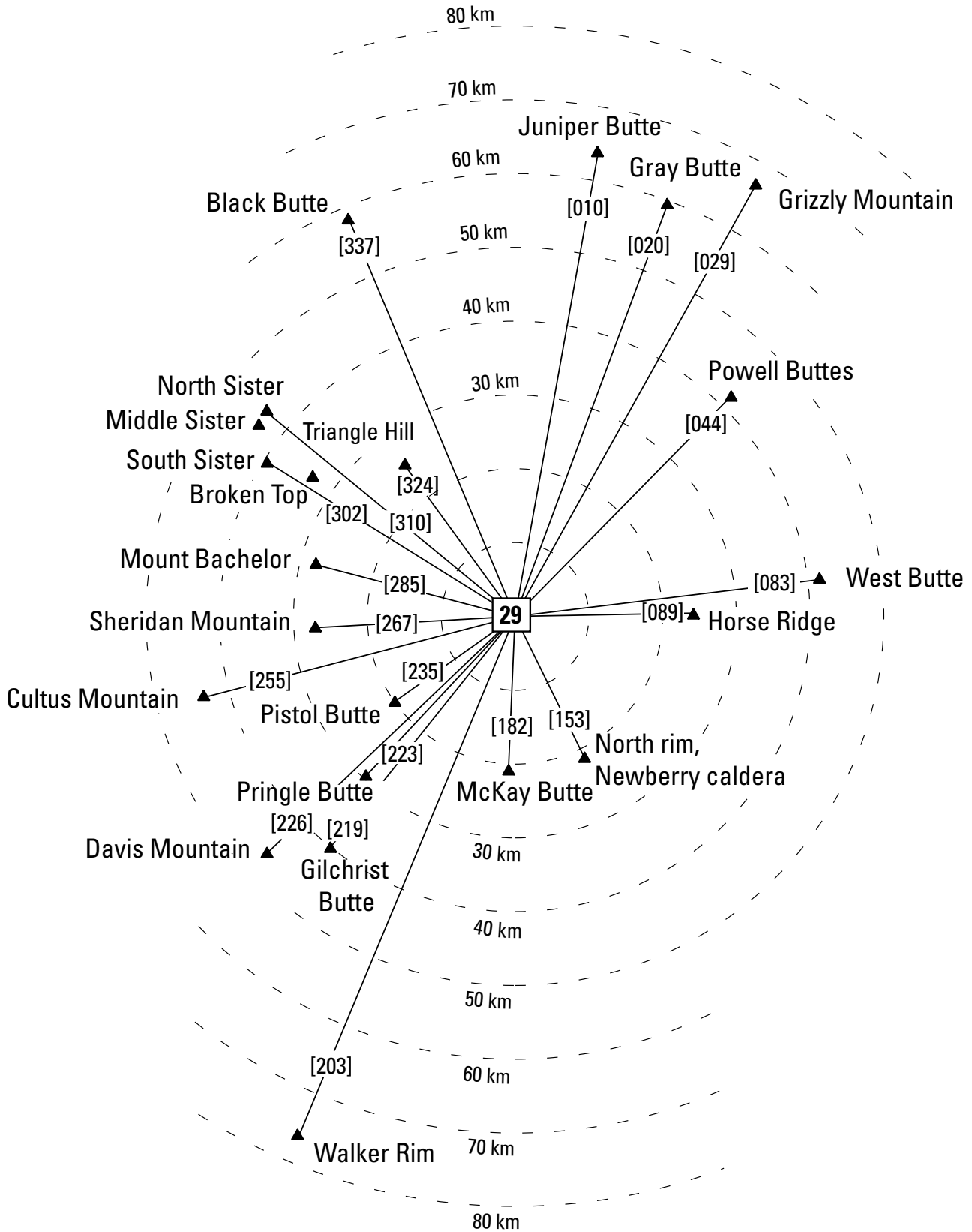


Figure 51. Compass-wheel diagram showing distances (dashed lines) and approximate azimuthal directions (in brackets) to peaks and other features (triangles) that are visible from top of Lava Butte (Stop 29; relative location shown by stop number in white rectangle). Modified from Sherrod and others (2002).

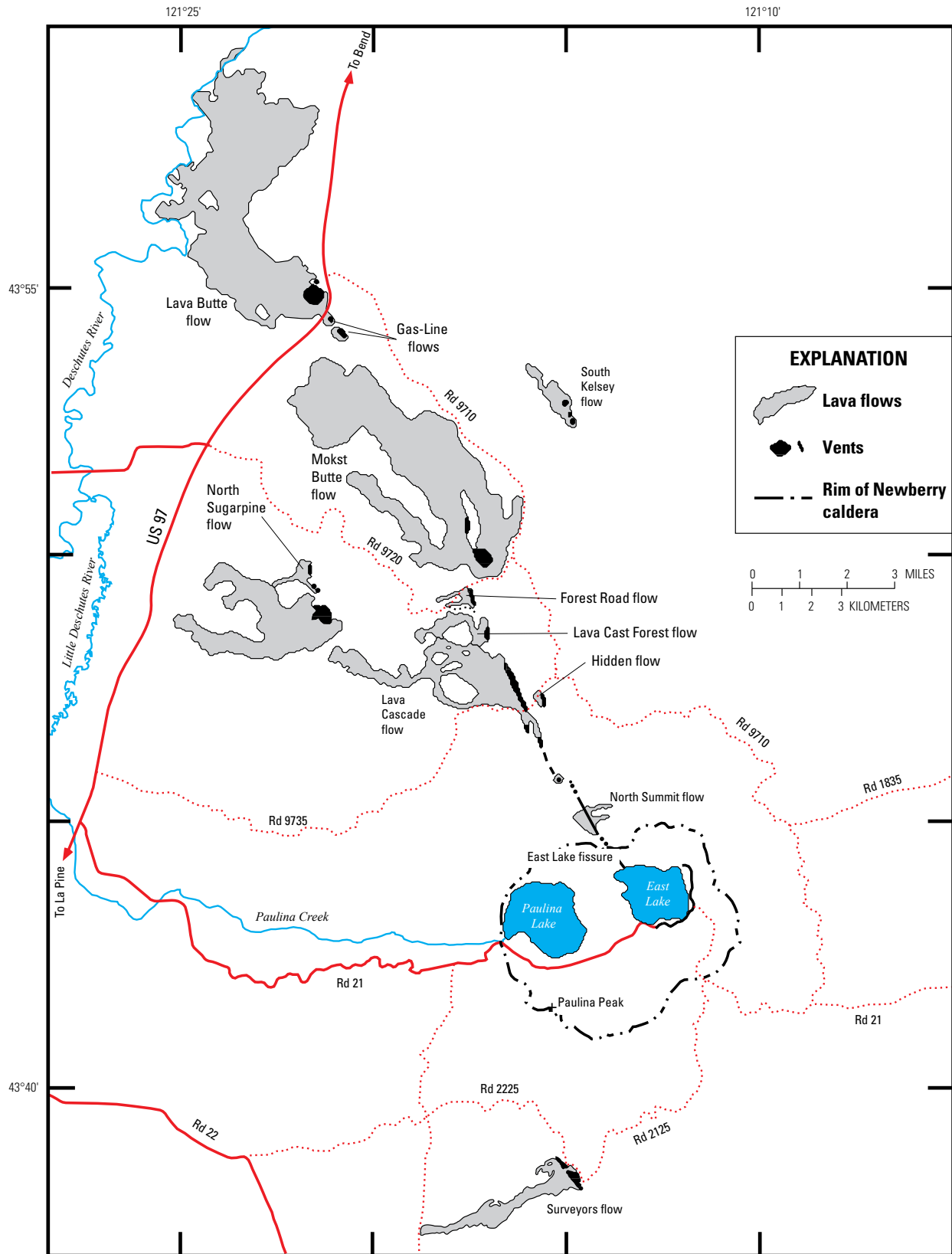


Figure 52. Map showing vents, fissures, and lava flows of “northwest rift zone” of Newberry Volcano, which postdates deposition of Mazama ash. Modified from Jensen (2006). Red solid lines show highways and paved roads; red dotted lines show four-wheel-drive roads. Drainage, highways, paved roads, and four-wheel-drive roads traced from U.S. Geological Survey 1:24,000-scale quadrangle maps.

eruptions. Lava Butte and Mokst Butte are large cinder cones that produced extensive ‘a’ā lava flows and tephra blankets, which are products indicative of energetic Strombolian or perhaps violent Strombolian-style activity.

[Modified from Cashman and others (2009)]

Lava flows of the “northwest rift zone” merge with lava flows from the Cascade Range to form the northern limit of the La Pine Subbasin, a relation that has probably existed for a substantial part of the history of the subbasin. Emplacement of the Lava Butte flow diverted the Deschutes River, forcing the river to establish a new channel along the western margin of the lava flow. The topographic gradient increases abruptly north of the contact between the lava of Newberry Volcano and lava from the Cascade Range, from relatively flat in the sediment-filled basin south of here to prominently northward sloping to the north. The stream gradient reflects this topographic change: the Deschutes River drops a mere 0.48 m/km along the 71-km-long reach between Wickiup Reservoir and Benham Falls, whereas, north of Benham Falls, the gradient steepens dramatically to 8.7 m/km along the 18.5-km-long reach to Bend.

The slope of the water table also increases north of Benham Falls, but to a greater degree. The water table is roughly 3 m below the land surface in much of the La Pine Subbasin. Starting at Sunriver, 8 km southwest of Lava Butte, the water table slopes northward so steeply that at Bend the depth to water is 170 to 200 m below the land surface. Near the river at Benham Falls, the water table is at an altitude of about 1,260 m and is 1.5 to 5 m below the land surface (fig. 53). In downtown Bend, the water table is at an altitude of 940 m, and the land-surface elevation is 1,110 m.

Stop 30. Dillon Falls—Incursion of the Lava Butte Flow into the Deschutes River

Directions to Stop 30

Exit the west end of the Lava Lands Visitor Center parking area and turn left (east) onto Forest Service Road 9702 (Crawford Road). Take an immediate right (south) in about 180 feet (50 m) onto Cottonwood Road, then follow Cottonwood Road for about 2 miles (3.2 km) to the junction with Highway 97. Turn right (north) to merge with Highway 97 northbound toward Bend. Follow Highway 97 for about 11 miles (17.7 km) to Reed Market Road (Exit 139). After exiting Highway 97, turn left (west) onto SW Reed Market Road and follow it for about 1.6 miles (2.6 km). You will pass through four traffic circles on this route; at each of these four traffic circles, continue west on SW Reed Market Road. At the fifth traffic circle, take the third exit onto SW Century Drive, which is marked with a sign for Mount Bachelor Ski Area and “Cascades Lakes;” SW Century Drive will become Highway 46 (also known as Cascade Lakes Highway). Continue on Highway 46 for about 4.9 miles (7.9 km) to Forest Service Road 41 (Conklin Road) and turn left (south); the turn is marked with a sign for “Deschutes River Recreation Sites.” Follow Forest Road 41 (Conklin Road) for about 2.6 miles (4.2 km) to Forest Service Road 600 and turn left (southeast); the turn is marked with a sign for Dillon Falls. Follow Forest Road 600 about 0.8 miles (1.3 km) to the end of the road. Several spur roads are along the route; stay to the left at each junction. The road ends at a small parking area and picnic area. Display a Northwest Forest Pass in your vehicle when parked.

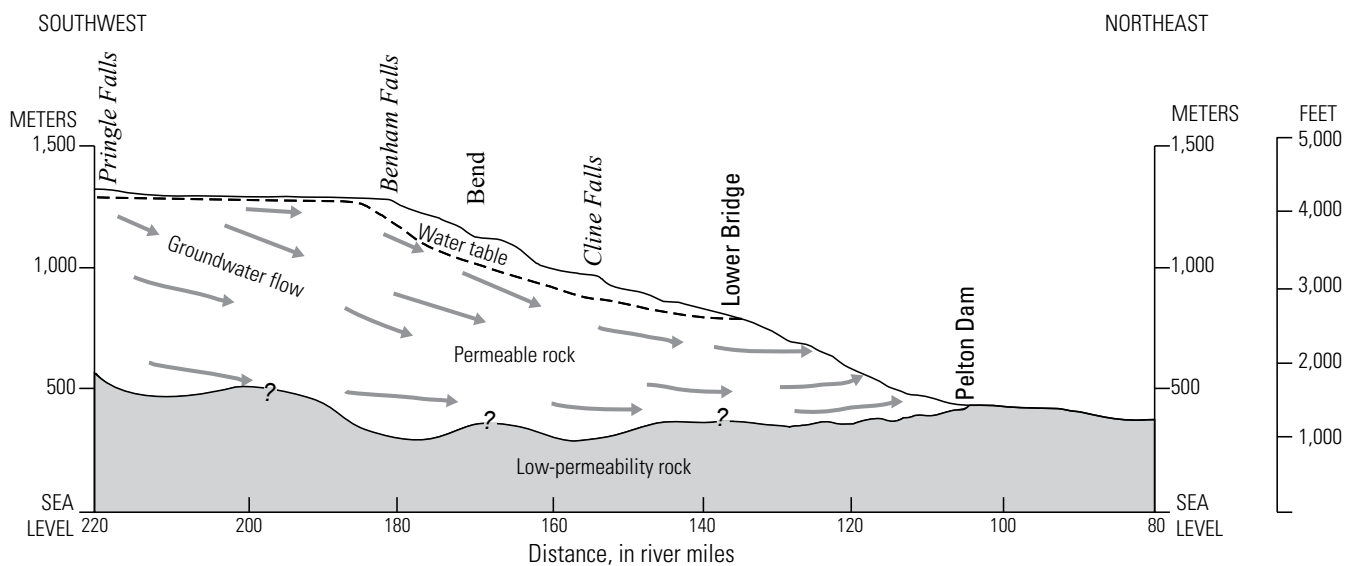


Figure 53. Diagrammatic cross section of elevation profile of Deschutes River, showing effect of geology and topography on groundwater flow (arrows) and discharge along Deschutes River from Benham Falls to Pelton Dam. Area of groundwater discharge to Deschutes River is between water table (dashed line) at Lower Bridge and contact with low-permeability rock at Pelton Dam; queries indicate that identity and (or) existence of contact between permeable and low-permeability rock is uncertain. Modified from Gannett and others (2001).

Discussion of Stop 30

[Modified from Cashman and others (2009)]

Lava flows from Lava Butte entered the Deschutes River in several places, most of which are now marked by rapids. Jensen (2006) provided a detailed reconstruction (which we summarize here) of the preeruption Deschutes River channel, the syneruptive and posteruptive extents of a lava-dammed lake that once existed upstream from here (informally called “Lake Benham”), and the gradual creation of the present-day river channel.

The lava-flow lobe that entered the Deschutes River south of Benham Falls dammed the river to create “Lake Benham” (fig. 54). Radiocarbon dating of roots helped constrain the timing (and extent) of this lake: immediately following the eruption (ca. 7,000 calendar years B.P.), the elevation of “Lake Benham” was 1,274 m; by 5,890 ¹⁴C yr B.P., the lake elevation had dropped, stabilizing at 1,268 m. Dating of the plant material from the top of the diatomaceous lake sediments indicated that the lake existed until 1,950 ¹⁴C yr B.P., by which time the Deschutes River had reestablished itself and its flow was sufficient to drain the lake; however, a series of meadows upstream and downstream of Dillon Falls suggests that the river reestablished itself gradually, forming

a sequence of temporary lakes where the lava flow invaded its channel, which then existed until the river was able to carve a new channel through the lava flow. Alternatively, depending on the timing of lava incursions into the river channel, these meadows may reflect temporary lakes that formed by the syneruptive displacement of the river (that is, before the formation of “Lake Benham”). Determining the exact timing of the lava’s interactions with the river along this stretch of the modern Deschutes River will require further, more detailed studies of sediments preserved within the meadows.

From Benham Falls, the modern Deschutes River follows the margin of the Lava Butte flow until it reenters the old channel at Dillon Falls. Below Dillon Falls, the old channel is blocked by the Lava Butte flow in two more locations before the end of the lava flow is reached downstream of Lava Island Falls (Jensen and others, 2009).

A key geomorphic constraint on the time required for the Deschutes River to reexcavate its valley or to incise new canyons after damming by lava flows is the reinitiation of bedload transport across the impounding lava dam. Moving bedload serves as “tools” (Sklar and Dietrich, 2001) to abrade the dam, and such tools would be sparse until the impounded

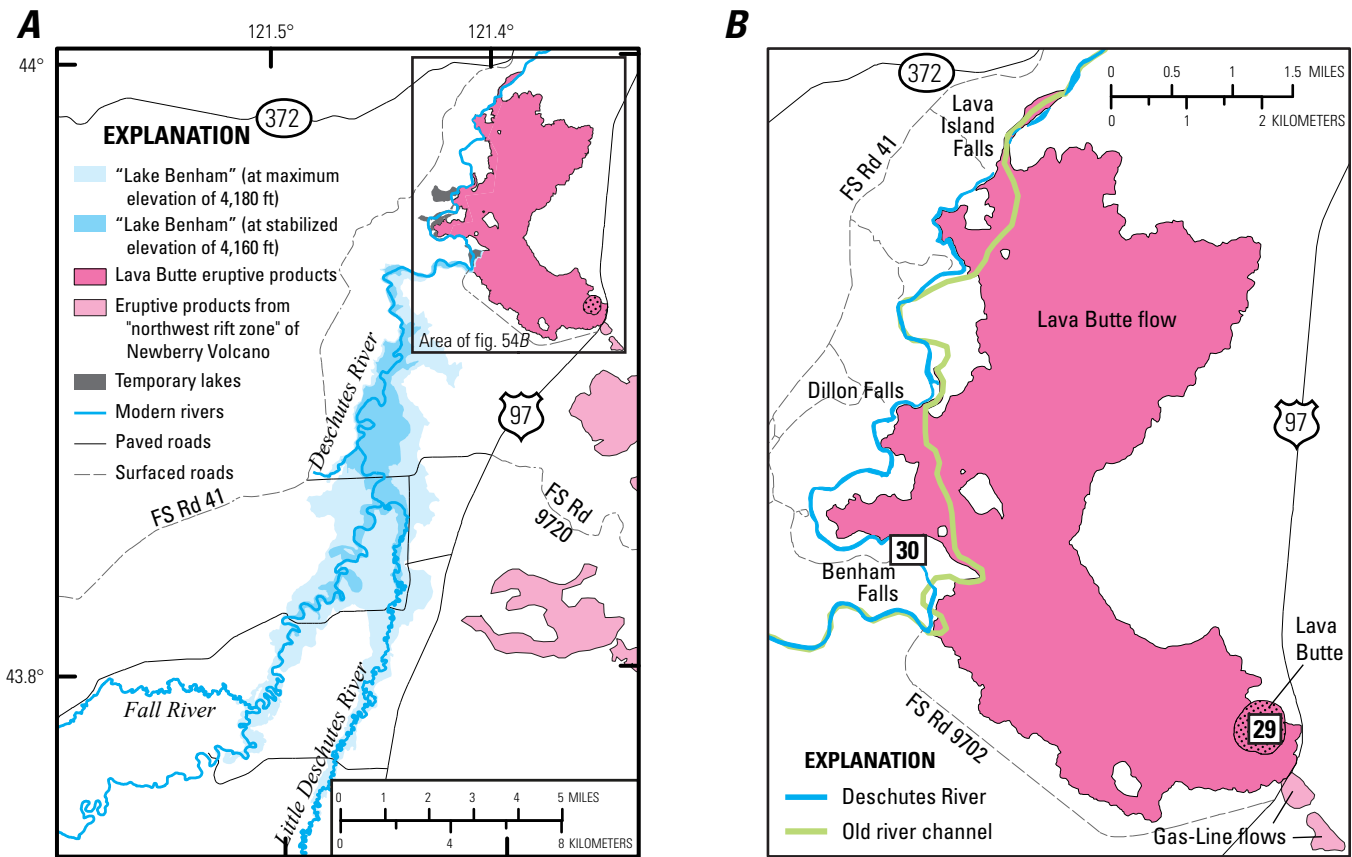


Figure 54. A, Map showing maximum and stabilized extents of “Lake Benham,” formed when young (7,000 ¹⁴C yr B.P.) lava flow from Lava Butte (stippled area) blocked ancestral Deschutes River. B, Map showing Lava Butte (stippled area) and Lava Butte flow, as well as channels of modern and ancestral (inferred) Deschutes River. Both maps modified from Jensen (2006). Base map features (drainage, highways and paved roads [solid red lines], and four-wheel-drive roads [dashed red lines]) traced from U.S. Geological Survey 1:24,000-scale quadrangle maps.

lake fills with sediment, allowing throughgoing bedload transport. In addition, past and present upstream natural dams, such as “Lake Benham” behind the lava dam that now forms Benham Falls, likely have limited downstream transport of bedload in a watershed that has an exceptionally low sediment load (O’Connor and others, 2003). These factors, in combination with the extremely stable flow regime, limit the frequency of bedload transport events and hinder fluvial incision of knickpoints such as Benham Falls and Dillon Falls. In particular, erosion of Dillon Falls probably did not commence in earnest until after “Lake Benham” had drained.

Benham Falls was investigated in the early 20th century as a potential site for a power-generation facility or a reservoir for irrigation (U.S. Reclamation Service, 1914); drill holes for site surveys in this area showed that the depth of the ancestral Deschutes River canyon was 24 m lower than that of the modern river channel. The site studies also concluded that any dam site near Benham Falls would leak badly; however, dams were successfully built upstream to form Crane Prairie and Wickiup Reservoirs. That water flows through the Lava Butte flow is indicated by local springs at the base of the lava flow near Dillon Falls, suggesting that “Lake Benham” may have been impounded by a leaky, rather than impermeable, lava dam.

Groundwater studies show a net transfer of water from the river into the lava flow that is driven by the northward-increasing depth to the water table in this area (as was discussed at Stop 29). South of Sunriver, the Deschutes River system gains water owing to groundwater discharge, and major spring complexes are common. North of Sunriver, the streams lose water to the groundwater system as groundwater altitudes drop far below stream levels. For example, stream-gage data from the 1940s and 1950s showed that the Deschutes River lost an average of 0.68 m³/s between Sunriver and Benham Falls. The average loss between Benham Falls and Lava Island Falls, about 12 km downstream, is 2.3 m³/s. Most of the loss likely happens where the channel crosses, or is adjacent to, the lava flows from Lava Butte. The Lava Butte lavas are sufficiently young that fractures have not been sealed by sediment, and water easily leaks through the streambed or channel walls and into underlying lava flows.

Note that tomorrow, in stops farther north on our return to Portland, we will see where conditions are reversed and the regional water table is above river level, which causes groundwater to once again discharge to streams. The relation between topography and groundwater level in the upper Deschutes Basin is shown diagrammatically in figure 53.

Stop 31. Mount Bachelor

Directions to Stop 31

From Dillon Falls, return to Highway 46 (also known as Cascade Lakes Highway or SW Century Drive). Turn left (west) onto Highway 46 and continue for about 14.2 miles (22.9 km) to Mount Bachelor. Where the road splits, take a slight left (slightly west) off Highway 46 following the signs for West Village Lodge.

Continue on this road for about 0.8 miles (1.3 km) to the parking area for West Village Lodge. A Northwest Forest Pass is not required when parked here.

Proceed to the ticket office to purchase tickets for the Pine Marten Express ski lift to Pine Marten Lodge. Lift schedules and prices vary annually; check with Mount Bachelor (<https://www.mtbachelor.com/>) for current information. Alternatively, Pine Marten Lodge may be reached by a hiking trail.

Discussion of Stop 31

[Modified from Scott and Gardner (1990)]

The Mount Bachelor volcanic chain provides another example of the type and scale of mafic activity that has occurred in the High Cascades. The Mount Bachelor volcanic chain, which is 25 km long, produced lava flows that cover 250 km² and constitute a total volume of 30 to 50 km³. Vents of the Mount Bachelor volcanic chain define a north-northeast-trending alignment of cinder cones, lava flows, and shield volcanoes, a direction that is consistent with many other late Pleistocene and Holocene vents in the region (fig. 3).

Eruptive activity along the chain was not continuous but, instead, occurred from localized segments of the chain, in four discrete eruptive episodes that date from about 18 to about 8 ka. The youngest vent of the Mount Bachelor chain is “Egan Cone,” a cinder cone on the north flank of Mount Bachelor. Mazama ash lies on unweathered or slightly weathered scoria from “Egan Cone,” indicating that tephra from the cone is only slightly older than Mazama ash.

The compositions of lavas from the Mount Bachelor volcanic chain are interesting in that they include both types of basaltic andesite that are common in the region: those of the Mount Washington type and those of the North Sister type (fig. 55; see also, Hughes and Taylor, 1986; Gardner, 1994). Eruption of both types occurred throughout the life of the chain, but the least SiO₂-rich lava was invariably of the Mount Washington type (fig. 55).

[Modified from Fierstein and others (2011)]

Pine Marten Lodge offers spectacular views of the glaciated volcanoes of the Three Sisters volcanic cluster and the Broken Top area, which form a spectacular 20-km-long reach of high peaks along the crest of the Cascade Range. Though contiguous and grouped by name, the volcanoes of the Three Sisters volcanic cluster are geologically quite different from one another. North Sister (3,074 m) is a monotonously mafic edifice (Schmidt and Grunder, 2009) that ranges in age from about 400 to about 11 ka. Middle Sister (3,062 m) is an andesite-basalt-dacite cone built between 48 and 14 ka. South Sister, the highest in the cluster (3,157 m), is a basalt-free edifice that has alternated between rhyolitic and intermediate-composition modes repeatedly from 50 to 2 ka. South Sister, once considered the youngest stratovolcano in the cluster (Wozniak, 1982; Clark, 1983), is largely contemporaneous with Middle Sister.

A comparison of the compositions of rocks of the Three Sisters volcanic cluster is shown in figure 56. The eruptive

Figure 55. Graphs showing Zr versus FeO*/MgO (measure of fractionation; FeO* is total Fe calculated as FeO) for chain of lava flows in Mount Bachelor region (data from Gardner, 1994). Data for basalt erupted from Cayuse Crater (postglacial cinder cone on south flank of Broken Top) are highlighted in figures 55B and 55C. *A*, Comparison of data for basaltic andesite lava flows in region (R. Conrey, unpub. data, 2003) with those for lava flows from Mount Bachelor. Both “typical” Mount Washington type and incompatible-element-poor North Sister type of lava (Hughes and Taylor, 1986; Schmidt and Grunder, 2009) were erupted at Mount Bachelor (Gardner, 1994). *B*, Data for Mount Bachelor lava flows, plotted by SiO₂ content; lava flows that have lowest Zr, FeO*/MgO, and SiO₂ contents are of Mount Washington type (Hughes and Taylor, 1986). *C*, Data for Mount Bachelor lava flows plotted as function of eruptive unit (Gardner, 1994). Both Mount Washington– and North Sister–type lavas were coerupted throughout lifetime of eruptive activity in Mount Bachelor region.

life of North Sister lasted for about 70,000 years; however, its composition is very homogeneous. In contrast, both Middle Sister and South Sister have erupted a wide compositional range of lavas, although the dearth of rhyodacite is surprising. The most silicic lava known in the High Cascades comes from Middle Sister; however, the volcano lacks the less silicic rhyolites that are common at South Sister. Notable at Middle Sister is one of the oldest eruptions, an andesite of the North Sister type that has very low zirconium concentrations. Overall, Middle Sister intermediate-composition lavas tend to have higher zirconium contents than do similar lavas at South Sister.

Broken Top, an older (about 300–150 ka), glacially scoured volcano centered 6 km east-southeast of South Sister, is an extensive mafic shield topped by a modest stratocone, which together span a wide compositional range (51–70 percent SiO₂). Cayuse Crater, on the south-southwest flank of Broken Top, is a much younger basaltic cinder cone and lava flow that is not related to Broken Top.

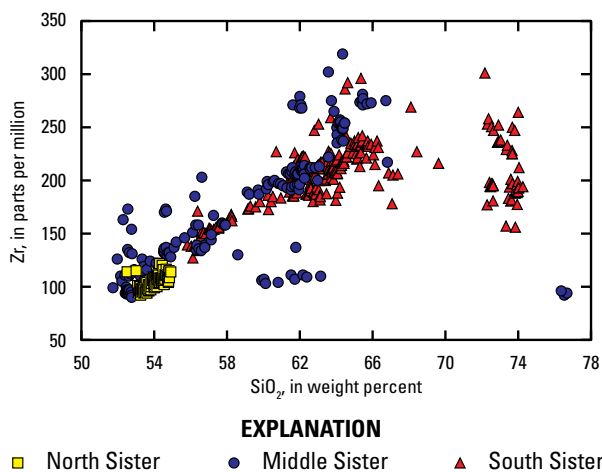
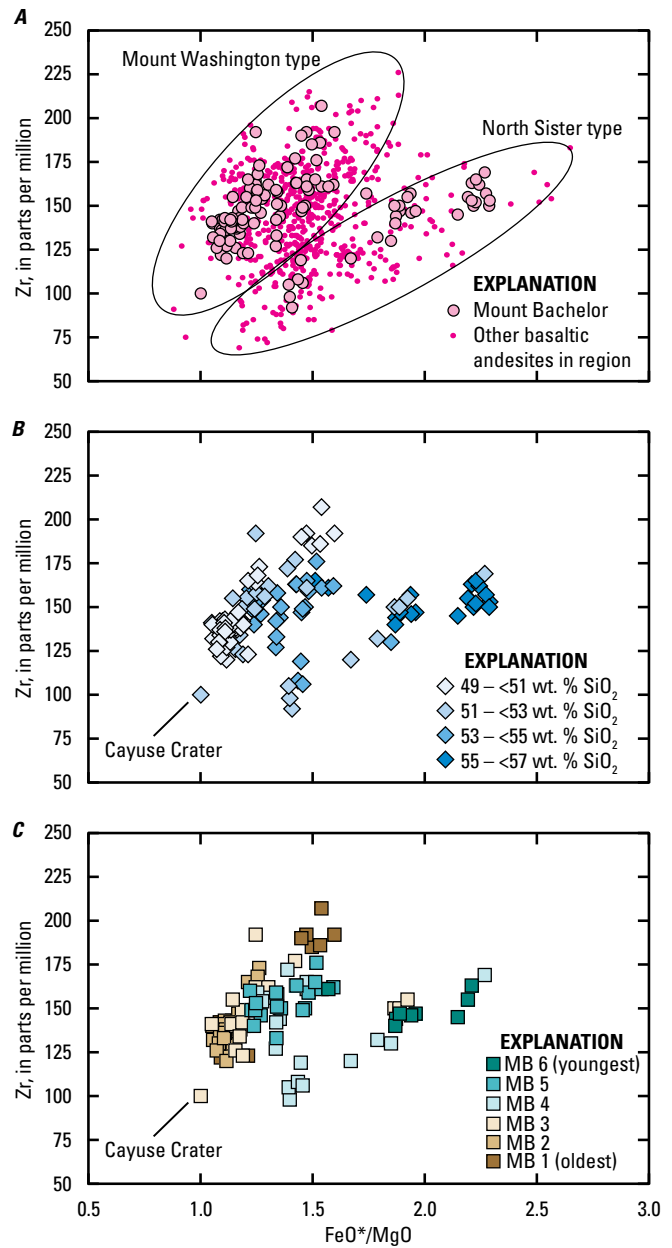


Figure 56. Zr versus SiO₂ contents of lava flows from Three Sisters volcanoes (data from Hildreth and others, 2012; Schmidt and Grunder, 2011).



Postglacial mafic eruptions are more common in the Three Sisters reach than anywhere else along the axis of the Cascade Range (Hildreth, 2007). The McKenzie Pass volcanic field (seen on Day 4) produced some of the youngest of these eruptions. Around the periphery of South Sister, Le Conte Crater to the southwest, the “Katsuk-Talapus chain” to the south, the Mount Bachelor chain and “Egan Cone” cluster to the south-southeast, and Cayuse Crater to the southeast, all appear to have erupted in the interval from 17 to 8 ka, during deglaciation or in early postglacial time, and they all are older than the Mazama ash (7.7 ka).

Postglacial rhyolite erupted from fissures on the southwest, southeast, and northeast flanks of South Sister. Together these form the about-2-ka Rock Mesa and the Devils Hill chain of vents, which produced domes, lava flows, tephra, and small pyroclastic

flows (Scott, 1987). Rapid snowmelt early in each eruption also triggered a few small lahars (Scott, 1987).

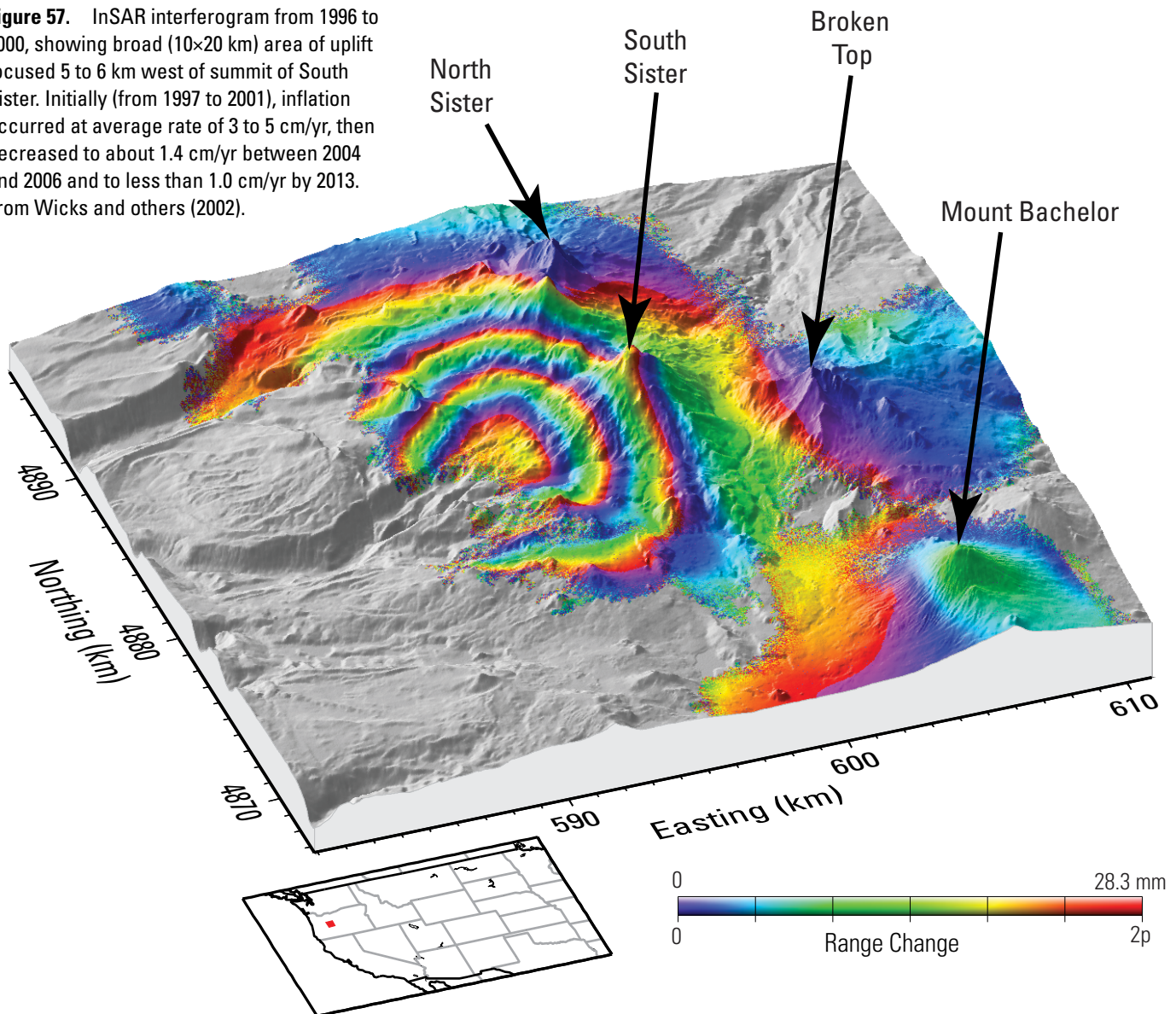
The most recent unrest in the area has been uplift centered about 5 km west of South Sister, recognized by InSAR (interferometric synthetic aperture radar) satellite imagery in 2001 (fig. 57; see also, Wicks and others, 2002). Geophysical models have suggested that the uplift was caused by an intracrustal intrusion (Dzurisin and others, 2009), possibly involving mafic magma similar to that which was erupted during the middle to late Holocene a few kilometers to the north (for example, Collier Cone, Four in One Cone, Yapoah Crater). Uplift west of South Sister coincides with elevated water temperatures, elevated chloride and sulfate concentrations, and elevated $^3\text{He}/^4\text{He}$ ratios observed in nearby springs (Evans and others, 2004; Ingebritsen and others, 2014).

Stop 32. Sparks Lake

Directions to Stop 32

Return to the West Village Lodge parking area and exit toward Highway 46 (also known as Cascade Lakes Highway). In about 0.8 miles (1.3 km), turn left (northwest) onto Highway 46 and continue for about 3.9 miles (6.3 km) to Forest Service Road 46-400, which is marked with a sign for Sparks Lake Recreation Area; turn left (south) onto Forest Road 46-400. Stay left at the intersection for Soda Creek Campground and continue for about 1.6 miles (2.6 km) to the parking area for the Sparks Lake Boat Ramp and the trailhead for the Ray Atkeson Loop Trail. Display a Northwest Forest Pass in your vehicle when parked.

Figure 57. InSAR interferogram from 1996 to 2000, showing broad (10×20 km) area of uplift focused 5 to 6 km west of summit of South Sister. Initially (from 1997 to 2001), inflation occurred at average rate of 3 to 5 cm/yr, then decreased to about 1.4 cm/yr between 2004 and 2006 and to less than 1.0 cm/yr by 2013. From Wicks and others (2002).



Discussion of Stop 32

Sparks Lake is dammed by mafic lava flows from “Egan Cone” on the north flank of Mount Bachelor, as well as by older mafic flows from a north-south-trending chain of three unnamed cinder cones, located about 3 km east of the lake and about 1 km northwest of “Egan Cone” (Fierstein and others, 2011). Two older mafic units are exposed along the eastern shore of the south arm of the lake. Unlike the younger flows from “Egan Cone” and the three unnamed cones, these older flows are cut by several linear rifts 1 to 15 m wide and as much as 5 m deep (Fierstein and others, 2011). Flow features and cracks are exposed along the about-2.5-mile-long (4-km-long) Ray Atkeson Loop Trail, named for Ray Atkeson, Oregon’s Photographer Laureate from 1987 to 1990. Several sections of the trail go through deep rifts in the older basalt flows, exposing prismatically jointed and block-jointed interiors. Water from Sparks Lake drains into fractures and rifts of the lava flows along the eastern and southeastern margins of the lake.

The western shore of Sparks Lake is bordered by basaltic and basaltic andesite lavas, hyaloclastite, and cinder cones of the late Pleistocene Talapus and Katsuk Buttes (Fierstein and others, 2011). This 6-km-long chain of vents includes two subaerially erupted cones and, at the north end of the chain, about 140 m of hyaloclastite tuff that may have erupted through meltwater when the Sparks Lake area was occupied by late Pleistocene ice (Scott and Gardner, 1992).

On October 7, 1966, a lake dammed by a Neoglacial-age moraine on the east flank of Broken Top released 140,000 m³ of water, lowering the lake level by 4.4 m and partially breaching the moraine dam (O’Connor and others, 2001a). The resulting debris flow traveled about 10 km total and was eventually channeled down the Soda Creek drainage to Sparks Lake meadow (O’Connor and others, 2001a). Debris was deposited onto Highway 46 (Nolf, 1969), and fine-grained flood sediment from the event still covers about 35 to 45 percent of Sparks Lake meadow south of the road (Scott and Gardner, 1990). The lake, which did not completely empty, still holds 200,000 m³ of water and has a maximum depth of 13.7 m (O’Connor and others, 2001a). This debris flow was one of about a dozen from lakes dammed by Neoglacial moraines on central Oregon Cascade Range volcanoes (O’Connor and others, 2001a). All debris flows occurred after 1930, and all were from areas vacated by retreating glaciers since the Little Ice Age maximum ice advance in the mid-1800s. The potential for such a flood or debris flow from Carver Lake, at the foot of Prouty Glacier on the east side of South Sister, has resulted in a special flood-hazard delineation within the city of Sisters.

Stop 33. Lava Lakes Fen

Directions to Stop 33

From Sparks Lake, return to Highway 46 and turn left (west). Continue for about 12.5 miles (20.1 km) to a small pullout on the left (east) side of the road, which is marked with two interpretive

signs about fens. The pullout is about 0.3 miles (0.5 km) past the left turn into Lava Lake Recreation Site.

Discussion of Stop 33

[Modified from Aldous and others (2015)]

Lava Lake fen is one of a handful of unique wetlands in the central Oregon Cascades that can be classified as a fen. Fens develop where groundwater discharges into the biologically active zone of soil at a rate that is both sufficient and constant enough to promote peat accretion. These wetland areas harbor high species richness and endemism owing to their unique hydrogeologic, edaphic, and geochemical conditions (Amon and others, 2002; Bedford and Godwin, 2003). Montane fens may be spatially distant from more extensive riparian and floodplain wetland complexes and river networks, yet they are integrally linked to the freshwater landscape as headwater areas or through subsurface flows.

Analysis of the geology of mapped wetlands in the central Oregon Cascades shows that fens are found where two conditions are present. First, they are found almost exclusively in areas of glacial till, and second, they are found where the glacial till is mantled by coarse pumice sand, typically from the eruption of Mount Mazama. In the southern part of the central Oregon Cascades, closer to Mount Mazama, approximately 50 percent of wetlands on glacial till are fens, compared to 13 percent in the northern part of the central Oregon Cascades (that is, south of Mount Jefferson). Furthermore, peat has never been observed beneath the pumice deposits (the peat is always above the pumice layers), supporting the conclusion that pumice is necessary for fens to develop, an indication that glacial tills alone do not provide an environment for peat development. However, as little as a few tens of centimeters of pumice sand on top of glacial till can create the conditions necessary for peat development.

Although the role of pumice is not fully understood, its presence may have transformed the landscape to favor peat accretion by any or all of the following mechanisms: (1) by increasing shallow groundwater storage, (2) by providing a laterally extensive medium for the movement of shallow groundwater, and (3) by diffusing discharge of small springs from the pumice itself or from permeable zones in the underlying till. Moderate discharge velocity and diffusive discharge are identified as potentially important conditions for peat development (Almendinger and Leete, 1998; Amon and others, 2002).

Lava Lake fen and other fens in the central Oregon Cascades may be vulnerable to climate change on the basis of their locations and the expected changes in their hydrology during projected future climate conditions. Warming in the Pacific Northwest is expected to result in shifts in winter precipitation from snow to rain in the Cascade Range (Elsner and others, 2010; Mote and Salathé, 2010). Snow in the Cascade Range is most sensitive to projected warming between elevations of 1,000 to 2,000 m (Nolin and Daly, 2006; Sproles and others, 2013). This elevation range is projected to change

from a seasonal snow zone, in which snow accumulates all winter and melts in the spring, to a transient snow zone, in which snow both falls and melts multiple times throughout the winter, causing decreases in basinwide snow-water storage of as much as 56 percent (Sproles and others, 2013). The median elevation of fens in the central Oregon Cascades is 1,462 m (standard deviation, 229 m), which is near the middle of the elevation range of “at risk” snow, where winter snowpack is most vulnerable to climate change (Nolan and Daly, 2006).

Stop 34. Pilot Butte

Directions to Stop 34

From Lava Lake fen, return to Bend on Highway 46. When you reach Bend, the first traffic circle is at the intersection of Mount Washington Drive and Highway 46 (also known as SW Century Drive); take the second exit from the traffic circle (SW Century Drive) and continue northeast. Stay on SW Century Drive for about 2.2 miles (3.5 km), passing through three traffic circles; at each traffic circle, continue north on SW Century Drive (which becomes NW 14th Street). The fourth traffic circle is at the intersection of NW 14th Street and NW Newport Avenue; take the first exit from the traffic circle onto eastbound NW Newport Avenue and continue for about 2.2 miles (3.5 km), passing through one traffic circle and several stoplights. Continue east on NW Newport Avenue (which becomes NW Greenwood Avenue and then NE Greenwood Avenue) to Pilot Butte Summit Drive; turn left (north) onto Pilot Butte Summit Drive, at the Oregon State Parks sign. Continue on Pilot Butte Summit Drive for about 1.1 miles (1.8 km) to the top of the Pilot Butte.

If Pilot Butte Summit Drive is closed, or if you prefer to hike to the top of Pilot Butte, continue east on NE Greenwood Avenue, past Pilot Butte Summit Drive, for about 0.8 miles (1.3 km), then turn left (north) onto NE Azure Drive. The turn is marked with an Oregon State Parks sign for the Pilot Butte Trailhead. Continue for about 0.1 miles (0.2 km) on NE Azure Drive and then turn left (north) onto NE Savannah Drive. Continue for about 350 feet (0.1 km) on NE Savannah Drive, then turn left (east) onto NE Linnea Drive. Continue for about 0.2 miles (0.3 km) to the parking area for the Pilot Butte Trailhead.

Discussion of Stop 34

Pilot Butte is a Pleistocene (188±42 ka; Donnelly-Nolan and others, 2000) cinder cone that has a basaltic andesite lava flow exposed north of the cone. The cone and associated lava flow are surrounded by about-78-ka basalt flows from the north slope of Newberry Volcano (Jensen and others, 2009).

The summit of Pilot Butte offers splendid views of the entire Bend area. Most of the southern skyline is dominated by Newberry Volcano and the many cinder cones that dot its flanks. To the west are hundreds of cinder cones, domes, large and small shield volcanoes, and stratovolcanoes of the Cascade Range. To the northeast are the Ochoco Mountains and, in the middle

distance, the postcaldera domes of the about-29.5-Ma Crooked River caldera (McCloughry and others, 2008). Figure 58 shows a simplified compass wheel that indicates the directions and distances to many features that are visible from the summit of Pilot Butte on a clear day.

The summit of Pilot Butte is a good place to summarize the variety of recent volcanic activity that has occurred in the central Oregon Cascades and to discuss volcanic hazards. The close proximity of multiple, recently active volcanoes to densely populated areas means that future volcanic activity poses significant hazards to regional transportation, infrastructure, agriculture, and public health. Despite the abundance of recent mafic activity in the central Oregon Cascades, volcanic hazards presented by these types of eruptions have not been fully studied. As we have seen at several locations during this field trip, eruptions at mafic vents can last for several decades. Eruption styles can vary considerably from vent to vent, sometimes producing extensive lava flows and multiple tephra blankets. Recent lava flows from regional mafic vents covered areas that are now covered by densely populated urban areas and are crossed by major highways, railroads, and power and gas lines. Many of these lava flows interacted with water, forming lava dams and interrupting or altering streamflows. If similar eruptive episodes were to occur today, lava flows could cause extensive damage to central Oregon communities, and tephra eruptions could pose even broader hazards if winds were blowing toward developed or agricultural areas.

Regional hazard assessments need to address this variety of volcanic hazards, but traditional hazard assessments typically focus on individual volcanoes rather than individual communities. Because many central Oregon communities are at risk from multiple hazards presented by numerous vents, a better approach would be to address the range of hazards that threaten each community, rather than the hazards presented by each volcano, especially because future eruptive activity might not be limited to the summit or flanks of long-lived composite volcanoes but, rather, might occur anywhere in the region.

A community-based approach to assessing the volcanic hazards and risks to Auckland, New Zealand, was described in Magill and Blong (2005a,b). Communities in central Oregon are similar to Auckland in that they could be affected by a variety of volcanic hazards, both proximal and distal, as well as by eruptions of both mafic and silicic materials. Community-based hazard assessments could not only address the hazards and risks presented by multiple vents but could also give local and regional agencies specific, community-focused information to include in their emergency response plans. For these reasons, it is important that future hazard assessments in central Oregon focus on individual communities, rather than on individual volcanoes.

End of Day 5: Bend

Today’s itinerary ends at Pilot Butte, which is within the city limits of Bend. We encourage you to explore Bend as time allows until our departure for Portland tomorrow morning.

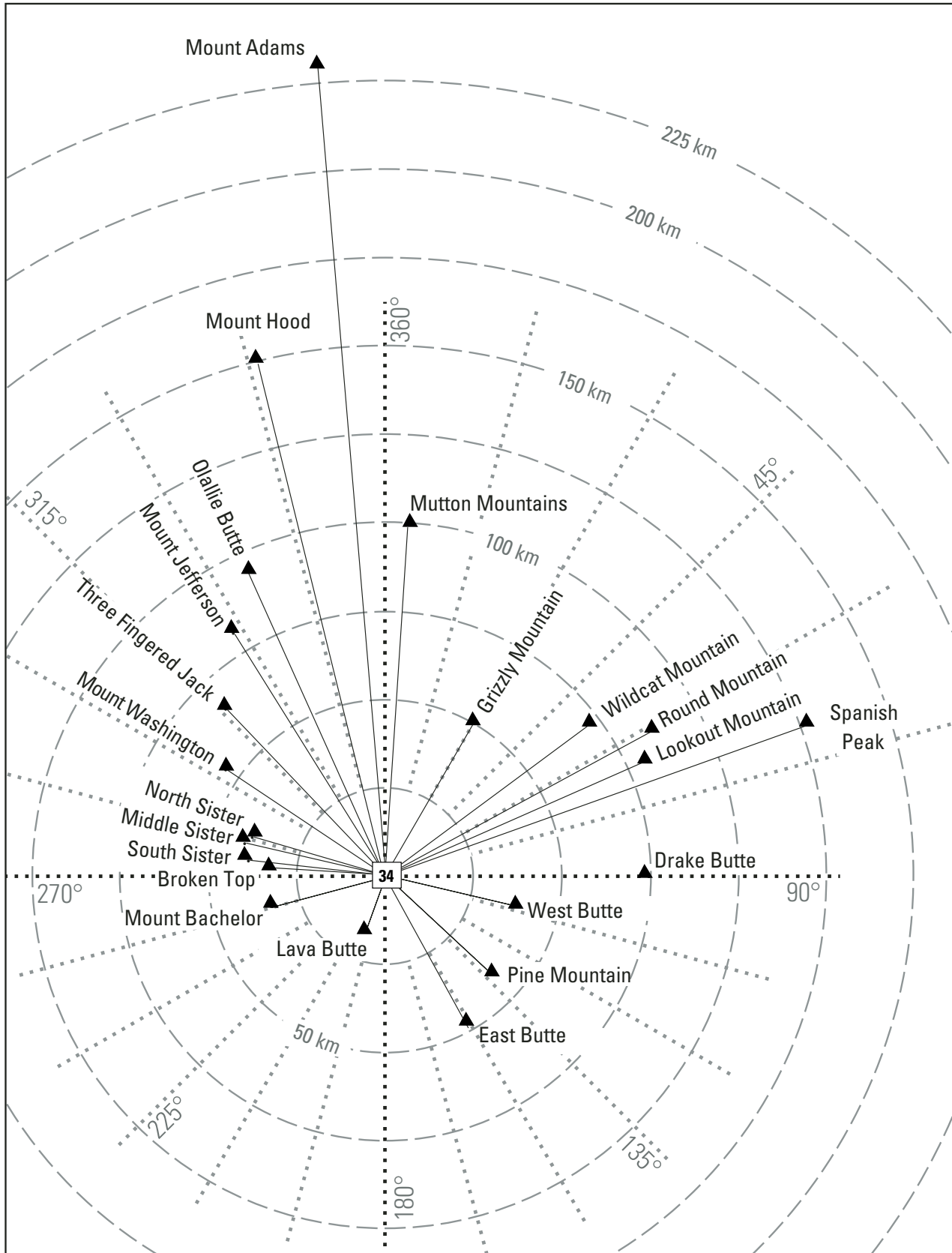


Figure 58. Compass-wheel diagram showing distances (dashed lines) and approximate azimuthal directions (dotted lines) to peaks and other features (triangles) that are visible from top of Pilot Butte (Stop 34; relative location shown by stop number in white rectangle). Azimuthal directions are given in 15° increments. Modified from Jensen and others (2009).

Day 6. Bend to Portland

On Day 6 of the field trip, we will return to Portland, stopping at a few places along the way (fig. 59). We will begin by looking at surface-water diversions in Bend (Stop 35). On the way back to Portland, we will make stops at the bridge at Peter Skene Ogden State Park (Stop 36) and at the Lake Billy Chinook overlook (Stop 37). Our last stop before Portland will be at Timberline Lodge on Mount Hood (Stop 38), where we will eat lunch.

Stop 35. Surface-Water Diversions in Bend

Directions to Stop 35

Head north on Highway 97 from Bend, then take the Revere Avenue–Downtown exit (Exit 137). Drive straight

through the traffic signal onto Division Street. Proceed on Division Street for 0.5 miles (0.8 km) from the traffic signal to Riverview Park. Park in the tiny parking area on the west (left) side of road. The diversion dam and head gates can be seen just north of the parking area.

Discussion of Stop 35

[Modified from Sherrod and others (2002) and Cashman and others (2009)]

At this stop we can see the dam and headgates for diversion into the North Unit and Pilot Butte Canals (fig. 60). The dam, near river mile 165, was constructed in the early 1900s as part of the diversions (K.G. Gorman, oral commun., 2001). It also once served as a hydropower impoundment. Some of the original power-generating equipment is still visible downstream from the dam. During the irrigation season, water is diverted from the Deschutes River between Lava Butte and

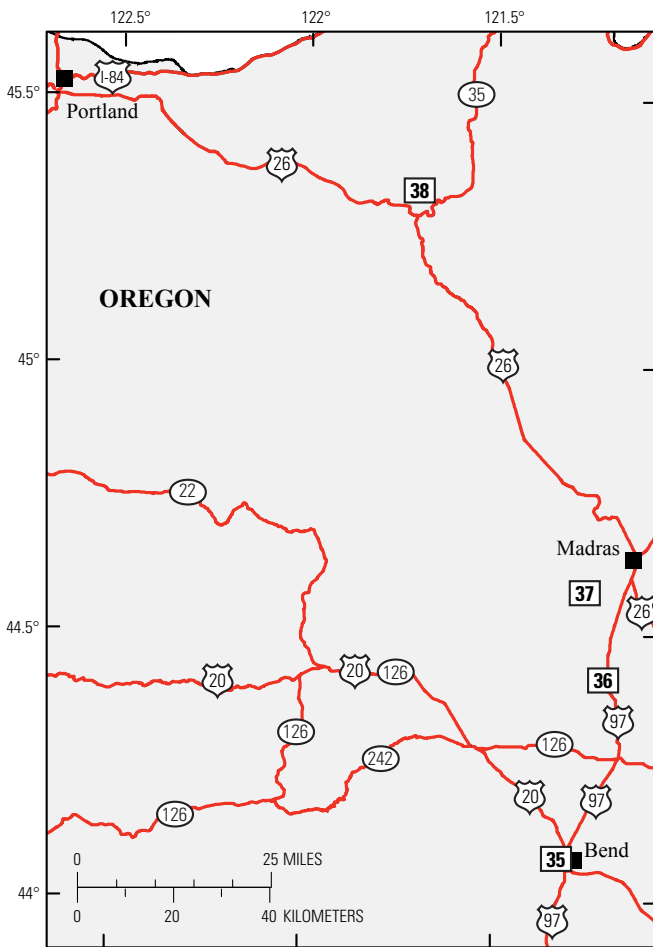


Figure 59. Index map of part of northwestern Oregon, showing locations of field-trip stops on Day 6. Field-trip stops shown by white rectangles; stop numbers are inside rectangles. Roads from Oregon Department of Transportation (2015). Oregon state outline (heavy lines along top edge of figure) from Bureau of Land Management (2001).

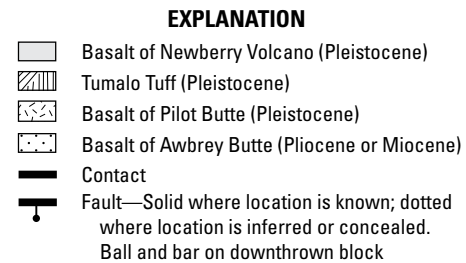
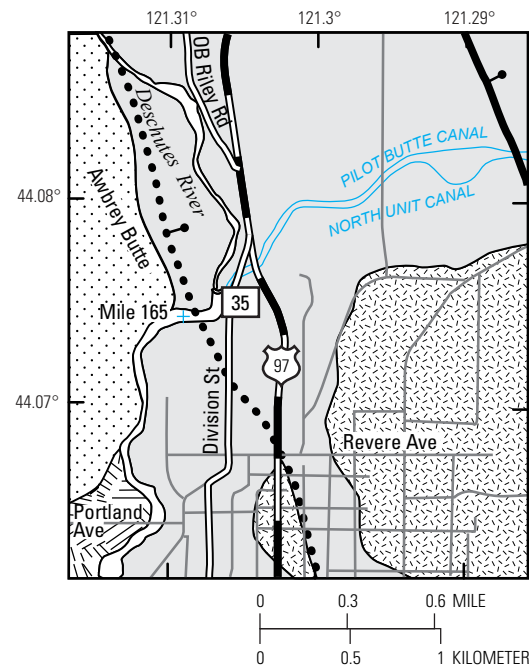


Figure 60. Map showing diversions of Deschutes River for North Unit and Pilot Butte Canals north of Bend. Field-trip stop shown by white rectangle; stop number is inside rectangle. Modified from Sherrod and others (2002).

Bend into irrigation canals at a rate of approximately 57 m³/s (2,000 ft³/s) (Gannett and others, 2001); the average annual rate is about 28 m³/s (1,000 ft³/s). The North Unit and Pilot Butte Canals account for roughly one-half of the total diversion.

Most canals in the area are unlined and leak considerably; overall transmission losses approach 50 percent, and the losses are even greater where the canals cross fractured Pleistocene lava. The water lost from the canals infiltrates and recharges the groundwater system. Although the canals lose large amounts of water, the Deschutes River north of Bend shows little or no loss, probably because the lava in the stream channel north of Bend is sufficiently old that fractures have been sealed by sediment. Total canal losses north of Bend approach a mean annual rate of 14 m³/s (500 ft³/s), more than 10 percent of the long-term average recharge from precipitation in the entire upper Deschutes Basin, which is about 108 m³/s (3,800 ft³/s) (Gannett and others, 2001).

Groundwater-flow directions inferred from head maps (fig. 42) suggest that the lost canal water should flow toward the lower Crooked River; comparing rates of estimated canal losses with long-term streamflow records confirms that this is the case. Figure 61 shows the estimated annual mean canal losses from 1905 to 1998; also shown are the mean flows of the lower Crooked River for the month of August during the same period. Because flows of the lower Crooked River during August are almost entirely from spring discharge, variations in mean flows during August are a good proxy for variations in groundwater discharge (baseflow). As shown in figure

61, baseflow to the lower Crooked River increased by an amount similar to the estimated canal losses throughout most of the 20th century. This relation has implications for water management, as efforts to conserve water by lining the canals will result in reduced streamflow in the lower Crooked River.

Many wells in the Bend area have static water levels greater than 200 m below the land surface. Some wells, however, have depths to water that range from 30 to 60 m. Many of these shallower saturated zones are artificially recharged from canal leakage and deep percolation of irrigation water. Historical data are insufficient to determine precisely how much shallow groundwater is canal derived and how much might result from natural stream leakage.

Groundwater levels show varying rates of response to changes in canal flow that depend on the permeability of bedrock, as described in detail by Gannett and others (2001). For example, the static water level in a well 5 km southeast of this location, which was drilled into fractured lava 1 km from the Arnold Canal, responds within a few days after annual canal operation begins (fig. 62A). In contrast, a well on the north side of Redmond was drilled in an area mapped as the 4- to 3-Ma basalt of Dry River, and it yields water from underlying sedimentary strata of the Deschutes Formation. The water level in this well, located 0.4 km west of the Pilot Butte Canal, has a greater lag time and more subdued response (fig. 62B); it begins to respond two months after annual canal operation begins, and it peaks one to two months after the canals are shut off for the year.

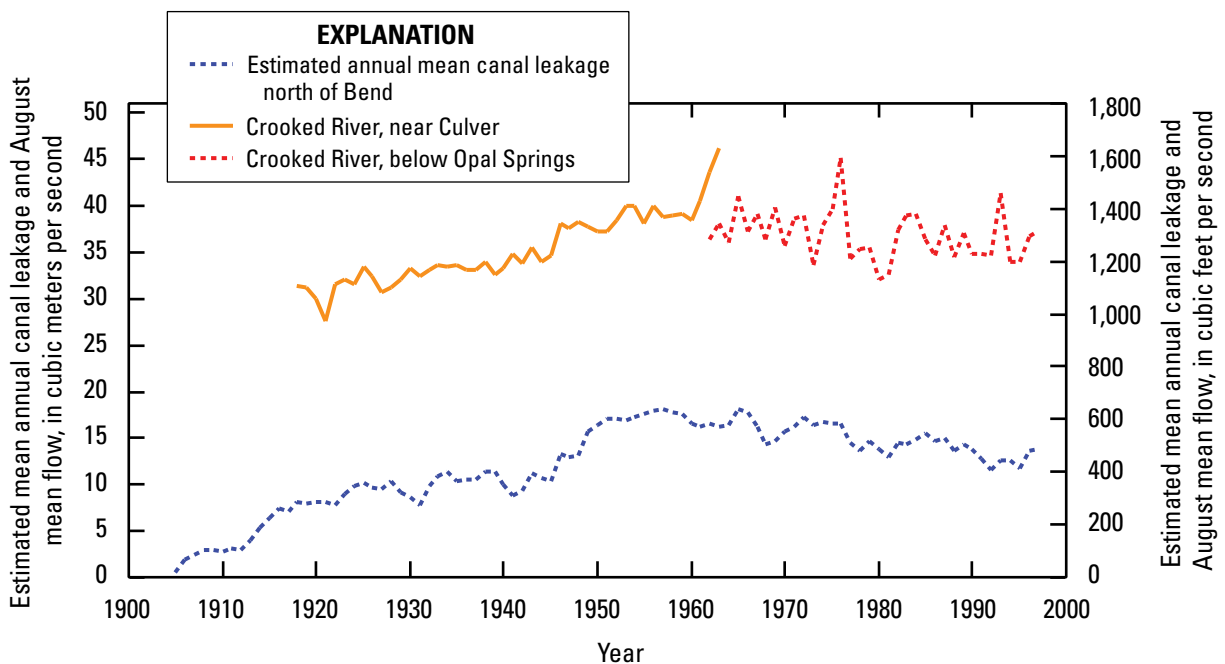


Figure 61. Hydrograph showing estimated canal leakage north of Bend and August mean flow of Crooked River. Modified from Gannett and others (2001), from Cashman and others (2009).

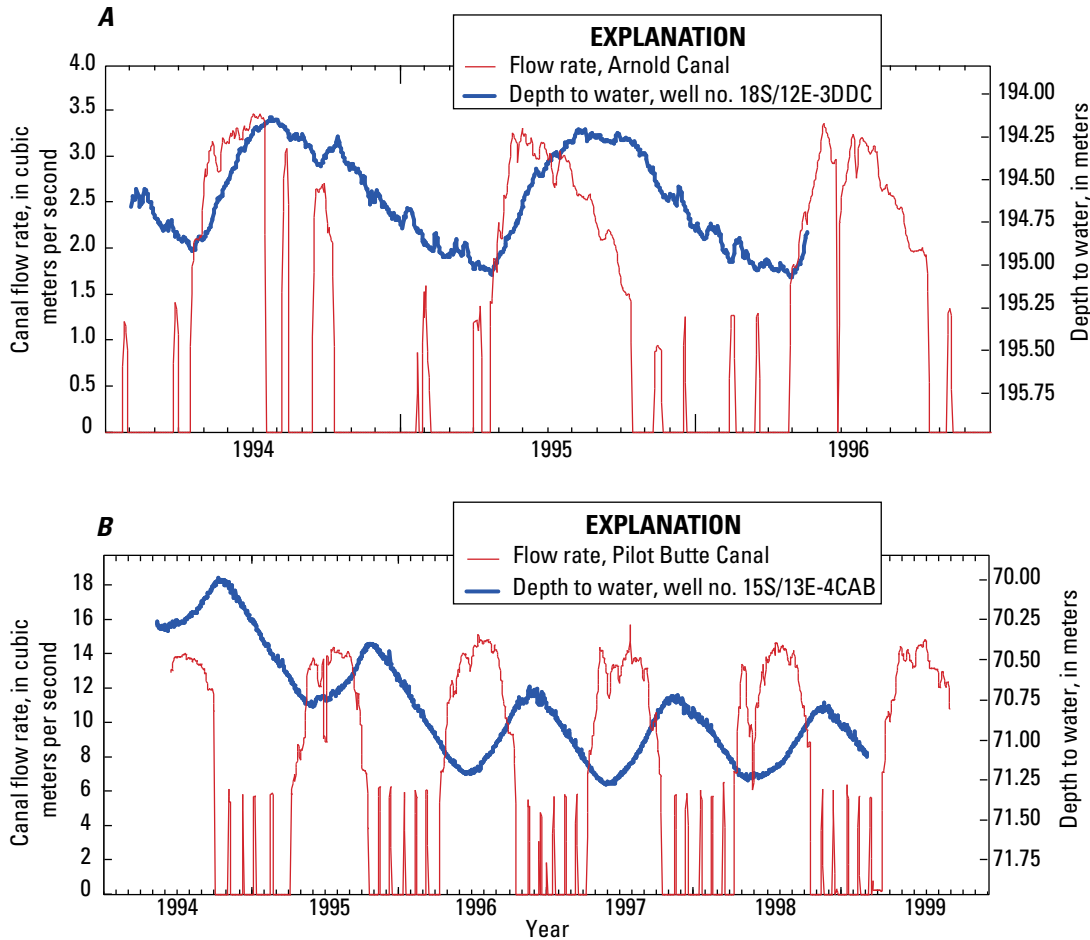


Figure 62. Hydrographs showing relation between groundwater fluctuations and canal operation. *A*, Well and canal-water fluctuations at Arnold Canal, near Bend. Canal flows through highly permeable late Quaternary lava flows. *B*, Well and canal-water fluctuations at Pilot Butte Canal, near Redmond. Canal flows through Miocene and early Pliocene lava flows and sedimentary strata. Modified from Gannett and others (2001), from Cashman and others (2009).

Stop 36. Bridge at Peter Skene Ogden State Park—Canyon-Filling Lava Flows

Directions to Stop 36

Return to Highway 97 and head north toward Redmond and Portland. About 2 miles (3.2 km) north of the small town of Terrebonne, turn left at Peter Skene Ogden State Park. From the parking area, the footpath north leads to restrooms, drinking water, and a spectacular view of the Crooked River Gorge from the footbridge.

Discussion of Stop 36

[Modified from Sherrod and others (2002)]

Where Highway 97 crosses the Crooked River Gorge, middle Pleistocene basalt forms most of the canyon walls. These lava flows were erupted from vents on the north flank of

Newberry Volcano and flowed northward across the broad plain that extends to Redmond. The lava poured into the ancestral Crooked River canyon 9 km southeast of the bridge at Peter Skene Ogden State Park and flowed downstream beyond the bridge at least another 8 km, more than 55 km from the vent area. Lava flows also entered the Deschutes River and flowed to Lake Billy Chinook, at least 65 km from the vent.

The elevation of the Crooked River at the Highway 97 crossing is approximately 750 m. At this level, the Crooked River has incised to the depth of the regional water table. Synoptic streamflow measurements taken in 1994 (fig. 63) showed that the Crooked River gained about 2 m³/s (70 ft³/s) from groundwater discharge between “Trail Crossing,” about 3.2 km upstream from (northeast of) this location, to Osborne Canyon, about 7.2 km downstream from (northwest of) here. Along the 11.2-km-long reach downstream from Osborne Canyon to the gage above Lake Billy Chinook, the river gained an additional 28.3 m³/s (1,000 ft³/s), making this reach one of the principal groundwater-discharge areas in the basin.

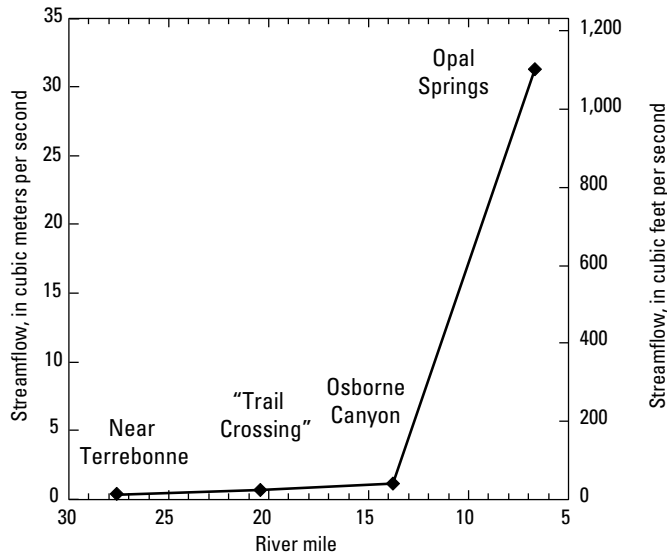


Figure 63. Graph of streamflow of lower Crooked River, as measured between river miles 28 and 7 during July 1994, showing gain at Osborne Canyon owing to groundwater discharge. Modified from Gannett and others (2001), from Cashman and others (2009).

The hills to the east are part of the upthrown block of the Cyrus Springs Fault Zone (Smith and others, 1998), and they define the northwestern margin of the about-29.5-Ma Crooked River caldera (McClaghry and others, 2008). Rocks as young as the Prineville Basalt (15.8 Ma) were involved in this faulting, whereas rocks of the Deschutes Formation, the next youngest unit preserved, are not faulted. Thus, faulting occurred after the early Oligocene and before the late Miocene, and it may be entirely of earliest or middle late Miocene age.

Rocks of the John Day Formation have low permeability because the tuffaceous material has mostly devitrified to clay and other minerals. Lava flows within the formation are weathered and contain abundant secondary minerals. Strata of the John Day Formation act as a barrier to regional groundwater flow and, along with age-equivalent strata from the Cascade Range, are considered to be the lower boundary of the regional groundwater-flow system throughout much of the Deschutes Basin. The overlying middle Miocene Prineville Basalt is locally fractured and contains permeable interflow zones, and it is used as a source of water in some places.

Stop 37. Lake Billy Chinook Overlook

Directions to Stop 37

Return to Highway 97 and turn left (north). Continue on Highway 97 for about 7 miles (11.3 km), then turn left (northwest) onto SW Culver Highway (marked with a sign for Culver and for Round Butte Dam, as well as an Oregon State Parks sign for The Cove Palisades State Park). Continue on SW Culver Highway for

about 2.3 miles (3.7 km), then turn right (north) onto 1st Avenue; after about 0.3 miles (0.5 km), turn left (west) onto C Street (marked with a sign for The Cove Palisades State Park), which becomes SW Huber Lane. Continue west on SW Huber Lane for about 0.9 miles (1.4 km), then turn right (north) onto SW Feather Drive; after about 0.9 miles (1.4 km), turn left (west) onto SW Fisch Lane and continue west for about 0.5 miles (0.8 km), until SW Fisch Lane turns north and becomes SW Frazier Drive. After another about 0.5 miles (0.8 km), turn left (west) onto SW Peck Road and continue west for about 0.3 miles (0.5 km), then turn right onto SW Mountain View Drive¹¹ (marked with an Oregon State Parks sign for Round Butte Overlook Park). Continue on SW Mountain View Drive for about 2.1 miles (3.4 km) along the rim of Crooked River Gorge to Round Butte Overlook Park, the third scenic viewpoint on the left.

Discussion of Stop 37

[Modified from Sherrod and others (2002)]

The Round Butte Overlook Park provides a view of the canyons of the Crooked and Deschutes Rivers, just upstream of their confluence. Lake Billy Chinook is impounded behind Round Butte Dam, which was completed in 1964. Our east-rim overlook is situated on the about-5-Ma basalt of Tetherow Butte (Smith, 1986b), and sedimentary rocks of the Deschutes Formation form much of the canyon walls. The far rim (that is, the west rim of Deschutes River canyon) is capped by the basalt of Lower Desert (Smith, 1986b), which has normal-polarity magnetization; its isotopic age is 5.43 ± 0.05 Ma (Sherrod and others, 2004), but its magnetization suggests that it, too, is about 5 Ma in age (fig. 64).

Also visible from our overlook is The Island, the narrow, flat-topped ridge that separates the Crooked and Deschutes Rivers. The Island is an erosional remnant of a reversely polarized, 1.19-Ma intracanyon lava flow unit, the basalt of The Island. Our overlook rim is at an elevation of 786 m; the elevation of the reservoir pool is 593 m (1,945 ft), and that of the canyon floor, now flooded, is about 488 m. Photographs taken from this same spot in August 1925 by Harold T. Stearns provide a glimpse of the prereservoir exposures (fig. 65); the prominent lava flows at the base of the canyon (fig. 65B) belong to the 7.42-Ma Pelton basalt member, the lowest lava-flow member of the Deschutes Formation (Stearns, 1931; Smith, 1986b).

The Pelton basalt member of the Deschutes Formation (which is not visible from our overlook but which can be observed from within the canyon) consists of several lava flows of olivine tholeiite, some of which contain thin sedimentary interbeds (Smith, 1986b). A flow in the Pelton basalt member has been dated at 7.42 ± 0.22 Ma (Smith and others, 1987), and the unit is as thick as 30 m near Pelton Dam (Smith, 1987a). The Pelton basalt member is exposed as far south as Round Butte Dam, and it was also mapped another 6.4 km south of the mouth of the Crooked

¹¹Note that, if you continue on SW Peck Road without turning onto SW Mountain View Drive, you will be able to experience the geologically interesting drive into The Cove Palisades State Park.

Figure 64. Correlation of ages (dots) of selected samples in Deschutes Basin with paleomagnetic timescale. Polarity of remanent magnetization of samples indicated by fill color of bars showing standard deviations (black, normal polarity; white, reversed polarity). Remanent magnetization of samples determined using portable fluxgate magnetometer. Paleomagnetic timescale from Cande and Kent (1992); see Sherrod and others (2004) for references to age data and descriptions of map units. Modified from Sherrod and others (2002).

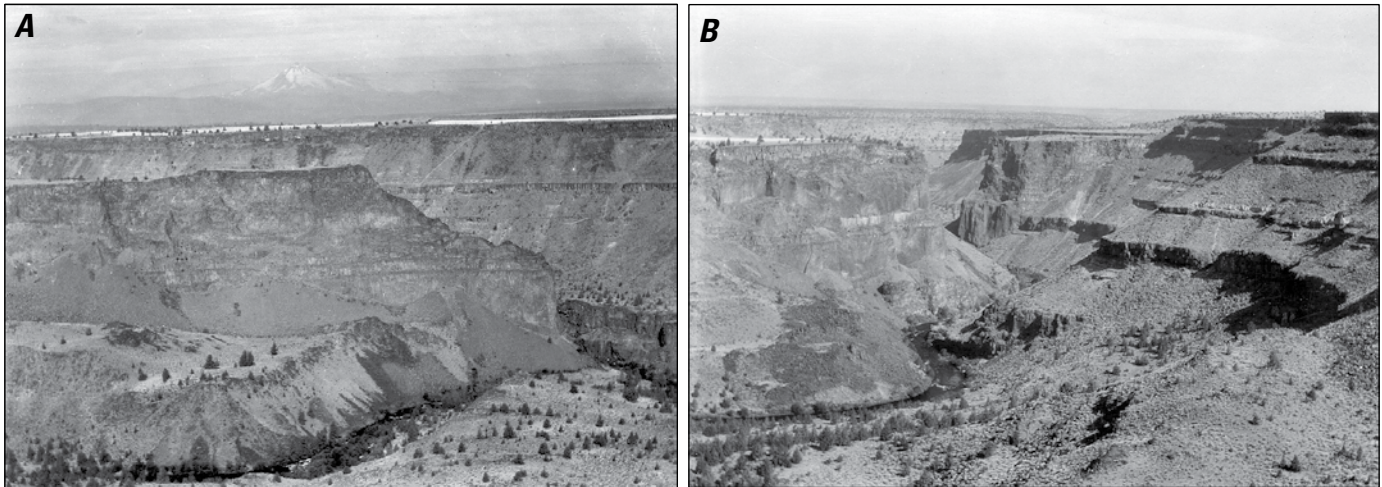
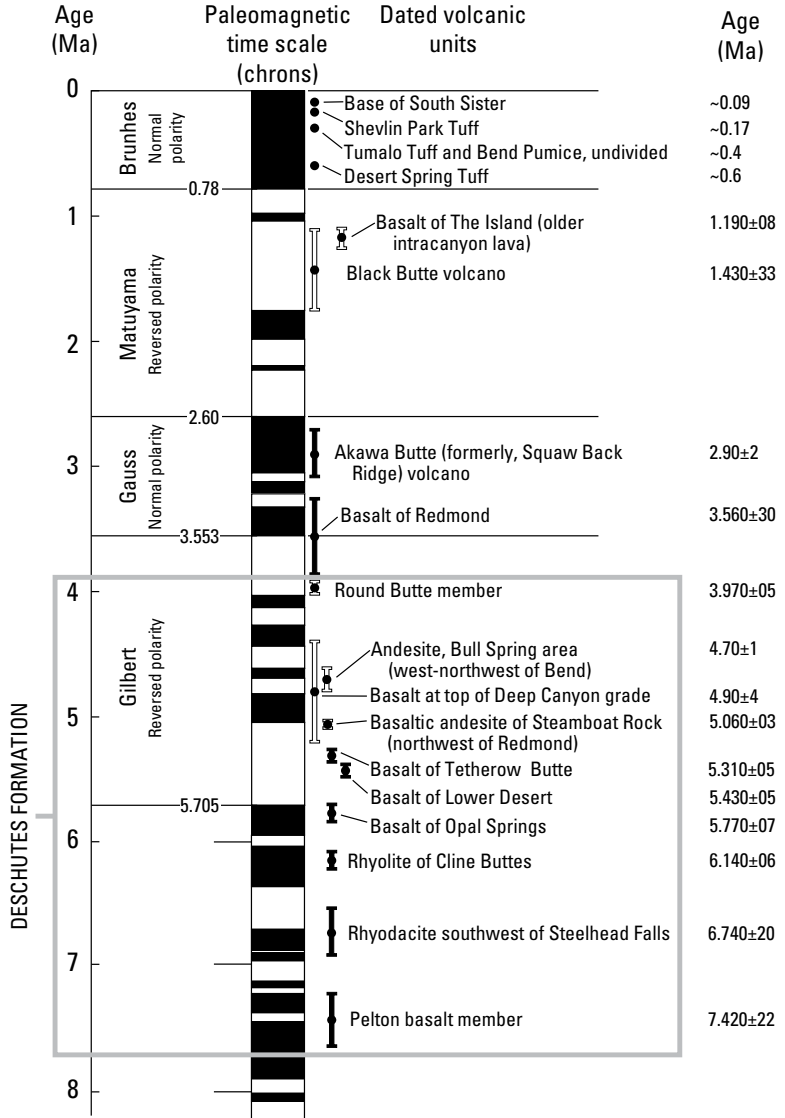


Figure 65. Photographs into canyons of Crooked and Deschutes Rivers taken in August 1925, prior to inundation by Lake Billy Chinook, from SE¼ sec. 35, T. 11 S., R. 12 E. Photographs by H.T. Stearns. From Sherrod and others (2002). *A*, View to west across Crooked River canyon to The Island (prominent ridge in middle of photograph) and, beyond it, to west rim of Deschutes River canyon. Confluence of Deschutes and Crooked Rivers is in lower right foreground; snow-covered Mount Jefferson, 45 km to west-northwest, is barely visible in center background. *B*, View to north (downstream) into Deschutes River canyon. Confluence of Deschutes and Crooked Rivers is at lower left edge of photograph.

River (Stearns, 1931) before the exposure was buried by the impoundment of Lake Billy Chinook.

As is the case for the basalt of Opal Springs, a considerable amount of groundwater does discharge from springs in the Pelton basalt member. Stearns (1931) observed that the Pelton basalt is the stratum from which springs issue in the lower Crooked River below about river mile 4, as well as along the Deschutes River from its confluence with the Crooked River to below its confluence with the Metolius River. Stearns (1931) also noted a large spring that issued from the Pelton basalt member in the forebay of the power plant that once existed about 1.6 km upstream of this location. He also documented a line of springs that extend 1.2 km along the west bank of the Deschutes River, about 0.8 km upstream from its confluence with the Metolius River; these springs have an estimated discharge of between 2.3 and 2.8 m³/s (80 and 100 ft³/s, respectively). Groundwater discharge into Lake Billy Chinook is estimated from stream-gage data to be approximately 12 m³/s (420 ft³/s); most of this discharge is likely from the Pelton basalt member (Gannett and others, 2001).

The Pelton basalt member extends in the subsurface southward beyond its now-submerged exposure in the canyon. Wells drilled at river level near Opal Springs (river mile 6.7) penetrated the Pelton basalt member at a depth of approximately 110 m. The Pelton basalt member is a productive aquifer at this location: wells encountered artesian pressures of approximately 344 kilopascals (50 lb/in²) at land surface and artesian flow rates of as much as 0.32 m³/s (5,000 gal/min).

The Pelton basalt member, the lowest lava sequence in the Deschutes Formation, is effectively the base of the permeable section in the Deschutes Formation, although Smith (1987a,b) mapped a thin layer of Deschutes Formation sediment underlying it. The contact between the Deschutes Formation and its underlying units is exposed about 8 km north of here. At that location, most of the groundwater flowing from the upper basin in the Deschutes Formation has discharged into the river system. Depending on location, the Deschutes Formation is in unconformable contact with either the underlying middle Miocene Simtustus Formation or the upper Oligocene to lower Miocene John Day Formation. Mapping by Smith (1987a,b) and Smith and Hayman (1987) showed that rocks of the Simtustus Formation and the Prineville Basalt typically separate those of the Deschutes Formation and the John Day Formation in the Deschutes River canyon. West of the canyon, the Deschutes Formation directly overlies the John Day Formation in many places.

The Simtustus Formation (which is not visible from our overlook but which can be observed from within the canyon) is a sequence of middle Miocene volcanogenic sandstone, mudstone, and tuff that is conformable on, and interbedded with, lava of the Prineville Basalt (Smith, 1986a). The Simtustus Formation, which is as thick as 65 m, was deposited across an area almost 20 km wide; deposition occurred in response to drainage-system disruption by lava flows of the Columbia River Basalt Group and the Prineville Basalt (Smith, 1986a). The Simtustus Formation is exposed from the Deschutes River canyon to east of Gateway, 27 km northeast of this location. Although its hydrologic

characteristics are unknown, it is thought to be a hydrologically insignificant stratigraphic unit because of its location, limited areal extent, and relative thinness.

The Prineville Basalt (which is also not visible from our overlook but which can be observed from within the canyon) is a sequence of relatively evolved lava flows exposed sporadically across north-central Oregon. Of middle Miocene age, the unit includes flows that have both normal- and reversed-polarity magnetization, and so it is thought to have been erupted during a short time period about 15.8 Ma, when the Earth's magnetic field was changing polarity from reversed to normal (Hooper and others, 1993). In the Deschutes Basin, the Prineville Basalt is as thick as 200 m, and it is exposed east of Powell Buttes, east of Smith Rock, and along the Deschutes River from Pelton Dam downstream toward Cow Canyon, 20 km northeast of Gateway (Smith, 1986b). The Prineville Basalt may underlie the Deschutes Formation in much of the east half of the basin; stratigraphic separation between the two formations is relatively small, depending on the thickness of intervening middle Miocene strata of the Simtustus Formation.

The hydrologic characteristics of the Prineville Basalt are poorly known. It is generally less permeable than the Deschutes Formation, and we know of no published reports of major springs issuing from the unit. It is, however, used locally as a source of water for domestic wells and a few irrigation wells.

About 13 km north of this location, just below Pelton Dam, the John Day Formation (not visible from here) is exposed in the Deschutes River canyon. The John Day Formation in this area primarily consists of light-colored tuff, lapilli-stone, fine-grained volcanic sandstone, and mudstone (Smith, 1987a,b). The John Day Formation has very low permeability, and it is considered to be the basement of the regional groundwater system (Sceva, 1968; Gannett and others, 2001). In contrast to the upper basin, little groundwater does discharge into the Deschutes River downstream from where it intersects with the John Day Formation.

Stop 38. Timberline Lodge at Mount Hood

Directions to Stop 38

[Note that we are providing two options to travel to Stop 38 from the intersection of SW Mountain View Drive and SW Belmont Lane: (1) the more interesting but slower Pelton Dam route; and (2) the faster, mostly highway Madras route]

Exiting the overlook, turn left (north) onto SW Mountain View Drive and proceed about 1.8 miles (2.9 km) to the junction with SW Round Butte Drive. Bear left and remain on SW Mountain View Drive, following it to a 'T' junction with SW Belmont Lane; turn right (east) onto SW Belmont Lane.

Directions for Option 1, the Pelton Dam Route—From the intersection with SW Mountain View Drive, continue on SW Belmont Lane for about 1.4 miles (2.3 km), then turn left (north) onto SW Elk Drive, which becomes NW Pelton Dam Road and descends into Willow Creek canyon. About 300 m past the major switchback is a roadcut in the Pelton basalt

member, the oldest basalt in the Deschutes Formation. Remain on NW Pelton Dam Road for about 4 miles (6.4 km) to its junction with Highway 26; along the way you will see good exposures of the Prineville basalt and the interbedded Simtustus Formation (Smith and Priest, 1983). Turn left (north) onto Highway 26 and proceed for 50 miles (80 km) through Warm Springs, the Warm Springs Reservation, and U.S. Forest Service lands to the Highway 35 junction.

Directions for Option 2, the Madras Route—From the intersection with SW Mountain View Drive, continue on SW Belmont Lane for about 7.3 miles (11.7 km) to its intersection with Highway 97 in Madras. Turn left (north) onto Highway 97, which becomes Highway 26 at the north end of Madras; follow Highway 26 for 61 miles (98 km) through Warm Springs, the Warm Springs Reservation, and U.S. Forest Service lands to the Highway 35 junction.

Continuation of Directions for Both Routes—At the junction of Highway 26 with Highway 35, stay to the left and continue west on Highway 26 (follow the signs for Government Camp and Portland); about 2 miles (3.5 km) past the Highway 35 junction, turn right (north) onto State Highway 173 (also known as Timberline Highway) and proceed to Timberline Lodge. A quarry in the Mount Hood andesite is on the north (right) side of the road, not far past the first hairpin turn (about 3 miles [4.5 km] from Highway 26).

In Transit—The Geology En Route from the Deschutes River near Warm Springs to Mount Hood

[Geology modified from Conrey and others (2004)]

Ascending the grade from Warm Springs, roadcuts show the monotonously tan beds of the John Day Formation, here believed to be about 20 Ma and tilted southward. Near the top of the grade, roadcuts show the now-thin tuffs and sediment of the Deschutes Formation; at the crest, the highway cuts through the overlying basalt of Miller Flat (about 4 Ma). Past the crest, the highway offers few exposures until it crosses Mill Creek canyon, where a thick section of basalt is exposed; north of Mill Creek canyon, the basalt section is overlain by the informally named “Shitike” formation (R. Conrey, unpub. data, 1996), a younger and less voluminous sequence that is related to the Deschutes Formation. Distal “Shitike” (a Native American location name, pronounced *shh-dike*) strata can be seen in some roadcuts.

Visible on the left (west) side of the highway is Mount Jefferson; the domes in the foreground beneath the peak (North and Shitike Buttes) are of Gauss-normal age (3.6–2.6 Ma), and they are part of the evidence for the longevity of the Mount Jefferson volcanic center. Closer to, and immediately west of, the highway are Hehe Butte and the Sidwalter Buttes, Pliocene rhyolite domes built atop the basalt of Miller Flat; they are partly surrounded by the late Pliocene lava flows, tuff, and sedimentary strata of the “Shitike” formation. East of the highway are the anticlinal Mutton Mountains, which are underlain by rocks of the John Day Formation (40–20 Ma). After the highway crosses the

Warm Springs River, the mafic lava flows that are so common between stratovolcanoes to the south die out about halfway between Mount Jefferson and Mount Hood, and so the volcanic arc loses expression; here, the arc is underlain chiefly by older, reversed-polarity rocks that are highly weathered and poorly exposed. As the highway approaches Mount Hood, the exposures become better; some large escarpments of late Miocene and Pliocene rocks can be seen on the right (east) side of the highway, on the far (east) side of the upper White River valley. Close to Mount Hood, after the junction with Highway 35, roadcuts are largely in andesite lava flows from Mount Hood.

Discussion of Stop 38

Timberline Lodge, on the south side of Mount Hood, was constructed from 1936 to 1938 by employees from the Works Progress Administration, with the help of local artisans. Dedicated by President Franklin D. Roosevelt on September 28, 1937, the lodge contains wonderful carvings and hand-woven draperies, as well as extensive stone, iron, and glass work. Local materials were used, many of them recycled: for example, the stair posts were carved from old cedar telephone poles, and old tire chains were used to make the fireplace screens. Some of the outside views for the movie “The Shining” were filmed at Timberline Lodge.

Timberline Lodge is built on an extensive fan of lahar deposits and pyroclastic flows produced by an eruption about 1.5 ka from Crater Rock dome, near the summit of Mount Hood (Scott and others, 1997). The youngest lahar deposits and pyroclastic flows from Mount Hood are only slightly more than 200 years old, part of the “Old Maid” eruptive period (Crandell, 1980; Cameron and Pringle, 1987; Pierson and others, 2011). Those eruptions began in 1781, and they continued until about 1793 (Pierson and others, 2011). During the 1792 explorations of the Columbia River upstream from the Pacific Ocean, a sand bar was described that extended from the mouth of the Sandy River, which drains the south and west flanks of Mount Hood (Pierson and others, 2011). In the fall of 1805, the Lewis and Clark expedition descended the Columbia River, and they noted that the mouth of the Sandy River—which they named the “Quicksand River”—was very wide and shallow where it enters the Columbia River, owing to the large sediment load. The “sand” was actually volcanoclastic sediment moving down the Sandy River drainage from Mount Hood. Similar deposits from an older eruptive period (the “Polallie” period, from 20–13 ka) are distributed in all major drainages around the volcano (Scott and others, 1997).

Crater Rock is the prominent dome visible just beneath the summit on the south side of Mount Hood. Fumaroles are active near the eastern base of Crater Rock, in an area aptly named Devils Kitchen; climbers often encounter a strong sulfur smell when passing through “the Kitchen” on their way to the summit. Temperatures of water vapor from the fumaroles are near boiling, despite mixing with meteoric snowmelt, which suggests a strong fluid upflow (Ingebritsen and others, 2014). The fluid, chiefly water, is driven by magmatic heat, as indicated by its high $^3\text{He}/^4\text{He}$ ratio, as high as 7.6 times the atmospheric ratio (Ra) (Ingebritsen and others, 2014).

Mount Hood has a long record of intermediate-composition (55–64 percent SiO₂) volcanism that extends back to 1.5 Ma (Scott and others, 1997). Most eruptions have been from near the present-day summit region, and, thus, a large stratovolcano has been constructed; in contrast, eruptions from the smaller cone at Mount Jefferson were spread out over a broader field, and they also are of a wider range of compositions (50–72 percent SiO₂). Kent and others (2010) argued that andesite-dominated stratovolcanoes such as Mount Hood are restricted in composition because their eruptions are all from mafic magma recharge and that the mixing of resident silicic magma with recharged mafic magma inevitably leads to the production of andesitic magma.

End of Day 6: Return to Portland

Directions to Portland

Return to Highway 26 on State Highway 173 (Timberline Highway), then turn right (west) toward Portland. Remain on Highway 26 for 39 miles (63 km) through Sandy to the outskirts of Gresham, where Highway 26 splits off to the left and SE

Burnside Road continues straight ahead; stay on SE Burnside Road, which soon becomes NE Burnside Road. About 0.7 miles (1.1 km) past the split, turn right (north) onto NE Hogan Drive, which becomes NE 242nd Drive and then NE 238th Drive. Follow NE 238th Drive to Interstate 84, then take the westbound onramp for Interstate 84 toward Portland.

Acknowledgments

We thank the many workers who have studied the central Oregon Cascades and produced a wealth of knowledge on this special place. In particular, we thank authors of previous field guides (see introduction) and geologic maps of the region. We are grateful to Marshall Gannett (U.S. Geological Survey [USGS]), Sarah Lewis (Oregon State University), and Anne Jefferson (Kent University) for answering detailed questions, often at short notice. This field guide was improved by comments by reviewers Elizabeth Safran (Lewis and Clark College) and Mariek Schmidt (Brock University) and our editor Taryn Lindquist (USGS). And finally, work by Natalia I. Deligne was supported by the GNS Science Core Research Programme.

References Cited

- Aldous, A.R., Gannett, M.W., Keith, M., and O'Connor, J.E., 2015, Geologic and geomorphic controls on the occurrence of fens in the Oregon Cascades and implications for vulnerability and conservation: *Wetlands*, v. 35, p. 757–767, doi:10.1007/s13157-015-0667-x.
- Alexander, D., 2013, Volcanic ash in the atmosphere and risks for civil aviation—A study in European crisis management: *International Journal of Disaster Risk Science*, v. 4, no. 1, p. 9–19, doi:10.1007/s13753-013-0003-0.
- Allègre, C.J., Treuil, M., Minster, J.-F., Minster, B., and Albarède, F., 1977, Systematic use of trace elements in igneous processes, Part I—Fractional crystallization processes in volcanic suites: *Contributions to Mineralogy and Petrology*, v. 60, no. 1, p. 57–75, doi:10.1007/BF00372851.
- Allen, J.E., 1966, The Cascade Range volcanic-tectonic depression of Oregon, *in* Transactions of the Lunar Geological Field Conference, Bend, Oregon, August 1965: Oregon Department of Mineral Industries, p. 21–23.
- Almendinger, J.E., and Leete, J.H., 1998, Regional and local hydrogeology of calcareous fens in the Minnesota River basin, USA: *Wetlands*, v. 18, no. 2, p. 184–202, doi:10.1007/BF03161655.
- Amon, J.P., Thompson, C.A., Carpenter, Q.J., and Miner, J., 2002, Temperate zone fens of the glaciated midwestern USA: *Wetlands*, v. 22, no. 2, p. 301–317, doi:10.1672/0277-5212(2002)022[0301:TZFOG]2.0.CO;2.
- Ankney, M.E., Johnson, C.M., Bacon, C.R., Beard, B.L., and Jicha, B.R., 2013, Distinguishing lower and upper crustal processes in magmas erupted during the buildup to the 7.7 ka climactic eruption of Mount Mazama, Crater Lake, Oregon, using ^{238}U – ^{230}Th disequilibria: *Contributions to Mineralogy and Petrology*, v. 166, no. 2, p. 563–585, doi:10.1007/s00410-013-0891-4.
- Armstrong, R.L., Taylor, E.M., Hales, P.O., and Parker, D.J., 1975, K–Ar dates for volcanic rocks, central Cascade Range of Oregon: *Isochron/West*, v. 13, p. 5–10.
- Avramenko, W., 1981, Volcanism and structure in the vicinity of Echo Mountain, central Oregon Cascade Range: Eugene, University of Oregon, M.S. thesis, 156 p.
- Bacon, C.R., 1990, Calc-alkaline, shoshonitic and primitive tholeiitic lavas from monogenetic volcanoes near Crater Lake, Oregon: *Journal of Petrology*, v. 31, no. 1, p. 135–166, doi:10.1093/petrology/31.1.135.
- Barratt, B., and Fuller, G., 2010, Analysis of the impact of Heathrow and Gatwick airport closures on local air quality during Eyjafjallajökull eruption 15th–17th April 2010: Vienna, Austria, European Geophysical Union General Assembly, Geophysical Research Abstracts, v. 12, EGU2010-15764, available at <http://meetingorganizer.copernicus.org/EGU2010/EGU2010-15764.pdf>.
- Bedford, B.L., and Godwin, K.S., 2003, Fens of the United States—Distribution, characteristics, and scientific connection versus legal isolation: *Wetlands*, v. 23, no. 3, p. 608–629, doi:10.1672/0277-5212(2003)023[0608:FOTUSD]2.0.CO;2.
- Benson, G.T., 1965, The age of Clear Lake, Oregon: *The Ore Bin*, v. 27, p. 37–40.
- Black, G.L., Woller, N.M., and Ferns, M.L., 1987, Geologic map of the Crescent Mountain area, Linn County, Oregon: Oregon Department of Geology and Mineral Industries Map GMS-47, scale 1:62,500.
- Blackwell, D.D., Bowen, R.G., Hull, D.A., Riccio, H., and Steele, J.L., 1982, Heat flow, arc volcanism, and subduction in northern Oregon: *Journal of Geophysical Research*, v. 87, no. B10, p. 8735–8754, doi:10.1029/JB087iB10p08735.
- Bureau of Land Management, 2001, Oregon state boundaries—2001: Oregon Spatial Data Library, available at <http://spatialdata.oregonexplorer.info/geoportal/details?id=cf375eb0ff7042d99daea17a776821a8>.
- Büttner, R., Dellino, P., and Zimanowski, B., 1999, Identifying magma-water interaction from the surface features of ash particles: *Nature*, v. 401, p. 688–690, doi:10.1038/44364.
- Cameron, K.A., and Pringle, P.T., 1987, A detailed chronology of the most recent major eruptive period at Mount Hood, Oregon: *Geological Society of America Bulletin*, v. 99, no. 6, p. 845–851, doi:10.1130/0016-7606(1987)99<845:ADCOTM>2.0.CO;2.
- Cande, S.C., and Kent, D.V., 1992, A new geomagnetic polarity time scale for the Late Cretaceous and Cenozoic: *Journal of Geophysical Research*, v. 97, no. B10, p. 13,917–13,951, doi:10.1029/92JB01202.
- Cashman, K.V., Deligne, N.I., Gannett, M.W., Grant, G.E., and Jefferson, A., 2009, Fire and water—Volcanology, geomorphology, and hydrogeology of the Cascade Range, central Oregon, *in* O'Connor, J.E., Dorsey, R.J., and Madin, I.P., eds., *Volcanoes to vineyards—Geologic field trips through the dynamic landscape of the Pacific Northwest: Geological Society of America Field Guide 15*, p. 539–582, doi:10.1130/2009.fl.d015(26).

- Champion, D.E., 1980, Holocene geomagnetic secular variation in the western United States: U.S. Geological Survey Open-File Report 80–824, 314 p.
- Chatters, R.M., 1968, Washington State University Natural Radiocarbon Measurements I: Radiocarbon, v. 10, no. 2, p. 479–498.
- Clark, J.G., 1983, Geology and petrology of South Sister volcano, High Cascade Range, Oregon: Eugene, University of Oregon, Ph.D. dissertation, 235 p.
- Clyne, M.A., and Muffler, L.J.P., 2010, Geologic map of Lassen Volcanic National Park and vicinity, California: U.S. Geological Survey Scientific Investigations Map 2899, pamphlet 116 p., 3 sheets, scale 1:50,000, available at <https://pubs.usgs.gov/sim/2899/>.
- Conrey, R.M., 1991, Geology and petrology of the Mt. Jefferson area, High Cascade Range, Oregon: Pullman, Washington State University, Ph.D. dissertation, 357 p.
- Conrey, R.M., Grunder, A., and Schmidt, M.E., 2004, State of the Cascade arc—Stratocone persistence, mafic lava shields, and pyroclastic volcanism associated with intra-arc rift propagation; introduction to the geology of the north-central Oregon Cascade Range along arc rift propagation: Oregon Department of Geology and Mineral Industries Open-File Report O-04-04, 43 p., available at <http://www.oregongeology.org/pubs/ofr/O-04-04.pdf>.
- Conrey, R.M., Hooper, P.R., Larson, P.B., Chesley, J., and Ruiz, J., 2001, Trace element and isotopic evidence for two types of crustal melting beneath a High Cascade volcanic center, Mt. Jefferson, Oregon: Contributions to Mineralogy and Petrology, v. 141, no. 6, p. 710–732, doi:10.1007/s004100100259.
- Conrey, R.M., Taylor, E.M., Donnelly-Nolan, J.M., and Sherrod, D.R., 2002a, North-central Oregon Cascades—Exploring petrologic and tectonic intimacy in a propagating intra-arc rift, *in* Moore, G.W., ed., Field guide to geologic processes in Cascadia: Oregon Department of Geology and Mineral Industries Special Paper 36, p. 47–90.
- Conrey, R.M., Taylor, E.M., Sherrod, D.R., Donnelly-Nolan, J.M., and Bullen, T.D., 2002b, Desert Spring tuff, central Oregon Cascade Range—New perspectives on source, genesis, and hazards: Geological Society of America Abstracts with Programs, v. 34, p. A–92.
- Cook, R.J., Barron, J.C., Papendick, R.I., and Williams, G.J., 1981, Impact on agriculture of the Mount St. Helens eruptions: Science, v. 211, no. 4477, p. 16–22, doi:10.1126/science.211.4477.16.
- Craig, E.S., 1993, Open vertical volcanic conduits—A preliminary investigation of an unusual volcanic cave form with examples from Newberry Volcano and the Central High Cascades of Oregon, *in* Halliday, W.R., ed., Proceedings of the Third International Symposium on Vulcanospeleology: International Speleological Foundation, p. 7–17.
- Craig, H.M., Wilson, T.M., Stewart, C., Villarosa, G., Outes, V., Cronin, S.J., and Jenkins, S.F., 2016, Agricultural impact assessment and management after three widespread tephra falls in Patagonia, South America: Natural Hazards, v. 82, no. 2, p. 1167–1229, doi:10.1007/s11069-016-2240-1.
- Crandell, D.R., 1980, Recent eruptive history of Mount Hood, Oregon, and potential hazards from future eruptions: U.S. Geological Survey Bulletin 1492, 81 p.
- Deardorff, N.D., and Cashman, K.V., 2012, Emplacement conditions of the c. 1,600 BP Collier Cone lava flow, Oregon—A LiDAR investigation: Bulletin of Volcanology, v. 74, p. 2051–2066.
- Deligne, N.I., 2012, After the flow—Landscape response to the emplacement of Holocene lava flows, central Oregon Cascades, USA: Eugene, University of Oregon, Ph.D. dissertation, 217 p.
- Deligne, N.I., Cashman, K.V., and Roering, J.J., 2013, After the lava flow—The importance of external soil sources for plant colonization of recent lava flows in the central Oregon Cascades, USA: Geomorphology, v. 202, p. 15–32, doi:10.1016/j.geomorph.2012.12.009.
- Deligne, N.I., Conrey, R.M., Cashman, K.V., Champion, D.E., and Amidon, W.H., 2016, Holocene volcanism of the upper McKenzie River catchment, central Oregon Cascades, USA: Geological Society of America Bulletin, v. 128, nos. 11–12, p. 1618–1635, doi:10.1130/B31405.1.
- Dellino, P., Gudmundsson, M.T., Larsen, G., Mele, D., Stevenson, J.A., Thordarson, T., and Zimanowski, B., 2012, Ash from the Eyjafjallajökull eruption (Iceland)—Fragmentation processes and aerodynamic behavior: Journal of Geophysical Research, v. 117, no. B9, p. 1–10, doi:10.1029/2011JB008726.
- Dellino, P., and Kyriakopoulos, K., 2003, Phreatomagmatic ash from the ongoing eruption of Etna reaching the Greek island of Cefalonia: Journal of Volcanology and Geothermal Research, v. 126, p. 341–345, doi:10.1016/S0377-0273(03)00154-9.
- Donnelly-Nolan, J.M., Champion, D.E., and Lanphere, M.A., 2000, North flank stratigraphy revealed by new work at Newberry volcano, Oregon, *in* Jensen, R.A., and Chitwood, L.A., eds., What's new at Newberry Volcano, Oregon: Friends of the Pleistocene, Eighth Annual Pacific Northwest Cell Field Trip, Guidebook, p. 177–180.

- Dreher, D.M., 2004, Effects of input and redistribution processes on in-stream wood abundance and arrangement in Lookout Creek, western Cascades Range, Oregon: Corvallis, Oregon State University, M.S. thesis, 143 p.
- Dzurisin, D., Lisowski, M., and Wicks, C.W., 2009, Continuing inflation at Three Sisters volcanic center, central Oregon Cascade Range, USA, from GPS, leveling, and InSAR observations: *Bulletin of Volcanology*, v. 71, no. 10, p. 1091–1110, doi:10.1007/s00445-009-0296-4.
- Elsner, M.M., Cuo, L., Voisin, N., Deems, J.S., Hamlet, A.F., Vano, J.A., Mickelson, K.E.B., Lee, S., and Lettenmaier, D.P., 2010, Implications of 21st century climate change for the hydrology of Washington State: *Climate Change*, v. 102, no. 1, p. 225–260, doi:10.1007/s10584-010-9855-0.
- Erlund, E.J., Cashman, K.V., Wallace, P.J., Pioli, L., Rosi, M., Johnson, E., and Delgado Granados, H., 2010, Compositional evolution of magma from Parícutin Volcano, Mexico—The tephra record: *Journal of Volcanology and Geothermal Research*, v. 197, nos. 1–4, p. 167–187, doi:10.1016/j.jvolgeores.2009.09.015.
- Evans, W.C., Van Soest, M.C., Mariner, R.H., Hurwitz, S., Ingebritsen, S.E., Wicks, C.W., Jr., and Schmidt, M.E., 2004, Magmatic intrusion west of Three Sisters, central Oregon, USA—The perspective from spring geochemistry: *Geology*, v. 32, no. 1, p. 69–72, doi:10.1130/G19974.1.
- Faustini, J.M., 2001, Stream channel response to peak flows in a fifth-order mountain watershed: Corvallis, Oregon State University, Ph.D. dissertation, 339 p.
- Fierstein, J., Hildreth, W., and Calvert, A.T., 2011, Eruptive history of South Sister, Oregon Cascades: *Journal of Volcanology and Geothermal Research*, v. 207, nos. 3–4, p. 145–179, doi:10.1016/j.jvolgeores.2011.06.003.
- Fisher, R.V., and Schmincke, H.-U., 1984, *Pyroclastic rocks*: Berlin, Springer-Verlag, 472 p.
- Fries, C.J., 1953, Volumes and weights of pyroclastic material, lava, and water erupted by Parícutin volcano, Michoacán, Mexico: *Transactions of the American Geophysical Union*, v. 34, p. 603–616.
- Gannett, M.W., and Lite, K.E., Jr., 2004, Simulation of regional ground-water flow in the upper Deschutes Basin, Oregon: U.S. Geological Survey Water-Resources Investigations Report 03–4195, 84 p., available at <https://pubs.usgs.gov/wri/wri034195/>.
- Gannett, M.W., Lite, K.E., Jr., Morgan, D.S., and Collins, C.A., 2001, Groundwater hydrology of the upper Deschutes Basin, Oregon: U.S. Geological Survey Water-Resources Investigation Report 00–4162, 77 p., available at <https://pubs.usgs.gov/wri/wri004162/>.
- Gannett, M.W., Manga, M., and Lite, K.E., Jr., 2003, Groundwater hydrology of the upper Deschutes Basin and its influence on streamflow, *in* O'Connor, J.E., and Grant, G.E. eds., *A peculiar river—Geology, geomorphology, and hydrology of the Deschutes River*, Oregon: American Geophysical Union, Water Science and Application, v. 7, p. 31–49.
- Gardner, C.A., 1994, Temporal, spatial and petrologic variations of lava flows from the Mount Bachelor volcanic chain, central Oregon High Cascades: U.S. Geological Survey Open-File Report 94–261, p. 100.
- Grant, G.E., 1997, A geomorphic basis for interpreting the hydrologic behavior of large river basins, *in* Laenan, A., and Dunnette, D., eds., *River quality, dynamics and restoration*: New York, CRC Press, p. 105–116.
- Grant, G.E., and Swanson, F.J., 1995, Morphology and processes of valley floors in mountain streams, western Cascades, Oregon, *in* Costa, J.E., and others, eds., *Natural and anthropogenic influences in fluvial geomorphology—The Wolman volume*: American Geophysical Union, Geophysical Monograph 89, p. 83–101.
- Grant, G.E., Swanson, F.J., and Wolman, M.G., 1990, Pattern and origin of stepped-bed morphology in high-gradient streams, Western Cascades, Oregon: *Geological Society of America Bulletin*, v. 102, no. 3, p. 340–352, doi:10.1130/0016-7606(1990)102<0340:PAOOSB>2.3.CO;2.
- Gudmundsson, M.T., Pedersen, R., Vogfjörð, K., Thorbjarnardóttir, B., Jakobsdóttir, S., and Roberts, M.J., 2010, Eruptions of Eyjafjallajökull Volcano, Iceland: EOS, *Transactions of the American Geophysical Union*, v. 91, no. 21, p. 190–191, doi:10.1029/2010EO210002.
- Gudmundsson, M.T., Thordarson, T., Höskuldsson, A., Larsen, G., Björnsson, H., Prata, F.J., Oddsson, B., Magnússon, E., Högnadóttir, T., Peterson, G.N., Hayward, C.L., Stevenson, J.A., and Jónsdóttir, I., 2012, Ash generation and distribution from the April-May 2010 eruption of Eyjafjallajökull, Iceland: *Scientific Reports*, v. 2, no. 572, doi:10.1038/srep00572.
- Hallett, O.J., Hills, L.V., and Clague, J.J., 1997, New accelerator mass spectrometry radiocarbon ages for the Mazama tephra layer from Kootenay National Park, British Columbia, Canada: *Canadian Journal of Earth Sciences*, v. 34, no. 9, p. 1202–1209, doi:10.1139/e17-096.
- Heiken, G.H., 1972, Morphology and petrography of volcanic ashes: *Geological Society of America Bulletin*, v. 83, no. 7, p. 1961–1988, doi:10.1130/0016-7606(1972)83[1961:MAPOV A]2.0.CO;2.
- Hildreth, W., 2007, Quaternary magmatism in the Cascades—Geologic perspectives: U.S. Geological Survey Professional Paper 1744, 136 p., available at <https://pubs.usgs.gov/pp/pp1744/>.

- Hildreth, W., Fierstein, J., and Calvert, A.T., 2012, Geologic map of Three Sisters volcanic cluster, Cascade Range, Oregon: U.S. Geological Survey Scientific Investigations Map 3186, pamphlet 107 p., 2 sheets, scale 1:24,000, available at <http://pubs.usgs.gov/sim/3186/>.
- Hill, B.E., 1985, Petrology of the Bend Pumice and Tumalo Tuff, a Pleistocene Cascade eruption involving magma mixing: Corvallis, Oregon State University, M.S. thesis, 101 p.
- Hill, B.E., 1988, The Tumalo volcanic center—A large Pleistocene vent complex on the east flank of the Oregon central High Cascades: Geological Society of America Abstracts with Programs, v. 20, no. 7, p. A398.
- Hill, B.E., 1992, Petrogenesis of compositionally distinct silicic volcanoes in the Three Sisters region of the Oregon Cascade Range—The effects of crustal extension on the development of continental arc silicic magmatism: Corvallis, Oregon State University, Ph.D. dissertation, 235 p.
- Hill, B.E., Connor, C.B., Jarzempa, M.S., La Femina, P., Navarro, M., and Strauch, W., 1998, 1995 eruption of Cerro Negro volcano, Nicaragua, and risk assessment for future eruptions: Geological Society of America Bulletin, v. 110, no. 10, p. 1231–1241, doi:10.1130/0016-7606(1998)110<1231:EOCNV N>2.3.CO;2.
- Hill, B.E., and Duncan, R.A., 1990, The timing and significance of silicic magmatism in the Three Sisters region of the Oregon High Cascades: EOS, Transactions of the American Geophysical Union, v. 71, p. 1614.
- Hill, B.E., and Priest, G.R., 1992, Geologic setting of the Santiam Pass area, central Cascade Range, Oregon, in Hill, B.E., ed., Geology and geothermal resources of the Santiam Pass area of the Oregon Cascade Range, Deschutes, Jefferson, and Linn Counties, Oregon: Oregon Department of Geology and Mineral Industries Open-File Report O-92-3, p. 5–18.
- Hill, B.E., and Taylor, E.M., 1990, Oregon central High Cascade pyroclastic units in the vicinity of Bend, Oregon: Oregon Geology, v. 52, no. 6, p. 125–126, 139–140.
- Hooper, P.R., Steele, W.K., Conrey, R.M., Smith, G.A., Anderson, J.L., Bailey, D.G., Beeson, M.H., Tolan, T.L., and Urbanczyk, K.M., 1993, The Prineville Basalt, north-central Oregon: Oregon Geology, v. 55, no. 1, p. 3–12.
- Hopson, R.E., 1960, Collier Glacier—A photographic record: Mazama, v. 42, no. 13, p. 15–26.
- Houghton, B.F., and Gonnermann, H.M., 2008, Basaltic explosive volcanism—Constraints from deposits and models: Chemie der Erde, v. 68, no. 2, p. 117–140, doi:10.1016/j.chemer.2008.04.002.
- Hughes, S.S., and Taylor, E.M., 1986, Geochemistry, petrogenesis, and tectonic implications of central High Cascade mafic platform lavas: Geological Society of America Bulletin, v. 97, no. 8, p. 1024–1036, doi:10.1130/0016-7606(1986)97<1024:GPATIO>2.0.CO;2.
- Ingebritsen, S.E., Mariner, R.H., and Sherrod, D.R., 1994, Hydrothermal systems of the Cascade Range, north-central Oregon: U.S. Geological Survey Professional Paper 1044-L, 86 p.
- Ingebritsen, S.E., Randolph-Flagg, N.G., Gelwick, K.D., Lundstrom, E.A., Crankshaw, J.M., Murveit, A.M., Schmidt, M.E., Bergfeld, D., Spicer, K.R., Tucker, D.S., Mariner, R.H., and Evans, A.C., 2014, Hydrothermal monitoring in a quiescent volcanic arc—Cascade Range, northwestern United States: Geofluids, v. 14, no. 3, p. 326–346, doi:10.1111/gfl.12079.
- Ingebritsen, S.E., Sherrod, D.R., and Mariner, R.H., 1992, Rates and patterns of groundwater flow in the Cascade Range volcanic arc, and the effect on subsurface temperatures: Journal of Geophysical Research, v. 97, p. 4599–4627, doi:10.1029/91JB03064.
- Iverson, R.M., LaHusen, R.G., and Costa, J.E., 1992, Debris-flow flume at H.J. Andrews Experimental Forest, Oregon: U.S. Geological Survey Open-File Report 92–483, 2 p.
- James, E.R., Manga, M., and Rose, T.P., 1999, CO₂ degassing in the Oregon Cascades: Geology, v. 27, no. 9, p. 823–826, doi:10.1130/0091-7613(1999)027<0823:CDITOC>2.3.CO;2.
- James, E.R., Manga, M., Rose, T.P., and Hudson, G.B., 2000, The use of temperature and the isotopes of O, H, C, and noble gases to determine the pattern and spatial extent of groundwater flow: Journal of Hydrology, v. 237, nos. 1–2, p. 100–112, doi:10.1016/S0022-1694(00)00303-6.
- Jefferson, A., and Grant, G., 2003, Recharge areas and discharge of groundwater in a young volcanic landscape, McKenzie River, Oregon: Geological Society of America Abstracts with Programs, v. 35, no. 6, p. 373.
- Jefferson, A., Grant, G., and Lewis, S., 2007, A river runs underneath it—Geological control of spring and channel systems and management implications, Cascade Range, Oregon, in Furniss, M.J., Clifton, C.F., and Ronnenberg, K.L., eds., Advancing the fundamental sciences: Proceedings, Forest Service National Earth Sciences Conference, Portland, Oregon, PNW-GTR-689, U.S. Department of Agriculture, Forest Service, Pacific Northwest Research Station, p. 391–400.
- Jefferson, A., Grant, G.E., Lewis, S.L., and Lancaster, S.T., 2010, Coevolution of hydrology and topography on a basalt landscape in the Oregon Cascade Range, USA: Earth Surface Processes and Landforms, v. 35, no. 7, p. 803–816, doi:10.1002/esp.1976.

- Jefferson, A., Grant, G., and Rose, T., 2006, Influence of volcanic history on groundwater patterns on the west slope of the Oregon High Cascades: *Water Resources Research*, v. 42, W12411, 15 p., doi:10.1029/2005WR004812.
- Jefferson, A., Nolin, A., Lewis, S., and Tague, C., 2008, Hydrogeologic controls on streamflow sensitivity to climatic variability: *Hydrological Processes*, v. 22, no. 22, p. 4371–4385, doi:10.1002/hyp.7041.
- Jensen, R.A., 2006, *Roadside guide to the geology and history of Newberry Volcano* (4th ed.): Bend, Oregon, CenOreGeoPub, 182 p.
- Jensen, R.A., Donnelly-Nolan, J.M., and McKay, D., 2009, A field guide to Newberry Volcano, Oregon, in O'Connor, J.E., Dorsey, R.J., and Madin, I.P., eds., *Volcanoes to vineyards—Geologic field trips through the dynamic landscapes of the Pacific Northwest: Geological Society of America Field Guide 15*, p. 53–79, doi:10.1130/2009.fld015(03).
- Johnson, D.M., Petersen, R.R., Lycan, D.R., and Sweet, J.W., 1985, *Atlas of Oregon lakes*: Corvallis, Oregon State University Press, 317 p.
- Kent, A.J.R., Darr, C., Koleszar, A.M., Salisbury, M., and Cooper, K.M., 2010, Preferential eruption of andesitic magmas through recharge filtering: *Nature Geoscience*, v. 3, p. 631–636, doi:10.1038/NGEO924.
- Koch, R.D., Ramsey, D.W., Sherrod, D.R., Taylor, E.M., Ferns, M.L., Scott, W.E., Conrey, R.M., and Smith, G.A., 2010, Database for the geologic map of the Bend 30- × 60-minute quadrangle, central Oregon: U.S. Geological Survey Data Series 303, available at <https://pubs.usgs.gov/ds/303/>.
- Kuehn, S.C., and Negrini, R.M., 2010, A 250 k.y. record of Cascade arc pyroclastic volcanism from late Pleistocene lacustrine sediments near Summer Lake, Oregon, USA: *Geosphere*, v. 6, no. 4, p. 397–429, doi:10.1130/GES00515.1.
- Lanphere, M.A., Champion, D.E., Christiansen, R.L., Donnelly-Nolan, J.M., Fleck, R.J., Sarna-Wojcicki, A.M., Obradovich, J.D., and Izett, G.A., 1999, Evolution of tephra dating in the Western United States: *Geological Society of America Abstract with Programs*, v. 31, p. A–73.
- Lawrence, R.D., 1976, Strike-slip faulting terminates the Basin and Range province in Oregon: *Geological Society of America Bulletin*, v. 87, no. 6, p. 846–850, doi:10.1130/0016-7606(1976)87<846:SFTTBA>2.0.CO;2.
- Le Bas, M.J., Le Maitre, R.W., Streckeisen, A., and Zanettin, B., 1986, A chemical classification of volcanic rocks based on the total alkali-silica diagram: *Journal of Petrology*, v. 27, no. 3, p. 745–750, doi:10.1093/petrology/27.3.745.
- Legg, N.T., Meigs, A.J., Grant, G.E., and Kennard, P., 2014, Debris flow initiation in proglacial gullies on Mount Rainier, Washington: *Geomorphology*, v. 226, p. 249–260, doi:10.1016/j.geomorph.2014.08.003.
- Lescinsky, D.T., and Fink, J.H., 2000, Lava and ice interaction at stratovolcanoes—Use of characteristic features to determine past glacial extents and future volcanic hazards: *Journal of Geophysical Research*, v. 105, p. 23,711–23,726, doi:10.1029/2000JB900214.
- Licciardi, J.M., Kurz, M.D., Clark, P.U., and Brook, E.J., 1999, Calibration of cosmogenic ³He production rates from Holocene lava flows in Oregon, USA, and effects of the Earth's magnetic field: *Earth and Planetary Science Letters*, v. 172, nos. 3–4, p. 261–271, doi:10.1016/S0012-821X(99)00204-6.
- Lite, K.E., Jr., and Gannett, M.W., 2002, *Geologic framework of the regional ground-water flow system in the upper Deschutes Basin, Oregon*: U.S. Geological Survey Water-Resources Investigations Report 02–4015, 44 p., available at <https://pubs.usgs.gov/wri/2002/4015/wri02-4015.pdf>.
- Luhr, J.F., and Simkin, T., 1993, *Paricutin—The volcano born in a Mexican cornfield*: Geoscience Press, 427 p.
- Lund, E.H., 1977, Geology and hydrology of the Lost Creek glacial trough: *The Ore Bin*, v. 39, no. 9, p. 141–156.
- MacLeod, N.S., Sherrod, D.R., Chitwood, L.A., and Jensen, R.A., 1995, *Geologic map of Newberry volcano, Deschutes, Klamath, and Lake Counties, Oregon*: U.S. Geological Survey Miscellaneous Investigations Series Map I–2455, 2 sheets, scale 1:62,500, pamphlet 23 p., available at <https://pubs.usgs.gov/imap/2455/>.
- Magill, C., and Blong, R., 2005a, Volcanic risk ranking for Auckland, New Zealand—I. Methodology and hazard investigation: *Bulletin of Volcanology*, v. 67, no. 4, p. 331–339, doi:10.1007/s00445-004-0374-6.
- Magill, C., and Blong, R., 2005b, Volcanic risk ranking for Auckland, New Zealand—II. Hazard consequences and risk calculation: *Bulletin of Volcanology*, v. 67, no. 4, p. 340–349, doi:10.1007/s00445-004-0375-5.
- Manga, M., and Kirchner, J.W., 2000, Stress partitioning in streams by large woody debris: *Water Resources Research*, v. 36, no. 8, p. 2373–2379, doi:10.1029/2000WR900153.
- Massey, N.W.D., MacIntyre, D.G., Desjardins, P.J., and Coonel, R.T., 2005, *Digital geology map of British Columbia*: British Columbia (Canada) Ministry of Energy and Mines Geofile 2005-1, available at <http://www.empr.gov.bc.ca/Mining/Geoscience/PublicationsCatalogue/GeoFiles/Pages/2005-1.aspx>.

- McCaffrey, R., Qamar, A.I., King, R.W., Wells, R., Khazaradze, G., Williams, C.A., Stevens, C.W., Vollick, J.J., and Zwick, P.C., 2007, Fault locking, block rotation and crustal deformation in the Pacific Northwest: *Geophysical Journal International*, v. 169, no. 3, p. 1315–1340, doi:10.1111/j.1365-246X.2007.03371.x.
- McCloughry, J.D., Ferns, M.L., Gordon, C.L., and Patridge, K.A., 2008, A field guide to the volcanic stratigraphy of the Oligocene Crooked River caldera, Crook Deschutes, and Jefferson Counties, Oregon: *Oregon Geology*, v. 69, no. 1, p. 25–44.
- McDannel, A.K., 1989, Geology of the southernmost Deschutes basin, Tumalo quadrangle, Deschutes County, Oregon: Corvallis, Oregon State University, M.S. thesis, 166 p.
- Mckay, D., 2012, Recent mafic eruptions at Newberry Volcano and in the central Oregon Cascades—Physical volcanology and implications for hazards: Eugene, University of Oregon, Ph.D. dissertation, 146 p.
- Mckay, D., Donnelly-Nolan, J.M., Jensen, R.A., and Champion, D.E., 2009, The post-Mazama northwest rift zone eruption at Newberry Volcano, Oregon, *in* O'Connor, J.E., Dorsey, R.J., and Madin, I.P., eds., *Volcanoes to vineyards—Geologic field trips through the dynamic landscape of the Pacific Northwest: Geological Society of America Field Guide 15*, p. 91–110, doi:10.1130/2009.fld015(05).
- Meinzer, O.C., 1927, Large springs in the United States: U.S. Geological Survey Water-Supply Paper 557, 94 p.
- Mimura, K., 1984, Imbrication, flow direction and possible source areas of the pumice-flow tuffs near Bend, Oregon, U.S.A.: *Journal of Volcanology and Geothermal Research*, v. 21, nos. 1–2, p. 45–60, doi:10.1016/0377-0273(84)90015-5.
- Mimura, K., 1992, Reconnaissance geologic map of the west half of the Bend and the east half of the Shevlin Park 7 1/2' quadrangles, Deschutes County, Oregon: U.S. Geological Survey Miscellaneous Field Studies Map MF-2189, scale 1:24,000, available at <https://pubs.er.usgs.gov/publication/mf2189>.
- Mordensky, S.P., 2012, The plumbing systems and parental magma compositions of shield volcanoes in the central Oregon High Cascades as inferred from melt inclusion data: Eugene, University of Oregon, M.S. thesis, 120 p.
- Mote, P.W., 2003, Trends in snow water equivalent in the Pacific Northwest and their climatic causes: *Geophysical Research Letters*: v. 30, no. 12, p. 1601, doi:10.1029/2003GL017258.
- Mote, P.W., Hamlet, A.F., Clark, M., and Lettenmaier, D.P., 2005, Declining mountain snowpack in western North America: *Bulletin of the American Meteorological Society*, v. 86, no. 1, p. 39–49, doi:10.1175/BAMS-86-1-39.
- Mote, P.W., and Salathé, E.P., 2010, Future climate in the Pacific Northwest: *Climatic Change*, v. 102, no. 1, p. 29–50, doi:10.1007/s10584-010-9848-z.
- Nakamura, F., and Swanson, F.J., 1993, Effects of coarse woody debris on morphology and sediment storage of a mountain stream system in western Oregon: *Earth Surface Processes and Landforms*, v. 18, no. 1, p. 43–61, doi:10.1002/esp.3290180104.
- National Center for Airborne Laser Mapping, 2008, North Sister, OR—Collier Cone lava flow: Open Topography, doi:10.5069/G9WM1BB6.
- Nolf, B., 1969, Broken Top breaks—Flood released by erosion of glacial moraine: *Oregon Department of Geology and Mineral Industries, Ore Bin*, v. 31, no. 11, p. 182–188.
- Nolin, A.W., and Daly, C., 2006, Mapping “at-risk” snow in the Pacific Northwest, U.S.A.: *Journal of Hydrometeorology*, v. 7, p. 1164–1173, doi:10.1175/JHM543.1.
- O'Connor, J.E., 2013, Our vanishing glaciers—One hundred years of glacier retreat in the Three Sisters Area, Oregon Cascade Range: *Oregon Historical Quarterly*, v. 114, no. 4, p. 402–427, doi:10.5403/oregonhistq.114.4.0402.
- O'Connor, J.E., and Costa, J.E., 1993, Geologic and hydrologic hazards in glacierized basins resulting from 19th and 20th century global warming: *Natural Hazards*, v. 8, no. 2, p. 121–140, doi:10.1007/BF00605437.
- O'Connor, J.E., Grant, G., and Haluska, T.L., 2003, Overview of geology, hydrology, geomorphology and sediment budget of the Deschutes River Basin, Oregon—A peculiar river: *Water Science and Application*, v. 7, p. 7–30.
- O'Connor, J.E., Hardison, J.H., III, and Costa, J.E., 2001a, Debris flows from failures of Neoglacial-age moraine dams in the Three Sisters and Mount Jefferson Wilderness areas, Oregon: U.S. Geological Survey Professional Paper 1606, 93 p., 2 plates, available at <https://pubs.er.usgs.gov/publication/pp1606>.
- O'Connor, J.E., Sarna-Wojcicki, A., Wozniak, K.C., Polette, D.J., and Fleck, R.J., 2001b, Origin, extent, and thickness of Quaternary geologic units in the Willamette Valley, Oregon: U.S. Geological Survey Professional Paper 1620, 52 p., available at <https://pubs.usgs.gov/pp/1620/>.
- Ohlschlager, J.G., 2015, Glacier change on the Three Sisters volcanoes, Oregon—1900–2010: Portland, Ore., Portland State University, M.S. thesis, 144 p., available at http://pdxscholar.library.pdx.edu/open_access_etds/2448.

- Oregon Department of Fish and Wildlife, 1982, Trout Management Plan—Lost Lake, *in* Trout Mini-Management Plans: Oregon Department of Fish and Wildlife, p. 172–178, available at <http://library.state.or.us/repository/2016/201604040825111/index.pdf>.
- Oregon Department of Geology and Mineral Industries, 2007–2010, Oregon Department of Geology and Mineral Industries Lidar Program data: Open Topography, doi:10.5069/G9QC01D1.
- Oregon Department of Geology and Mineral Industries, 2011a, Mount Washington: Oregon Department of Geology and Mineral Industries Lidar Data Quadrangle, available at <http://www.oregongeology.org/pubs/ldq/p-LDQ.htm>.
- Oregon Department of Geology and Mineral Industries, 2011b, North Sister: Oregon Department of Geology and Mineral Industries Lidar Data Quadrangle, available at <http://www.oregongeology.org/pubs/ldq/p-LDQ.htm>.
- Oregon Department of Transportation, 2015, Oregon signed routes—2015: Oregon Spatial Data Library, available at <http://spatialdata.oregonexplorer.info/geoportal/details?id=d9b426c59f1a4160a12798c8c4864f1a>.
- Oregon Department of Transportation, 2016, Oregon city limits—2016: Oregon Spatial Data Library, available at <http://spatialdata.oregonexplorer.info/geoportal/details?id=607b9a8e31874380a7a371c5048cd600>.
- Oregon Geospatial Enterprise Office, 2008, Oregon 10m [sic] digital elevation model (DEM): Oregon Spatial Data Library, available at <http://spatialdata.oregonexplorer.info/geoportal/details?id=7a82c1be50504f56a9d49d13c7b4d9aa>.
- Oregon Watershed Enhancement Board, 2014–2016, Oregon watershed councils—2014: Oregon Spatial Data Library, available at <http://spatialdata.oregonexplorer.info/geoportal/details?id=8091c70c2e7347d4ba0f8d8d0c5647c>.
- Ort, M.H., Elson, M.D., Anderson, K.C., Duffield, W.A., Hooten, J.A., Champion, D.E., and Waring, G., 2008, Effects of scoria cone eruptions on nearby human communities: *Geological Society of America Bulletin*, v. 120, nos. 3–4, p. 476–486, doi:10.1130/B26061.1.
- Pacific Northwest Hydrography Framework, 2005a, Oregon hydrography water courses—2005, available at <http://spatialdata.oregonexplorer.info/geoportal/details?id=3439a3c43f9f4c4499802f55898b7dd8>.
- Pacific Northwest Hydrography Framework, 2005b, Oregon water bodies—2005: Oregon Spatial Data Library, available at <http://spatialdata.oregonexplorer.info/geoportal/details?id=c4119ef0b66d4219b080d91c495525e9>.
- Parfitt, E.A., 1998, A study of clast size distribution, ash deposition and fragmentation in Hawaiian-style volcanic eruptions: *Journal of Volcanology and Geothermal Research*, v. 84, nos. 3–4, p. 197–208, doi:10.1016/S0377-0273(98)00042-0.
- Perron, J.T., and Fagherazzi, S., 2012, The legacy of initial conditions in landscape evolution: *Earth Surface Processes and Landforms*, v. 37, no. 1, p. 52–63, doi:10.1002/esp.2205.
- Peterson, N.V., and Groh, E.A., 1965, Lunar Geological Field Conference Guide Book: Oregon Department of Geology and Mineral Industries Bulletin 57, 51 p.
- Pierson, T.C., Pringle, P.T., and Cameron, K.A., 2011, Magnitude and timing of downstream channel aggradation and degradation in response to a dome-building eruption at Mount Hood, Oregon: *Geological Society of America Bulletin*, v. 123, nos. 1–2, p. 3–20, doi:10.1130/B30127.1.
- Pioli, L., Erlund, E., Johnson, E., Cashman, K., Wallace, P., Rosi, M., and Delgado Granados, H., 2008, Explosive dynamics of violent Strombolian eruptions—The eruption of Parícutin volcano 1943–1952 (Mexico): *Earth and Planetary Science Letters*, v. 271, nos. 1–4, p. 359–368, doi:10.1016/J.epsl.2008.04.026.
- Pirot, R., 2010, Initiation zone characterization of debris flows in November, 2006, Mount Hood, Oregon: Portland, Ore., Portland State University, M.S. thesis, 179 p.
- Priest, G.R., Woller, N.M., and Ferns, M.L., 1987, Geologic map of the Breitenbush River area, Linn and Marion Counties, Oregon: Oregon Department of Geology and Mineral Industries Map GMS–46, scale 1:62,500.
- Priest, G.R., Black, G.L., Woller, N.M., and Taylor, E.M., 1988, Geologic map of the McKenzie Bridge quadrangle, Lane County, Oregon: Oregon Department of Geology and Mineral Industries Geological Map Series GMS-48, scale 1:62,500.
- Redmond, K.T., 1990, Crater Lake climate and lake level variability, *in* Drake, E.T., Larson, G.L., Dymond, J., and Collier, R., eds., *Crater Lake—An Ecosystem Study*: San Francisco, Calif., American Association for the Advancement of Science, p. 127–141.
- Robinson, Joel E., Hildreth, Wes, Fierstein, Judy, and Calvert, Andrew T., 2012, Database for the geologic map of Three Sisters volcanic cluster, Cascade Range, Oregon, *in* Hildreth, Wes, Fierstein, Judy, and Calvert, Andrew T., *Geologic map of Three Sisters volcanic cluster, Cascade Range, Oregon*: U.S. Geological Survey Scientific Investigations Map 3186, pamphlet 107 p., 2 sheets, scale 1:24,000, available at <http://pubs.usgs.gov/sim/3186/>.

- Rowe, M.C., Kent, A.J.R., and Nielsen, R.L., 2009, Subduction influence on oxygen fugacity and trace and volatile elements in basalts across the Cascade volcanic arc: *Journal of Petrology*, v. 50, no. 1, p. 61–91, doi:10.1093/petrology/egn072.
- Ruscitto, D., Wallace, P.J., Johnson, E.R., Kent, A., and Bindeman, I.N., 2010, Volatile contents of mafic magmas from cinder cones in the Central Oregon High Cascades—Implications for magma formation and mantle conditions in a hot arc: *Earth and Planetary Science Letters*, v. 298, nos. 1–2, p. 153–161, doi:10.1016/j.epsl.2010.07.037.
- Russell, I.C., 1905, Geology and water resources of central Oregon: U.S. Geological Survey Bulletin 252, 138 p.
- Sceva, J.E., 1968, Liquid waste disposal in the lava terrane of central Oregon: U.S. Department of the Interior, Federal Water Pollution Control Administration, Technical Projects Branch Report No. FR-4, 66 p.
- Schick, J.D., 1994, Origin of compositional variability of the lavas at Collier Cone, High Cascades, Oregon: Eugene, University of Oregon, M.S. thesis, 142 p.
- Schmidt, M.E., 2005, Deep crustal and mantle inputs to North Sister volcano, Oregon High Cascade Range: Corvallis, Oregon State University, Ph.D. dissertation, 197 p.
- Schmidt, M.E., and Grunder, A.L., 2009, The evolution of North Sister—A volcano shaped by extension and ice in the central Oregon Cascade arc: *Geological Society of America Bulletin*, v. 121, nos. 5–6, p. 643–662, doi:10.1130/B26442.1.
- Schmidt, M.E., and Grunder, A.L., 2011, Deep mafic roots to arc volcanoes—Mafic recharge and differentiation of basaltic andesite at North Sister volcano, Oregon Cascades: *Journal of Petrology*, v. 52, no. 3, p. 603–641, doi:10.1093/petrology/egq094.
- Schmidt, M.E., Grunder, A.L., and Rowe, M.C., 2008, Segmentation of the Cascades Arc as indicated by Sr and Nd isotopic variation among diverse primitive basalts: *Earth and Planetary Science Letters*, v. 266, nos. 1–2, p. 166–181, doi:10.1016/j.epsl.2007.11.013.
- Scott, W.E., 1977, Quaternary glaciation and volcanism, Metolius River area, Oregon: *Geological Society of America Bulletin*, v. 88, no. 1, p. 113–124, doi:10.1130/0016-7606(1977)88<113:QGAVMR>2.0.CO;2.
- Scott, W.E., 1987, Holocene rhyodacite eruptions on the flanks of South Sister volcano, Oregon, *in* Fink, J.H., ed., *The emplacement of silicic domes and lava flows*: *Geological Society of America Special Paper* 212, p. 35–53.
- Scott, W.E., 1990, Temporal relations between eruptions of the Mount Bachelor volcanic chain and fluctuations of late Quaternary glaciers: *Oregon Geology*, v. 52, p. 114–117.
- Scott, W.E., and Gardner, C.A., 1990, Field trip guide to the central Oregon High Cascades—Part 1. Mount Bachelor–South Sister area: *Oregon Geology*, v. 52, p. 99–117.
- Scott, W.E., and Gardner, C.A., 1992, Geologic map of the Mount Bachelor volcanic chain and surrounding area, Cascade Range, Oregon: U.S. Geological Survey Miscellaneous Investigations Series Map I–1967, scale 1:50,000.
- Scott, W.E., Gardner, C.A., Sherrod, D.R., Tilling, R.I., Lanphere, M.A., and Conrey, R.M., 1997, Geologic history of Mount Hood volcano, Oregon—A field trip guidebook: U.S. Geological Survey Open-File Report 97–0263, 38 p.
- Seegerstrom, K., 1956, Erosion studies at Parícutin, State of Michoacán, Mexico: U.S. Geological Survey Bulletin 965A, 164 p.
- Sherrod, D.R., 1986, Geology, petrology, and volcanic history of a portion of the Cascade Range between latitudes 43–44 degrees N., central Oregon, U.S.A.: Santa Barbara, University of California, Ph.D. dissertation, 640 p.
- Sherrod, D.R., Gannett, M.W., and Lite, K.E., Jr., 2002, Hydrogeology of the upper Deschutes Basin, central Oregon—A young basin adjacent to the Cascade volcanic arc, *in* Moore, G.E., ed., *Field guide to geologic processes in Cascadia*: Oregon Department of Geology and Mineral Industries Special Paper 36, p. 109–144.
- Sherrod, D.R., and Smith, J.G., 1990, Quaternary extrusion rates of the Cascade Range, northwestern United States and southern British Columbia: *Journal of Geophysical Research*, v. 95, no. B12, p. 465–474, doi:10.1029/JB095iB12p19465.
- Sherrod, D.R., and Smith, J.G., 2000, Geologic map of upper Eocene to Holocene volcanic and related rocks in the Cascade Range, Oregon: U.S. Geological Survey Miscellaneous Investigations Series Map I–2569, 2 sheets, scale 1:500,000, pamphlet 49 p., available at <https://pubs.usgs.gov/imap/i2569/>.
- Sherrod, D.R., Taylor, E.M., Ferns, M.L., Scott, W.E., Conrey, R.M., and Smith, G.A., 2004, Geologic map of the Bend 30- × 60-minute quadrangle, central Oregon: U.S. Geological Survey Geologic Investigations Series Map I–2683, 2 sheets, scale 1:100,000, pamphlet 49 p., available at <https://pubs.usgs.gov/imap/i2683/>.
- Sherrod, D.R., and Wills, B.B., 2014, Debris flow from 2012 failure of moraine-dammed lake, Three Fingered Jack volcano, Mount Jefferson Wilderness, Oregon: U.S. Geological Survey Scientific Investigations Report 2014–5208, 13 p., available at <http://dx.doi.org/10.3133/sir20145208>.

- Sklar, L.S., and Dietrich, W.E., 2001, Sediment and rock strength controls on river incision into bedrock: *Geology*, v. 29, no. 12, p. 1080–1090, doi:10.1130/0091-7613(2001)029<1087:SARS CO>2.0.CO;2.
- Smith, G.A., 1986a, Simtustus Formation—Paleogeographic and stratigraphic significance of a newly defined Miocene unit in the Deschutes Basin, central Oregon: *Oregon Geology*, v. 48, no. 6, p. 63–72.
- Smith, G.A., 1986b, Stratigraphy, sedimentology, and petrology of Neogene rocks in the Deschutes Basin, central Oregon—A record of continental margin volcanism and its influence on fluvial sedimentation in an arc adjacent basin: Corvallis, Oregon State University, Ph.D. dissertation, 467 p.
- Smith, G.A., 1987a, Geologic map of the Madras West and Madras East quadrangles, Jefferson County, Oregon: Oregon Department of Geology and Mineral Industries Geological Map Series GMS-45, scale 1:24,000.
- Smith, G.A., 1987b, Geologic map of the Seekseequa Junction and a portion of the Metolius Bench quadrangles, Jefferson County, Oregon: Oregon Department of Geology and Mineral Industries Geological Map Series GMS-44, scale 1:24,000.
- Smith, G.A., and Hayman, G.A., 1987, Geologic map of the Eagle Butte and Gateway quadrangles, Jefferson and Wasco Counties, Oregon: Oregon Department of Geology and Mineral Industries Geological Map Series GMS-43, scale 1:24,000.
- Smith, G.A., Manchester, S.R., Ashwill, M., McIntosh, W.C., and Conrey, R.M., 1998, Late Eocene–early Oligocene tectonism, volcanism, and floristic change near Gray Butte, central Oregon: *Geological Society of America Bulletin*, v. 110, no. 6, p. 759–778, doi:10.1130/0016-7606(1998)110<0759:LEEOTV>2.3.CO;2.
- Smith, G.A., and Priest, G.R., 1983, A field trip guide to the central Oregon Cascades—First day, Mount Hood–Deschutes basin: *Oregon Geology*, v. 45, p. 119–126.
- Smith, G.A., Snee, L.W., and Taylor, E.M., 1987, Stratigraphic, sedimentologic, and petrologic record of late Miocene subsidence of the central Oregon High Cascades: *Geology*, v. 15, no. 5, p. 389–392, doi:10.1130/0091-7613(1987)15<389:SSAPRO>2.0.CO;2.
- Smith, G.A., and Taylor, E.M., 1983, The central Oregon High Cascade graben—What? Where? When?: *Transactions of the Geothermal Resources Council*, v. 7, p. 275–279.
- Smith, J.G., 1993, Geologic map of upper Eocene to Holocene volcanic and related rocks in the Cascade Range, Washington: U.S. Geological Survey Miscellaneous Investigations Series Map I-2005, 2 sheets, scale 1:500,000, pamphlet 20 p., available at <https://pubs.usgs.gov/imap/2005/>.
- Sproles, E.A., Nolin, A.W., Rittger, K., and Painter, T.H., 2013, Climate change impacts on maritime mountain snowpack in the Oregon Cascades: *Hydrology and Earth System Sciences*, v. 17, p. 2581–2597.
- Stearns, H.T., 1929, Geology and water resources of the upper McKenzie Valley, Oregon: U.S. Geological Survey Water-Supply Paper 597–D, 20 p.
- Stearns, H.T., 1931, Geology and water resources of the middle Deschutes River basin, Oregon: U.S. Geological Survey Water-Supply Paper 637–D, p. 125–212.
- Swanson, F.J., and Jones, J.A., 2002, Geomorphology and hydrology of the H.J. Andrews Experimental Forest, Blue River, Oregon, *in* Moore, G.W., ed., *Field guide to geologic processes in Cascadia—Field trips to accompany the 98th annual meeting of the Cordilleran section of the Geological Society of America*, Corvallis, Oregon: Portland, Oregon Department of Geology and Mineral Industries Special Paper 36, p. 288–314.
- Sweeney, K., and Roering, J.E., 2017, Rapid incision of a late Holocene lava flow—Insights from LiDAR, alluvial stratigraphy, and numerical modeling: *Geological Society of America Bulletin*, v. 129, nos. 3–4, p. 500–512, doi:10.1130/B31537.1.
- Tague, C., Farrell, M., Grant, G., Choate, J., and Jefferson, A., 2008, Deep groundwater mediates streamflow response to climate warming in the Oregon Cascades: *Climatic Change*, v. 86, no. 1, p. 189–210, doi:10.1007/S10584-007-9294-8.
- Tague, C., and Grant, G.E., 2004, A geological framework for interpreting the low flow regimes of Cascade streams, Willamette River Basin, Oregon: *Water Resources Research*, v. 40, no. W04303, doi:10.1029/2003WR002629.
- Tague, C., and Grant, G.E., 2009, Groundwater dynamics mediate low flow response to global warming in snow-dominated alpine regions: *Water Resources Research*, v. 45, no. W07421, doi:10.1029/2008WR007179.
- Taylor, E.M., 1965, Recent volcanism between Three Fingered Jack and North Sister, Oregon Cascade range: *The Ore Bin*, v. 27, p. 121–147.
- Taylor, E.M., 1968, Roadside geology, Santiam and McKenzie Pass Highways, Oregon, *in* Dole, H.M., ed., *Andesite conference guidebook*: Portland, Oregon Department of Geology and Mineral Industries, p. 3–33.
- Taylor, E.M., 1978, Field geology of S.W. Broken Top quadrangle, Oregon: Oregon Department of Geology and Mineral Industries Special Paper 2, 50 p., scale 1:24,000.

- Taylor, E.M., 1981, Central High Cascade roadside geology, *in* Johnston, D.A., and Donnelly-Nolan, J.M., eds., Guides to some volcanic terranes in Washington, Idaho, Oregon, and northern California: U.S. Geological Survey Circular 838, p. 55–83.
- Taylor, E.M., 1987, Field geology of the northwest quarter of the Broken Top 15' quadrangle, Deschutes County, Oregon: Oregon Department of Geology and Mineral Industries Special Paper 21, 20 p., scale 1:24,000.
- Taylor, E.M., 1990a, Sand Mountain, Oregon and Belknap, Oregon, *in* Wood, C.A., and Kienle, J., eds., Volcanoes of North America (United States and Canada): Cambridge, U.K., Cambridge University Press, p. 180–183.
- Taylor, E.M., 1990b, Volcanic history and tectonic development of the central High Cascade Range, Oregon: *Journal of Geophysical Research*, v. 95, no. B12, p. 19,611–19,622, doi:10.1029/JB095iB12p19611.
- Taylor, E.M., 1998, Geologic map of the Henkle Butte quadrangle, Deschutes County, Oregon: Oregon Department of Geology and Mineral Industries Geological Map Series GMS-95, scale 1:24,000.
- Taylor, E.M., and Ferns, M.L., 1994, Geology and mineral resource map of the Tumalo Dam quadrangle, Deschutes County, Oregon: Oregon Department of Geology and Mineral Industries Geological Map Series GMS-81, scale 1:24,000.
- Taylor, E.M., and Ferns, M.L., 1995, Geologic map of the Three Creek Butte quadrangle, Deschutes County, Oregon: Oregon Department of Geology and Mineral Industries Map GMS-87, scale 1:24,000.
- The Beer Detective, 2014, Bend's water quality: The Beer Detective website, accessed July 13, 2016, at <https://thebeerdetective.wordpress.com/2014/07/11/bends-water-quality/>.
- U.S. Forest Service, 2017, National Forest System trails: U.S. Forest Service FSGeodata Clearinghouse, available at <https://data.fs.usda.gov/geodata/edw/datasets.php?dsetCategory=transportation>.
- U.S. Reclamation Service, 1914, Deschutes Project: U.S. Reclamation Service [currently the Bureau of Reclamation] Deschutes Project folio, 147 p., 79 sheets.
- Walker, G.P.L., 1973, Explosive volcanic eruptions—A new classification scheme: *International Journal of Earth Sciences*, v. 62, no. 2, p. 431–446, doi:10.1007/BF01840108.
- Walker, G.P.L., and Croasdale, R., 1972, Characteristics of some basaltic pyroclastics: *Bulletin of Volcanology*, v. 35, no. 2, p. 303–317, doi:10.1007/BF02596957.
- Walker, G.W., and MacLeod, N.S., 1991, Geologic map of Oregon: U.S. Geological Survey, 2 sheets, scale 1:500,000.
- Walker, G.W., and Nolf, B., 1981, High lava plains, Brothers fault zone to Harney Basin, Oregon, *in* Johnston, D.A., and Donnelly-Nolan, J., eds., Guides to some volcanic terranes in Washington, Idaho, Oregon, and northern California: U.S. Geological Survey Circular 838, p. 105–118.
- Waters, A.C., and Fisher, R.V., 1971, Base surges and their deposits, Capelinhos and Taal volcanoes: *Journal of Geophysical Research*, v. 76, no. 23, p. 5496–5614, doi:10.1029/JB076i023p05596.
- Webster, J.R., 1992, Petrology of Quaternary volcanics of the Broken Top and Diamond Peak areas, central and south-central Oregon High Cascades—Evidence for varied magmatic processes from two contrasting volcanic centers: Bloomington, Indiana University, Ph.D. dissertation, 412 p.
- Wells, R.E., and McCaffrey, R., 2013, Steady rotation of the Cascade arc: *Geology*, v. 41, no. 9, p. 1027–1030, doi:10.1130/G34514.1.
- Wells, R.E., Weaver, C.S., and Blakely, R.J., 1998, Fore-arc migration in Cascadia and its neotectonic significance: *Geology*, v. 26, no. 8, p. 759–762, doi:10.1130/0091-7613(1998)026<0759:FAMICA>2.3.CO;2.
- Whiting, P.J., and Moog, D.B., 2001, The geometric, sedimentologic, and hydrologic attributes of spring-dominated channels in volcanic areas: *Geomorphology*, v. 39, nos. 3–4, p. 131–149, doi:10.1016/S0169-555X(00)00103-3.
- Whiting, P.J., and Stamm, J., 1995, The hydrology and form of spring dominated channels: *Geomorphology*, v. 12, no., 3, p. 223–240, doi:10.1016/0169-555X(95)00006-Q.
- Wicks, C.W., Jr., Dzurisin, D., Ingebritsen, S., Thatcher, W., Lu, Z., and Iverson, J., 2002, Magmatic activity beneath the quiescent Three Sisters volcanic center, central Oregon Cascade Range, USA: *Geophysical Research Letters*, v. 29, no. 7, p. 1122, doi:10.1029/2001GL014205.
- Wilcox, R.E., 1954, Petrology of Paricutin volcano, Mexico: U.S. Geological Survey Bulletin 965–C, p. 281–353.
- Williams, H., 1957, A geologic map of the Bend quadrangle, and a reconnaissance geologic map of the central portion of the High Cascade Mountains: Oregon Department of Geology and Mineral Industries, 2 sheets, scales 1:125,000, 1:250,000.
- Williams, H., 1976, The ancient volcanoes of Oregon: Eugene, University of Oregon Press, Condon Lectures, 70 p.

- Wilson, T., Cole, J., Cronin, S., Stewart, C., and Johnston, D., 2011, Impacts on agriculture following the 1991 eruption of Vulcan Hudson, Patagonia—Lessons for recovery: *Natural Hazards*, v. 57, no. 2, p. 185–212, doi:10.1007/s11069-010-9604-8.
- Winch, M.T., 1984–85, Tumalo—Thirsty land: *Oregon Historical Quarterly*, v. 85, no. 4, p. 341–374; v. 86, no. 1, p. 47–79, no. 2, p. 153–182, no. 3, p. 269–297.
- Wohletz, K.H., 1983. Mechanisms of hydrovolcanic pyroclast formation—Grain-size, scanning electron microscopy, and experimental studies: *Journal of Volcanology Geothermal Research*, v. 17, nos. 1–4, p. 31–64, doi:10.1016/0377-0273(83)90061-6.
- Wozniak, K.C., 1982, Geology of the northern part of the southeast Three Sisters quadrangle, Oregon: Corvallis, Oregon State University, M.S. thesis, 98 p.
- Yogodzinski, G.M., 1985, The Deschutes Formation—High Cascades transition in the Whitewater River Area, Jefferson County, Oregon: Corvallis, Oregon State University, M.S. thesis, 165 p.

Menlo Park Publishing Service Center, California
Manuscript approved July 6, 2017
Edited by Taryn A. Lindquist
Design and layout by Vivian Nguyen and Cory Hurd

